A STUDY OF THE VAPOUR-LIQUID EQUILIBRIA OF THE SYSTEM AMMONIA - CARBON DIOXIDE - WATER

IN RELATION TO THE SYNTHESIS OF UREA

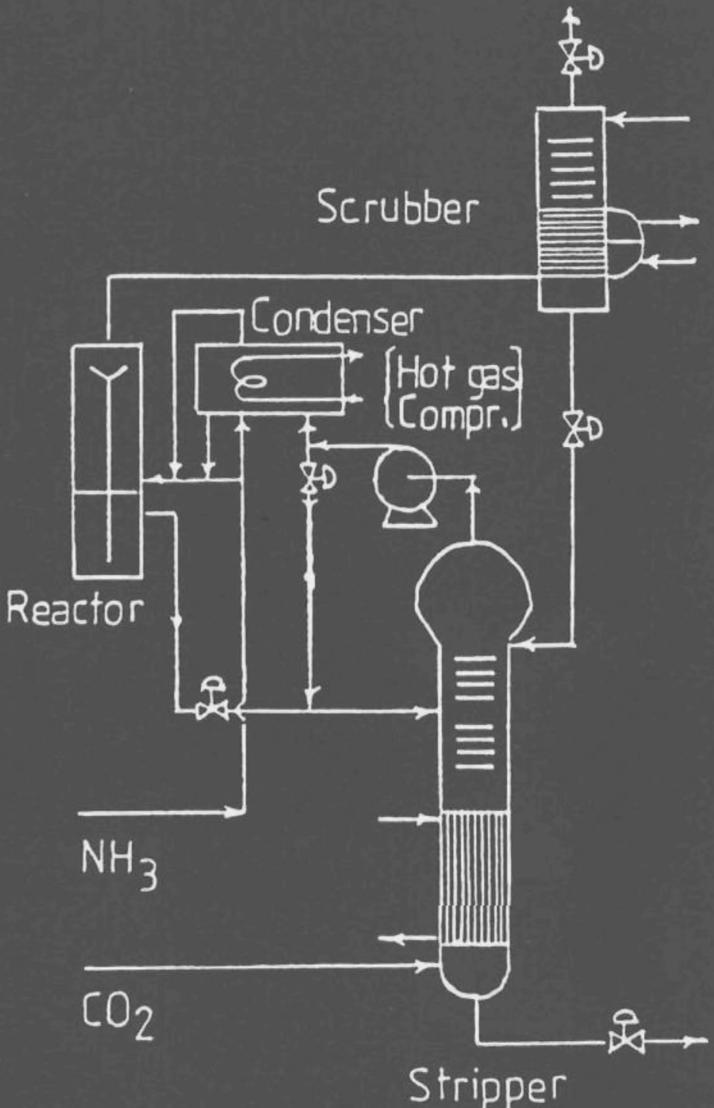

Krishnan RAMASAMY

A STUDY OF THE VAPOUR-LIQUID EQUILIBRIA OF THE SYSTEM AMMONIA - CARBON DIOXIDE - WATER IN RELATION TO THE SYNTHESIS OF UREA

A STUDY OF THE VAPOUR-LIQUID EQUILIBRIA OF THE SYSTEM AMMONIA - CARBON DIOXIDE - WATER IN RELATION TO THE SYNTHESIS OF UREA

PROEFSCHRIFT

ter verkrijging van de graad van doctor
aan de Technische Universiteit Delft,
op gezag van de Rector Magnificus, prof.dr. J.M. Dirken,
in het openbaar te verdedigen ten overstaan van
het College van Dekanen
op donderdag 17 maart 1988 te 14.00 uur

door

Krishnan RAMASAMY
Scheikundig ingenieur
geboren te Kandanur, Tamil Nadu
INDIA

1988

Dit proefschrift is goedgekeurd door de promotoren Prof. Drs. P.J. van den Berg en Prof. Dr. Ir. J. de Swaan Arons.

De promotiecommissie wordt gevormd door:

voorzitter:	
Prof. Dr. J.M. Dirken	(Rector Magnificus Technische Universiteit Delft)
promotoren:	
Prof. Drs. P.J. van den Berg	(Technische Universiteit Delft, Faculteit der Scheikundige Technologie en der Materiaalkunde)
Prof. Dr. Ir. J. de Swaan Arons	(Technische Universiteit Delft, Faculteit der Scheikundige Technologie en der Materiaalkunde)
toegevoegd promotor:	
Dr. Ir. S.M. Lemkowitz	(Technische Universiteit Delft, Faculteit der Scheikundige Technologie en der Materiaalkunde)
leden:	
Prof. Dr. Ir. J. de Graauw	(Technische Universiteit Delft, Faculteit der Scheikundige Technologie en der Materiaalkunde)
Prof. Ir. J.A. Wesselingh	(Technische Universiteit Delft, Faculteit der Scheikundige Technologie en der Materiaalkunde)
Prof. Dr. Ir. H.C.A. van Beek	(Technische Universiteit Delft, Faculteit der Scheikundige Technologie en der Materiaalkunde)
Dr. Ir. M.G.R.T. de Cooker	(DSM, Stamicarbon, Geleen)

STELLINGEN

1. There appears to be no reason why the two objectives (namely, the minimum pressure needed to effect urea synthesis and the maximum possible conversion to urea) cannot be met simultaneously.

- This dissertation p 195.

2. The phase rule dictates only the dimensionality of the state space and states nothing about the representation of it.... What is needed is a fundamentally new way of presentation (of the reactive phase equilibria) through manifolds.

- This dissertation p 99.

3. Thermodynamic textbooks usually define azeotropy as a state in which the two phase compositions are equal. Such a receipe although factual gives a poor perspective of azeotropy by missing the aspect of phase reactions. Many thermodynamic features have two aspects; one by viewing the feature as a state produced by a phenomenon and the other by viewing it as a phenomenon induced by a state. Both are valid view points, and one is the inverse of the other.

- This dissertation p 90.

4. The combination of modern applied thermodynamics with its high-powered calculational tools and classical phase theory with its far-reaching suggestiveness can be synergistic in devising new chemical engineering applications. Such a synergistic influence can be clearly seen in the development of urea processes.

- This dissertation p 64.

5. A widespread category mistake in chemistry is the confusion of thermodynamics with statistical mechanics, of chemical kinetics with collision theory, and taking the concept of chemical substances as being on equal footing with molecules.

- H.Primas, "Chemistry and complementarity", Chemia, 1982, Vol.36, No.7/8, p 298

6. Just as the university has changed from a center of learning to a social experience for the masses, so research, which bagan as a vocation and became a profession, has sunk to a trade if not a racket.

- C. Truesdell in his sixth lecture titled "Method and taste in natural philosophy", Six lectures, Springer Verlag.

7. Having identified the Sumerian civilization, the Egyptian civilization and the Indus civilization, the archaeology of the Africa - middle east Asia - Indian Sub-continent region has come to a plateau by being unable to delve beyond 3500 B.C. To progress further, one has to accept the hypothesis of the lost Lemurian Sub-continent and turn to deep water archaeology. All factual evidences point to a now submerged region extending from South India to Madagascar.

8. Considering the north Indian languages (together with Sanskrit) and the Europian languages as two branches of a single Indo-Europian tree is only a first step. Most probably, the Dravidian languages form an earlier branch of the same tree.

9. Any westener who likes to understand India's problems is better advised to think of Europe as if it were a single country, having been colonised for 400 years and become free only 40 years ago. If major economic developments had taken place only in these 40 years, that too in a regionally uneven manner, is it not natural that the multinational question in a "single republic" reality gets accentuated ? This aspect is the core of present day India's problems including Punjab. (Incidentally, the problems in Srilanka and Pakistan are also due to the multinational syndrome.)

10. Unless plant physiologists and geneticists work intensively on cassava, sorghum and millet, the green revolution in Africa will remain an empty phrase.

11. As long as the structural imbalances in the north-south economic interactions are not minimised, there will always be butter mountains and milk lakes of Europe together with the starvation of Sahel republics.

12. Almost all countries practice some form of human discrimination in the name of colour, race, language, religion and caste. The more developed the country, the more subtle and hypocritical this discrimination becomes.

13. The scenario of the nuclear winter (or, is it the nuclear autumn ?) will propel the East-West negotiators into realizing the absurdity of nuclear deterrence; the mistake of Hiroshima and Nagasaki will not be repeated.

14. The climate of a country and the hotness of its cuisines bear direct relationship with one another, with very few (happy) exceptions.

ACKNOWLEDGEMENTS

No man is an island, and no major effort, these days, is solo. Even a symphony created by a composer requires many others to realize it. Science is no exception; so is the present research work and this dissertation.

There were many who supported, helped, and even participated in my research efforts. In the first instance, there was the management of Southern Petrochemical Industries Corporation Limited, INDIA who reposed such a confidence in me and who did not mind giving a unique study leave period and its allied beneficial conditions. Secondly, there was the Canadian Commonwealth Scholarship Authorities who understood my reason for switching over from McGill, Montreal to Delft, the Netherlands and allowed me to opt out of the Commonwealth Scholarship Programme.

In Delft itself, the list of those who assisted is endless. The foremost was Dr.Ir.Saul.M.Lemkowitz. Straight from the day I landed in Netherlands, Saul has been a friend, philosopher and guide. He exposed me to the grandeur of phase theory, the intricacies of urea research, and the underlying mosaic of Dutch society. Then there was Prof.Drs.P.J.van den Berg, my promotor, who placed so much faith in me that I felt inspired to accomplish most of what I set out to do. There was also the urea research group at Dutch State Mines, especially Dr.Ir. Mario de Cooker, who continually followed the progress of my research and offered constructive criticisms, making the TUD - DSM urea discussions particularly lively. Here I should also mention the limited phase equilibria data which DSM gave me for use in my optimization programmes and for the permission they gave to cite from internal reports of DSM, in reference to Dr.H.A.G.Chermin's work.

Within Delft University of Technology, I should particularly mention the Physical and Inorganic Group, especially Prof.Dr.Ir.J.de swaan Arons, my co-promotor, (who brought a new enthusiaism into urea research and helped me at a crucial time so that the progress from then on was swift and smooth) and Dr.Ir.H.J. van der Kooi, for the productive discussions we had during the periodic urea project meetings.

Within the Laboratory of Chemical Technology, the efforts of A.A.M.Pruisken, W.J.Mulhuizen, M.T. van Thielen, W. Kerkhoven and P.Oudijn in building the experimental equipment, giving a concrete shape to my conceptual ideas, needs to be specially mentioned. I should also add P.Verbooij and P.Beekmans of the Instrument workshop into this special group of technical artisans for whom perfection was the watchword.

In the actual execution of the work, Rob van der Steen participated in trying out various ideas on gas analysis and Jaco Siegert worked on the liquid phase analysis. Further there was the special analysis help given with no hesitation by

Drs.H.G.Mercus, L.A.A.Peffer, B.Norder and H.L.Jansma.

Once the data were collected and the model was conceptualized, the whole effort was to translate the data into a parameter optimization software. Here I have to mention Evangelos Gogolides (who quickly grasped the dimension of the problem and came out with a software, excluding the gas phase section, in no time), Jan. M. de Rijke (who included the gas phase section, trimmed the software and chose a better optimization subroutine) and Fritz. P.C. Baak (who validated the programme at high temperatures).

I should also mention Jan Bakker who helped me in tracing a number of references besides the absorbing discussions on languages, Peter van Halderen who sorted out the word processing difficuties and Dr. P.J.W. Schuyl who made it possible to get a LaserJet print of this dissertation.

Finally, I should offer a thousand thanks to my wife Sala who never questioned my wisdom to choose but who always kept reminding me of the sustained efforts to move on the chosen path. There have been sagging moments through this research period and at each time she was the one who cheered me up in the company of my children, Ramu and Poo and got me into doing what I had to complete.

TABLE OF CONTENTS

3.3. The ternary system NH_3-CO_2-H_2O

3.5.2. The development of equilibrium manifold

4. THE EXPERIMENTAL STUDY

5. THERMODYNAMIC DESCRIPTION OF THE REACTIVE VLE IN THE SYSTEM OF NH_3-CO_2-H_2O THROUGH AN ION SPECIFIC INTERACTION MODEL

6. APPLICATION OF THE PHASE EQUILIBRIA PRINCIPLES TOWARDS THE DESIGN OF UREA PROCESSES AND ESPECIALLY WITH REFERENCE TO THE HOT GAS RECYCLE PROCESS

APPENDIX B. THE PROGRAMMES USED IN THE PRE-DESIGN OF THE IMPROVED TUD HOT GAS RECYCLE PROCESS

APPENDIX C. THE GAS PHASE ANALYSIS OF THE NH_3-CO_2-H_2O MIXTURES: THE METHOD, THE PROBLEMS FACED AND THE SOLUTIONS

APPENDIX D. THE LIQUID PHASE ANALYSIS

SUMMARY

The present dissertation is concerned with studying the reactive vapour- liquid equilibria of the NH_3-CO_2-H_2O system (with the equilibrium concentration of urea) in the pressure range of $5.41 < p < 30$ bar and the temperature range of $88.7 < T < 130^o$ C. The need for this study arose out of the earlier research concerning a revival of the Hot Gas Recycle Process (HGRP) for synthesizing urea. Especially the Delft researchers S.M. Lemkowitz and P. Verbrugge have worked and published on this subject and its related phase equilibria.

This dissertation consists of six chapters and four appendices. The first chapter starts with explaining the relevance of urea in alleviating the world food problem. Later it raises the problem of capacity utilization of urea plants, especially with reference to developing nations. Then it concentrates on the basic issue of the highly energy-intensive character of the urea processes and the efforts made to reduce these energy requirements. It also describes the effort taken by Delft University of Technology (TUD) in reviving the HGRP. The chapter ends with the statement of the present research objectives.

The second chapter discusses the molecular aspects of the basic components, NH_3, H_2O and CO_2, together with the phase equilibria of the important binary systems, NH_3-H_2O, CO_2-H_2O, NH_3-CO_2, H_2O-NH_2CONH_2, NH_3-NH_2CONH_2 and CO_2-NH_2CONH_2. The molecular aspects of urea-like species, especially carbamic acid, are also treated in the second chapter. These discussions are included to help the reader in appreciating the complexities of these relevant systems and to justify the inclusion of various parameters in the model developed in Chapter 5.

The third chapter begins with a description of the multiphase equilibria of the ternary system without the presence of urea. The earlier work is critically reviewed, and the probable behaviour of the system at high pressures (not yet researched) is sketched in detail. Subsequently a few important details, like the topology of the bubble- and dew-point surfaces, including the gas- and liquid-ridge curves on these surfaces, and the residue and distillate curves of this system (especially the boundary distillation line) are discussed. Later the phase behaviour of the ternary system ($2NH_3$)-NH_2CONH_2-H_2O is discussed. Subsequently, in order to present and understand the phase equilibria of the chemically reactive systems, like the NH_3-CO_2-H_2O system, the manifold representation of reactive equilibria is elaborated upon followed by a description of the five dimensional phase behaviour of the quarternary system ($2NH_3$)-CO_2-H_2O-NH_2CONH_2 and its eventual transformation to the four dimensional ternary system ($2NH_3$)-CO_2-H_2O with the equilibrium concentration of urea.

In the fourth chapter the rationale behind the choice of the system and the

experimental apparatus are first described. Then a description of the measurement procedures, the experimental difficulties and the suitable solutions follows. The control measurements of the known binary system NH_3-H_2O are then presented. Then a detailed description of the measured vapour-liquid equilibria of the chosen ternary system within the above-mentioned pressure and temperature ranges follows. Also the complementary results obtained by other researchers are included in the description and the discussion.

Chapter 5 begins with a review of electrolyte solution theory; here the theory of Pitzer plays an important role. A greater part of this chapter is devoted to the development of a specific molecular-thermodynamic model (to describe the measured phase behaviour) and to the optimization procedure for obtaining the model parameters. In general, the developed model appears to fit the experimental results adequately. Around the narrow regions close to the binary systems, NH_3-H_2O and CO_2-H_2O, the correspondence between the measured value and the calculated one is less than satisfactory. This difference might be due to the numerical problem of small numbers caused by the usage of the unweighted objective function. The other troublesome region is closer to the "tongue-tip" of the bubble-point curve (at constant pressure and temperature) where small analysis errors can make or break a fit. One important conclusion concerning the model is that the incorporation of urea formation reaction along with the ionic reactions is of major importance.

In the sixth chapter our own phase model along with other published models of this system are specially applied, to the maximal extent possible, in combination with the principles of phase theory towards the pre-design of an improved version of the HGRP for the production of urea. A new design approach is chosen with the goal of simultaneously achieving a minimal bubble-point, a maximal conversion, an optimal temperature, and an optimal $(NH_3)/(CO_2)$ mole ratio in a urea reactor for a given $(H_2O)/(CO_2)$ mole ratio. Utilizing the above models and principles the conditions of the reactor, the hot-gas condenser, and the stripper are calculated as completely as possible. Also the compressor calculations in regard to the handling of the hot gas recycle and the fresh CO_2 feed are carried out. An optimization procedure for determining the optimal stripper pressure is also skeched. However, in all these model calculations, the numerical value of many thermodynamic properties are either not fully known or known only with insufficient accuracy. Hence it is not possible to make an accurate economic comparison between a HGRP and a stripping process.

The dissertation ends with four appendices. Appendix A treats the solid-gas equilibria of ammonium carbamate. This is done to determine those p-T conditions at which only the vapour-liquid equilibria exist over the entire composition region. Appendix B incorporates the programmes utilized for fixing the conditions of the reactor, the condenser and the compressor of the improved TUD HGRP. Appendix C treats the gas phase analysis using Gas Chromotography, the problems faced in the analysis, and the simple and novel approaches taken for establishing the optimal parameter values of the GC analysis equipment. Appendix D describes in brief the liquid phase analysis.

CHAPTER 1

INTRODUCTION

1.1. *The scenario*:

Human achievements in the area of agriculture are phenomenal, especially in the last three decades. Dramatic production increases in this period have occurred all over the world, excepting perhaps the African continent, in the important cereals, namely wheat, rice and corn. These increases have become possible mainly due to the use of high yielding seeds. Since the pioneering efforts of Norman Borlaug in the 1950's, the high yielding wheat strains, tried first in Mexico, and the corn strains, tried first in the U.S., have laid the basis for the green revolution. A similar breakthrough for rice was achieved by the International Rice research Institute at the Philippines when it developed the strains of IR-8 and IR-22 [1]. These high yielding strains, however, cannot themselves cause the miracle. Assured irrigation, sound water management, optimal agronomic practices and profuse application of fertilizers and pesticides are some of the integral parts of the whole effort. Even though many of the high yielding strains are sterile and their development leads to a reduced cereal genetic pool, the farmer's resort to these varieties has gone unabated. Similarly, the intensive application of fertilizers has become perennial to achieve a bountiful harvest. In fact, one can state [2] that about 15% of the total cereal production, (or to state differently, 30% of the incremental cereal production, as well as 56% of the incremental cereal yield) during the 1948-52 to

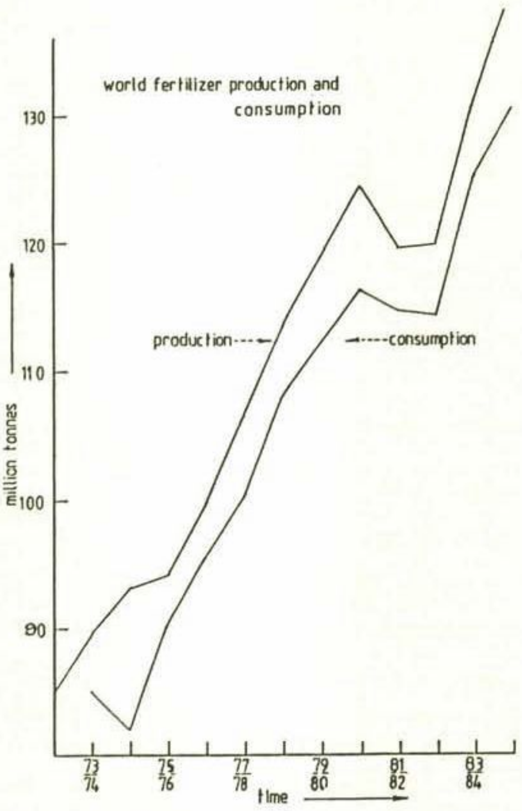

Fig.1.1.*World fertilizer production and consumption as per the FAO statistics (1982)* [3]

1972-73 period in the developing market economies can be attributed to fertilizer use. This being the case, it is no wonder that the world fertilizer production and consumption have grown enormously over the last decade [3]. (See Fig. 1.1 and 1.2.)

However, one should not read too much between the lines. Like a statistician drowned in a lake of 6 inch average depth, the conclusions based on these production figures about the general progress of the community of nations can become catastrophic. After all, these figures do not convey the lopsided growth patterns which are both inter-regional and intra-regional.

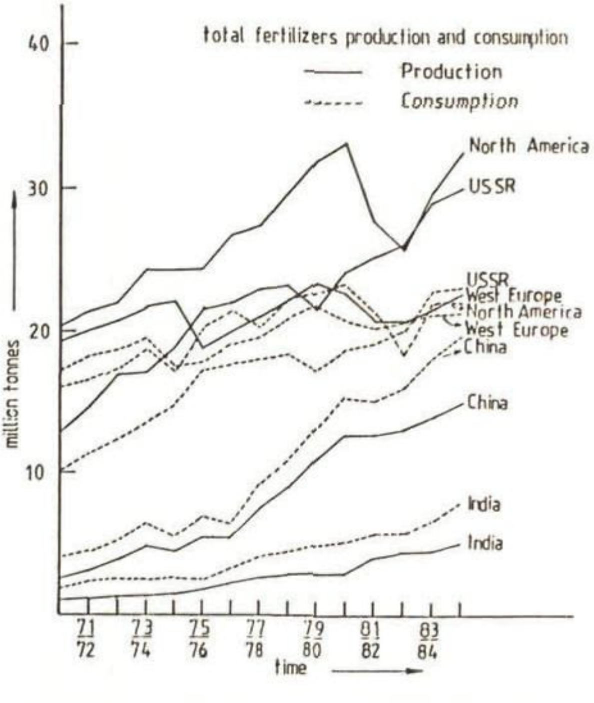

Fig. 1.2. *Fertilizer production and consumption in selected regions and countries as given by the 1983 FAO statistics on food and fertilizers [3].*

One of the factors of this uneven growth, namely weather conditions, is almost unpredictable. Properly speaking, the achievements in food production are better assessed against a backdrop of periodical weather disasters, such as a late arrival of monsoon in the Indian sub-continent, a drought in East Africa or Brazil or a frozen harvest in the Soviet Union.

Likewise there is one more perspective of the uneven growth. This is connected with the very high price the developing nations are paying on the social front for the increased production. The new found prosperity of the *nouve riche* and the intense struggle of the ancient poor caused by the green revolution create havoc in the social relations of the developing nations. The social fabric of most of these nations is torn to the core. Haunted by the Malthusian nightmare, this uneven growth has almost become a crisis and a challenge in the Africa and Indian subcontinent. The only way to redress the crisis is to further produce (which means more fertilizers and better farm practices) or, perish. The active role of nitrogenous fertilizers and especially urea is a cornerstone in this colossal effort to produce the cereals and to sustain the population.

1.2. *The relevance of urea as a nitrogenous fertilizer:*

In spite of the fact that urea was synthesized in 1812 by Davy and in 1828 by Wohler, and that the easiest and the only method of manufacture from NH_3 and CO_2 was suggested by Basaroff in 1868 [4], urea remained a curiosity among the chemists until well in the 20th century.

It was only in the 1950's with the high yielding strains and especially with rice that urea attained its prominence. Rice crop needs a large dosage of nitrogen and urea contains a high nitrogen nutrient per unit mass (about 46.3 wt%). It easily hydrolyses in water producing ammonium salts. Through microbial actions, these salts are further transformed into nitrates and thus become available to the rice crop.

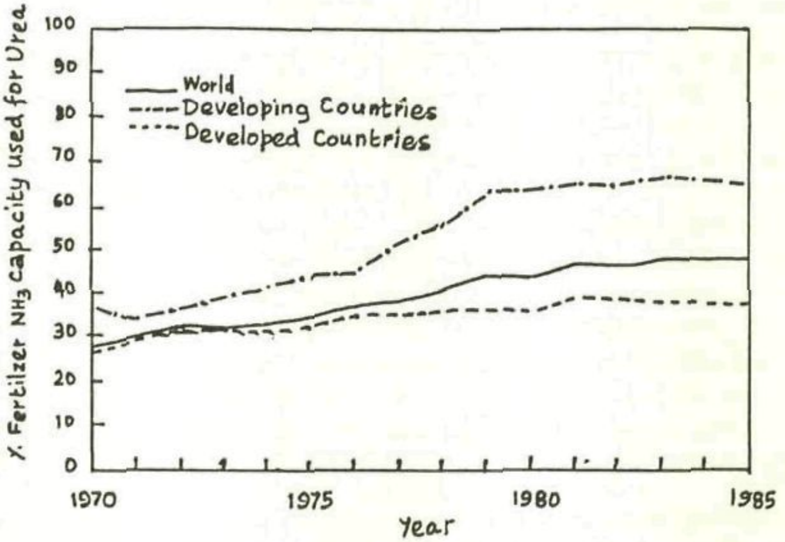

Fig. 1.3. *The growth of world urea production and that of selected regions as given by the 1982 IFDC report [5] and the 1983 FAO statistics [3]. For the years beyond 1982, only the IFDC projected values are plotted.*

Moreover urea does not leave any residue, as do some other nitrogenous fertilizers, such as ammonium sulphate and ammonium chloride.

Given urea's propensity *to fertilize soil, its low handling and distribution* costs on a nutrient basis, and the possibilities of scale economies in the production process, it is only natural that urea production grew by leaps and bounds all over the world [3]. See Fig. 1.3. The share of urea in the world nitrogen capacity increased from 31% in 1971 to 45% in 1979 and was projected to be 49% in 1985. In the developing countries the share was projected to be 67% in 1985 [5]. This phenomenal growth is occurring, even though urea production is highly energy intensive. According to one calculation by the International Fertilizer Development Center (IFDC) [5] it requires almost 79.6 GJ to deliver 1 mt. of nitrogen to the farmer in the form of urea, which is by far the largest energy requirement of any nitrogenous fertilizer. In fact many experts [6] question the whole *rationale* behind the choice of urea as a major nitrogenous source, mainly on this account and due to the poor nitrogen use efficiency of urea. Yet the farmer continues to buy urea, perhaps due to intense greening of the leaves and the rapid vegetative growth observed within days of application.

1.3. *The capacity utilization and energy consumption of urea plants*:

The ability to produce urea in large quantities at attractive prices depends on two factors, namely the capacity utilization and the energy usage.

Capacity utilization is the percentage of the nameplate capacity utilized over an accepted norm period of 330 days. It is a function of three different factors, namely the plant availability, the onstream factor and the onstream efficiency. The plant availability highlights the number of days the plant was available for production over a year, the rest of the time the plant not being available due to internal reasons. Additionally there might be downtime due to external reasons even though the plant was available. If the total downtime due to internal and external reasons is subtracted from 365 days, the onstream time is obtained. The onstream factor tells the onstream time as a percentage of 365 days. The onstream efficiency further measures the performance of the plant in the time it has run. Of the three factors mentioned, the plant availability and the onstream efficiency fall largely within the purview of the process designer, while the onstream factor is mostly in the plant operator's domain.

Each of these three factors is problematic in developing countries. To improve the plant availability it is necessary to have reliable running machinaries and simple flowsheets. The need for flowsheet simplicity is obvious by the popularity of some modern processes called stripping processes. To reduce the downtime due to external reasons, such as frequent power failures and insufficient raw-material availabilty in these countries, the plant operators have to resort to captive power units, and tone up ammonia plant operation. Also they have to store a large amount of spares to meet equipment failures. Furthermore, the plant operators have to identify the design inadequacies limiting the onstream efficiency in close co-operation with the process suppliers and rectify them at the earliest. Even new processes have to be assessed in terms of the possible operating problems related to capacity utilization.

Concerning the second aspect, the energy usage, the total energy consumed for urea production can be split into three categories, one for the energy required to produce the raw material NH_3 and the other two for the energy consumed in the synthesis (including decomposition and recovery stages) and finishing sections. The second raw material CO_2, being a byproduct of the ammonia plant, can be considered to be produced with no energy expenditure.

As a concrete example [7], the energies consumed in the three catagories by the existing urea plants in the U.S. and what would be the possible future energy savings through adopting new designs are listed in Table 1.1.

Table 1.1. *Present energy use and possible energy savings in the U.S. urea plants as given by the IFDC report of May 1982 [5].*

Category	Energy use Present (GJ/mt of N)	%	Future (GJ/mt of N)	%	Energy Savings %
Ammonia input	58.7	73.7	44.0	81.2	25
Synthesis	12.0	15.1	6.7	12.4	44
Finishing	8.9	11.2	3.5	6.5	61
Prilled Urea total	79.6	100.0	54.2	100.0	32

The necessity of designing energy efficient urea processes is highlighted on two accounts. The first concerns the upstream side, where novel ammonia flowsheets are offered with energy consumption close to only 42.9 GJ/mt of N leading indirectly to a reduced availability of surplus steam for the whole fertilizer complex. The second account occurs on the downstream side where the following argument given by G.M. Blouin of TVA [8] appears to be very relevant.

"In the final analysis, what is required for an agricultural crop is a balanced mixture of nitrogen, phosphorous and potash nutrients. The potash nutrient is usually obtained with almost no choice in the form of muriate of potash (KCl), mined in countries like Canada, USSR and now, Brazil. Fortunately, there is a choice in obtaining the NP fertilizers. One choice is the urea - ammonium phosphate (UAP) and the other is the ammonium nitrophosphate (ANP)". Among these choices and for the same raw material cost, Blouin argues that the ANP route may be cheaper than the UAP route, since 73% of the energy spent in the UAP route is utilized in the urea process itself. This aspect appears to be true even with the best commercial urea process at present. Such a conclusion challenges urea process developers to devise a still more energy efficient process; otherwise the validity of the ANP route becomes too obvious to ignore.

1.4. *The rise of new processes*:

Rising to the challenge, urea process designers are now offering new processes like the ACES process offered by Toyo Engineering [9], the IDR process offered by Tecnimont [10], the SRR process offered by Ammonia Casale [11] and the improved versions of the stripping processes offered by Stamicarbon [12] and SNAM progetti [13]. One common aspect of all these processes is the isobaric synthesis loop comprising a reactor, a so-called stripper and a condenser.

To understand the term stripping, one has to go into the chemistry of urea manufacture. Urea is produced by the reaction of ammonia and carbon dioxide to form ammonium carbamate followed by dehydration. While the first reaction is almost complete, the second reaction, namely the dehydration, is thermodynamically limited. Hence, to get increased conversion, all the available processes employ excess ammonia which is to be expelled later along with the decomposition of the unconverted ammonium carbamate in the downstream equipment. In the older processes, these two objectives are achieved by sequential pressure reductions and recovery in aqueous solution. In the stripping processes the same are accomplished by the alteration of partial pressures of the components, without reducing the total pressure, through the admission of one of the reagents, namely either carbon dioxide or ammonia. For example, in the case of CO_2 stripping process, the reactor outlet stream becomes lean in NH_3 and CO_2 after an intense contact with the fresh CO_2, employed as a stripping agent. Similarly one can work with fresh NH_3 as a stripping agent. The advantages of the stripping technique are many and are discussed in the following paragraphs.

Taking a specific example of the Stamicarbon stripping process, the three major advantages of the process have always been the high reactor pressure close to the minimal bubble-point conditions of the system, the high stripping efficiency leading to low NH_3 and CO_2 concentrations at the exit of the stripper (hence no need for an intermediate recovery stage), and the near azeotropic condensation in the HP condenser. However, these features are achieved at a cost of relatively low conversion in the reactor (60%). By contrast, the old solution recycle processes rely on the high conversion in the reactor together with a complex heat exchange network to produce a competitive energy economy. Still the simplicity of the Stamicarbon flowsheets carried the day, and more than 40% of the urea plants presently existing came to be built on their scheme.

But, once the Stamicarbon patents on the CO_2 stripping expired, other process suppliers started combining their old advantage of the high conversion with that of the high pressure condensation (which in these processes is non-azeotropic) through CO_2 stripping. Still, these new stripping processes, now very much competitive with that of Stamicarbon, could not achieve a high stripping efficiency due to inherent constraints, like the high $(NH_3)/(CO_2)$ ratio at the inlet of the stripper. By stripping efficiency, it is meant of the percentage of the incoming ammonia which is transferred to the gas phase. It has been observed that the $(NH_2)/(CO_2)$ ratio of the inlet stream has a large bearing on the stripping efficiency achieved. Beyond a critical ratio, there is a decrease in the stripping efficiency leading to higher ammonia content in the outgoing liquid stream and hence a need for additional recovery at an intermediate pressure. However, in the case of Stamicarbon process with a high stripping efficiency, only a single low pressure recovery is required.

1.5. *The Hot Gas Recycle Process (HGRP)*:

The claims and counter-claims of the various urea process suppliers in the pages of "Nitrogen" magazine [14] regarding the energy usage is an indication of the present intense competition existing in the field. On seeing these process developments in the urea technology, a concerned observer might well definitely ask, "Is this all that is possible ? Can we not get a flow sheet combining the high stripping efficiency and the HP condensation with a maximal conversion and minimal bubble-point pressure in the reactor ?" The answer is definitely affirmative, if we revive the now defunct concept of hot gas recycle process (HGRP). The idea is simple. Stripping at a low pressure and condensation at a high pressure are advantageous to achieve energy economy. In the old solution recycle processes, the decomposer and the condenser were at a low pressure and the reactor at a high pressure. In the stripping processes, all the three are at the same high pressure. In the HGRP, the reactor and the condenser will be at the high pressure and the stripper at a low pressure. The gases from the low pressure stripper will be compressed before being sent to the HP condenser.

The idea of a HGRP is not something new. It was in fact the pioneering urea process [15] developed in the 1940's by I.G.Farben of Germany. The process adopted by I.G. Farben was, however, plagued with a number of operating problems, like excessive corrosion in the hot gas compressor, unduly large energy consumption and frequent machinery failures. Subsequent to the war, both Chemico of the United States and Norsk Hydro of Norway started working on variations and patented a number of them [16,17,18,19]. None of the patented HGR processes were ever tried on a pilot plant level, since the market in the 1960's was already clamouring for the then recent CO_2 stripping process. The future of the HGRP was left hanging due to a perceived problem regarding the hot gas compressor. When no new process company came forward to revive the HGRP, it was left to Delft university of Technology (TUD) to do so.

Lemkowitz and van den Berg brought forth a newer version of the HGRP and also constructed an actual HGR-pilot plant [20]. Lemkowitz studied the bubble- and dew-*points of the NH_3-CO_2-H_2O system at the synthesis conditions; he also performed the* static and dynamic corrosion studies on a turbo-impeller by subjecting it to hot gas compositions above the dew-point conditions, and proved convincingly the possibility of running a turbocompressor at high temperature. As a result, the technical feasibility of the HGRP (especially the fact that the NH_3-CO_2-H_2O mixture could be compressed without any corrosion whatsoever by working at temperatures above the dew-points,) was clearly established [20,21,22], but not the economic viability, which required further studies.

1.6. *The follow-up to the study of Lemkowitz:*

The questions left unanswered in Lemkowitz's study are the following:

1. Can one achieve simultaneously a maximum equilibrium conversion and a minimum bubble-point pressure together with an optimum $(NH_3)/(CO_2)$ mole ratio and optimum temperature for a given $(H_2O)/(CO_2)$ mole ratio?
2. What is the maximum condenser temperature one can reach?
3. How does one fix the stripper pressure?

In order to answer these questions, Verbrugge [23] began investigating the NH_3-CO_2-H_2O system at physical equilibrium with no urea formation. Soon it was realized that the experimental observations were tedious and quite involved in terms of reliable gas and liquid phase analyses. Accordingly he had to limit his study to temperature range of 40°C to 90°C and at just 1.03 bar (abs.) pressure.

The present study is a sequel to Verbrugge's work and a bridge to the work of Lemkowitz. Unlike Verbrugge, the present author studied the ternary system at chemical equilibrium (i.e., with equilibrium concentration of urea) but at a pressure range of 5.41 to 30 bar and a temperature range of 88.7 to 130°C.

1.7. *The major aspects of the present research programme:*

The major aspects of the present research programme were concerned with establishing reliable sampling and analysis procedures, collecting isothermal-isobaric data and obtaining an accurate thermodynamic description using modern electrolyte theories.

The necessity of reliable sampling and analysis procedures needs no emphasis, given the fact that both NH_3 and H_2O are polar and that they influence one another's elution in gas-solid chromotography. Similarly the liquid phase analysis of NH_3 and CO_2 is quite tricky, especially in the presence of urea.

The insistence on the isobaric-isothermal working in the present study was *intentional. In this way the consistency* of the data can be easily checked with regard to tie-line crossings, the demarcation of the VLE region in p-T cross sections and the transparent viewing of the 3-dimensional isothermal (or isobaric) diagram without going through model calculations.

The third aspect, namely the thermodynamic description, was spurred by the recent developments in electrolyte theories. Pitzer and his coworkers have suggested an ion-interaction model applicable for concentrated solutions of multi-electrolytes. This model has also been attempted recently for the NH_3-CO_2-H_2O system, especially for the mild concentrations [24,25,26]. However, the application was not complete. Hence it was proposed in the present study to test the ion-interaction model quite thoroughly even for the region of high concentrations.

Also it was proposed in the present programme to describe the inter-related component systems, both from a phenomenological phase-theoretical view point and from a molecular-interactions view point.

Finally a few optimum parameters of a HGRP are derived through the simple empirical models given in the literature.

The fruits and results of the present research programme along with the discussions of the relevant literature are described in the succeeding pages.

Reference:

1. Swaminathan,M.S., "Rice", Scientific American, 1983, pp 63-71.
2. Pinstrup-Anderson,P., "Preliminary estimates of the contribution of fertilizers to cereal production in developing market economies", Journal of Economics,1976, vol.12, pp 169-172.
3. FAO statistics on food and fertilizers, 1983, Rome.
4. Chao, G.T.Y., "Urea, its properties and manufacture", Chao's Institute, 3014- Larkwood St., West Covina, Calif., p 2.
5. Mudahar, M.S. and T.P.Hignett, " Energy and fertilizer-policy implications and options for developing countries", Technical bulletin 20, IFDC, May 1982, p 45.
6. *ibid*, p 166.
7. *ibid*, p 121.
8. Blouin, G.M., " Energy requirements for high nitrogen fertilizers ", CEP, April 1984, pp 40-44.
9. Jojima, T. et al, "Commercially proven new urea technologies", CEP, April 1984, pp 31-35.
10. Pagani, G. and L.Mariani, "The IDR process: An economical way of producing urea", CEP, April 1984, pp 45-48.
11. Zardi, U., "Revamping urea plants economically", CEP, April 1984, pp 36-39.
12. Dooyeweerd, E. and J.Meessen, "How do power and steam prices affect urea plant design ?", CEP, April 1984, pp 54-57.
13. "SNAM Progetti's newest urea process", Hydrocarbon Processing, July 1975, pp 102-104.

14a. Dooyeweerd, E. and J.Meessen, "comparison of the energy consumptions of low energy urea technologies", Nitrogen, 1983, May-June, No.143, pp 32-38.

14b. Pagani,G., "IDR technology cuts to a minimum the energy consumption in urea plants", Nitrogen, 1983, september-october, No.145, pp 35-37.

15a. Dewling, W.L.E. and S.Robell, "Urea manufacture at the I.G.Farben-Industrie Plant at Oppau", FIAT final report 889, 3 september, 1946, 29 pages.

15b. Fromholz, A.Z, FIAT final report 889 supplement, 3 september,1946, 4 pages.

16. Cook, L.H., Chemico, US patent 3301897, Jan 31, 1967.
17. Cook, L.H., Chemico, US patent 3370090, Feb 20, 1968.
18. Cook, L.H., Chemico, US patent 3816528, Jan 11, 1974.
19. Norsk-Hydro-Ellektrisk Kvaelstotfaktieselskab, British patent 1129787, Oct 9, 1968.
20. Lemkowitz, S.M., "Phase and corrosion studies of the ammonia - carbon dioxide - water system at the conditions of the hot gas recirculation process for the synthesis of urea", PhD thesis, Delft University of Technology, The Netherlands, 1975, 191 pages.
21. Lemkowitz, S.M., de Cooker, M.G.R.T., and van den Berg, P.J., " Some fundamental

aspects of urea technology," paper presented before The Fertilizer Society, London, on December, 14th, 1972, 115 pages. Published as Proceedings No. 131 of The Fertilizer Society.

22. Written contributions to proceedings 131 (Lemkowitz, S.M., de Cooker, M.G.R.T., and van den Berg, P.J., " Some fundamental aspects of urea technology,") of the Fertilizer Society, London, 1972.

23. Verbrugge, P., "Vapour-liquid equilibria of the ammonia - carbon dioxide - water system", PhD thesis, Delft University of Technology, The Netherlands, 1979, 133 pages.

24. Chen, CC. et al. "Extension and application of the Pitzer equation for vapor-liquid equilibrium of aqueous electrolyte systems with molecular solutes", AIChE J., 1979, vol.25, no.5, pp 820-831.

25. Pawlikowski, E.M. et al, "Phase equilibria for aqueous solutions of ammonia and carbon dioxide", I&EC process des.dev., 1982, vol.21, no.4, pp 764-770.

26. Müller, G., " Experimentelle Untersuchung Des Dampf-flussigkeits-Gleichgewichts im system ammoniak-kohlendioxid-wasser zwischen 100 und 200°C bei drucken bis 90 bar", (in German), PhD thesis, University of Kaiserlautern, 1983.

THE MOLECULAR CHARACTERISTICS OF THE SPECIES INVOLVED IN THE NH_3-CO_2-H_2O SYSTEM AND THEIR RELEVANCE TO THE BINARY VAPOUR-LIQUID EQUILIBRIA.

2.1. *Introduction*:

It is only natural that phase equilibria studies play an important role in the development of urea processes, since these processes involve intense contacts of liquid and vapour. Along with development of reliable pumps and compressors and new fabrication materials, the phase equilibria studies have brought many advances in urea technology in the form of solution recycle processes, stripping processes and their latest combination breeds. However, there is still a need for new process development, mainly because of the increased demand on plant reliability and energy economy in the days ahead.

Presently, the need to have a better understanding of the phase equilibria of the NH_3-CO_2-H_2O system can be emphazised on the following grounds.

1. It is advantageous to achieve simultaneously a maximal conversion to urea, a minimal bubble point pressure, an optimal $(NH_3)/(CO_2)$ mole ratio and an optimal temperature for a given mole ratio of $(CO_2)/(H_2O)$.
2. Energy exchanges involved in the decomposition and recovery steps can be integrated to get a near self-sufficiency in energy, if quantitative thermodynamic descriptions of the phase equilibria and a satisfactory method of estimating the enthalpies of the process streams are available.
3. Condensing and absorbing the recycled gas mixture with or without the use of external water at the maximal temperature for a selected pressure is essential in reducing the energy rejected to cooling water.
4. A knowledge of the solid-liquid and the solid-liquid-gas equilibria is needed to prevent operating problems like clogging of pipe lines and control valve damage due to solid formation at the design stage itself.
5. A quantitative description of the phase equilibria is needed for flowsheeting programs meant to optimize the third generation urea processes.

Although most of the above aspects appear to be achievable, there are many conceptual and practical difficulties to contend with. One of the major difficulties is understanding the relevant phase equilibria themselves. Quite a number of complex phenomena occur in the systems relevant to urea technology, such as ternary saddle azeotropy [1], the existence of complex solid-liquid-gas equilibria in which up to five solid species can occur, the existence of quadruple points and possibly a quintuple point [2], liquid-liquid immiscibility [2,3] and unusual critical behaviour [1,2]. Yet on the molecular level, the relevant systems contain only the three basic species NH_3,CO_2 and H_2O along with other relatively simple species derived from them.

The fact that complex and unusual phenomena such as these mentioned above occur in systems composed of relatively simple species raises a number of questions, one of which is the relation of the molecular characteristics of these species to the gross phase equilibrium behaviour of the systems composed of these species. The major emphasis in this chapter is towards describing these relations in detail, mainly with respect to the binary systems.

2.2. *Characterisation of a multi-species system*:

Any discussion of physico-chemical equilibria has to start with the characterisation of the involved species with reference to chosen pressure and temperature ranges. All possible species are either identified through chemical analyses or through postulation. Contrary to the expectation of many a chemist, fixing the number of species becomes really arbitrary, since refining the chemical analysis procedures tend to indicate more and more species. Once the species are fixed, it is natural to ask whether their composition can be changed arbitrarily. The answer is negative due to reaction constraints and material balances which limit the species compositions to particular ranges. Additionally there is an electroneutrality constraint in the case of ionic species. Hence one should say that there is a *minimum number of species*, called *components*, to which the origin of all the *remaining species* can be attributed. For a simple system, this minimum number can be fixed heuristically (i.e. through ad hoc means). In fairly complicated systems, such simple procedures, unless handled properly, may lead to non-unique results. In such cases the number of the components can be found systematically by the following method [4,5,6].

Knowing the formulae of all the species, one can first write an element-species matrix whose ij'th unit will denote the number of i'th atoms in the j'th species. For example the following element-species matrix (augmented with a row of charges held by each species) can be written for the present system.

	Species present									
	NH_3	CO_2	H_2O	H^+	NH_4^+	$CO_3^=$	HCO_3^-	NH_2COO^-	OH^-	NH_2CONH_2
Number of N atoms	1	0	0	0	1	0	0	1	0	2
Number of C atoms	0	1	0	0	0	1	1	1	0	1
Number of H atoms	3	0	2	1	4	0	1	2	1	4
Number of O atoms	0	2	1	0	0	3	3	2	1	2
Amount of charge e	0	0	0	1	1	-2	-1	-1	-1	0

One can now find the rank of the matrix through row transformations.

	Species present									
	NH_3	CO_2	H_2O	H^+	NH_4^+	$CO_3^{=}$	HCO_3^-	NH_2COO^-	OH^-	NH_2CONH_2
N	1	0	0	0	1	0	0	1	0	2
C	0	1	0	0	0	1	1	1	0	1
(O-2*C)	0	0	1	0	0	1	1	0	1	-1
e	0	0	0	1	1	-2	-1	-1	-1	0
(H+4*C-3*N -2*O-e)	0	0	0	0	0	0	0	0	0	0

The rank of the above row echelon matrix turns out be four; hence there are only four basic species (which may be chosen as NH_3, CO_2, H_2O and H^+); all other species can be derived from them. In other words, the following reaction set can be written in terms of the stoichiometric transformation matrix.

$$\begin{array}{l} NH_4^+ \\ CO_3^{=} \\ HCO_3^- \\ NH_2COO^- \\ OH^- \\ NH_2CONH_2 \end{array} = \begin{array}{rrrr} 1 & 0 & 0 & 1 \\ 0 & 1 & 1 & -2 \\ 0 & 1 & 1 & -1 \\ 1 & 1 & 0 & -1 \\ 0 & 0 & 1 & -1 \\ 2 & 1 & -1 & 0 \end{array} * \begin{array}{l} NH_3 \\ CO_2 \\ H_2O \\ H^+ \end{array} \qquad \text{(eq. 2.1)}$$

From the above stoichiometric transformation matrix, one can also write the following material and charge balances valid for any single phase.

$$\begin{array}{l} \{NH_3\} \\ \{CO_2\} \\ \{H_2O\} \\ \{\text{Charge } e\} \end{array} = \begin{array}{l} \langle NH_3 \rangle \\ \langle CO_2 \rangle \\ \langle H_2O \rangle \\ \langle H^+ \rangle \end{array} + \begin{array}{rrrrrr} 1 & 0 & 0 & 1 & 0 & 2 \\ 0 & 1 & 1 & 1 & 0 & 1 \\ 0 & 1 & 1 & 0 & 1 & -1 \\ 1 & -2 & -1 & -1 & -1 & 0 \end{array} * \begin{array}{l} \langle NH_4^+ \rangle \\ \langle CO_3^{=} \rangle \\ \langle HCO_3^- \rangle \\ \langle NH_2COO^- \rangle \\ \langle OH^- \rangle \\ \langle NH_2CONH_2 \rangle \end{array} \qquad \text{(eq. 2.2)}$$

In the above balances, the braces ({ }) denote the amounts in moles of the basic species, and the angular brackets (< >) denote the amounts in moles of the individual species at any chosen moment.

Now posing the electroneutrality condition leaves only three independent balances and hence only three gross amounts which are known variously as "the component compositions", "the reaction invariant compositions", "the gross phase compositions", etc. It can be said that the stoichiometry places constraints only on the *number of the components* and *not* on the *amounts* or the *kinds*. The components can, of course, be chosen arbitrarily. In the present case, ammonia, carbon dioxide and water are chosen as components as these are the simplest species present and are the substances from which the reaction mixture is prepared in practice. Correspondingly all other species become the derived ones.

2.3. *Characterising the systems relevant to urea technology*:

There are four binary systems, two ternary systems and one quarternary system which are relevant to urea technology.

The four binary systems are as follows.

1. The ammonia - water system.
2. The carbon dioxide - water system.
3. The ammonia - carbon dioxide system.
4. The urea - water system.

Unlike the first two systems, the last two, namely the NH_3-CO_2 and the urea-water systems, are not strictly binary in wide pressure and temperature ranges [1]. Above 100°C and at pressures above the corresponding decomposition pressures of ammonium carbamate, urea formation becomes appreciable in the NH_3-CO_2 system producing water as a by-product. The occurrence of this reaction alters the character of the phase equilibria due to changes in solubilities of NH_3 and CO_2 in the liquid phase which now includes urea and water. Consequently the NH_3-CO_2 system has to be treated as pseudo-binary above 100°C by posing the condition that urea formation does not occur. Such a treatment has its utility in describing a high pressure carbamate condenser in urea processes.

Likewise the urea-water system, which is useful for the design of evaporators and crystallizers, transforms into a ternary system at temperatures above 100°C due to urea hydrolysis.

Now coming to the quarternary system of NH_3-CO_2-H_2O-NH_2CONH_2, one can propose a similar pseudo-equilibrium by neglecting the slow reactions such as urea hydrolysis and considering only the fast ones. Such a proposal is useful in designing decomposers / strippers of urea processes. Subsequently, the design can be tuned with results obtained from a kinetic study of urea hydrolysis.

Regarding the ternary systems, one can speak of the two different systems of NH_3-CO_2-H_2O, namely, one in which the relatively slow urea formation and urea hydrolysis go to complete chemical equilibrium (i.e. equilibrium concentration of urea is present) and another in which the same reactions are hypothetically prohibited from proceeding. (i.e. no urea is present.) The equilibrium study of urea hydrolysis at low concentrations of urea (around 1-3 %) is quite important for the design of urea hydrolysers employed in effluent treatments.

In the light of the above discussion, three multicomponent systems can be considered as follows:

- The NH_3- CO_2- H_2O ternary system with the equilibrium concentration of the species urea.
- The NH_3- CO_2- H_2O - NH_2CONH_2 pseudo-quarternary system.
- The NH_3- CO_2- H_2O ternary system without the species urea.

Each of the above systems exhibits subtle differences relative to others, and, in turn, such differences are harnessed into individual applications on urea reactors, decomposers and condensers. However, these differences have not been fully appreciated in urea technology literature and, often, insufficient distinctions have been made as to the type of systems considered. Even in experimental studies [7,8,9,10,11,12], a few authors did not mention the time involved in attaining the equilibrium and, as a result, there is no way of demarcating the system they are referring to. Furthermore a number of investigators [8,9,10,13,14] studying the ternary system did not analyse the liquid phase for the presence of urea. Similarly many authors studying the quarternary system [10,11] did not clarify whether the reported urea concentration was the one they started with or the one they *analysed* after the equilibrium was attained. In fact, as mentioned earlier, it is above all the urea formation reaction with its by-product water which necessitates all these

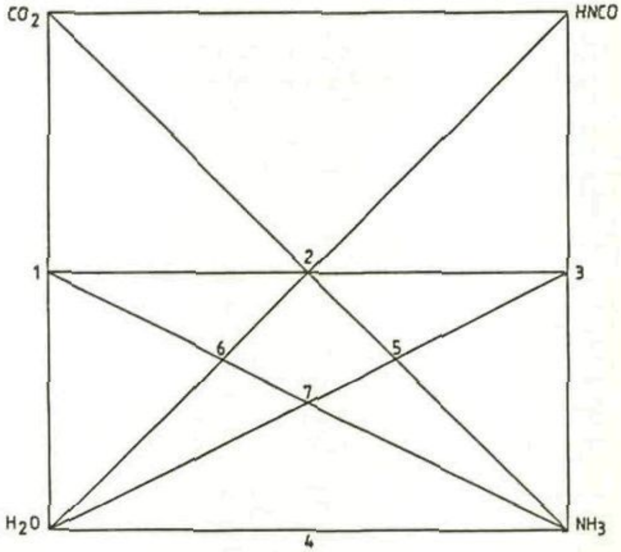

Fig. 2.1. *Composition plane of the NH_3-CO_2-H_2O-UREA system with the molecular species marked at their stoichiometric composition.*

1.H_2CO_3 2.NH_2COOH 3.NH_2CONH_2 4.NH_4OH 5.NH_4COONH_2 6.NH_4HCO_3 7.$(NH_4)_2CO_3$

distinctions and makes an adequate theoretical description all the more difficult and, interestingly, brings forth a new insight into the application of thermodynamic phase theory to reactive systems, as will be illustrated in the next chapter.

In order to visualize the possible phase equilibria to be described in the succeeding pages, a composition plane is presented in the Fig 2.1. In this plane all the molecular species are marked at their stoichiometric compositions. As decribed below, each of these species, both in its ionic and molecular form, affects the phase equilibria of the related systems through its structure, its intermolecular attraction and its ability to protonate or de-protonate.

2.4. *The molecular characteristics of water and ammonia relevant to the pure component and solution behaviour*:

First, the simpler species ammonia and water and their related cations may be considered with special reference to the ammonium ion.

1. Water and ammonia are respectively the most stable hydrides of oxygen and nitrogen. Geometrically the molecular orbitals of these two species form a slightly distorted tetrahedral structure with an O or an N atom at their respective centres. As shown in the Fig 2.2., water has two protonated orbitals extending to the two corners and two non-bonding orbitals directed to the remaining corners, while ammonia has three protonated orbitals extending to the three corners with the non-bonding orbital pointing to the remaining corner. Disregarding the non-bonding orbitals, ammonia forms a trigonal pyramidal molecule and water an angular molecule [15].

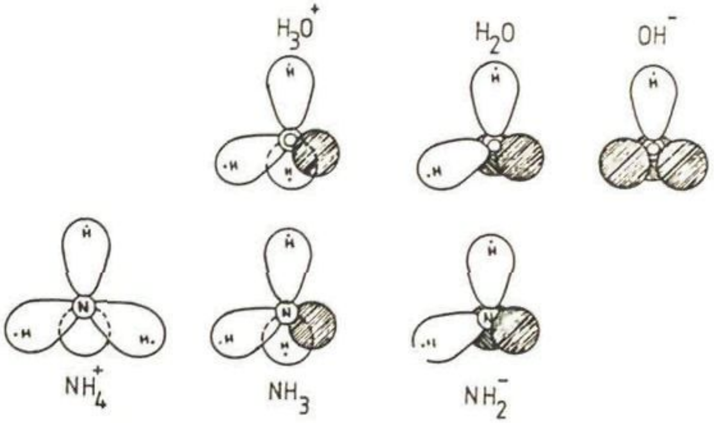

Fig. 2.2. *The molecular structure of ammonia, water, and their cations and anions. The shaded regions are the non-bonding orbitals and the non-shaded ones are the protonated orbitals. The protons are surrounded by the electron cloud. The orbital length of N-H bond does not differ much from that of the O-H bond.*

2. Both water and ammonia are able to solvate anions and cations by orienting their protonated and non-bonding orbitals. Due to the excess of protonated orbitals, NH_3 strongly interacts with anions leading to the preferential solvation of anions over cations [16]. For example if NaCl is added to a strong aqua-ammonia solution, more NH_3 molecules will be found around the chloride ions than around the sodium ions. Water molecules do not have such a preference. In fact, the nature of the anion markedly influences the solubilities in liquid ammonia [17]. Most ammonium salts with the exception of the oxyacid salts such as sulphates, sulphites, carbonates, carbamates, phosphates and arsenates, are soluble and act as acids in liquid ammonia. Some ammonium salts, such as nitrate, thiocyanate and acetate, are extremely soluble in liquid ammonia [16].

3. Both water and ammonia are capable of hydrogen bonding due to powerful attraction of the highly dense electron cloud of one molecule for a proton of a neighbouring molecule. Due to the equal numbers of the protonated and the non-bonding orbitals and also due to tetrahedral geometry, water molecules form three dimensional networks of various sizes [18]. In contrast, ammonia molecules form only chains and rings of different lengths [17,18]. Due to this relatively reduced association, ammonia is much more volatile than water. To some extent, the high critical pressure and critical temperature of water compared to ammonia can be explained by the same association effects [16,18].

4. As suggested by Bernal and Fowler [18] and later corroborated by others [19,20,21], the extraordinary proton mobility in water is due to the same extended three dimensional network of water. Similar increased mobility is not observed in liquid ammonia [16,22]. The high proton mobility in water can induce a water dimer to act as an acid-base bifunctional catalyst in several solvent mediated reactions like the hydration of CO_2. Such an active solvent catalysis exhibited by water is treated later in the section on CO_2 (section 2.7.6).

5. While polar contributions through the permanent dipole moments exceed by at least five fold the polarizability and dispersion forces of the water molecule, the relative contributions of these forces in the ammonia molecule exhibit an even balance, as shown in Table 2.1 [23]. Such a combination of forces makes ammonia a

Table 2.1. *Relative magnitudes of intermolecular forces between two identical molecules at 0^oC*

Molecule	Forces(erg.cm^6*10^{60})		
	Dipole	Induction	Dispersion
NH_3	82.6	9.77	70.5
H_2O	203.0	10.80	38.1

better solvent than water for solutes having polarisable electrons [22]. Obvious examples are the hydrocarbons.

6. The high dielectric constant of water(78) compared to that of ammonia (23) suggests that ion pairing is potentially less frequent in water [16,22].

7. At a given temperature, water is more ionised than ammonia due to the equal number of the protonated and non-bonding orbitals and the ease with which random proton migrations are possible in water. The ionic product for ammonia is 10^{-29} compared to the value of 10^{-14} for water at 25°C [24]. Based on the protonic solvent theory, water is more acidic than ammonia.

8. Protolytic equilibria in an aqeous solution and in an ammoniacal solution differ widely leading to "differentiation" and "levelling" effects [27].

For example in water, the degrees of dissociation of acetic acid and the HSO_4^- ion at equal concentrations of 0.1 M are limited and different. Such partial dissociations enable one to distinguish between these two species in terms of pH. Consequently it can be said that water "differentiates" the acetic acid and the HSO_4^- ion in terms of the protolytic equilibria.

In liquid ammonia, however, the same two solutes at the same concentration of 0.1 M are found to be completely dissociated. The ammoniacal acetic acid solution and the ammoniacal alkali bisulphate solution contain only negligible amounts of the undissociated acetic acid and undissociated HSO_4^- ion, respectively. Such behaviour implies that ammonia "levels" both the acetic acid and the HSO_4^- ion and that one can not distinguish experimentally the different acid-base behaviours of these two acids in ammoniacal solutions [24].

It is quite important in solution chemistry whether the solvent exhibits a differentiating effect or a levelling effect on solutes. In aqueous solutions, acids stronger than H_3O^+ and bases stronger than OH^-, being respectively unstable as the protonated and de-protonated species [28], are completely levelled. Similarly in the ammoniacal solutions, acids stronger than the NH_4^+ and bases stronger than the NH_2^- are completely levelled.

Consequently water has a levelling effect on strong acids (like HCl, $HClO_4$ and sulphonic acids) and strong bases (like alkali hydroxides, DEA, MEA and tetra alkyl ammonium bases), while ammonia has a levelling effect on strong acids and a differentiating effect on strong bases [24].

Differences in the acid-base behaviour of urea and urea-like solutes in these two solvents can also be understood in terms of the protolytic equilibria. For example in water, urea is a weak base while guanidine is a rather strong base and cyanamide a relatively weak acid. In liquid ammonia, however, [16,22] all these substances actually behave as acids capable of reacting with metallic amides and, in some cases, with metals themselves to form salts.

9. There are three different mechanisms through which a solute can exist in solution with water, if dissolution by chemical reaction is excluded. These mechanisms can be described as follows:

i) If the solute molecules are polar, simply structured and not unduly restrained by their molecular sizes and the energy barriers for bond rotation, then these molecules can enter into the hydrogen bonded network of water, leading to a loose but still three dimensional structure [29,30]. A prime example of such a solute is NH_3. A second example is NH_4F, the only known ionic compound having an appreciable solubility in ice [31]. Evidence for the possibility of NH_4F entering into the three dimensional network of water has accrued recently, when it was reported that NH_4F has very little influence on the radial distribution functions and the infra red spectrum of water [32,33].

ii)If the solute molecules are nonpolar, small sized and nearly spherical, then these molecules can occupy the interstices of the hydrogen bonded structure [34]. An appropriate example is methane. The tetrahedral CH_4, being incapable of forming hydrogen bonds, can easily insert itself into the interstices of the three dimensional network of water, since the size of the methane molecule is similar to the size of the water molecule. Still the solubility of methane is limited due to other reasons such as polarizability, inertness etc.

iii) The third mechanism is by dilution (i.e. by mixing with the monomer water). Species for which the above two mechanisms are precluded by their sizes, their geometries, or their potential barriers are forced to adopt this dilution mechanism. Obvious examples are the large sized iodides and carbon dioxide. The structure of CO_2 and its influence on the solubility in water are dicussed later in this chapter (section 2.7).

All the three mechanisms may be utilized simultaneously by a solute. Due to the predominant three dimensional structure, a solute molecule which preferentially utilizes the first mechanism dissolves well in water compared to solutes using the remaining ones. In the present case one can readily understand the difference in the solubility of NH_3 and CO_2 in water on the above basis.

Dissolution in liquid ammonia can also be explained through mechanisms similar to those of water. Dissolution occurs either by interfering with and enlarging the ring / chain formation or by simple dilution [18]. Examples of species which do likewise are the amides and the flourides [17].

10. Both in water and in ammonia it is possible to consider the hydrogen bonded molecules to be a separate species called the bulk species and the monomer as the dense species. In this model of water and ammonia, originally proposed by Bernal and Fowler [18] and later developed by Frank, Evans and Wen [29,30], a dynamic equilibrium is assumed to exist between the two species, here shown with water as an example.

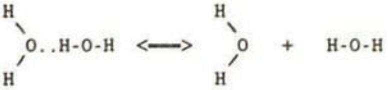

(eq. 2.3)

Species I (Bulk) Species II (Dense)

This model assumes that an increase in temperature shifts the equilibrium towards the dense species. In other words, increasing the temperature causes more hydrogen bonds to break leading to reduced dissolving capacity by the above mentioned first dissolution mechanism. Recently, it has become possible to quantify this concept of structure both by infrared and by Raman spectroscopy [35,36]. For example, in a near infrared study of water, the ratio of the differential absorbances of the bands at 1160 nm and 1240 nm was shown to be dependent on the extent of the hydrogen bonded species relative to that of the monomer species. Further, through the effect of temperature on this ratio the enthalpy of formation of the bulk species from the dense species was estimated to be about 2.45 to 2.6 kcal mol^{-1} [35]. These values are comparable to the value of 2.55 kcal mol^{-1} obtained from Raman Spectroscopic measurements [36].

11. The effect of ionic species in changing the water structure was shown originally by Bernal and Fowler [18] to be similar to the effect of temperature variation. For example, let the conversion of species I (bulk) to species II (dense) at 25°C by the addition of $NaClO_4$ be 20% resulting in a 0.5 M solution. If the same conversion is obtained by raising the temperature from 25°C to 40°C, then the effects can be said to be similar, and one can define an equivalent structural temperature shift which in this case is 15°C for a 0.5 M $NaClO_4$ solution at 25°C. Similarly one *can find out the structural temperature shift for each ion at any chosen concentration* and at 25°C.

If a salt favours the forward reaction of breaking the hydrogen bonds (i.e. eq.2.3), it is classified as structure breaking. It it does the reverse, it is called structure making. In order to appreciate these differences in the character of the various salts, the structural temperature shifts of a number of salts are presented in Table 2.2. All salts having a negative ΔT^* are classified as structure makers in water. It can be observed that these values are positive for salts like $NaClO_4$, and negative for salts like Na_2SO_4.

The equivalent structural temperature shift just defined and discussed is meaningful only when the solution is so dilute that the solute-solute interactions can be neglected. In concentrated solutions such interactions would mask the effects caused by the ion-solvent interactions on the solvent structure.

Table 2.2. *The equivalent structural temperature shift (ΔT^*) for various inorganic salts at 298 K (0.5 m concentration) [36]*

1:1 Electrolytes	ΔT^* K	2:1 and 1:2 Electrolytes	ΔT^* K
$NaPF_6$	23.0	Na_2SO_4	-1.6
$NaClO_4$	16.0	Na_2SO_3	-4.2
$NaBF_4$	14.0	$Na_2S_2O_3$	+4.8
$NaClO_3$	7.6	Na_2CO_3	-7.0
$NaNO_3$	7.4	$MgCl_2$	-2.4
$NaBrO_3$	6.8	$CaCl_2$	+4.0
NaCN	5.2	$SrCl_2$	+4.5
NaSCN	4.4	$BaCl_2$	+3.4

12. The ion-solvent interactions affect the binary phase equilibria substantially through the salting-out phenomena. For example it has been observed that the addition of $NaClO_4$ even up to a molality of 6 does not affect the activity coefficient of NH_3 in the NH_3-H_2O system, while the addition of NaCl increases the ammonia activity and the addition of LiBr decreases the same [37].

13. In what was seen as an extention of their original model for water, Frank and Wen [29] proposed a simple interpretation of the ionic hydration in dilute solutions. Since their concepts will be used often later, the essential features of their model are described below. Their model has features similar to the models proposed by Gurney [38] and Samoilov [39].

According to these models, there is a primary region, called the first cosphere, around an ionic solute in which the solvent molecules are more or less immobilized through electrostatic forces. The solvent properties in the primary cosphere can be very different from those in the bulk. An example would be the dielectric saturation of the primary cosphere. These models further propose a second cosphere (surrounding the first one) in which the organisation of water molecules is suggested to be more random than the "normal" (bulk) water. Surrounding the broken water structure of the second cosphere is third region in which the long range ionic influence is considered to prevail but not the structure breaking influence. Samoilov attributes a dynamic character for all these regions and Gurney proposes competition between these regions. Depending on the relative influences of these regions, ionic species can again be classified to be structure making or structure breaking.

Given the complexities of ionic hydration even at extreme dilutions, these models are very successful in giving a qualitatively satisfactory picture of the hydration phenomenon. Although similar models can be proposed in principle for the ammoniacal solutions, no references could be found to review such attempts.

The most interesting question regarding the phenomena of structure making and breaking with respect to the thermodynamic description of the NH_3-CO_2-H_2O system will be the effect of ammonium salts, especially the carbonate, the bicarbonate and the carbamate, on the structure of the solvent water. Unfortunately no experimental studies have been reported due to difficulties in preparing single electrolyte solutions of each of these salts in water. Consequently the possible trends can only be speculated based on the related studies of the ammonium halides, ammonium nitrate, alkali carbonates and other relevant salts in water. Leaving the anions to be discussed later in the chapter, the ammonium ion is treated in the following section.

2.5. *The interaction of the ammonium ion with water*:

1. The ammonium ion and the water molecule have almost identical masses (respectively 18.03 and 18.015) and partial molar volumes (18 ml). These species also have very similar bond angles (109.5° for NH_4^+ and 104.5° for H_2O) and interatomic distances (ranging from 10.1 to 10.3 nm) [15]. Both H_2O and the NH_4^+ ion form hydrogen bonds of almost the same strength [15].

2. In a Raman spectroscopic study of ammonium nitrate solutions at various concentrations [40], it was reported that the ammonium ion, even in concentrated solutions, did not influence either the frequency or the half width of the Raman band of the nitrate ion. This result is quite unlike that of the alkali ions, say the potassium or the sodium ion, which influenced these behaviours rather substantially at high concentrations. To phrase it anthropomorphically, the nitrate ion does not appear to perceive the change in its local environment when ammonium ions replace water molecules in concentrated solutions.

3. The apparent molar volume of ammonium chloride in aqueous solution is approximately equal to the molar volume of two moles of water, and the temperature dependences of these volumes near 35°C are also practically identical [41]. The difference between the partial molar entropy of ammonium chloride and the entropy of water is the smallest of all alkali chlorides [42]. The differential enthalpy of solution of NH_3 in water is almost unchanged by the addition of ammonium chloride up to a salt molality of 2 [43]. Viscosities of ammonium chloride solutions also show the smallest deviation (<1%) from water when compared to all other alkali chlorides [44]. Furthermore in a study of electrolyte solutions employing NMR spectroscopy it was found that ammonium chloride does not markedly affect the proton resonance of water

[45]. An infrared spectroscopic study provides additional evidence of the negligible influence of the ammonium ion on the water structure [32,33].

4. In a recent molecular dynamics study [46] on the ionic co-ordination of the NH_4^+ ion in water it was reported that, unlike the behaviour observed with other alkali cations, there is a lack of strong orientational ordering of the water molecules with respect to the NH_4^+ ion in the first co-ordination shell. To quote the same authors, "the water molecules arrange themselves in a way that resembles the hydrogen-bond network around a central water molecule, although here the oxygen atoms are all directed towards one of the NH_4^+ hydrogens". In other words, interpreting this effect in terms of the Frank and Wen model, it appears that the first cosphere structurally resembles the tertiary bulk region of the "normal" water and the influence of the structure broken second cosphere is minimal around an ammonium ion in the aqueous solution.

5. As mentioned earlier in section 2.4.9.1, there is a remarkable similarity between NH_4F crystals and ice.

The literature is replete with evidence and arguments as given above to characterize the behaviour of the NH_4 ion in water. See for example Conway [36].

On the basis of this background regarding the molecular characteristics of water, ammonia and their related ionic species, one can now look into the phase behaviour of the ammonia-water binary system.

2.6. *The ammonia-water binary system*:

This system is of interest not only to urea manufacture but also to ammonia manufacture (especially with the recent aqueous absorption-desorption techniques in the ammonia synthesis loops) and sour water stripping processes.

Dissolution of ammonia in water, as suggested earlier, is both physical and chemical at low concentrations and low temperatures. Chemical reaction is spontaneous at these conditions, since a proton from the water molecule, experiencing a higher repulsion from the effective nuclear charge of the oxygen atom, tends to migrate to the non-bonding orbital of ammonia, where it comes under the repulsion of the lower effective nuclear charge of the nitrogen atom [15].

$$NH_3 + H_2O \Longleftrightarrow NH_4^+ + OH^- \qquad \text{(eq. 2.4)}$$

A reversal of the proton migration occurs when there is an addition of energy and an increase in entropy (i.e. the randomness) of the system. Also with increasing temperature a large proportion of NH_4^+ ions hydrolyses to give free ammonia and oxonium ions.

$$NH_4^+ + H_2O \longleftrightarrow NH_3 + H_3O^+ \qquad \text{(eq. 2.5)}$$

In other words, ammonia is a weak electrolyte at high temperatures [47]. As said earlier there is an energetically favoured process of dissolution by the formation of hydrogen bonds (here indicated by a dotted line).

$$NH_3 + H_2O \longleftrightarrow NH_3 \ldots\ldots H_2O \qquad \text{(eq. 2.6)}$$

Correspondingly, many authors explained the vapour-liquid behaviour of the ammonia-water system largely on the basis of physical dissolution without any consideration of the ionization reaction [48,49,50].

Gas-liquid equilibrium behaviour of the NH_3-H_2O system has been experimentally studied by a number of researchers up to a temperature of 350°C [14,49,51,52,53,54,55,56].

As the earlier discussions in the section 2.4 suggest, the ammonia-water molecular interactions are very strong leading to a large solubility of ammonia in water.

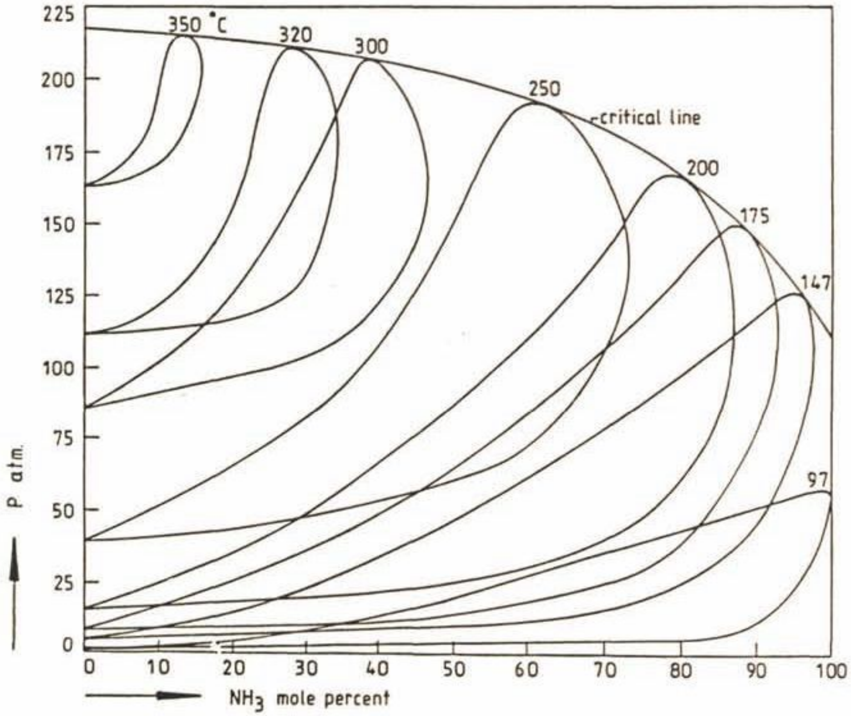

Fig.2.3. *The p-T-composition behaviour of the NH_3-H_2O system shown through a projection on the temperature scale. Various temperature cross sections are also marked together with the projection of the critical curve [56].*

This is reflected in the highly non-ideal thermodynamic behaviour of the bubble-point surface, which exhibits a strong curvature, as shown in Fig. 2.3. No unusual phenomena are observed in the critical line behaviour. The critical line starts at the critical point of ammonia and rises gradually with a moderate slope until it ends at the critical point of water. It appears that all the non-ideality of the system NH_3 - H_2O can be ascribed to the intrinsic non-idealities of the pure component behaviour with no new phenomenon arising due to mixing. However, the bubble- and dew-point surfaces have not yet been accurately determined above 20 bar and 120°C in the literature.

Unlike the previous attempts on modeling the phase equilibria of the NH_3 - H_2O system, an unconventional attempt by Edwards and Prauznitz [45] and its improvement by Won et al [50] were very successful in describing the phase behaviour up to 20 bar and to about 100°C. At higher pressures and temperatures and close to the critical conditions, the model has not been tested. A recent model proposed by Gubbins and Twu [57] based on a perturbation theory with a hard sphere reference potential is claimed to represent the binary polar systems well at these conditions. Gubbins and Twu have applied their model to polar-nonpolar systems (Xe/HCl, Xe/HBr), polar-polar systems (HCl/HBr), quadrupolar-quadrupolar systems (CO_2 / C_2H_2, CO_2/C_2H_4, CO_2/C_2H_6) and nonpolar-octopolar systems (Ar/CH_4, Kr/CH_4, Kr / CF_4). They have also applied their model to a ternary system ($CO_2/C_2H_4/$ C_2H_6). Although they suggest the applicability of their model to associating systems like ammonia-water, no attempt has so far been made to apply their model to this system.

Having discussed in detail the behaviour of NH_3 and H_2O both as pure components and in solution, one can now turn to CO_2.

2.7. *The molecular characteristics of carbon dioxide relevant to the pure component and solution behaviour*:

1. Carbon dioxide is a triatomic 16 electron molecule. As Fig. 2.4a. shows, it has a linear spine involving two bonding orbitals, two non-bonding orbitals, a bonding orbital and two non-bonding orbitals [15]. The two non-bonding orbitals at the end oxygen atoms exhibit a weekly antibonding character near the outer rim. A time averaged model of the cloud looks like a hollow hyperbolic barrel (Fig.2.4a), slightly thinned nearer to the carbon atom and bulged on both sides due to the high concentration of electronic charge adjacent to the oxygen atoms. The front of the bulge is presumed to exhibit the above-mentioned mild antibonding character [15].

2. Although eight electrons in the bonding and an equal number in the bonding are involved, the electrons in both types of bonding orbitals are pulled close to the oxygen atom due to its intrinsically high effective nuclear charge.

This phenomenon results in the reduction of nuclear shielding on the carbon atom and in turn makes the central carbon atom much more electrophilic than it usually is in other molecules, like for example the saturated hydrocarbons [15]. Also the bond lengths approach those of triple bonds with only a double bond strength [15]. All these features seem to indicate a nucleophilic attack on the central carbon atom by a reactive molecule or an ion [15]. In the present system the heightened effective nuclear charge of the central carbon atom enables CO_2 to capture species like NH_3 and H_2O containing non-bonding orbitals to form anions like HCO_3^-, CO_3^- and NH_2COO^- and also neutral molecules like NH_2COOH and NH_2CONH_2.

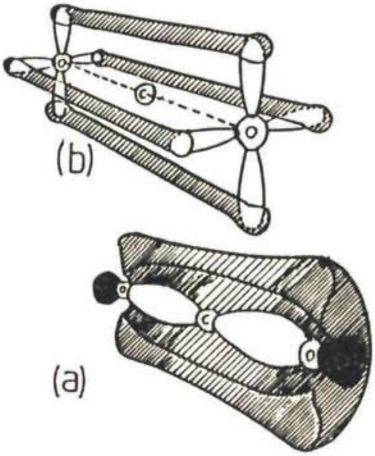

Fig. 2.4.b. *Instant location of π orbitals.*

Fig. 2.4.a. *Time averaged location of all electron clouds in CO_2. The shaded orbitals are the non-bonding orbitals, and the striped ones are the π orbitals. The σ orbitals are shown non-shaded. [15]*

3. The negative charges at the two oxygen atoms and the positive charges at the carbon atom (exhibiting a bidirectional influence) constitute a linear quadrupole affecting the physical properties of the molecule, in spite of the lack of dipole character.

4. Since the π electron barrel of one CO_2 molecule shields its own carbon atom from the intermolecular attraction of the other CO_2 molecules like a protective sleeve and also since the rim of the barrel exhibits a mild antibonding character, the CO_2 molecule lacks self association. Even the van der Waals forces are relatively small in CO_2 leading to a low critical pressure and critical temperature. Also the range of pressure and temperature in which CO_2 exists as a liquid is narrow.

5. When CO_2 is dissolved in polar solvents like water and ammonia, it acts as an ansolvo acid by acting on the dissociation equilibrium of the solvent. In other words, it increases the concentration of the solvent cations by combining with the solvent anions [58].

For example with water , the relevant reactions are:

$$2\,H_2O \quad \text{—} \quad H_3O^+ + OH^- \qquad \text{(eq. 2.7)}$$

$$CO_2 + OH^- \quad \text{—} \quad HCO_3^- \qquad \text{(eq. 2.8)}$$

Similarly with liquid ammonia, the reactions are:

$$2\,NH_3 \quad \text{—} \quad NH_4^+ + NH_2^- \qquad \text{(eq. 2.9)}$$

$$CO_2 + NH_2^- \quad \text{—} \quad NH_2COO^- \qquad \text{(eq. 2.10)}$$

Although the above two schemes look similar, there is a subtle but important difference in the way CO_2 disturbs the dissociation equilibria. This aspect can be readily noted by the discussion on the differentiating and levelling effects (given in section 2.4.8). The argument runs as follows.

Since CO_2 is less acidic, in terms of the Lewis definition of acidity, than the characteristic cation (H_3O^+) of water, it falls within the differentiating range of water (pK_a- 0 to 14). Hence there is a considerable amount of water left un-ionized subsequent to the reaction equilibria (eq.2.7 and 2.8). In the case of ammonia, CO_2, being more (Lewis) acidic than the characteristic cation (NH_4^+), is completely levelled (i.e. consumed) causing the equilibria (eq.2.9 and 2.10) to move very much towards the right; there will thus be more NH_4^+ ions and far less free NH_3, unlike the aqueous system where the formation of H_3O^+ ions is less prolific. For the same reason it is almost impossible to observe experimentally the amide ion in the ammoniacal CO_2 solution, while the OH^- ion is easily observed in the aqueous CO_2 solution.

In an effort to explain the phenomema of azeotropy in terms of dissociating compound formation, Khmara [59] suggested a probable reason for not observing azeotropy in the CO_2-H_2O system. This reason was none other than what has been so far alluded to during the discussion on differentiation and levelling; the reaction equilibria (eq. 2.7 and eq. 2.8) are strongly displaced to the left. Unlike NH_4COONH_2, which is relatively stable even above the critical point of ammonia and carbon dioxide, carbonic acid is hardly a viable species.

6. In a theoretical study of the formation of carbonic acid through the hydra*tion of CO_2, Nguyen and Ha [60] presented information which adduced to the validity* of the above mentioned mechanism (eq.2.7 and 2.8). They proposed an active catalytic role for a second water molecule in the formation of H_2CO_3.

$$CO_2 + 2H_2O \longleftrightarrow H_2CO_3 + H_2O \qquad \text{(eq. 2.11)}$$

After having established the stablity of a six membered cyclic complex (see Fig. 2.5) involving one molecule of carbon dioxide and a dimer of water, they suggested that the reaction of CO_2 with the water dimer is clearly favoured through an energy advantage over that with one water molecule. Also the activation energy calculated

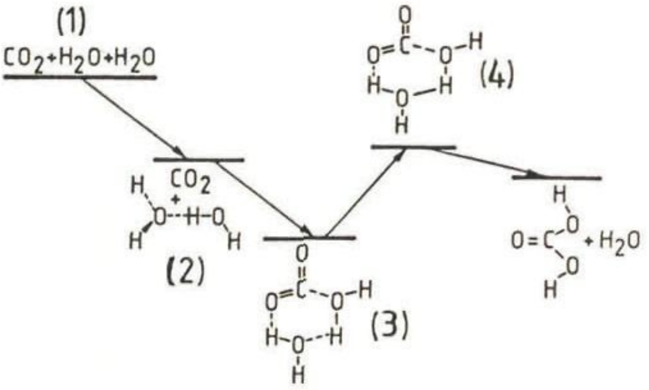

Fig.2.5. *The mechanism of carbonic acid formation proposed by Nguyen and Ha. Species (4) is a transition complex. Species (3) is the stable cyclic complex mentioned in the text.*

for the proposed mechanism closely approximates the experimental results found in the aqueous CO_2 solution. In the proposed mechanism shown in the Fig. 2.5, the water dimer is presumed to act under its ionized form ($H_3O^+.OH^-$). Thus water is transformed into an acid-base bifunctional catalyst through the formation of H_3O^+ and OH^-. Consequently the addition of OH^- to the carbon atom (now without an activation barrier) is facilitated by the simultaneous capture of the excess charges by the H_3O^+ ion.

A mechanism similar to that of Nguyen and Ha utilizing the concept of the cyclic complex had also been proposed earlier by Pocker and Bjorkquist [61] in a stopped flow study of the carbon dioxide hydration.

The importance of the six membered complex in the carbonic acid formation has its parallel in the formation of ammonium carbamate. In a very recent low temperature infrared study of solid ammonium carbamate [62] the existence of a six membered cyclic complex composed of one molecule of CO_2 and a dimer of ammonia was proposed. The suggested structure of the cyclic complex in which one ammonia molecule is bonded straight to the central carbon atom and the other ammonia molecule is hydrogen bonded to the end oxygen atom resembles very much the cyclic complex proposed by Nguyen and Ha for the aqueous system. It is quite probable, although it was not suggested in the infrared study, that a similar bifunctional active catalytic role is played by the ammonia dimer in the formation of ammonium carbamate. However, it was suggested in the same study that the proton transfer in the cyclic complex of carbon dioxide diammoniate occurs at about - 80°C to form ammonium carbamate.

The central feature of the above proposals for the cyclic complexes lies in the fact that the simultaneous proton transfer to the central carbon atom with nucleophilic bond fomation is much more favourable than the sequential process. As the reader will appreciate in the succeeding section 2.14.1, such a cyclic complex might indeed play a crucial role in the formation of ammonium carbamate even in aqueous solutions.

7. The ease with which CO_2 reacts with ammonia in the liquid phase to form carbamate through the reaction (eq.2.10) partially explains the unlikelihood of observing free CO_2 in significant amounts in a liquid phase containing ammonium carbamate and ammonia. Whether CO_2 has a poor physical solubility in the molten carbamate is difficult to establish experimentally. Purely on the theoretical grounds discussed so far, however, we can venture to suggest that this solubility has to be very small.

8. In addition to the primary reactions already mentioned (eq. 2.7, and eq. 2.8), there are also secondary reactions involving CO_2. For example with water, the carbonate formation is favoured at high pH and at high temperatures.

$$HCO_3^- + H_2O \longleftrightarrow H_3O^+ + CO_3^= \qquad \text{(eq. 2.13)}$$

Similarly with ammonia, the following two step reaction may be considered as the secondary one.

$$NH_2COOH + NH_2^- \longleftrightarrow NH_2CONH_2 + OH^- \qquad \text{(eq. 2.14)}$$

$$NH_4^+ + OH^- \longleftrightarrow NH_3 + H_2O \qquad \text{(eq 2.15)}$$

Both these schemes (eq. 2.13 and the combination of eq. 2.14 and 2.15) represent the reversals of natural spontaneous reactions, since the proton migrates from an atom having a low effective nuclear charge (C in the case of eq. 2.13 and N in the case of eq. 2.15) to an atom having a high effective nuclear charge (O in both the schemes). Hence these reactions require an addition of energy and an increase in entropy in order to proceed. Given the characteristics of the levelling and differentiating effects previously mentioned in section 2.4.8 for the solvents ammonia and water, it can be inferred that the progress of the reaction (eq. 2.13) will be much more limited than that of the reaction (eq. 2.14 and eq. 2.15)

The similarity of the above two schemes emphasizes the influence of solvent dissociation equilibria on the progress of individual reactions. Such decisive influence of the solvent enables the preparation of certain compounds in NH_3 which are otherwise impossible in water [22].

9. Faced with a restricted possibility of dissolution in water through chemical means, CO_2 does not easily enter into physical dissolution either, since its own structure prohibits it from forming hydrogen bonds with water molecules. If a protonated orbital of one water molecule aligns with the non-bonding orbital of the CO_2

molecule (Fig. 2.4a and Fig. 2.4b), the second protonated orbital of the same water molecule (which is at an angle of 104.5° with the first) comes directly under the influence of the antibonding orbital of the CO_2 molecule leading to the repulsion of the water molecule.

Likewise, as discussed earlier (section 2.4.9.iii), the possibilities for entering into the interstices of the water structure or being attracted by the van der Waals forces of the monomer water are very much limited for CO_2.

2.8. *The CO_2-H_2O system:*

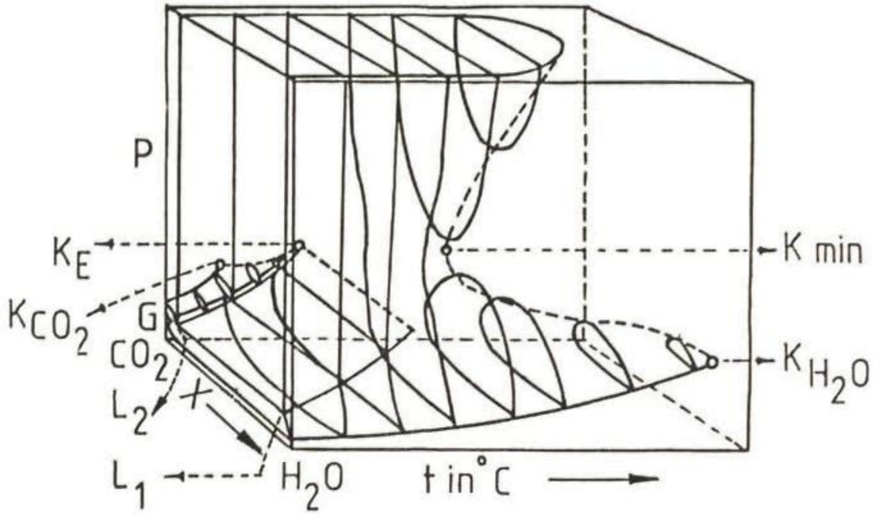

Fig. 2.6. *p-T-x diagram for the CO_2-H_2O system. K_E denotes the lower critical endpoint and K_{min} -the minimum critical point. L_1 and L_2 are the liquid phases. [69]*

Much of the unusual phase behaviour of the CO_2-H_2O system has been observed in geochemical studies [63,64,65,66,67,68]. The steep bubble- and dew-point surfaces are widely separated at temperatures below 200°C and are near to pure component p-T planes even at thousands of atmospheres. Below 250°C, the gas phase contains little water even at high pressures ($p>1000$ bar). The behaviour of the critical line with two branches is unusual. One branch starting at the critical point of CO_2 ends at a point called the lower critical end point (31.5°C, 74 bar, 99.95% CO_2). The second branch beginning at the critical point of water (T= 347°C), as shown in Fig. 2.6, first falls gradually to a minimum critical point around (266°C, 2450 bar, 41.5% CO_2), and later reverses direction heading for high temperatures and pressures. Between 40°C and 265°C no critical behaviour is observed. Above 266°C fluid immiscibility occurs. There is also the formation of an addition compound $CO_2.6H_2O$ [69]. The reader is refered to Gmelin [70] for further details on the CO_2-H_2O system.

Describing the CO_2-H_2O system quantitatively through the use of the classical Krichevsky-Illinskaya equation seems to work reliably up to about 300°C as long as the mole fraction of CO_2 does not exceed 0.1 [66,71]. Beyond that concentration, the unreliability of the experimental data published for temperatures from 50°C to 200°C [66] is too poor to attempt a model.

A number of features observed in the CO_2-H_2O system have their analogues in the system NH_3-CO_2 which is decribed in the next section.

2.9. *The NH_3-CO_2 system*:

The NH_3-CO_2 system is of fundamental importance to urea synthesis. It remains purely binary until about 100°C. Thereafter, it can be treated as pseudo-binary from 100°C to perhaps about 160°C, if the slight formation of urea is neglected. Beyond 160°C, the pseudo-binary treatment is quite unrealistic. The utility of the pseudo-binary treatment is related to two facts, namely:

i. the residence time in the urea process high pressure condenser is short enough to warrant the neglect of urea formation, and

ii. the inlet gases of the high pressure condenser contain very little water (usually about 4 to 6 mole%), and hence the phase equilibrium behaviour is largely determined by the binary system NH_3-CO_2.

Over and above the practical utility, the NH_3-CO_2 system is interesting also from a scientific viewpoint due to a number of observed or inferred phase phenomema [1], such as a maximal temperature azeotrope, liquid-liquid immiscibility in the CO_2-lean region (relative to the stoichiometric composition of ammonium carbamate), and a lower critical end point in the CO_2-rich region.

In spite of the importance of the system NH_3-CO_2, realized as early as the 1930's, the amount of published experimental data is seriously inadequate. For example, the density of solid ammonium carbamate, whose value is needed at least at one temperature for any meaningful calculation of the S-G equilibria of the NH_3-CO_2 system at high pressures and temperatures, was not known until recently through a crystallographic study [72]. Similarly in the region of liquid-liquid immiscibility the number and the quality of tie-line data [3] are, respectively, too few and too poor to be of any possible use in application. In what follows the available literature data are used to describe qualitatively the binary / pseudo-binary system of NH_3-CO_2; also these results are presented in Fig.2.7.

The central aspect of the NH_3-CO_2 system is, of course, the formation of ammonium carbamate, a dissociating compound. Solid ammonium carbamate is hydrogen bonded in all three directions. The hydrogen atoms of each NH_4^+ are hydrogen bonded to the oxygen atoms of four separate carbamate ions, and each carbamate oxygen is bonded to two different NH_4^+ ions. There is also a hydrogen bond between the centrosymmetric pairs of carbamate ions similar to that of primary amide structures. Curiously, one of the hydrogen atoms of the carbamate ion is not involved in hydrogen bonds [72]. Further, the ease of dissociation of solid NH_4COONH_2 appears to be due to low potential barrier for a proton transfer from the ammonium ion to the carbamate ion [73].

Starting the description of the p-T-x space model from 20°C as illustrated in Fig. 2.7.1, the p-x cross section is found to contain a 'shallow trough' representing the solid-vapour equilibria and two envelopes at both corners representing the vapour-liquid equilibria. The minimum of the trough corresponds to the composition of ammonium carbamate and its sublimation pressure.(A quantitative description of the S-G equilibria is presented in appendix A.) There are two S-L-G equilibria, one occurring at a low pressure in the ammonia-rich region (relative to ammonium carbamate) and the other at a high pressure in the CO_2-rich region. Similar p-x cross sections (Fig. 2.7.2) can be constructed until the critical temperature of CO_2 (31.06°C) is reached. Crossing the critical temperature of CO_2, the CO_2-side vapour-liquid envelope starts to recede inwards until it becomes a lower critical end point, (which is estimated to occur at 32°C and 74 bar) (Fig. 2.7.3).

Further temperature increase changes the area demarcation little until about 116°C (Fig. 2.7.4, Fig. 2.7.5 and Fig. 2.7.6). At this temperature liquid-liquid immiscibility begins with the occurrence of a four phase equilibrium L_1-L_2-S-G (Fig. 2.7.7). This quadruple point is estimated to occur at 80 bar and 116°C with the mole % of NH_3 of the individual phases being: G-100%; L_1- >98%; L_2- approx.78%; S-66.667%. Further increase up to the ammonia critical temperature results in the growth of the L_1 region (Fig. 2.7.8). On passing the critical temperature of ammonia (132°C), the NH_3 side vapour-liquid envelope starts receeding inwards (Fig. 2.7.9). At about 133°C the liquid immiscibility (L_1-L_2 equilibria) transforms into gas-liquid equilibria (Fig. 2.7.10).

At temperatures higher than 133°C, the enclosed L_2 region widens, and the critical solution line of the two liquid phases gradually transforms into a gas-liquid critical line. Just before 147°C another gas-liquid critical line starts in the CO_2 rich region (Fig. 2.7.11). At 147°C the azeotropic line starts (Fig. 2.7.12). Further increase brings out two gas-liquid envelopes on both sides of the azeotropic point and, in quick succession, the maximum sublimation point and the minimum melting point. The maximum sublimation point, often incorrectly referred to as the melting point, has been measured to be around 153-156°C and 88 bar [74]. Also, in a thermographic analysis of urea synthesis, Kucheryavyi et al [75] referred to the "melting point" of ammonium carbamate as 155°C and 75 atm. Unlike the maximum sublimation

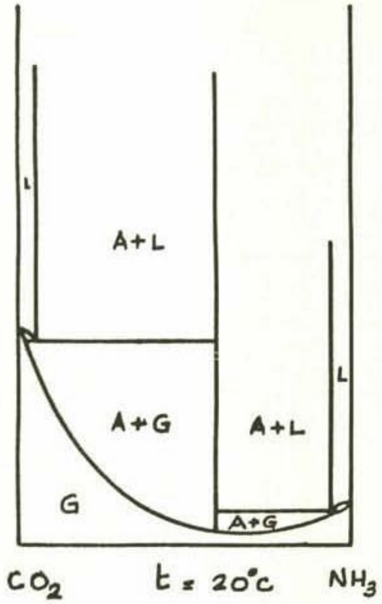

Fig. 2.7.1

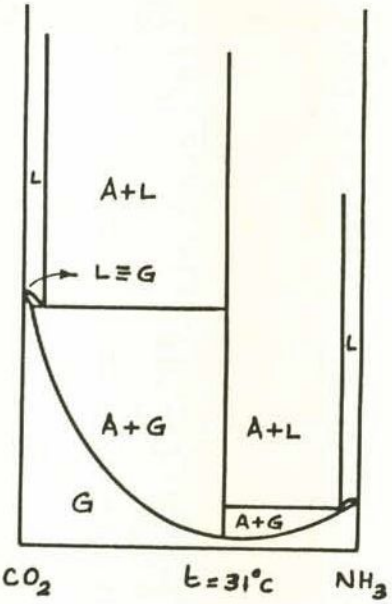

Fig. 2.7.2

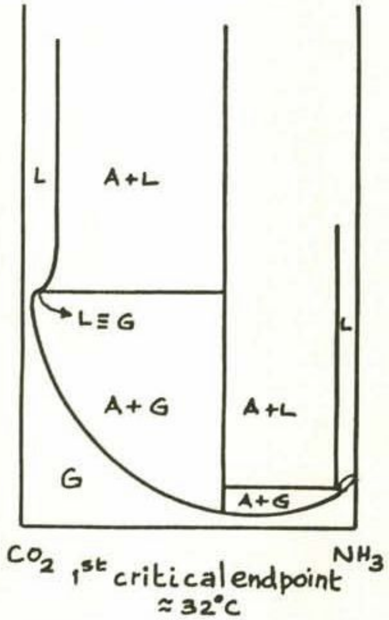

Fig. 2.7.3

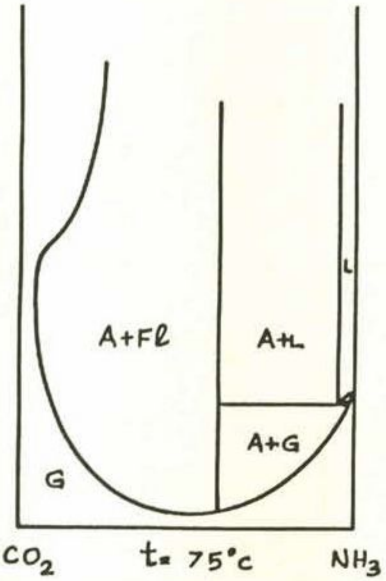

Fig. 2.7.4

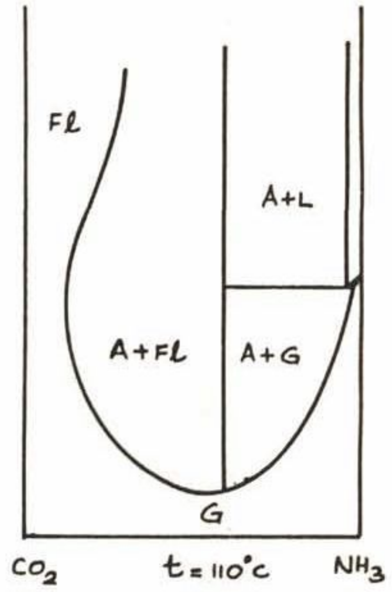

Fig. 2.7.5

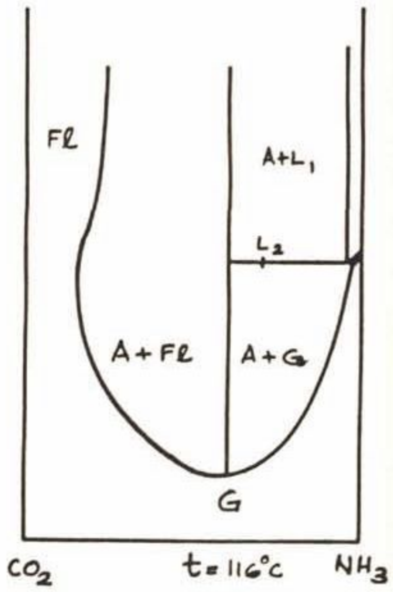

Fig. 2.7.6

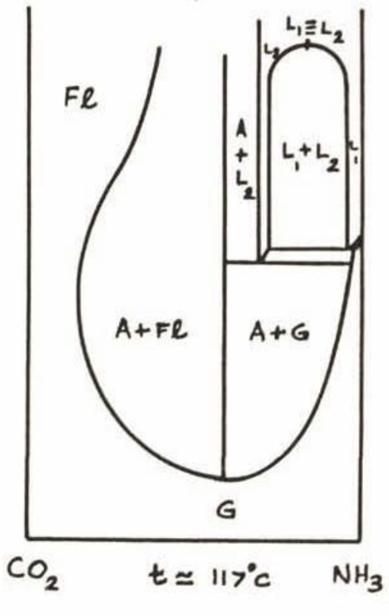

Fig. 2.7.7

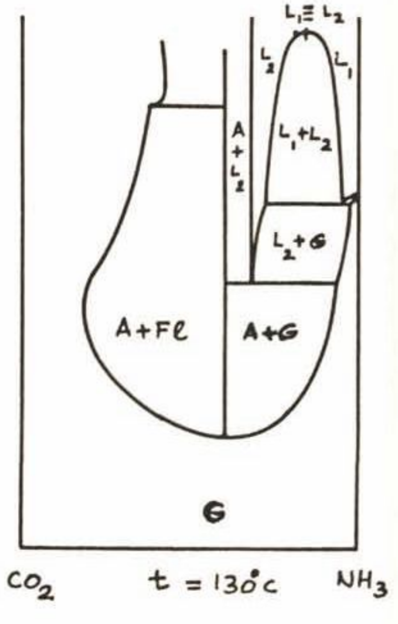

Fig. 2.7.8

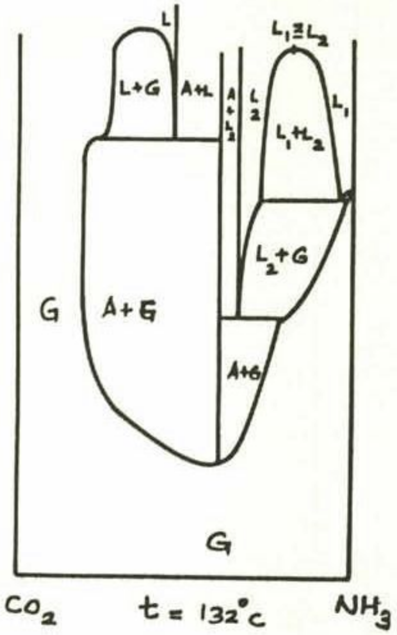

Fig. 2.7.9

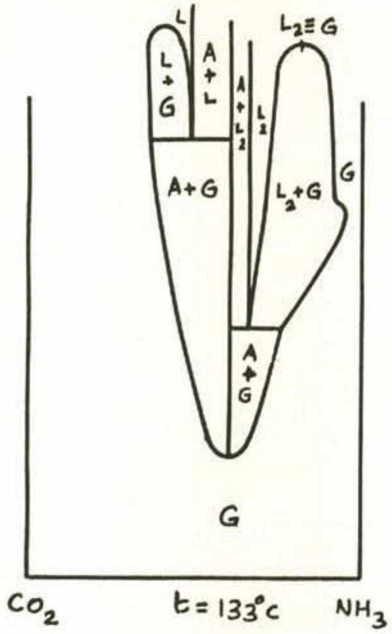

Fig. 2.7.10

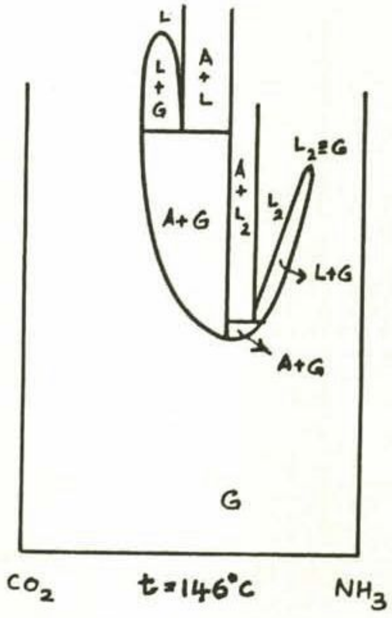

Fig. 2.7.11

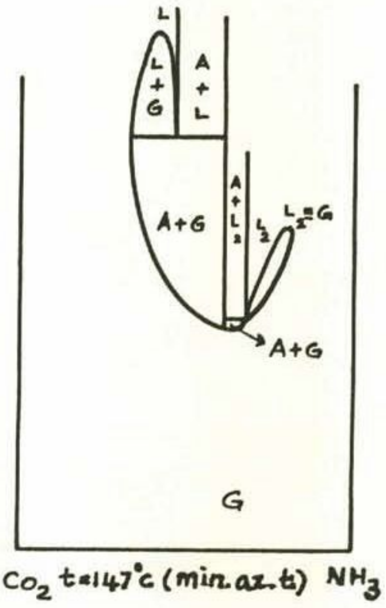

Fig. 2.7.12

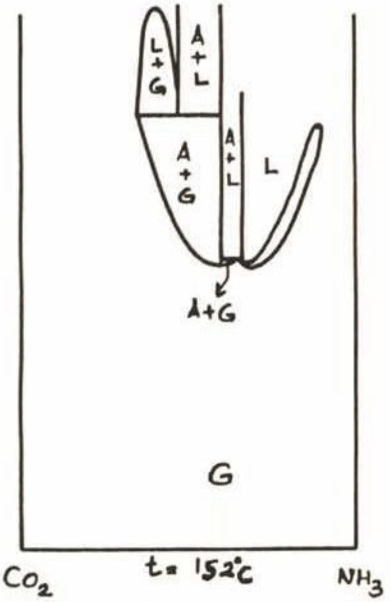

Fig. 2.7.13

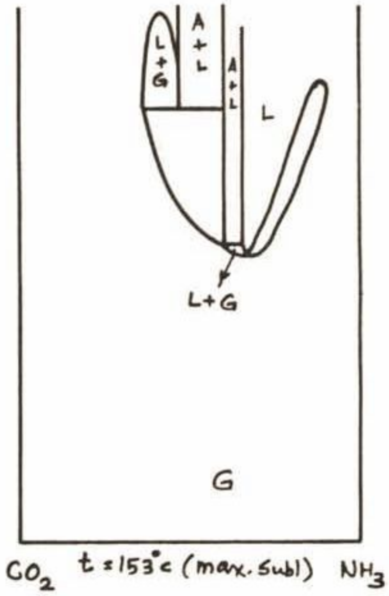

Fig. 2.7.14

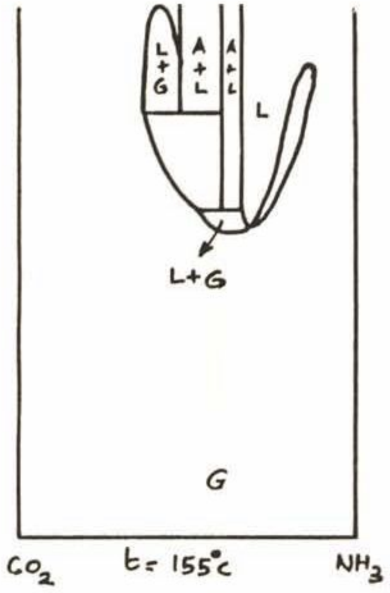

Fig. 2.7.15

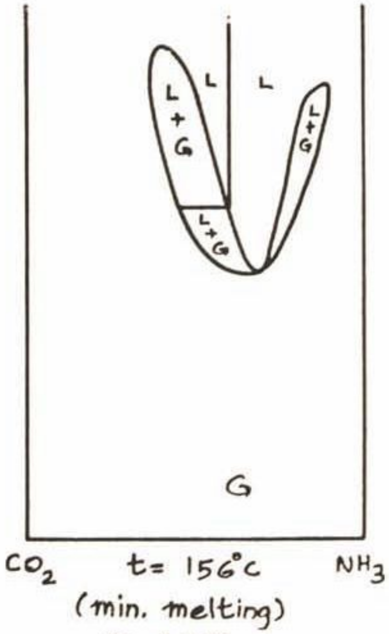

Fig. 2.7.16

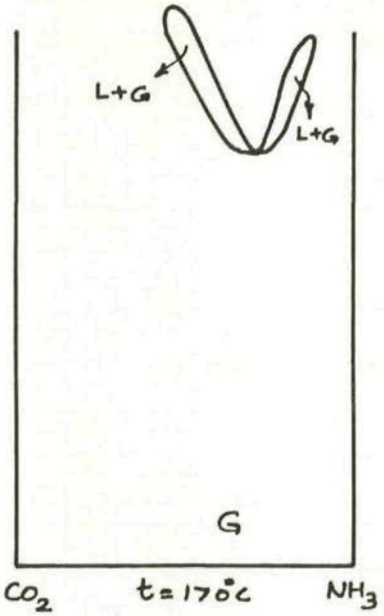

Fig. 2.7.17

point, which is the maximum temperature at which the gas and solid can coexist in the absence of liquid, the minimum melting point (i.e. the minimum temperature at which the solid and liquid can coexist in the absence of gas) is unknown and perhaps does not exist. Based on tentative grounds, Lemkowitz et al [1] arbitrarily assigned the point to occur at 155°C and 111.5 bar. Crossing the minimum melting point, there are exclusive vapour-liquid envelopes on both sides of the azeotropic point. These envelopes recede eventually into a critical end point above which only a fluid exists (Fig. 2.7.13, Fig. 2.7.14, Fig. 2.7.15, Fig. 2.7.16 and Fig. 2.7.17).

Zernike [69] states that a minimum azeotrope persisting up to the critical region is rare. The NH_3-CO_2 system appears to exhibit such rare behaviour.

The above explanation of the phase diagrams is, perhaps, too brief for readers not familiar with the phase theory. A detailed explanation of the same system from a p-T cross section viewpoint is presented by Lemkowitz et al [1]. The most important phase behaviour for the urea technology is the occurrence of azeotropy. As will be explained in the succeeding chapter, this behaviour in the binary system induces two top-ridge curves, one in the bubble-point surface and another in the dew-point surface of the NH_3-CO_2-H_2O ternary system (in which the species urea does not exist).

The operation of a high pressure condenser in the stripping processes around the top-ridge curves results in condensation at the highest possible temperature for a given pressure, leading to a substantial energy recovery. Also the condensation can be achieved with a minimum surface area (i.e. mimimal equipment size) in these processes, since it occurs at conditions close to the binary azeotrope and practically without diffusion limitations (i.e. analogous to pure component condensation). In fact, one of the factors which effectively clinched the commercial success of the stripping processes in the early seventies was this near-azeotropic condensation. It was a highly imaginative application of the principles of phase equilibria to a process design.

After having dealt at length with the behaviour of the basic species NH_3, CO_2 and H_2O, one can now turn to the larger species like urea and the anions.

2.10. *The molecular characteristics of urea and their relevance to the pure component and solution behaviour*:

1. The urea molecule is characterized by its planar structure with its lone C atom at the centre and two NH_2 groups and an O atom situated on the vertices of an almost equilateral triangle. The N-C-O and N-C-N bond angles are approximately 120°. The C-N bond lengths are shorter than the single bond lengths, and the H-N-H bond angles are approximately 104.5° [76,77,78]. See Fig.2.8.

Solid urea has four hydrogen bonds per molecule. The lone pair orbitals of the oxygen atom are the acceptor sites, and each amide group acts as a donor group. Just like the carbamate ion, one of the hydrogen atoms in the amide group does not appear to take part in hydrogen bonding [79,80].

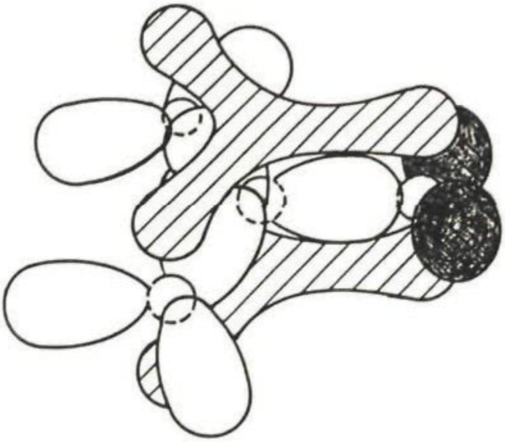

Fig.2.8.*Structural representation of an urea molecule. Shaded areas denote the nonbonding orbitals and striped areas denote* π *orbitals.*

2. The polar character of the urea molecule is caused by the presence of negatively charged non-bonding orbitals at the oxygen atom and the predominance of the positive charge at the protonated orbitals of the N atoms.

3. There is a specific difference in the behaviour of urea in aqueous and ammoniacal solutions. Urea acts as a proton acceptor in water unlike in ammonia, where it donates protons and form salts with strong bases like the alkalis [22].

4. Urea is one of the few substances which increases the dielectric constant of water on dissolution [81]. Such an increase reduces the energy required to dissolve an ionic solute in urea-water solution relative to that required in pure water. Consequently the solubilities of many ionic solutes excepting a few are higher in urea-water solutions than in pure water. For example, Bower and Robinson [82] report of the salting-in effect of NaCl at low and high urea concentrations and the contrary salting-out effect at moderate urea concentrations in the system NaCl-H_2O.

5. The effect of urea on the solubility of CO_2 in water at low temperature was studied by Kiss et al [83] in the early twenties and their data are plotted in Fig.2.9. From these data, it is difficult to say whether the solubility of CO_2 in water at high temperature is increased or decreased by adding urea.

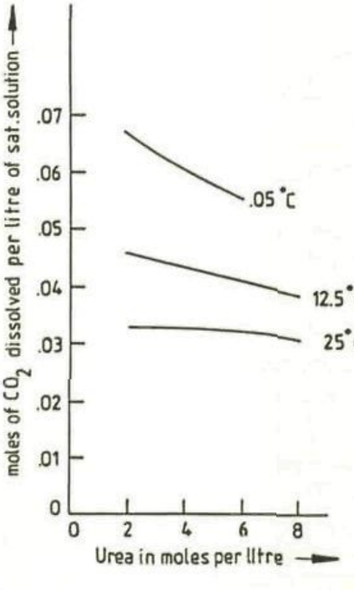

Fig. 2.9. *The effect of urea on the solubility of CO_2 in water [83]*

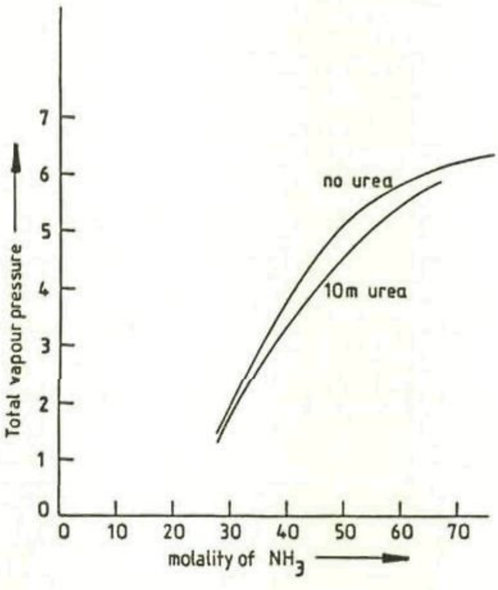

Fig. 2.10. *The effect of urea on the solubility of NH_3 in water. [84]*

6. The effect of urea on the solubility of NH_3 in water was studied by Worthington et al [84], again at low temperatures. Their recalculated results are presented in the Fig.2.10. It is notable that the presence of urea increases the solubility of ammonia in water and hence a reduction of vapour pressure. The effect of urea on aqueous NH_3-CO_2 mixtures was also observed to be similar [85].

7. In spite of the capability of the urea molecule to form hydrogen bonds in aqueous solution, both NMR and spectroscopic evidence indicate a lack of self association on dissolution [86]. Still self-association has often been invoked in the literature to explain the behaviour of urea in solution [87,88,89].

8. Divergent opinions exist in explaining the urea-water interactions. Some investigators [90,91,92] claim that urea can enter into the three dimensional network of water, while others [34,93] claim that the geometry of the urea molecule precludes it from entering into the same network.

Investigators who claim that urea is like the monomer water in its interactions with other water molecules cite a number of facts to support their claim. Similarity of the standard heat of solution of urea in water (3.5 kcal /mole) to the heat of fusion of urea (3.6 kcal/mole) [1] and the close agreement between the partial molar heat capacity of urea at infinite dilution and that of the solid urea [90] are just two examples of such evidence.

In terms of the structural geometry, an arbitrary water molecule can be said to interact with its neighbours through its two orbital pairs, namely:

i) the positively charged pair of the protonated orbitals, and
ii) the negatively charged pair of the non-bonding orbitals.

Likewise, an arbitrary urea molecule interacts with its neighbours through its two positive pairs of the protonated orbitals and one negative pair of the non-bonding orbital. Hence, given the fact that one of the hydrogen atoms of the amide groups in urea molecule does not form a hydrogen bond (as mentioned in point no.1 above), it is conceivable that the non-ideality of the urea solution is minimal, as it really does, due to similar orbital pair angles (for e.g., around 118^o for both urea and water [94,95,99]), intramolecular bond lengths (namely, N-H bond length in urea is 0.1 nm [94] and that of O-H in water is 0.096 nm [95,96]), and comparable attractive or repulsive forces [91,92].

In an effort to discern between the longstanding and differing opinions raised in the literature, two independent theoretical investigations (the so-called "computer experiments") [91,92] on the hydration of urea in an infinitely dilute solution were recently carried out, and the results are quite revealing.

Tanaka et al [91] have shown that the original water structure is changed only upto the second hydration shell near a urea molecule in an infinitely dilute solution. The urea-water interactions are claimed to be short ranged and short lived. According to their calculations, urea enters the water structure without appreciable distortion. The coordination number of water molecules around an urea molecule at a *distance of 40 nm is said to be the same as that in pure water. Also the water* molecules orient themselves separately to the *cis*-H of the amide group and the carbonyl lone-pair of the urea molecule. One of the hydrogen atoms of the amide group, namely the *trans*-H, does not take part in the hydrogen bonding. This behaviour in the urea solution is remarkably similar to that of solid urea, as given in point 1 above. Regarding the endothermic heat of mixing, Tanaka et al suggest the main cause to be the breaking of urea-urea hydrogen bonds. This is contrary to Frank and Franks [34], who attributes it to the change in water structure of the second cosphere.

Kuharski and Rossky [92] have adduced additional aruguments to these findings. They suggested that the average binding energy (i.e. the sum of all interaction energies attributed to one water molecule with all other water molecules in the vicinity) and the binding energy distribution of water molecules are the same in the primary solvation shell and the bulk region. Also the average number of hydrogen bonds formed by the water molecules in both the shell and the bulk region are deduced to be equal.

Such behaviour of urea appears to be similar to that of the ammonium ion; i.e., the first cosphere (or the primary solvation shell) and the bulk solvent are energetically similar, and the influence of the second cosphere is small.

2.11. *The urea-water system*:

The p-x behaviour of the urea-water system up to 80°C was investigated by Perman [97], while the vapour pressure of the saturated solution was studied by Kucheryavyi et al [98]. The system cannot be considered as binary when hydrolysis occurs at high temperatures and high water concentrations, and should be treated as a ternary with a *material balance constraint. However, the equilibrium studies on urea hydrolysis* [97,98] are very inadequate, in spite of their importance to the design of evaporators and crystallizers.

The system at low temperature is nearly ideal and the vapour pressure curve (i.e. the bubble-point behaviour) is regular (Fig. 2.11). A similar behaviour also occurs in the ternary NH_3-CO_2-H_2O system (with equilibrium concentration of urea and no excess NH_3 or CO_2) even at high temperatures without any modification, as observed by Lemkowitz et al [1].

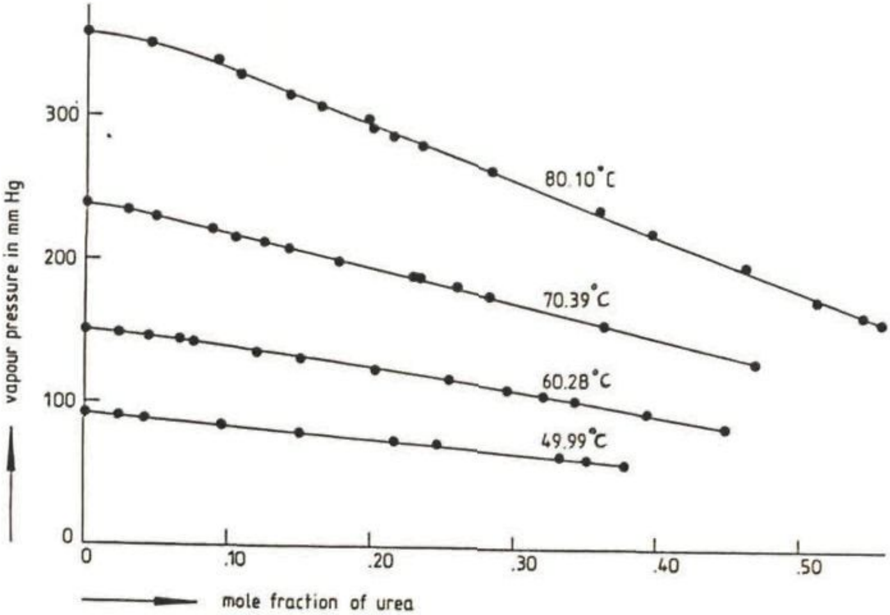

Fig. 2.11. *The p-x behaviour of the urea-water system [97].*

Essentially, two models have been proposed to explain the vapour-liquid behaviour and other thermodynamic properties of the urea-water system, namely:

i) the urea association model [87,88,89], and

ii) the water structure breaking model [34].

The urea association model considers the urea molecules to be associated (i.e. by forming dimers, trimers, etc.) and water to be essentially unassociated. It fits the experimental osmotic coefficients impressively well, in spite of the unrealistic assumption of the lack of water structure. However, the model predictions of the heat of solution values [34] are not yet satisfactory.

The water structure breaking model, also known as flickering cluster model, is based on the fact that, although the urea-water interactions are similar to water-water interactions, urea is precluded from entering the long range network of water by its incompatible geometry. Instead, urea is said to perturb the equilibrium between the structured and the unstructured water (i.e. the bulk and the dense species; see section 2.4.10). This model explains satisfactorily the qualitative behaviour of both the phase equilibria and the enthalpy aspects, although quantitatively there is much to be desired.

On the basis of the molecular dynamics calculations, the validity of the structure breaking model seems to be doubtful; yet, in their original studies, Frank and Franks applied their model to a 7 M urea solution and strongly argued the suitability of their model to the urea-water system. In a persuasive follow-up of the Frank and Franks model and in an application to describe the heat of solution of urea-like solutes, Barone et al [93] had this to say: "We believe that the excess thermodynamic properties of aqueous solutions of urea-like solutes are determined mainly by the rearrangement of water molecules. In other words, the processes in solution involve solute-solvent and solvent-solvent interactions rather than the solute-solute and solute-solvent interactions."

Thus, the interpretations regarding urea-water solutions still remain inconclusive. Perhaps the knots will be untied in the future and this long held controversy will be solved.

2.12. *The urea-ammonia system:*

The urea-ammonia system has been studied by Scholl and Davis [99], Jänecke [3] and Lemkowitz et al [1]. At high ammonia concentrations the system is quite stable. Irreversible chemical reactions leading to the formation of biuret, triuret, cyanuric acid etc. complicate the phase behaviour only at high temperatures and at high urea concentrations.

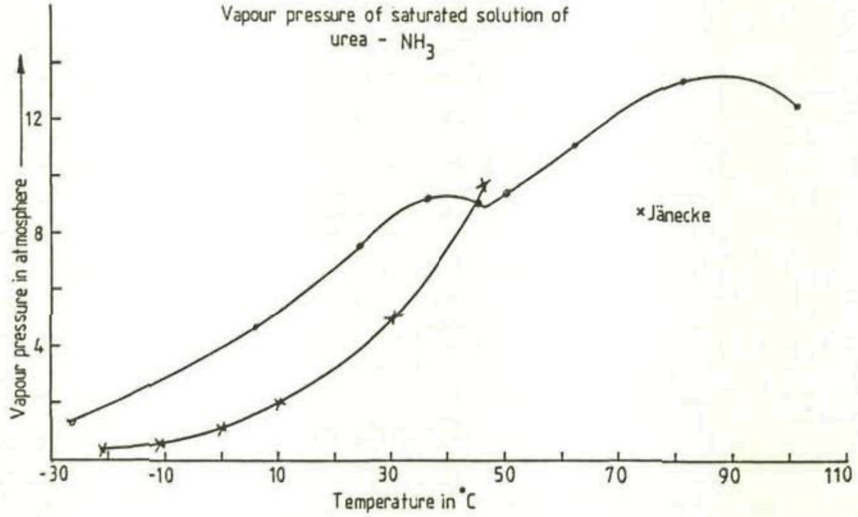

Fig.2.12.*Vapour pressure of saturated solution of Urea-NH_3.*
The curve with the cross marked points is due to Jänecke [3].

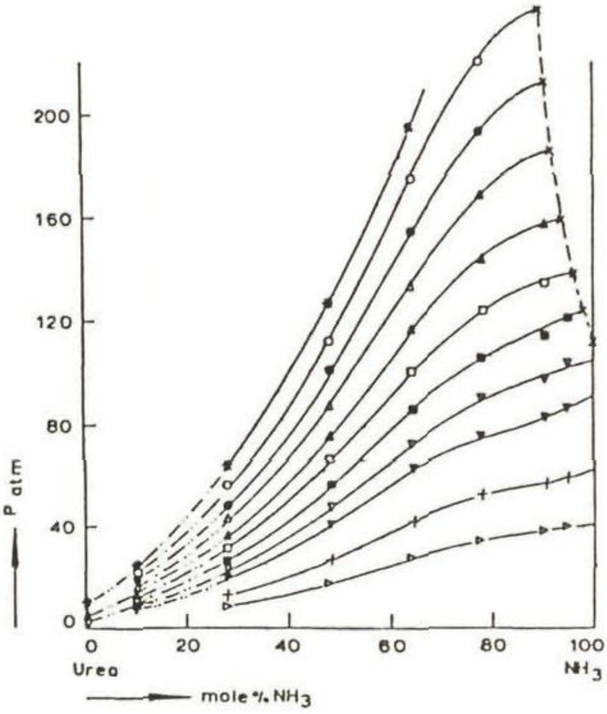

Fig.2.13.*The p-x behaviour of the ammonia-urea system.* ▷ , + , ▼ , ▽ , ■ , □ , ▲ , △ , ● , ○ , *and* ★ *refer to the bubble-points at temperatures, repectively, 80, 110, 120, 130, 140, 150, 160, 170, 180, 190, and 200° C. x - a critical point. [1]*

The equilibrium behaviour of the ammonia-urea system is quite analogous to that of the urea-water system. As noted earlier, the NH_3 molecule has no charged pairs. There is a single non-bonding orbital and a cluster of three protonated orbitals. The kind of interaction which an NH_3 molecule will experience with another NH_3 molecule may appear to be different from the interaction which it will experience with an urea molecule. But, given the tendency of NH_3 molecules to form hydrogen bonded chains and rings and the fact that one hydrogen atom in the urea NH_2 group does not take part in hydrogen bonding, it is possible that urea can form hydrogen bonds through utilization of just one acceptor site and one donor site. Hence it is not surprising that urea is ammonophilic. Such ammonophilicity is illustrated through the formation of an addition compound ($NH_2CONH_2.1NH_3$). The same compound exerts an appreciable influence on the saturation vapour pressure of the ammoniacal urea solutions, as seen in Fig. 2.12.

The similarity of the ammonia-urea and the ammonia-water systems in their phase behaviour was observed by Lemkowitz [1]. As can be seen in Fig. 2.13, the bubble-point behaviour and the critical line are regular. At high NH_3 concentrations in the liquid phase the vapour phase consists of almost pure NH_3. It is considered probable that urea can dissolve in supercritical NH_3 [1].

2.13. *The carbon dioxide-urea system*:

Phase equilibrium measurements of this system are extremely difficult and highly non-reproducible at temperatures above the melting point of urea (132.7°C) due to the rapid reaction of urea to form polymerisation products. The evolution of ammonia as a by-product complicates the measurements further by forming ammonium carbamate with the carbon dioxide present. The near equilibrium bubble-point measurements for 10.6 mole % CO_2 mixture are presented by Lemkowitz et al [1]. Through these measurements and due to similarity of urea and water in their orbital interactions with a third molecule it is possible that the CO_2-urea system is similar to the CO_2-H_2O system.

Whether the unusual behaviour of a critical line with lower critical end-points (as observed in the CO_2-H_2O and CO_2-NH_3 binary systems) and liquid-liquid immiscibility can also be expected to occur in the CO_2-urea system is a moot point over which one can only speculate.

After having discussed the binary equilibria and the relevant molecular characteristics of the simple species like ammonia, carbon dioxide, water, ammonium ion and urea, there is still one other aspect yet to be discussed, namely the molecular characteristics of the anions and species similar to urea.

2.14. *The molecular characteristics of the urea-like species and their relevance to the solution behaviour*:

Excluding the OH^- ion, whose structure resembles the species H_2O, NH_3, H_3O^+ and NH_4^+, there are three anionic species, namely the carbamate, bicarbonate and carbonate ions bearing a close resemblance to urea. Additionally there is a neutral molecule, carbamic acid (NH_2COOH), which is considered to be a major intermediate in *urea synthesis [100,101]. See Fig. 1.14.*

1. Carbamic acid, one of the simplest amino acids and also an amide analogue of carbonic acid, has never been isolated in the pure form, although a number of its salts are known. At 25°C its dissociation constant has been estimated to be around 10^{-9} [102]. Also it is suggested that it cannot exist as a zwitterion unlike other amino acids [73,103,104]. At high temperature, the formation of isocyanic acid (HNCO) by the dehydration of carbamic acid is quite possible, and, in fact, in one of the mechanisms proposed for the urea synthesis, such a dehydration step is considered to be important [100].

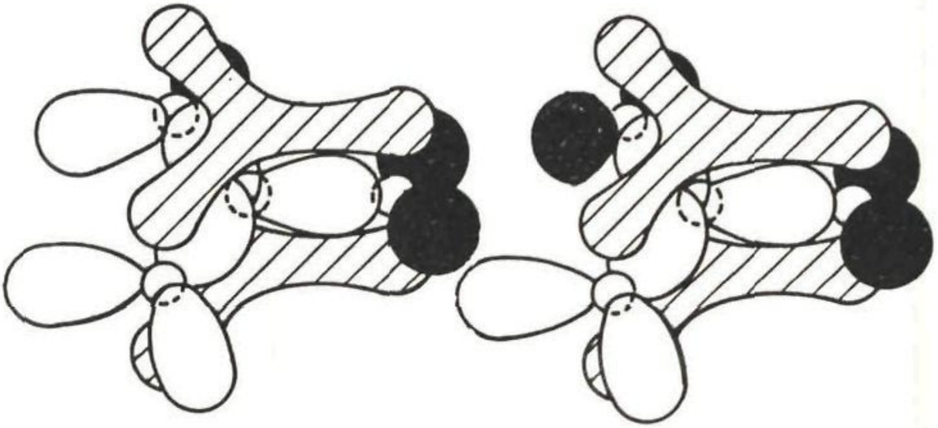

a. NH_2COOH *b.* NH_2COO^-

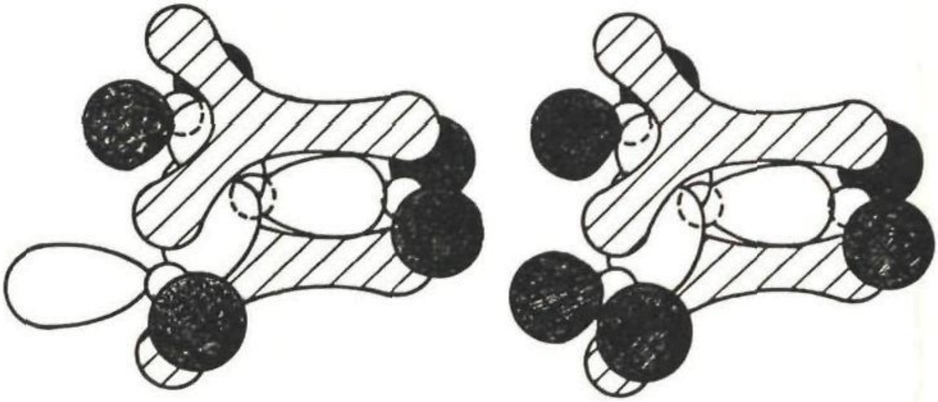

c. HCO_3^- *d.* $CO_3^=$

Fig. 2.14. *Molecular representation of urea-like species.*

The existence of carbamic acid in the NH_3-CO_2-H_2O solution has often been speculated [100,101], although no specific spectroscopic evidence has yet been found. However, Marion and Dutt [105] have presented arguments based on their calculations suggesting a plausible existence of the ion-pair $NH_4.HCO_3^o$. Such an ion-pair would, of course, be thermodynamically identical to a hydrated carbamic acid or to another ion-pair, oxonium carbamate ($H_3O^+.NH_2COO^-$). Similarly the ammonium carbonate ion-pair can be viewed as the ammonium carbamate monohydrate. In spite of these theoretical possibilities, however, the extent of ion pairing in the NH_3-CO_2-H_2O solution has not yet been experimentally investigated.

Additional support for the probable existence of carbamate in more than one form was found in a recent Laser Raman spectroscopic study on the NH_3-CO_2-H_2O system by van Eck [106]. This study was concerned with the *in situ* analysis of the species composition in a transparent high pressure equilibrium cell. On fitting the observed bands with Gauss/ Lorentian symmetrical peaks at the known fraquencies of carbamate [107], bicarbonate [108] and carbonate [109], it was found that the carbamate band was unsymmetrical, and at least two peaks were necessary to fit the observed band. The same behaviour, but to a much lesser extent, was seen with a solution of ammonium carbamate in formamide. The anomalous behaviour of the carbamate in the aqueous system persisted even at a pH of 14, and could not be explained by assuming conversion of carbamate to bicarbonate or carbonate. Van Eck suggested the possibility of a dynamic equilibrium, similar to the ones proposed for other simple amino acids [28], between the protonated and non-protonated species, as given below.

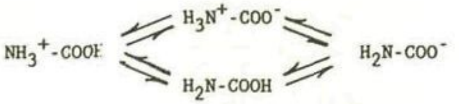

$$NH_3^+\text{-COOH} \begin{array}{c} \rightleftharpoons H_3N^+\text{-COO}^- \rightleftharpoons \\ \rightleftharpoons H_2N\text{-COOH} \rightleftharpoons \end{array} H_2N\text{-COO}^-$$

(eq. 2.16)

It is to be remarked, however, that the suggestion of the amino acid type equilibrium and especially the zwitterionic equilibrium is at variance with the conclusions of at least three related studies [73,103,104]. The fully protonated form NH_3^+COOH, if it exists, has to be short-lived in view of the potential barriers to form such species. In fact van Eck had discounted the possibility of observing this species. Among the remaining species, the carbamic acid is already stressed. The second most likely candidate to explain the unsymmetrical carbamate peak in the Laser Raman spectroscopic study would be the cyclic dimer of the carbamate ion, namely the stable dimer observed in the crystallographic study of NH_4COONH_2. (see section 2.9 and 2.14.3 below.)

2. The saturation of ionic solutions leading to the precipitation of solids occurs when the solvent molecules become incapable of blanketing the interionic forces. In the case of the ternary system to be considered in the next chapter, a number of solids are known to precipitate under varying conditions, namely ammonium bicarbonate, ammonium carbonate monohydrate, ammonium carbamate, a double salt of bicarbonate and carbonate monohydrate ($2NH_4HCO_3.(NH_4)_2CO_3.H_2O$) and another double salt of bicarbonate and carbamate ($NH_4HCO_3.NH_4COONH_2$) [2].

3. In order to quantify the ion-specific interactions in concentrated solutions, Friedman and Krishnan [110] presented two possible interactions involving ionic

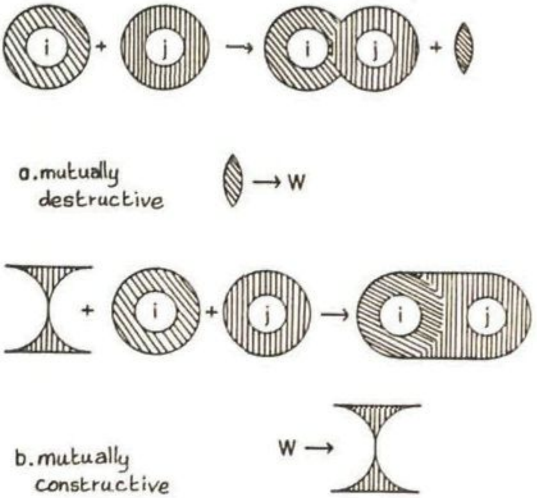

Fig. 2.15 *Ionic hydration interaction mechanisms suggested by Friedman and Krishnan [110]. 'a' denotes the relaxation of cosphere water into the bulk phase and 'b' denotes the inclusion of bulk water into the cosphere. Shaded portions denote the water regions involved.*

cosphere overlap namely, the "mutually destructive" one and the "mutually constructive" one. See Fig.2.15. In the first case some solvent in the overlapped cosphere is displaced into the bulk solvent. In the second, the overlapped cosphere takes up additional solvent molecules from the bulk region. Although the mutually destructive case is the normal one, there are cases for which the mutually constructive situation prevails. One of the significant overlap effects above the concentration of 1 M is the apparent solute-solute attractions caused by the solute-solvent interactions.

Such solvent mediated interactions can lead to associated species which are very similar to those existing in the solid crystals. For example in solid ammonium bicarbonate the bicarbonate ion is known to exist in an infinitely long polymer chain, while the same bicarbonate ion in the potassium salt exists as a cyclic dimer in an elongated benzene type hexagonal structure [111,112]. Similarly, as remarked earlier in the section 2.9, the carbamate ion in the ammonium carbamate crystal exists as a cyclic dimer. The carbonate monohydrate ion can also in principle be arranged into a polymeric sequence or into a dimer form, even though no crystallographic study has yet inferred such a sequence with the carbonate monohydrate. All these possibilities of the anion association in the crystal structure suggest that associated species can also exist in the concentrated solutions, in turn leading to the formation of solid phases on saturation. On the basis of the present inadequate knowledge, however, it is difficult to ascertain whether this hypothesis does indeed occur in reality. Perhaps future spectroscopic studies can clarify the situation.

4. While spectroscopic studies are successful in establishing species identities, their use in interpretation of the ionic interactions is problematic. For example spectroscopic studies have clarified the understanding of alkali nitrate solutions [113] through the effect of cations on the anion bands, while similar attempts on the alkali bicarbonate are inconclusive [114].

5. The phenomena of salting out, in which the solubilities of the volatile neutral solutes are reduced by the addition of salts, is difficult to establish quantitatively for the interested ammonium salts, since these salts react with water. Salting out depends on the ionic sizes, their charges, their concentrations, the nature of the non-electrolyte and the temperature. Although many studies [115,63,64,66] have established the solubility of CO_2 in aqueous alkali electrolytes to be lower than that in pure water, none of them are satisfactory due to their neglect of the simultaneous ionization reactions. The studies with ammonia are not hampered to the same degree, since the ionization of NH_3 is less severe in the aqueous alkali electrolytes. Attempts to explain the effects of alkali salts on the volatility of molecular solutes are very few. Recently, Pawlikowski et al [115] have done so regarding the effects of alkali salts on the volatility of NH_3 and CO_2 in terms of specific ionic contributions utilizing the model of McDevit and Long [116].

Further to these remarks on the characteristics of the urea-like solutes and how they affect the thermodynamic solution behaviour, the phase equilibria of the ternary and quarternary systems are discussed in the next chapter.

References:

1. Lemkowitz, S.M., "Phase and corrosion studies of the ammonia - carbon dioxide water system at the conditions of the hot gas recirculation process for the synthesis of urea", PhD thesis, Delft Univsity of Technology, The Netherlands, 1975, 191 pages.
2. Broers, J.N., "The phase behaviour of the ternary system ammonia - carbon dioxide - water at pressures of 1 to 20 atm and temperatures of 20 to 140°C," (in Dutch), Internal report, Department of chemical technology, Delft University of Technology, The Netherlands, 1974, 110 pages.
3. Jänecke, E., "Über das system: H_2O - CO_2 - NH_3, Fortsetzung," Z. Elektrochem. Angew. Phys. Chem., Bd. 35, No.9, 1929, pp. 716-727.
   ibid., Bd. 36, No.9, 1930, pp. 645-654.
4. Schneider, D.R. and G.V. Reklaitis, "On material balances for chemically reacting systems," Chem. Eng. Sci., 1975, vol. 30, pp. 243-247.
5. Upadhye, R.S., "Determining a set of independent chemical reactions," Computers and Chemical Engg, 1983, vol. 7, No.2, pp. 87- 92.
6. Whitwell, J.C. and S.R. Dartt, "Independent reactions in the presence of isomers," AIChE Journal 1973, vol. 19, No.6, pp. 1114-1120.
7. Yanagisawa, Y. et al, "Vapour-liquid equilibrium for the quarternary system of urea - ammonia - carbon dioxide - water," Nippon Kagaku Kaishi, 1975, (6), pp. *976-979 (Japanese)*
8. Takahashi, T., "Calculation of the equilibrium for the NH_3-CO_2-H_2O system by van Laar equation," Kogyo Kagaku Zasshi, 1962, vol. 65, pp. 837-843.
9. Takahashi, T. et al, "Equilibrium pressure for the NH_3-CO_2-H_2O system," Kogyo Kagaku Zasshi, 1962, vol. 65, pp. 743-745.
10. Otsuka, E.M. et al, "Equilibrium of the NH_3-CO_2-H_2O system," Kogyo Kagaku Zasshi, 1960, 63 (7), pp.1214-1218.
11. Othmer, D.F. and G.J. Frohlich, "CO_2 and NH_3 in aqueous ammonium nitrate solutions," I & E C Process Design and Develop., 1964, vol. 3, No.3, July pp.270-279.
12. Kotula, E., "A vapour-liquid equilibrium model of the NH_3-CO_2-H_2O-Urea system at elevated pressures," J. Chem. Tech. and Biotech., 1981, vol. 31, pp. 103-110.
13. Yanagisawa, Y. et al, "Vapour-Liquid equilibrium data for the ternary system NH_3-CO_2-H_2O," Nippon Kagaku Zasshi, 1973, (5), p 919
14. Pawlikowski, E.M. et al, "Phase equilibrium for aqueous solutions of ammonia and carbon dioxide," I & E C process Design and Develop., 1982, vol.21, pp. 764-770.
15. Ormerod, M. B., "The architecture and properties of matter", Edward Arnold (Publishers) Ltd., London, 1970
16. Audrieth, L.F. and J. Kleinberg, "Non-aqueous solvents," John wiley and Sons, 1953.

17. Lemly, A.T., "Hydrogen bonding phenomena" in the book "The Chemistry of Non-aqueous solvents - vol. IV," ed. by J.J. Lagowski, 1976, pp 56-66.
18. Bernal, J.D. and R.Fowler, " A theory of water and ionic solution with particular reference to hydrogen and hydroxyl ions," J. Chem. Phys., 1933, vol. 1, No.8, p 515.
19. Nemethy, G and H.A.Sheraga, "Structure of water - I", J. Chem. Phys., 1962, vol. 36, p 3382.
20. Samoilov, O.Ya., Zh. Struct. Khim., 1963, vol. 4, p 459.
21. Frank, H.S., "The proceedings of the conference on Desalination Research," Publication 942, National Academy of Sciences, National Research Council, Washington D.C., 1963, p 141.
22. Purcell and Kotz, "Inorganic Chemistry", W.B.Sanders Company, 1977.
23. Prauznitz, J.M., "Molecular Thermodynamics of Fluid phase equilibria," Prentice-Hall, 1969.
24. Huheey, J.E., "Inorganic chemistry-principles of structure and reactivity," 2nd ed.,1978, pp. 298-299.
25. Coulter, L.V. et al, J. Am. Chem. Soc., 1959, vol. 81, p. 2986.
26. Birchell, T and W.L. Jolly, "NMR study of weak acids in liquid ammonia," J. Am. Chem. Soc., 1965, vol. 87, No. 13, pp. 3007-3008.
27. Sisler, H.H.,"Chemistry of non-aqueous solvents," Reinhold, New york, 1961.
28. Stumm, W., and J.J. Morgon, "Aquatic Chemistry", Wiley-Interscience, 1970.
29. Frank, H.S. and Wen-Yang Wen, "Structural aspects of ion-solvent interaction in aqueous solutions: A suggested picture of water structure," Discussions of Faraday Society, 1957, vol. 24, pp. 133-140.
30. Frank, H.S. and M.W. Evans, "Free volume and entropy in condensed systems. III. Entropy in binary liquid mixtures; Partial molal entropy in dilute solutions; Structure and thermodynamics of aqueous electrolytes," J. Chem. Phys., 1945, vol. 13, p. 507.
31. Pauling, L., " The nature of the chemical bond," Cornell University Press, Ithaca, New York, 1960, 3rd ed., pp. 463-464.
32. Narten, A.H., J. Phys. Chem., 1970, vol. 74, p. 765.
33. Narten, A.H., J. Chem. Phys., 1969, vol. 51, p. 1108.
34. Frank, H.S. and F.Franks, J. Chem. Phys., 1968, vol. 48, p. 4746.
35. Paquette, J. and C. Jolicoeur, "A near-infrared study of the hydration of various ions and non-electrolytes," J. Solution. Chem., 1977, vol.6, p 403.
36. Conway, B.E., "Ionic hydration in chemistry and biophysics" Elsevier, 1981.
37. Durst, R.A. et al, "Mass spectrometric method for the determination of the activity coefficient of ammonia in aqueous salt solutions," The J. Phys. Chem. 1966, vol. 70, no. 6, pp. 2058-2061.
38. Gurney, R.W., "Ionic processes in solution", Dover Publications, N.Y.,1962.

39. Samoilov, O.Ya., " A new approach to the study of hydration of ions in aqueous solutions," Discussions of Faraday Society, 1957, vol. 24, p. 141.
40. Vollmar, P.M., "Ionic interactions in aqueous solution; A Raman Spectral study," J. Chem. Phys., 1963, vol 39, no. 9, pp. 22362248.
41. Fajans, K. and O. Johnson, "Apparent volumes of individual ions in aqueous solutions," J. Am. Chem. Soc., 1942, vol. 64, pp. 668-678.
42. Frank, H.S. amd A.L. Robinson, J. Chem. Phys., 1940, vol. 8, p. 933.
43. Worswick, R.D. et al, "The enthalpy of solution of ammonia in water and in aqueous solutions of ammonium chloride and ammonium bromide," J. Chem. Thermodynamics, 1974, vol. 6, pp..565-570.
44. Kaminsky, M., " Ion-Solvent interaction and viscosity of strong electrolyte solutions," Discussions of the Faraday Society, 1957, no. 24, pp. 171- 179.
45. Hindman, J.C., "Nuclear magnetic resonance effects in aqueous solutions of 1-1 electrolytes," J. Chem. phys., 1962, vol. 36, p.1000.
46. Böhm, H-J. and I.R. Macdonald, "An ab-initio potential energy function for $NH_4^+.H_2O$ and its use in the study of ionic co-ordination in solution," Trans. Fraraday soc. part II. Chem. Phys., 1984, vol.84, no.7, pp. 887-898.
47. Quist, A.S. and W.L.Marshall, "Ionization equilibria in ammonia-water solutions to 700° and to 4000 bars of pressure," J.Phys.Chem.,1968, vol.72, no.9, pp.3122.
48. Edwards, T.J., "Thermodynamics of vapour-liquid equilibria of the ammonia-water system," I & E C chem. Fundam., 1978, vol.17, no. 4, pp 264-269.
49. Müller, G.,"Experimentelle Untersuchung Des Dampf-flussigkeits-Gleichgewichts im System Ammoniak-Kohlendioxid-Wasser zwischen 100 und 200°C bei drucken bis 90 bar,"(in German), Ph D thesis, University of Kaiserlautern, 1983.
50. Won, K.W. et al, "Vapour-liquid equilibria of the ammonia-water system," Proceedings of phase equilibria and fluid properties in the chemical industry, EFCE Publ. Series, no. 11, Frankfurt/Main, 1980.
51. Wilson, T.A., Refrig. Eng., 1924, vol. 10, pp. 248-252.
52. Clifford, I.L. and E. Hunter, " The system NH_3-H_2O at temperatures up to 150°C and at pressures up to 20 atm.," J. Phys. Chem., 1933, vol. 37, pp 101-118.
53. Mollier, H., VDI- Zeitschrift, 1908, vol. 52, no. 33, pp. 1315-1320.
54. Perman, E.P., J. Chem. Soc., 1901, vol. 79, pp. 718-725.
ibid., 1903, vol. 83, pp. 1168-1184.
55. Pierre, B. Kylteknisk Tidskrift, 1959, vol. 14, pp. 89-90.
56. Tsiklis, D.S. et al, "Phase equilibria in the system NH_3-H_2O," Russian J. Phys. Chem., 1965, Vol. 39, no.12, pp. 1590-1592.
57. Gubbins, K.E. and C.H.Twu, "Thermodynamics of polyatomic fluid mixture - I Theory," Chem. Eng. Sci., 1978, vol. 33, pp. 863-878.
58. Waddington, "Non-aqueous solvents", Nelson, London, 1969.
59. Khmara, Yu. I., "A possible interpretation of azeotropy as a property of vapour-

liquid systems with chemical reactions," Russian J.Phys.Chem., 1982, vol.56 (2), pp. 651-659.

60. Nguyen, M.T. and Tae-Kyu Ha, "A theoretical study of the formation of carbonic acid from the hydration of carbon dioxide; A case of active solvent catalysis," J. Am. Chem. Soc., 1984, vol. 106, pp. 599-602.
61. Pocker, Y. and D.W. Bjorkquist, "Stopped flow studies of carbon dioxide hydration and bicarbonate dehydration in H_2O and D_2O: Acid-base and metal ion catalysis," J. Am. Chem. Soc., 1977, 99:20, sept 28.
62. Hisatsune, I.C., "Low temperature infrared study of ammonium carbamate formation," Can. J. Chem., 1984, vol. 62, pp. 945-948.
63. Ellis, A.J., "The solubility of carbon dioxide in water at high temperatures," Am. J. Sci., 1959, vol. 257, pp. 217-234.
64. Takenouchi, S. and G.C. Kennedy, "The binary system H_2O-CO_2 at high temperatures and pressures," Am. J. Sci., 1964, vol. 262, pp. 1055-1074.
65. Malinin, S.D., "The system water-carbon dioxide at high temperatures and pressures," Geochemistry, 1959, no. 3, pp. 292-304.
66. Malinin, S.D., "The thermodynamics of the CO_2-H_2O system," Geochemistry international, 1974, pp. 1060-1085.
67. Wiebe, P. and V.L. Gaddy, " The solubility in water of carbon dioxide at 50,75, 100°C, at pressures to 700 atm.," J. Am. Chem. soc., 1939, vol. 61, pp. 315-318.
68. Wiebe, P. and V.L. Gaddy, "Vapour phase composition of carbon dioxide-water mixtures at various temperatures and at pressures to 700 atm," J. Am. Chem. Soc., 1941, vol. 63, pp. 475- 477.
69. Zernike, "Chemical phase theory," Kluwer Publishing company, 1955.
70. Gmelin, "CO_2; C[c3] 2 Das system CO_2-wasser", p. 36.
71. Gibbs, R.E. and H.C. van Ness, "Solubility of gases in liquids in relation to the partial molar volumes of the solute, carbon dioxide-water," I & E C Fundam., 1971, vol. 10, no. 2, pp. 312-315.
72. Adams, J.M. and R.W. Small, "The crystal structure of ammonium carbamate," Acta Cryst., 1973, B29, pp. 2317-2319.
73. Frasco, D.L., "Infrared spectra of ammonium carbamate and Deutroammonium carbamate," J. Chem. Phys., 1964, vol. 41, no.7, pp. 2134-2140.
74. Kaasenbrood, P.J.C., "Phase equilibrium in the binary system NH_3-CO_2," DSM internal report.
75. Kucheryavyi, V.I. et al, "Molecular mechanism of the reaction of urea synthesis from ammonia and carbon dioxide in the liquid phase under high pressures," Zh. Prikl. Khim., 1974, vol. 47, no. 3, pp. 529-536.
76. Scalar, N. et al, "Thermal effects in urea: The crystal structure at -140°C and at room temperature," Acta Cryst., 1961, vol. 14, p.716.
77. Worsham Jr. and Levy, Acta Cryst., 1957, vol. 10, p. 319.

78. Caran and Donohue, Acta Cryst(B), 1969, vol. 25, p. 404

79. Vaughan, P. and J. Donohue, Acta Cryst., 1952, vol. 5, p. 530.

80. Suzuki, K., "Vapor pressures of molecular crystals. XI. Vapor pressures of crystalline Urea and Diformylhydrazine; Energies of hydrogen bonds in these crystals," Bullettin Chem. Soc. Japan, 1956, Jan, pp. 127-131.

81. Wyman, J., " Dielectric constants; Ethanol-Diethyl ether and urea-water solution between 0 and 58^oC," J. Am.Chem. Soc., 1933, vol 55, pp.4116-4121.

82. Bower, V.E. and R.A. Robinson, J. Phys. Chem., 1963, vol. 67, p. 1524.

83. Kiss et al, "Uber die loslichkeit von gassen in Wasswer - Nichtelectrolyt gemissen," Zeitschrift fur Anorg. und Alleg. Chem., 1937, Band 233, pp.346-352.

84. Worthington et al, "Physical properties of ammonia solutions: ammonium nitrate-ammonia-water and urea-ammonia-water," I & E C., vol. 44, no.4, pp.910-913.

85. Balyaev et al, Russian Journal of Inorganic Chemistry, 1966, vol. 11, no.6, pp. 787-789.

86. Finer, E.G. et al, "Nuclear Magnetic resonance studies of aqueous urea solutions, " J. Am. Chem. soc., 1972, vol. 94, no. 13, pp. 4424-4429.

87. Stokes, R.H., "Thermodynamics of aqueous urea solutions," Austral. J. Chem., 1967, vol. 20, pp. 2087-2100.

88. Schellman, J.A., C.R.Lab. Carlsberg, Ser. Chem., 1955, vol. 29, p. 223.

89. Kresheck, G.C. anmd H.A. Scheraga, J. Phys. Chem., 1955, vol. 69, p. 1704.

90. Mohammad Abu-Hamdiyyah, "The effect of urea on the structure of water and hydrophobic bonding," J. Phys. Chem., 1965, vol. 69, no. 8, pp. 2720-2725.

91. Tanaka, H. et al, "Computer experiment on aqueous solution. IV. Molecular dynamics calculation on the hydration of urea in an infinitely dilute aqueous solution with a new urea-water pair potential", J. Chem. Phys., vol. 80, no. 10, pp. 5170-5186.

92. Kuharski, R.A. and P.J. Rossky, "Molecular dynamics study of solvation in urea-water solution," J. Am. Chem. Soc., 1984, vol. 106, pp. 5786-5793, pp.5794-5800.

93. Barone, G. et al, "Heat of dilution of thiourea in aqueous solutions at 25^oC," Gazzetta Chemica Italiana, 1980, vol. 110, pp. 215-219.

94. van Alsenoy, C. et al, "Ab initio studies of structural features not easily amenable to experiment," J. Molecular Structure, 1981, vol. 76, pp.179-185.

95. Gussoni, M. et al, "Formation of weak hydrogen-bonded complexes as predicted by experimental atomic charges," Chem.Phys.Lett.,1983, vol.99, no.2, pp.101-106.

96. O'Reilly, D.E. et al, J. Chem. Phys., 1971, vol. 54, p. 96.

97. Perman, E.P. and T. Lovett, "Vapour pressure and heat of dilution of aqueous solutions," Faraday Soc. Trans., 1926, vol. 22, pp. 1-19.

98. Kucheryavyi, V.I. et al, "Equilibrium distribution of urea between liquid and vapor in the urea-water system," Zh.Prikl.Khim.,1969, vol.42, no.2, pp.446-447.

99. Scholl, W. and R.O.E.Davis,"Saturated solutions of urea in liquid ammonia,"I & E

C, 1934, vol. 26, no. 12, pp. 1299-1301.

100. Monzarch, E.M., "A quantum-chemical calculation of the activation energy of individual stages in the urea synthesis," Kinetica i Kataliz,1972, vol.13, no.3, pp. 672-677.

101. Kaasenbrood, P.J.C., "Nieuwe Ontwikkelingen bij de technische bereiding van ureum," Procestechniek, 15th March 1968, pp. 198-201.

102. Finn Christensson et al, "Equilibrium constants in the ammonium carbonate-carbaminate system. The acid dissociation constant of carbamic acid," Acta Chemica Scandinavica, 1978, vol. A32, no. 1, pp. 15-17.

103. Caplow, M., "Kinetics of carbamate formation and breakdown," J. Am. Chem. Soc., 1968, vol. 90, no. 24, pp.

104. Moodie, R.B. and P.J. Sansom, "The mechanism of decomposition of carbamate anions in aqueous solution," J. Chem. Research(S), 1979, pp. 390-391.

105. Marion, G.M. and G.R. Dutt,"Ion association in the ammonia-carbon dioxide," Soil.Sci.Soc., Amer.Proc., Division of Soil Chemistry, 1974, vol.38, pp.889-891.

106. van Eck, M.," Quantitative analysis of the urea synthesis by means of Laser Raman Spectrometry," Ph D Thesis, Delft University of Technology, The Netherlands, 1985, 101 pages.

107. van Eck, M., The analyst, 1983, vol. 108, p. 485.

108. Davis, A.R. and B.G. Oliver, "A vibrational spectroscopic study of the species present in the CO_2-H_2O system," J. Solution Chem., 1972, no. 76, p. 1565.

109. Bates, J.B. et al, J. Phys. Chem., 1972, vol. 76, p. 1565.

110. Friedman, H.L. and C.V. Krishnan in "Water - A comprehensive Treatise," ed. by F. Franks, Plenum, New York, 1973, Vol. 3, Chap. 1.

111. Nakamoto, K. et al, "Normal Co-ordinate analyses of Hydrogen-bonded compounds. IV. The acid carbonate ion," J. Chem. Phys., 1965, vol.43, no.4, pp. 1177-1181.

112. Nitta, I., "The crystal structure of potassium bicarbonate $KHCO_3$," Acta Cryst., 1952, vol. 5, p.292.

113. Irish, D.E. and A.R. Davis, "Interaction in aqueous alkali metal nitrate solutions," Can. J. Chem., 1968, vol. 46, pp. 943-951.

114. Oliver, B.G. and A.R.Davis, "Vibrational spectroscopic studies of aqueous alkali metal bicarbonate and carbonate solutions," Can.J.Chem.,1973, vol.151, pp.698-702.

115. Pawlikowski, E.M. and J.M. Prauznitz, "Estimation of Setchenow constants for nonplar gases in common salts at moderate temperatures," I & E C. Fundam., 1983, vol. 22, p. 86.

116. Long, F.A. and W.F. McDevit, "Activity coefficients of non-electrolyte solutes in aqueous salt solutions," Chem. Reviews, 1952, vol. 51, pp. 119-169.

CHAPTER 3

PHASE EQUILIBRIA OF THE TERNARY AND QUARTERNARY SYSTEMS COMPOSED OF AMMONIA, CARBON DIOXIDE, WATER AND UREA.

3.1. *Introduction*:

The presence of simultaneous phase and reaction equilibria in a number of associated systems leads to new phenomena, rich in their variations and poor in their amenability to quantitative description. This condition is especially evident when one of the components is water. For example, the systems hydrogen halide-water (HCl-H_2O, HBr-H_2O, HI-H_2O and HF-H_2O), nitric acid-water, formic acid-water and ethylene diamine-water all exhibit minimum azeotropy (maximum boiling point) and form addition compounds [1]. The systems composed of ammonia and hydrogen sulphide or hydrogen halide also form dissociating compounds and hence exhibit maximum sublimation points, minimum melting points and minimum azeotropy [1]. Similarly, the hydrogen halide-water and SO_2-water systems exhibit liquid-liquid immiscibility, again an unusual phenomenon. According to Zernike [1], a maximum in the boiling curve combined with demixing is rare, and he cites only the hydrogen halide-water systems.

It is in this rare class that one finds the system ammonia-carbon dioxide. The related system of carbon dioxide-water exhibits only demixing and compound formation [2]. Two other binary systems, namely the systems NH_3-H_2O and NH_3-urea, are known to form addition compounds, but do not show demixing [3]. There is also an azeotrope formed in the NH_3-H_2O system at an extremely low concentration of ammonia [4]. Of the two remaining systems, the urea-water system is regular with no unusual phenomena and the CO_2-urea system is experimentally inaccessible at temperatures above the melting point of urea ($T=132.5^oC$).

The interplay of these binary systems in forming ternary and quarternary systems creates further complications, new compounds and unusual behaviour. Although the ternary system NH_3-CO_2-H_2O has a long history of experimental studies and qualitative treatments, it still defies a thorough quantitative description. The complexity of the system makes all exhaustive attempts very difficult to sustain and to bring to fruition. Instead, quite a number of studies carried out in restricted ranges have met with success. For example, van Krevelen et al [5] described the vapour-liquid equilibria of dilute solutions (at low temperature and pressure with high ammonia to carbon dioxide ratios) rather satisfactorily. Frohlich [6], Wicar [7] and Verbrugge [8] had a limited success in empirically extending the model of van Krevelen et al to a moderately high concentration (10 molal ionic strength) with pressures ranging from 1 bar to 50 bar and temperatures up to 130°C. The recent attempts by Edwards et al [9], Pawlikowski et al [10] and Müller [11] using ionic interaction models are quite successful up to 100°C and up to a fairly large concentration of ammonia (>20 molal). Similarly, the equation of state proposed by Nakamura et al [12] enables one to calculate the S-G equilibria of ammonium carbamate extremely well utilizing the known data on the dissociation pressure (See appendix A).

Given the possibilities of modern molecular thermodynamic descriptions, it is imperative for phase equilibria investigators to have a qualitative understanding of the probable phase behaviour of the systems being studied. It is in this area where the phase theory can be immensely helpful. The combination of modern applied thermodynamics with its high-powered calculational tools and classical phase theory with its far-reaching suggestiveness can be synergistic in devising new chemical engineering applications. Such a synergistic influence can be clearly seen in the development of urea processes.

The phase equilibria of the ammonia-carbon dioxide-water systems (with and without the presence of urea), the ammonia-water-urea system and the ammonia- carbon dioxide-water-urea system are described in this chapter mainly with respect to experimental investigations found in the literature.

3.2. *Compounds occurring in the ternary system of NH_3-CO_2-H_2O (without the presence of urea)*:

Starting with the high pressure ($1<p<30$ bar) and high temperature ($80<T<120^{o}C$) description of the ammonia-carbon dioxide-water system (without the presence of urea), one finds four binary compounds and four ternary compounds occuring at conditions below 155°C [3,8]. The formulae of these compounds together with their symbols, as used in this chapter, are given below.

H - $CO_2.6H_2O$, B - NH_4HCO_3, A - NH_2COONH_4, C - $(NH_4)_2CO_3.H_2O$
$NH_3.2H_2O$, P - $2NH_4HCO_3.(NH_4)_2CO_3.H_2O$, $NH_3.H_2O$, R - $NH_4HCO_3.NH_2COONH_4$

The behaviour of the gas hydrates, the ammonium carbonate monohydrate and the ammonium sesquicarbonate monohydrate (i.e. the double salt of the bicarbonate and the carbonate monohydrate), which occur only at low temperatures, are not treated in this chapter, since their influence in the chosen pressure and temperature range is marginal. This leaves only ammonium bicarbonate (B), ammonium carbamate (A) and the double salt of carbamate and bicarbonate (R) as being relevant to the high temperature equilibria. Ammonium carbamate, treated in the last chapter at some length, is easily hydrolysed at temperatures below 58°C to ammonium carbonate (as shown below in (eq. 3.1)), which in turn crystallizes as the carbonate monohydrate just below 46°C [13]. In fact, it is possible to have appreciable concentrations of carbonate even at high temperatures.

$$NH_4COONH_2 \quad + \quad H_2O \longleftrightarrow \quad (NH_4)_2CO_3 \qquad \text{(eq. 3.1)}$$

3.2.1. *Ammonium bicarbonate*:

1. Crystallographically ammonium bicarbonate resembles sodium bicarbonate with its long and flat anionic chain [14] of hydrogen bonds as given below.

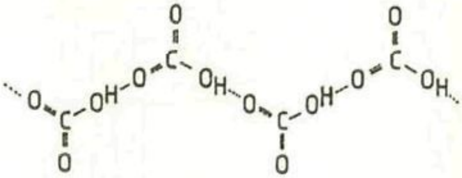

While the extent of H-bonding between the ammonium and bicarbonate ions in the ammonium bicarbonate crystal is not known, polymeric H-bonding is noted to be an unusual occurrence [15]. Such an infinitely long anionic H-bonding differs from the centrosymmetric cyclic bonding observed in potassium bicarbonate crystals [16] and, as given the last chapter, in ammonium carbamate crystals.

2. In spite of the difference in H-bonding, ammonium bicarbonate resembles ammonium carbamate in many ways. It is also a dissociating ammonium compound having a maximum sublimation point (19.5°C and 0.0466 to 0.052 bar [17]) and a minimum melting point (which was not observed but estimated [17] to occur at 114 ± 2°C and at a pressure exceeding 200 to 300 bar). The wide range of bicarbonate S-L-G equilibria (i.e. from 19.5° to 114°C) and its low sublimation pressure, compared respectively to the small range of carbamate S-L-G equilibria (from 153 to 156°C), and its sublimation pressure at equal temperatures probably indicates a greater stability of ammonium bicarbonate than ammonium carbamate. This high stability could be due to potential barriers placed against the proton transfer from the nitrogen atom of the NH_4^+ ion to the oxygen atom of the HCO_3^- ion.

3. Zernike [17] investigated S-L-G equilibria of ammonium bicarbonate and the p-T behaviour of the saturated bicarbonate solution. Also Stobiecki et al [18] studied the p-T behaviour of the same and presented their data under the mistaken *notion of being related to the sublimation behaviour. They were apparently not aware* of Zernike's work, and especially the low value of the maximum sublimation point of bicarbonate. In fact, by plotting on a p-T diagram (Fig. 3.1) their data can be seen to be similar to the S-L-G data of Zernike. These data are useful, as demonstrated in section 3.3.7, in establishing the boundaries of the S-L-G equilibria involving NH_4HCO_3 in the NH_3-CO_2-H_2O system. There is also one other vapour pressure study of ammonium bicarbonate by Bonnier [19], which differs by a constant value from these two groups of researchers. Studies of ammonium bicarbonate S-L-G equilibria are difficult due to the great difference in solubilities of NH_3 and CO_2 in water. In

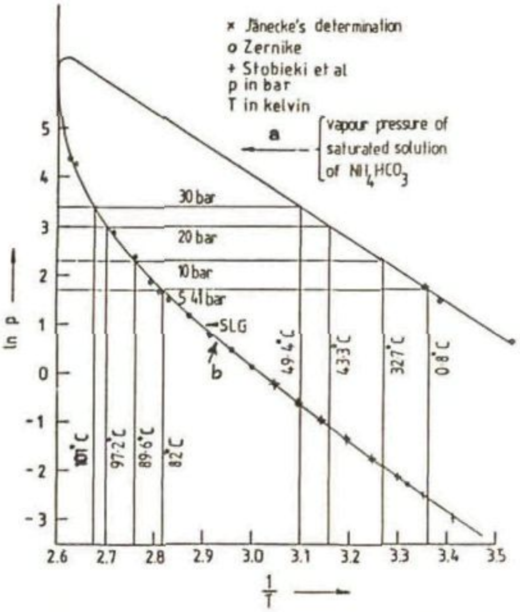

Fig. 3.1. a. *Vapour pressure curve of the saturated NH_4HCO_3 solution.* b. *S-L-G curve of NH_4HCO_3. In the figure, the S-L-G and boiling temperatures are also marked for the pressures 5.41 bar, 10 bar, 20 bar and 30 bar.*

fact, accurate S-L-G measurements necessitate that the mole ratio $(NH_3)/(CO_2)$ in the liquid phase be kept at unity. This is possible only when the vapour volume is kept extremely small. Failure to appreciate this important factor has led many investigators [20,21,22] to report much too low vapour pressures of the saturated solutions. As shown in Fig. 3.1, the correct vapour pressures are very high; such high pressures are necessary to maintain the poorly soluble CO_2 in the liquid phase.

4. If ammonium bicarbonate resembles ammonium carbamate as a dissociating compound, it is natural for the question to be raised as to why one does not observe any azeotropy induced by bicarbonate formation similar to that induced by carbamate formation. The answer to this question is easily provided by phase theory in terms of generalised models of dissociating compound behaviour.

Consider the system made of CO_2 and NH_4OH. The pure compound NH_4OH has not been isolated, and many investigators even doubt the existence of species like NH_4OH [23]. However, for pedagogical purposes one may consider the fully associated equimolar aqua-ammonia as NH_4OH. The pure component vapour pressure of NH_4OH may be presumed to be similar to that of H_2O (in view of its potential H-bonding capabilities) and hence low with respect to that of CO_2. For a binary system of this type with the vapour

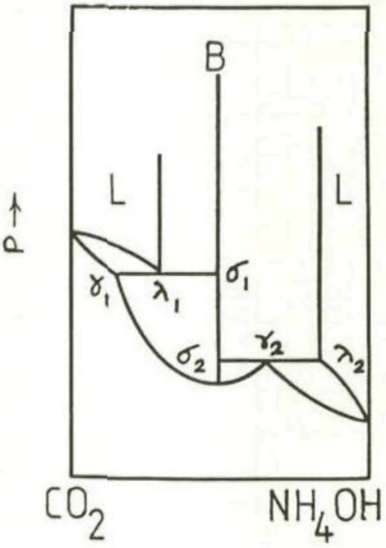

Fig. 3.2.1. Binary equilibria below the max. subl. point. $T < T_{msp}$

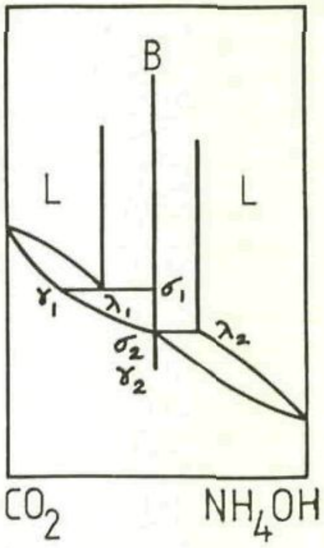

Fig. *3.2.2. Binary equilibria at the max. subl. point. $T = T_{msp}$*

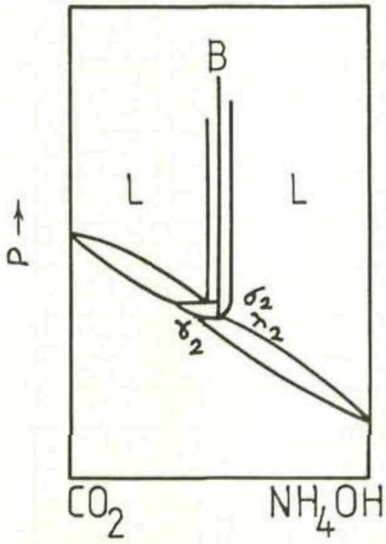

Fig. 3.2.3. *Binary equilibria at the minimum melting point, $T = T_{mmp}$*

pressure of the dissociating compound having a value between those of the original components, the probable p-x behaviour just below the maximum sublimation temperature, at the maximum sublimation temperature and at the minimum melting temperature, are shown respectively in figures 3.2.1, 3.2.2 and 3.2.3. All systems similar to the one shown above have been generally observed [1] not to exhibit azeotropy.

2.2. *The double salt (R) of carbamate (A) and bicarbonate (B)*:

1. Although no crystallographic study of the double salt (R) has been reported, infrared and optical study of its crystals [24] indicate similarities of the double salt with bicarbonate (B) and carbamate (A). Further one may suspect that the salt anions in the double salt are extensively H-bonded, since it dissociates easily into its constituent salts which are themselves H-bonded.

2. Terres and Behrens [25] studied the melting behaviour of B-R mixtures, while Jänecke [26] studied the melting of A-B mixtures. It can be inferred from these studies that the double salt is quite unstable above 100°C and it probably decomposes into carbamate and bicarbonate through a solid state reaction

$$R_s \longleftrightarrow A_s + B_s \qquad \text{(eq. 3.2)}$$

3. Broers [3] estimated the sublimation vapour pressure of the double salt (R) at 65°C to be 1 atm. He also established the probable existence of a quadruple point BRAL in the NH_3-CO_2-H_2O system at approximately 100°C with a liquid composition of 35 mole% NH_3 and 29 mole% CO_2. The pressure at the quadruple point was not estimated due to dearth of data on the R-L-G equilibria. There are three other quadruple points involving the salt R in addition to BRAL, all of which were determined by Guyer and Piechowicz [27]. The reader may refer to Broers [3] or Verbrugge [8] for the values of these quadruple points. Further, the pressure dependence of these quadruple points can be neglected, in view of the absence of the gas phase in these equilibria.

3.3. *The ternary system NH_3-CO_2-H_2O*:

3.3.1. *Characterization of the system*:

The ternary system NH_3-CO_2-H_2O involves both physical and chemical equilibria. The possible chemical reactions (involving either a simple proton transfer or a proton transfer coupled with nucleophilic bond formation) are as follows.

$$NH_3 + H_2O \longleftrightarrow NH_4^+ + OH^- \qquad \text{(eq. 3.3)}$$

$$CO_2 + H_2O \longleftrightarrow HCO_3^- + H^+ \qquad \text{(eq. 3.4)}$$

$$HCO_3^- \longleftrightarrow CO_3^{=} + H^+ \qquad \text{(eq. 3.5)}$$

$$H_2O \longleftrightarrow OH^- + H^+ \qquad \text{(eq. 3.6)}$$

$$NH_3 + HCO_3^- \longleftrightarrow NH_2COO^- + H_2O \qquad \text{(eq. 3.7)}$$

$$NH_4^+ + NH_2COO^- \longleftrightarrow NH_2CONH_2 + H_2O \qquad \text{(eq. 3.8)}$$

If the last reaction is artificially restricted from proceeding, one is left with 9 species, 3 components and 5 reactions together with one electroneutrality constaint. This means that at least three intensive thermodynamic properties (called "intensities" in the rest of this work) have to specified to fix a two phase equilibria and two intensities to fix a three phase equilibria. Accordingly the pressure, temperature and any one of the phase compositions may be chosen. The equilibria can be conveniently plotted in p-T cross sections drawn on triangular composition diagrams, as shown variously in this chapter. An advantage of this method is the immmediate visualization of the two phase tie-lines and a possible check on the inconsistency of data (like the crossing of tie-lines, the transformation of the vapour-liquid region into a three phase region, incompatibility with the tie-line data of the boundary binary systems, etc). (Interestingly enough, many researchers did not check their experimental results this way, and at least part of their data are found to be inconsistent.)

Early works prior to 1950's on the NH_3-CO_2-H_2O system were mostly concerned with the solid-liquid and vapour-liquid equilibria. Of the three major studies [25,26,27] on the solid-liquid equilibria, only two [25,26] have included high temperature data. In the 1960's, a follow up study of the S-L and S-L-G equilibria was published by a group of Japanese investigators [28]. In the next section, the S-L / S-L-G equilibria studies are first described in chronological order and the salient points are assessed later.

3.3.2. *Investigations of Terres et al on the S-L equilibria*:

Continuing the earlier work of their laboratory, Terres and Behrens [25] studied the S-L-G equilibria in the range of 80-135°C. Due to the corrosive nature of the solutions, all experiments were carried out in either rubber-lined or glass-lined vessels. The solutions were prepared by mixing either the bicarbonate or the carbamate salt with aqua-ammonia of known composition. The equilibrium vessel was manually shaken. The temperature at which the last trace of salts just dissolved was established visually, and was taken to be the solubility temperature for the given gross composition. The time needed to attain equilibrium was stated to be around 4 hrs (which appears to be rather short), and the pressures were said to be roughly in the range of 30 to 50 bar. After cooling the samples, the crystals were separated and microscopically investigated. In certain experiments, the liquid phase was also chemically analysed.

Although Terres et al clearly mentioned that their data concerned the S-L equilibria, one may easily infer the presence of a gas phase through indirect means. For each experimental composition, Terres et al gave the original composition of the

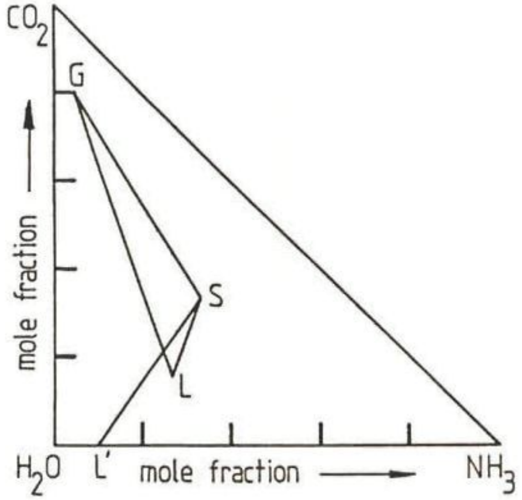

Fig. 3.3. *The presence of gas phase in Terres et al measurements.*

aqua ammonia solution and the salt employed for the preparation of the mixture. For example, as shown in Fig. 3.3, by mixing the salt S and an aqua ammonia solution of composition L', the final composition should be in the line connecting S and L'. Instead, the analysed liquid compositions of Terres et al were always very much different from those on the line, as composition L shows in Fig. 3.3. Such a differene is possible only when a significant amount of gas phase is also present. Since the S-L-G equilibria are strongly influened by pressure, specifying the liquid composition to be only a function of temperature which Terres and Behrens did, is incorrect.

One therefore has to conclude that the non-isobaric data of Terres and Behrens is only of qualitative significance. Even so, their pioneering investigations proved to be useful in organizing later studies. Qualitatively the picture they drew remained more or less valid through the succeeding studies.

In the range of 80 to 100°C, Terres and Behrens found three S-L regions associated with the three salts B, R and A and one quadruple point B-R-A-L (see section 3.2.2). The R-L equilibria region in the p-T cross sections was observed to shrink fast with increasing temperature. As mentioned earlier, Terres and Behrens also investigated the melting behaviour of R-B mixtures, which led them to conclude that the "melting point" of bicarbonate was around 106°C and that the salt R decomposed even in the solid state to bicarbonate and carbamate.

3.3.3. *Investigations of Jänecke on the S-L equilibria*:

Investigations of Jänecke were presented in a series of three articles [26,29,30] in the years 1929-1932. Leaving aside his third article [30] (which involved urea and its related species), one may consider the two investigations related to the NH_3-CO_2-H_2O system (without urea).

In his first article [29] Jänecke reported the solubility of ammonium bicarbonate in water. Experiments with low concentrations of bicarbonate were performed in glass vessels, while those with high concentrations were performed in metal autoclaves. It is not clear whether the maximum charge density (i.e. negligible amount of gas phase) was achieved in each experiment. As a result of these experiments and those concerning the melting behaviour of bicarbonate-carbamate mixtures, Jänecke arrived at the "melting point" of bicarbonate as 108°C with $p = 75$ to 78 atm (in a later article [26] 80 atm), which is quite below the value estimated by Zernike (114 ± 2°C and 200-300 atm) [17].

Considering the difficulties involved in measuring the high temperature solubility, the reliability of the earlier researchers' solubility data, presented here in Fig.3.4, is surprisingly good, but only up to about 100°C.

In the second article [26] Jänecke reported the solubility data of more than 250 mixtures. Each mixture was prepared by mixing either the bicarbonate or the carbamate with aqua-ammonia of known composition. Being well aware of the problems faced by Terres et al, Jänecke carried out his experiments in sealed glass tubes with known gross compositions. He chose the highest possible charge density in each tube in

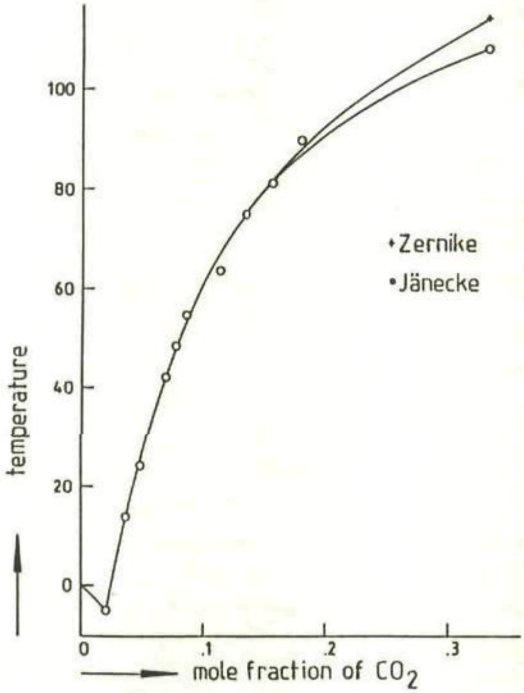

Fig. 3.4. *The solubility of NH_4HCO_3 in water.*

order to get a negligible vapour volume. Once again the temperature at which the last solid speck dissolved was taken as the solubility temperature for the given gross composition. Janecke did not carry out any liquid or gas phase analysis and also did not measure the pressure in the tubes. Often the glass tubes exploded leading to a need for placing them in metal autoclaves with high pressure glass windows. All the glass tubes placed outside the autoclaves were mechanically shaken while those placed inside (i.e. the high temperature equilibria mixtures) could not be stirred. Janecke did not state the time involved for attaining equilibrium, although he mentions the heating rate prior to the equilibrium as 10°C/hr. It is quite possible that equilibrium was not achieved in many experiments. The microscopic investigations of the crystals were performed after cooling the sealed tubes and breaking them.

Since Janecke did not separate the crystals before cooling, he relied mainly on discontinuities of the solubility isotherms to distinguish between the different S-L equilibria. This method can be very troublesome if there is appreciable scatter in the data. In fact, Janecke differs from Terres et al [25] in identifying the solids. He gives the composition of sesquicarbonate as unhydrated and discounts the possibility of a salt like R. Such conclusion is at odds with the results of the solubility studies of Guyer and Piechowicz [27], to be described shortly, and the optical and infrared studies of Scalar [24].

Through his experiments on the melting behaviour of bicarbonate-carbamate mixtures, Janecke also established the eutectic composition and temperature to be 35 mol% NH_3, 33 mol% CO_2 and 112°C, respectively. Furthermore his experiments on the liquid demixing are few and far between; his demarcation of the demixing region can be considered only as qualitative.

3.3.4. *Solubility investigations of Guyer and Piechowitz*:

In an effort to settle the controversy between Terres and Janecke, Guyer et al [27] carried out their experiments, by maintaining a constant pressure of 0.963 bar with mercury seal, in closed glass vessels. After reaching the equilibrium, both the liquid and the crystals were separately analysed. Unlike the previous two investigators, Guyer et al presented the interpolated liquid compositions (and not the raw data) of the S_1-S_2-L equilibria at various temperatures (the solids S_1 and S_2 being any two of the set A, B, C, P and R), the liquid compositions of B-L-G and A-L-G equilibria at various temperatures and the quadruple points (BPCL, PRCL and ARCL). Their values presented by Broers [3] and Verbrugge [8] are given here in Table 3.1 for the readers' convenience. One important and novel feature of the work of Guyer et al was a clear demarcation of the S-L equilibria as opposed to the S-L-G equilibria. They referred to the curve traced by the liquid compositions on the CO_2- side of the

Table.3.1. *The liquid compositions of the various equilibria studied by Guyer and Piechowitz at 0.963 bar.*

Related equilibria	T°C	Liquid composition in mole%	
		NH_3	CO_2
B-L-G ("CO_2 saturation line")	20	4.8	4.2
	25	5.3	4.7
	30	6.4	5.3
	35	7.8	6.0
	40	9.6	7.0
	45	12.0	8.1
	50	14.8	9.5
A-L-G ("NH_3 saturation line")	20	41.3	11.1
	25	40.6	12.2
	30	39.9	13.3
	35	39.4	14.2
	40	38.9	15.2
	45	38.6	16.1
	50	38.4	17.0
B-P-L	20	19.2	9.8
	25	19.6	10.1
	30	20.3	10.5
	33	25.8	13.0
B-R-L	35	27.2	13.5
	40	28.2	14.2
	45	29.0	15.0
	50	29.8	15.9
C-P-L	20	23.1	10.6
	25	26.8	12.6
P-R-L	30	27.8	13.4
C-R-L	30	29.0	13.4
A-C-L	20	39.1	11.9
	25	37.4	13.2
	30	36.0	14.3
A-R-L	35	36.4	15.1
	40	37.1	15.8
	45	37.7	16.4
	50	38.3	17.1
B-P-R-L	34	27.1	13.4
C-P-R-L	29	27.9	13.3
A-C-R-L	31	35.8	14.5

S-L-G equilibria (at various temperatures but at a constant pressure) as the "CO_2 saturation line" and a similar one on the NH_3-side as the "NH_3 saturation line".

In view of the care taken in organising their solubility experiments and their appreciation of keeping the vapour volume negligible, the data of Guyer et al appear to be quantitatively more reliable than those of all previous investigators in describing the probable behaviour of the ternary system at 1 atm pressure [3,8]. Since the maximum temperature reached in the work of Guyer et al was unfortunately only 50°C, one has to turn elsewhere, mainly to a group of Japanese investigators, for high temperature and high pressure measurements.

3.3.5. *Determinations of the saturated solution pressures by Takahashi et al*:

Not being aware of the work of Guyer and Piechowitz on the S-L and S-L-G equilibria at constant pressure, but conscious of the need for the knowledge of equilibrium pressures of the saturated solutions, Takahashi et al [28] set out to close the gap left by the earlier two investigators, especially by Jänecke.

They reported the results of 48 experiments performed in an autoclave of 50 ml capacity at a charge density of 0.6 gm/ml. In addition to charge density, the weight ratios $(NH_3)/(CO_2)$ and $(H_2O)/(CO_2]$ were considered as independent variables. After charging the autoclave, the temperature was raised slowly up to the solubility temperature of the given composition, as read from Jänecke [26,29]. Corresponding to this temperature, the average of two pressure readings, one on heating and the other on cooling, were taken as the equilibrium pressure.

Elegant though the technique is with no need for liquid phase analysis, there is one unanswered question (leaving aside the point about the literal and uncritical acceptance of Jänecke's solubility temperatures). Was the vapour volume negligible? This question is quite important, since Jänecke's solubility data were supposed to have been obtained with negligible vapour volume. While Takahashi et al were justified in choosing the independent variables as the $(NH_3)/(CO_2)$ ratio, the $(H_2O)/(CO_2)$ ratio and the charge density, interpreting their results in terms of equilibrium diagrams can be meaningful only when the vapour phase was indeed negligible; i.e., when the charge density equals the liquid density. Unfortunately, nowhere in their article have they mentioned this factor explicitly. However, in one figure of their article they do mention that the equilibrium pressures of the saturated solutions are plotted against the liquid composition. On the whole, their data is in a strange setting: an apparently valid set, but no clear statement of the experimental conditions. Similar lack of clarity prevails over their VLE data of the unsaturated solutions presented in the same article. The present author is unable to fix clearly whether their data refer to bubble point compositions or gross compositions.

If the data of Takahashi et al concerning the equilibrium pressures of the saturated solutions had indeed been obtained with negligible vapour volume, there is one important implication for the VLE experimental studies and for solid formation in industrial practice. The data of Takahashi et al suggest that, at pressures higher than about 1.5 bar and upon heating the system, the last S-L-G equilibria to transform into a L-G equilibria extending over the whole ternary composition range is the one involving only carbamate. This situation is in sharp contrast to the behaviour at lower pressures. For example at 1 atm. the last salt to dissolve completely is the double salt of carbamate and bicarbonate. (Refer to Fig. 2.11.g in Verbrugge's dissertation [8]. Also see the section 3.3.7 for further elaboration on this point.)

Prior to the above work on the vapour pressures of the saturated solutions, the same group of investigators carried out VLE studies. In one of their studies [31], presented by Otsuka et al, the onset of S-L-G equilibria is discussed in terms of its importance to the solution handling of urea processes, and just four liquid composition data on the NH_3-side A-L-G equilibria were given in the same article. Otsuka et al called the liquid phase composition of the S-L-G equilibria the "liquefying point (the translator's term)" at the chosen pressure and temperature. The locus of the "liquifying points" at constant pressure with varying temperatures would become "the NH_3 saturation line" or "the CO_2 saturation line" of Guyer and Piechowicz.

Before consolidating the salient points of the S-L / S-L-G equilibria, it is useful to describe next the earlier works on the vapour-liquid equilibria (VLE) at the chosen range of $80^oC<T<135^oC$ and $1<p<30$ bar.

3.3.6. *Vapour-liquid equilibria of the NH_3-CO_2-H_2O system*:

Previous studies on the VLE at near-atmospheric pressure and below 80^oC were reviewed by Broers [3] and Verbrugge [8]. At high pressures many researchers, like Otsuka et al [31], Takahashi [32], Jager et al [33,34], Schmidt [35], Yanagisawa et al [36,37], Pawlikowski et al [10] and Müller [11], studied the system NH_3-CO_2-H_2O (without urea). Further, there is the study by Frölich [6] on the quarternary system of NH_3-CO_2-H_2O-NH_4NO_3 and the VLE study of the present system by Koren and Andreatch [38] (utilizing infrared spectroscopy).

Otsuka et al measured the VLE at 20, 40 and 60^o C by the flow method and further at 80 and 100^o C using a stirred autoclave. In addition to temperature, two other variables, namely the wt.% of $((NH_3)+(CO_2))$ in the liquid phase and the gross wt. fraction $(CO_2)/((CO_2)+(NH_3))$ were chosen as independent variables. Based on their measurements, Otsuka et al established a pressure minimum at each of the temperatures studied, in the vicinity of the $(NH_4)_2CO_3$ stoichiometric composition. The data of Otsuka et al appear to be quite reliable and consistent with the generally accepted trend. (See figures 3.6.1 and 3.6.2).

Takahashi measured the VLE at two different pressures (2 and 15 Kg/cm^2 abs) with temperature and $(NH_3)/(CO_2)$ ratio in the gas phase as the other two variables. The low pressure experiments were performed by the flow method and the high pressure ones in an autoclave. The data at 2 Kg/cm^2 abs. appear to have a systematic error compared to the data of others. (See Fig. 3.6.1)

Jager et al studied the system NH_4COONH_2-NH_3-H_2O in the range of 40 to 100°C and up to 35 bar using both the flow and static methods. In their first study, they measured the vapour pressures of carbamate solutions of known composition by bubbling nitrogen at a very low flow rate of 2 l/hr for a period of 5 hrs, and analysing the saturated outlet stream for NH_3 and CO_2. Under the assumption of insignificant change in liquid composition, Jager et al plotted the solution vapour pressures against the carbamate compositions. Apparently the fact that carbamate in low concentrations hydrolyses easily to carbonate at temperatures below 58°C seems to have been overlooked. Their plot at 40°C is in conflict with the saturated solution compositions as measured by others [13]. In their second study with aqua-ammonia solutions of carbamate, Jager et al presented constant temperature and constant pressure sections obtained through a semi-empirical interpolation of their experimental data. Unfortunately, the data for carbamate-water solutions from their second study show inexplicable discrepancies with similar data of their first study. Moreover their high pressure data are incompatible with the VLE data of the system NH_3-H_2O [39]. Due to all these factors, one has to critically assess the data of Jager et al in relation to other sources before using them for any model evaluation.

Yanagisawa et al studied the ternary system at 20 Kg/cm^2 abs. and at varying temperatures. Known amounts of carbamate or bicarbonate salts together with aqua-ammonia were placed in a 500 ml autoclave. The contents of the closed autoclave were frozen and the air inside was evacuated. After the required temperature and pressure were established within 3 hrs during which the equilibrium was said to have been reached, the gas and liquid samples were drawn and analysed using a gas-solid chromotograph (Poropak Q coloumn of 2.5 m length and at 145°C), the accuracy of which was not given by the authors. Since previous experience [40] with poropak Q is not encouraging (due to small water peak occurring as shoulder in ammonia peak's tail), one has to approach their results with certain reservations. In fact, a number of Yanagisawa's data with NH_3 concentrations >95% are not consistent with the binary NH_3-H_2O vapour compositions, although the "tongue like" character of the bubble-point curve of the ternary system is confirmed qualitatively. They also suggested that the $(NH_3)/(CO_2)$ ratio in the gas phase is directly proportional to a similar ratio in the liquid phase with the constant of proportionality being only a function of temperature. It is not clear whether this conclusion is valid over the whole range of composition. Other literature sources mentioned at the beginning of this section do not confirm this behaviour in the whole composition range.

Recently Pawlikowski et al presented a few measurements of the NH_3-CO_2-H_2O system. All the data given were on the CO_2-rich side. The measurements were performed in an autoclave of about 1.85 l capacity. After an overnight equilibration, both the liquid and gas samples were analysed using gas-solid chromotography, just as Yanagisawa et al had done. There are, however, certain differences. The coloumn employed was Chromosorb 103, which is usually considered to give a better separation of polar gas mixtures than Poropak Q. The coloumn temperature was kept at 70°C until the ammonia peak began to elute; then the temperature was increased to 150°C to reduce the width of the water peak and thereby reduce the analysis time. Since Pawlikowski et al were mainly interested in the application to sour water stripping processes, they did not measure in a wide composition range. As is evident from Fig. 3.6.2 and Fig. 3.6.3, the data of Pawlikowski et al suffer from the inaccuracy of the vapour phase analysis. This is in contrast to their liquid phase analyses, which seem to be more or less consistent with data from other sources.

The latest series of investigations was carried out by Müller. He provided a large number of data including those of the binary systems NH_3-H_2O and CO_2-H_2O, over a wide pressure ($1<p<100$ bar) and temperature ($100<T<200$°C) range (254 ternary VLE data points and 89 binary VLE data points). Acknowledging the difficulty of liquid sampling from a pressurised vessel without disturbing the equilibrium and also the difficulty of liquid phase analysis itself, Müller analysed only the vapour composition. Measuring the liquid volume through a level indicator and knowing the amount of the materials charged into the autoclave, the liquid composition was calculated through material balances. Furthermore, in order to apply the material balances, the vapour density was calculated by means of the Nakamura et al [41] equation of state. This method differs from the approach of Kawasumi [42] and Durisch [43] who, in their investigations of the NH_3-CO_2-H_2O system (with equilibrium concentration of urea), measured the vapour density and did not resort to calculations.

Müller's experimental procedure was in principle a simple one. Starting from the ammonia-water binary side, measured amounts of CO_2 were added to get a series of ternary data points. Each of the data series was identified by the starting binary liquid phase ammonia composition and the temperature. The equilibration time for the binary ammonia-water system is stated to be more than 12 hrs and that for the ternary measurements, after the addition of CO_2, as about 2 hrs. The gas chromotographic analysis was performed using a Poropak T coloumn with an oven temperture of 95°C.

Due to the nature of the experimental procedure, it appears that the CO_2- rich ternary points, obtained usually at the end of a particular series, suffer from the

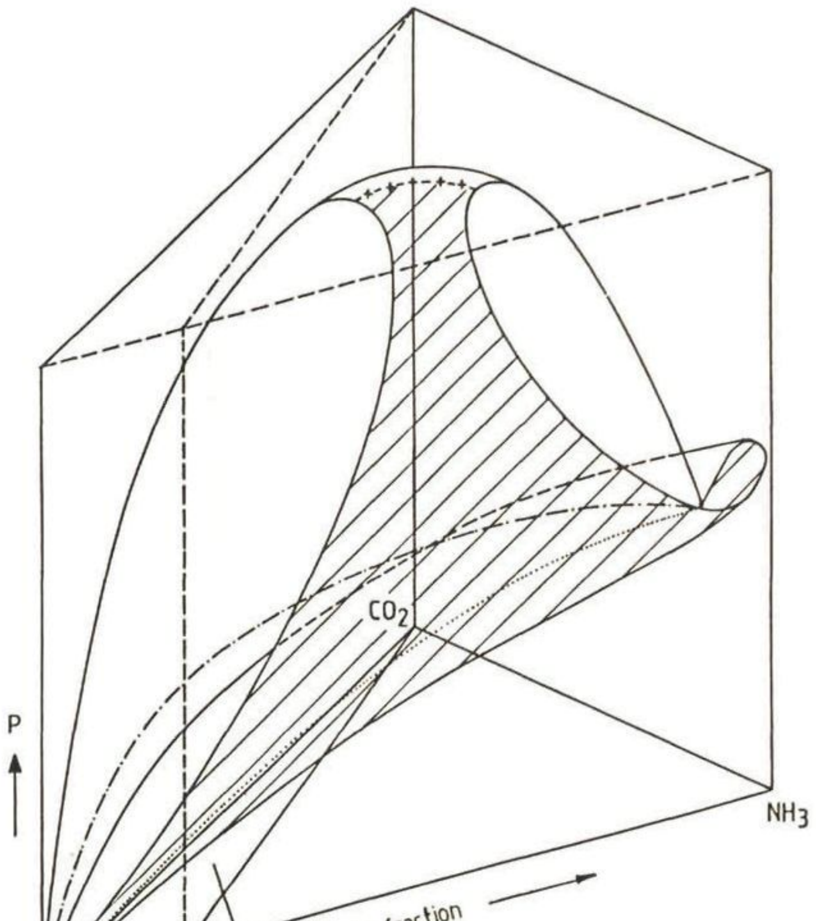

Fig. 3.5. *The p-x-y diagram of the ternary system at constant temperature. Dotted line - the gas ridge curve; Dot-dashed line - the liquid ridge curve; Plus-dashed line - the critical curve; Hatched area - the dew-point surface. Also a typical gross composition plane at constant* $(NH_3)/(CO_2)$ *is shown.*

Table 3.2.*The VLE data of the* NH_3-CO_2-H_2O *system at* $100^{o}C$ *and 2,3 and 6 bar. The data are mostly interpolated from the original sources.*

Investigator	Liquid composition		Gas composition		Pressure
	mole% NH_3	mole% CO_2	mole% NH_3	mole% CO_2	in bar
Pawlikowski	5.25	1.26	32.0	20.0	2
Takahashi	10.10	2.23	47.0	16.0	
Müller	6.2	1.6	33.5	18.5	
Müller	6.5	1.4	37.5	12.0	
Otsuka	6.7	1.6	35.3	13.0	
Pawlikowski	5.2	1.7	13.7	43.3	3
Müller	6.0	2.5	12.5	56.0	
Müller	6.5	2.7	13.0	55.0	
Müller	10.0	3.9	23.2	48.0	
Müller	11.2	3.8	37.0	34.5	
Otsuka	8.2	3.4	17.8	51.0	
Otsuka	12.9	1.1	64.7	3.3	
DSM	13.7	4.6	47.5	23.5	
Pawlikowski	5.2	2.7	4.2	77.5	6
Pawlikowski	13.8	6.4	10.0	74.2	
Müller	6.3	3.5	3.5	81.5	
Müller	9.8	5.2	6.7	78.5	
Müller	10.7	5.5	8.0	77.5	
Müller	22.0	10.5	20.0	68.2	
Müller	28.0	12.5	36.0	54.0	
Müller	28.8	9.2	80.0	7.5	
Müller	24.1	2.7	87.2	0.8	
DSM	7.2	4.1	11.7	77.0	
DSM	10.2	5.3	14.0	75.5	
DSM	32.9	13.0	74.5	14.2	
DSM	28.4	6.8	79.7	5.0	

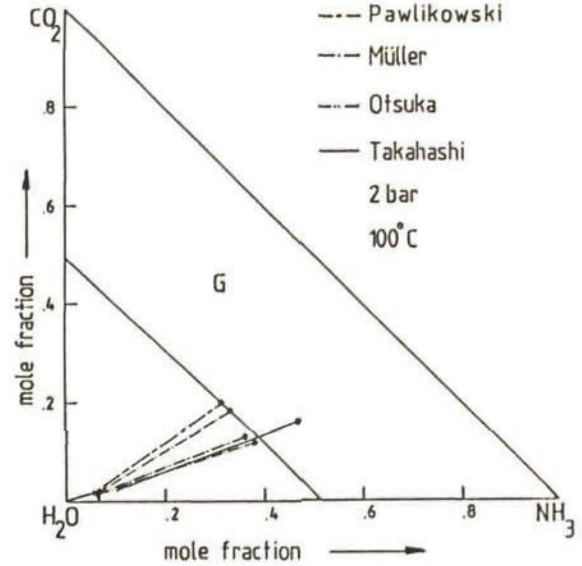

Fig. 3.6.1. *Vapour-liquid equilibria of NH_3-CO_2-H_2O system at 2 bar and 100°C. Some of the data marked in the figure are interpolated values.*

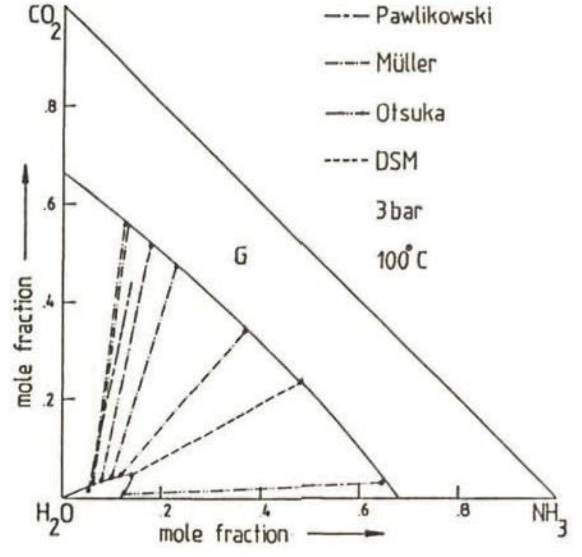

Fig. 3.6.2. *Vapour-liquid equilibria of NH_3-CO_2-H_2O system at 3 bar and 100°C. Some of the data marked in the figure are interpolated values.*

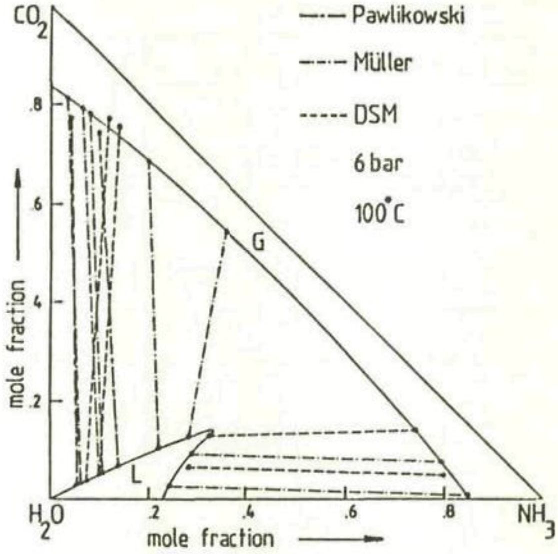

Fig. 3.6.3. *Vapour-liquid equilibria of NH_3-CO_2-H_2O system at 6 bar and 100°C. Some of the data marked in the figure are interpolated values.*

accumulated errors involved in the calculation of material balances. These errors are especially apparent in high temperature measurements. Further, Muller did not observe the pressure minimum for the data set at 140°C and higher, possibly due to the experimental procedure. As the reader may see in Fig. 3.5, which illustrates the p-x-y diagram at constant temperature, the pressure minimum is quite shallow at high temperatures, and it is most visible when the data are collected at constant water compositions. When one carries out experiments with the gross $(NH_3)/(H_2O)$ ratio kept nearly constant and the gross (CO_2) amount varied, as Muller did, it is easy to miss the pressure minimum because of the angle at which the overall gross composition plane (constant gross $(NH_3)/(H_2O)$ ratio plane) intersects the bubble-point surface. *(See Fig. 3.5 for an overview of the bubble-point and dew-point surfaces at constant* temperature. In this figure the gas and liquid ridge lines are also presented, the explanations of which will be given in the later part of this chapter.)

In general Muller's data appear to be reliable over the whole composition range at low temperatures and on the NH_3-rich side at high temperatures.

With this review on VLE, one would naturally like to compare the mutual consistency and the reliabilty of various data. Such a task is quite difficult in the range of interest, since these insufficient data have been obtained at very different conditions. Hence, falling back to the only recourse possible, the available original data and certain interpolated data at 100°C are presented in Table 3.2 and plotted in Fig. 3.6.1 to 3.6.3 at 2,3 and 6 bar. In these p-T sections the data of Jager et al could not be plotted due to insufficient data from their study.

Subsequent to these discussions on the G-L, S-L and S-L-G equilibria studies carried out by the earlier researchers, the probable behaviour of the NH_3-CO_2-H_2O system (without the species urea) are presented by consolidating the salient features in the following section.

3.3.7. *The probable behaviour of the NH_3-CO_2-H_2O system at high pressures and moderately high temperatures*:

Interest in the behaviour of NH_3-CO_2-H_2O system is based on two grounds:

1. It appears to be an unique example of a complex ternary system; hence there is a purely scientific value in presenting its behaviour.
2. The system is also of practical interest. Estimating the minimum temperature for each pressure at which a continous L-G region can exist in the p-T sections (starting from the CO_2-H_2O system to the NH_3-H_2O system without any intervening S-L or S-L-G equilibria, i.e. without the occurrence of crystallisation) is essential in applications related to urea and melamine manufactures. Such estimations help in the design of low pressure condensers and decomposers and in fixing the lowest allowable temperature of the pipelines, pumps and valves handling NH_3-CO_2-H_2O solutions. One may call this temperature "the S-L-G onset temperature" or "the minimum temperature for the absence of S-L-G".

Before proceeding to describe the behaviour, clarifying one aspect of terminology is in the interest of pedagogy. In a ternary system like the present one, the S-L-G equilibria is represented in constant p-T cross sections by a triangular region, as shown in Fig. 3.7. Within this triangular region of SLG, any given gross composition will split into three phases. The relative amounts of the individual phases depend solely upon the gross composition and the material balances. If the gross composition is very close to the vertex L, there will be a very large amount of liquid phase and very small amounts of gas and solid phases. Similarly close to the vertex G the gas phase predominates over the other two phases. Knowing the composition of G and L is relevant to every S-L-G equilibria for each p and T. In this system there are two S-L-G equilibria of which one is concerned with the CO_2-rich gas phase and the other with the NH_3-rich gas phase.

The locus of points like L involved in such S-L-G equilibria for various temperatures but at one pressure serve an important function of delimiting the G-L

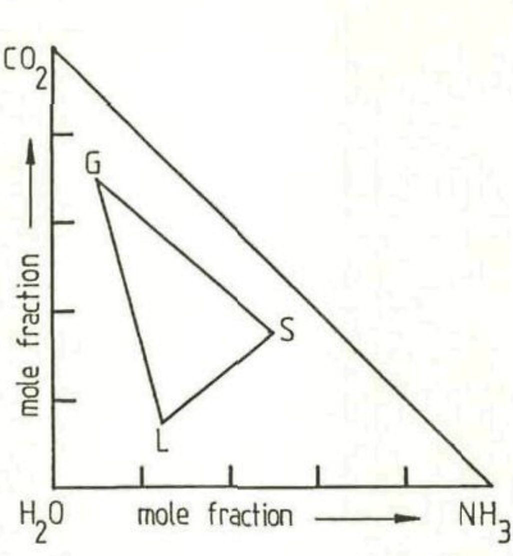

Fig. *3.7. Three phase S-L-G equilibria*

region. Such a locus of L-compositions has been variously termed in the literature as "the saturation line" (Guyer and Piechowitz), "the line of liquefying points" (Otsuka et al) and "the isobaric solubility line" (Takahashi et al). In the present writer's opinion, however, none of these terms capture the essential feature of the points in the said line, namely the insignificant proportions of solid and gas along with a large amount of liquid. In other words, there is simultaneously a tiny gas bubble and a tiny amount of solid ("frost") being present along with a very large amount of liquid phase. To imply this graphic description and to refer to the points like L clearly and consisely it is proposed to call them "the riming bubble-points". In a similar vein, one may call points like G "the riming dew-points". The term "riming" is used *exactly in the same sense of frosting (i.e.* the formation of ice crystals) in meteorological studies and was first suggested by Altmann [44].

It is the locus of the riming bubble-points for various temperatures but at constant pressure together with the loci of the double riming liquid compositions of the various S_1-S_2-L equilibria which are crucial in understanding the behaviour of the present system. All these loci are plotted in the Fig. 3.8. Since Guyer et al were the first investigators of the present ternary system to appreciate the importance of the riming bubble-points and since their data on the liquid composition loci of various S_1-S_2-L equilibria are the most reliable, their values are used for plotting such loci in Fig. 3.8. To extend their data to higher temperatures, both the data of Terres and Behrens and of Jänecke are employed with a reasonable (but admittedly subjective) extrapolation. The salt identifications of Guyer and Piechowitz are accepted for the reasons mentioned earlier in section 3.3.3. All the liquid compositions in Fig. 3.8 which can potentially exist in B-L or B-L-G equilibria and which are bounded by the liquid composition loci of the B-R-L equilibria and the B-P-L equilibria are said to constitute the riming field of the bicarbonate (RFB). Similarly other riming fields may be suitably defined. All the riming fields are marked in Fig. 3.8.

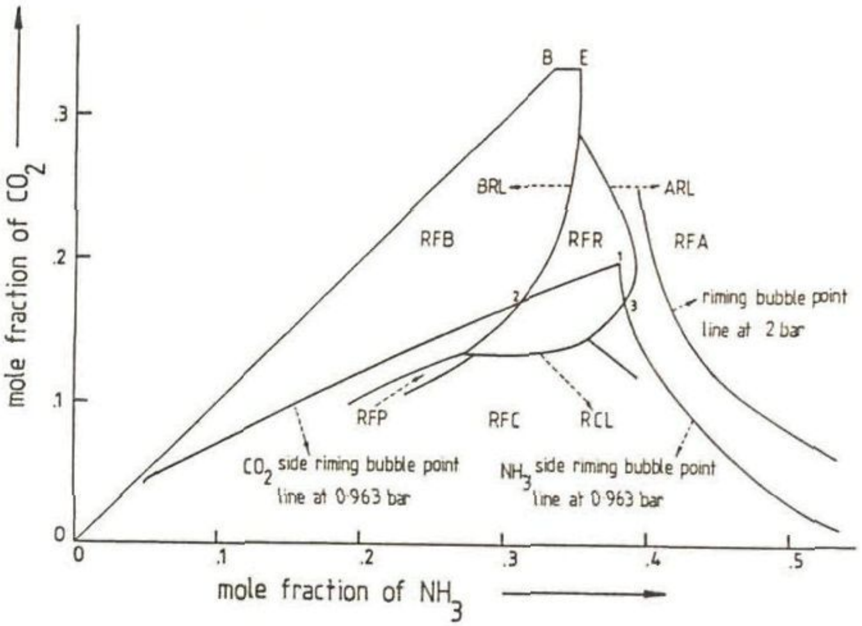

Fig. 3.8. *The loci of riming bubble points and the double riming liquid compositions. RFB denotes the riming field of B. Similarly RFR - R; RFA - A; RFC - C. B denotes the composition of bicarbonate and E denotes the eutectic of B and A. ARL, BRL and RCL denote the double riming boundary lines.*

As is evident in Fig. 3.8, the riming bubble-point curve at 0.963 bar (the curve measured by Guyer and Piechowitz) has a discontinuity at the point marked (1). The two branches (which are really the loci of the liquid compositions of the B-R-L and the A-R-L equilibria), on either side of the discontinuity, intersect the boundaries of the riming regions at two points marked (2) and (3) in the figure. The quadruple point BRLG (2) (31.0 mole% NH_3, 17.4 mole% CO_2 and 58°C), the quadruple point ARLG (3) (38.0 mole% NH_3, 17.2 mole% CO_2 and 52°C) and the S-L-G onset point (1) (35.5 mole% NH_3, 19.3 mole% CO_2 and 65°C) at 0.963 bar have been established and presented by Broers [3] and Verbrugge [8].

Unfortunately when it comes to higher pressures, one is hampered by the dearth of data and is therefore unable to trace similar CO_2-side branches of the riming bubble point curves. Regarding the NH_3-side branches, not withstanding the doubts mentioned earlier concerning the negligiblity of the vapour volume and also due to the lack of any other data, one may provisionally plot the data of Takahashi et al, as is done in Fig. 3.8.

Looking at the curvature of these NH_3 side branches of the riming bubble-point curves in the Fig. 3.8, one may assert that at pressures higher than 2 bar the discontinuities associated with the riming bubble-point curves have to occur in the riming field of A. It is to be emphasized that the present author does have reservation about such an inference, since it depends very much on the validity of the data of Takahashi et al. Nevertheless this inference, if found valid, answers one important querry, namely which salt is involved in the onset of S-L-G as the system is cooled from temperatures above that of the S-L-G onset. Incidentally such an inference brings forth a special feature of carbamate. Unlike the equilibria with the salt R, the S-L-G onset equilibria involving carbamate gives way simultaneously to two separate L-G and S-G equilibria on increasing the temperature. This behaviour is mainly due to the high minimum melting point of carbamate and because carbamate is a binary compound. In other words, the solid carbamate, on increase of temperature from the S-L-G onset, will always disappear only by sublimation and not by melting. The present writer is indebted to Dr.H.S. van der Kooi for clarifying this point.

There is one more interesting aspect of the present system. When the A-R-L boundary is intersected by the NH_3-side branch of the riming bubble-point curve (points like (3)) at pressures around 1 bar, the gas phase of the ARLG is NH_3-rich, and when the A-R-L boundary is intersected by the CO_2-side branch at pressures above 2 bar, it is CO_2-rich. Hence at an intermediate pressure when the discontinuity of the riming bubble-point curve falls right on the A-R-L boundary, one should get the ARLG point giving way directly to an L-G and A-G equilibria, as shown in Fig. 3.9.

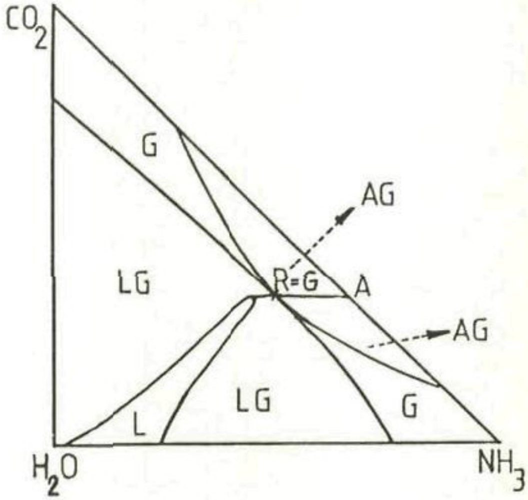

Fig. 3.9. *The ARLG quadruple point, giving rise to LG and AG equilibria directly upon a slight temperature increase. At the equilibrium, the probable composition of G = R.*

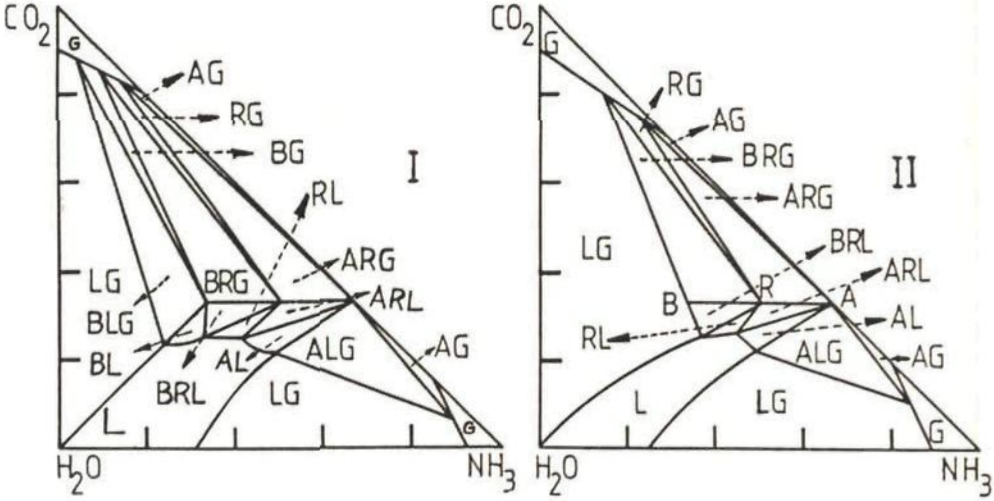

Fig. 3.10. *Multiphase equilibria of the NH_3-CO_2-H_2O system.*

I. Below the BRLG equilibria temperature. II. At BRLG equilibria temperature.

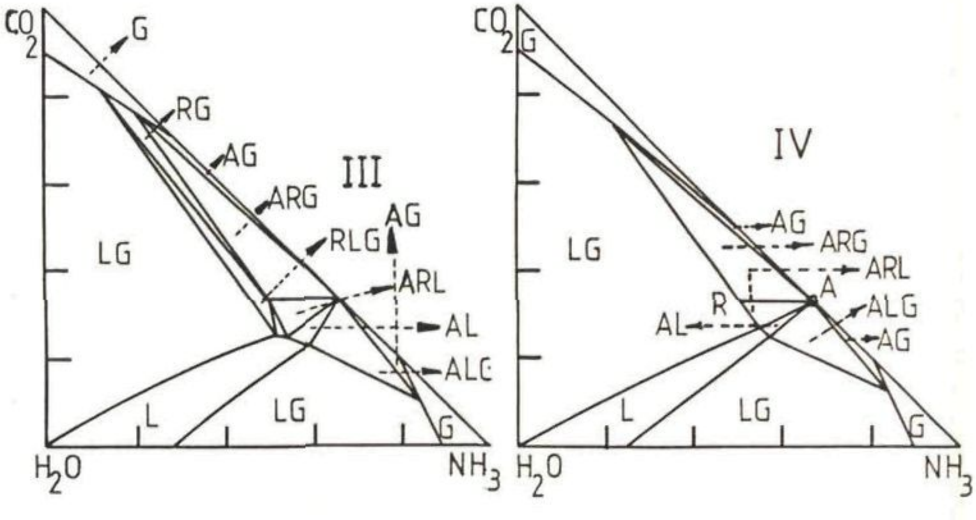

Fig. 3.10. *Multiphase equilibria of the NH_3-CO_2-H_2O system.*

III. Between BRLG and ARLG temperatures. IV. At ARLG equilibria temperature.

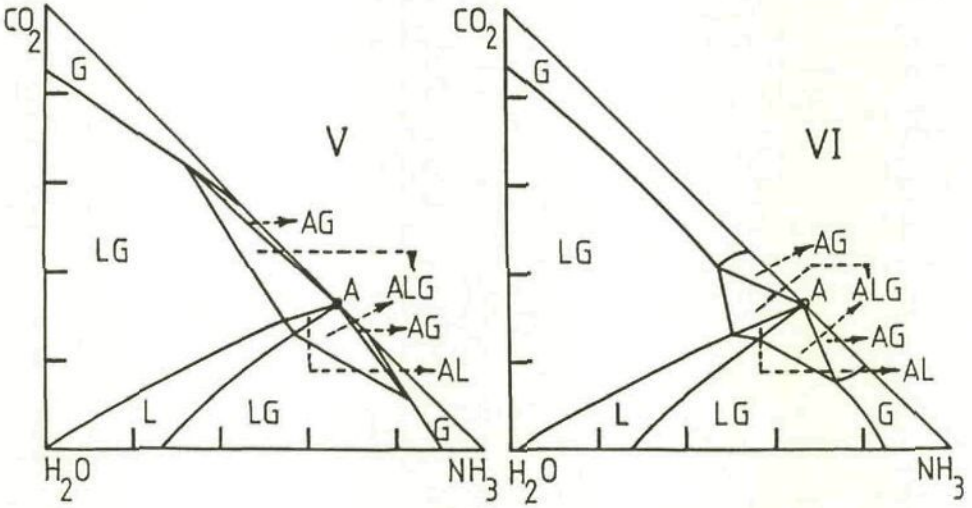

Fig. 3.10. *Multiphase equilibria of the NH_3-CO_2-H_2O system.*

V. Just above ARLG equilibria temperature. VI. Approaching ALG temperature.

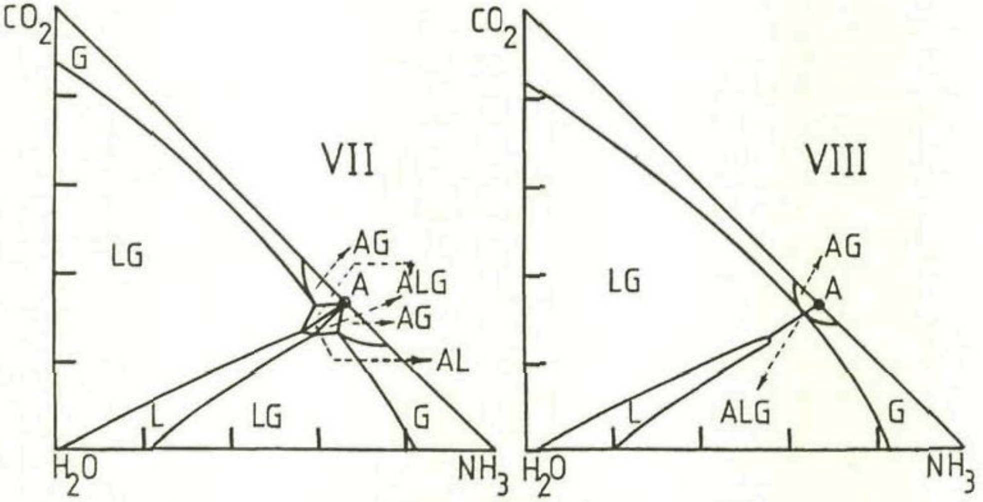

Fig. 3.10.*Multiphase equilibria of the NH_3-CO_2-H_2O system.*

VII. Close to ALG equilibria temperature. VIII. At ALG equilibria temperature.

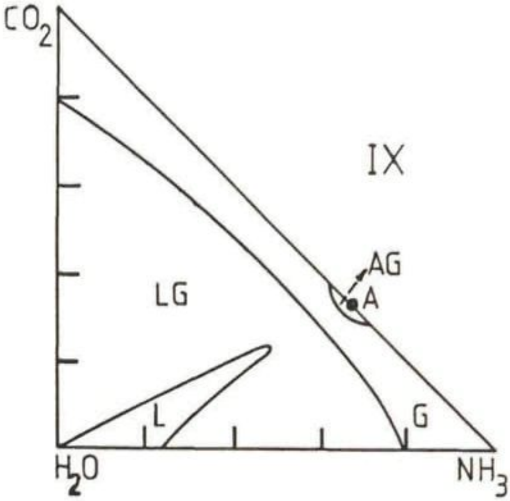

Fig. 3.10.*Multiphase equilibria of the NH_3-CO_2-H_2O system.*
IX. Continous LG and AG regions. Approaching AG equilibria temperature.

Consolidating various special features, the probable behaviour of the NH_3-CO_2-H_2O system at a pressure greater than 2 bar are qualitatively sketched in Fig. 3.10 (I) to (IX). There are four important p-T sections in Fig.3.10 related to the BRLG, ARLG, ALG onset, and AG equilibria. With the available data, only the first and the last equilibria temperatures for various pressures can be estimated, and these are usually sufficient for industrial applications and for planning VLE experiments.

Table 3.3. *BRLG and AG equilibria temperatures for the experimental pressures chosen in the present study.*

Pressure in bar	BRLG equil.temp. in °C	AG equil.temp. in °C
5.41	82.00	90.75
10.00	89.60	104.15
20.00	97.20	120.45
30.00	101.00	130.66

The BRLG temperature can be read from the data of bicarbonate S-L-G equilibria [17,18], since the gross composition equalling the bicarbonate composition has to be also in equilibrium with R in quartenary systems. The reader may refer to Fig. 3.8

once again to appreciate this argument. Further, the A-G equilibria temperature is the same as the dissociation temperature of ammonium carbamate at the given pressure. (See appendix A.) The BRLG and AG temperatures for the experimental pressures chosen in the present study are presented in Table 3.3.

3.3.8. *Topological features of the T-x surface and the distillation boundaries*:

Before concluding the discussion of the NH_3-CO_2-H_2O system (without urea), it is essential to understand two aspects related to the urea, melamine and sour water stripping processes. The first aspect concerns the pressure minima (temperature maxima) in the constant p-x (T-x) sections and the tongue-like character of the bubble-point curve in the constant p-T sections. The second aspect is related to the stripping technique in urea processes and the possibility of obtaining pure CO_2 and NH_3 through fractionation in the melamine and sour water stripping processes. Thermodynamically the second aspect is related to the distillation boundaries.

In this section, the topological features of the isobaric T-x surfaces or (equivalently the isothermal p-x surfaces) are treated first, followed by the distillation boundaries related to the T-x surface.

As asserted earlier, the only possible ternary phase equilibria above the decomposition temperature of NH_4COONH_2 at each pressure are the L-G equilibria covering the whole region of the ternary composition simplex extending from the CO_2-H_2O side to the NH_3-H_2O side. If the system were ideal, the isothermal bubble-point surface would be a two dimensional plane in the p-x space, and the dew-point surface would be a rectangular hyperboloid in the same space [1]. Instead, the presence of a binary azeotrope in the system (NH_3-CO_2) induces the bubble- and dew-point surfaces of the present system to buckle. In other words, the binary azeotropic point behaves as a mathematical "singularity" [45].

Azeotropy in two phase equilibria is a particular case of general phenomena known as phase reactions [46] during which the relative amounts of the phases at a given gross composition in a closed vessel can be changed at will by heating or cooling with no effect on the intensities like the phase compositions, pressure and temperature. Such phase reactions are not something unusual in phase equilibria. These are rather common occurrences. For example the process of pure component evaporation is a phase reaction. The consequence of phase reactions for a multicomponent VLE leads to special features, one of which can be understood easily in terms of material balances. Denoting the liquid compositions for components ($i = 1$ to c) as x_i, the gas compositions as y_i and the gross compositions as z_i, the material balances per mole of the gross amounts with L moles of liquid and (1-L) moles of gas can be written as follows.

$$L*x_i + (1-L)*y_i = z_i \qquad i = 1 \text{ to } (c-1) \qquad \text{(eq. 3.9)}$$

Remembering the functional dependence of y_i on x_i, p and T, one can differentiate the above relations with respect to L and get the following:

$$(x_i - y_i) + L*\left(\frac{dx_i}{dL}\right) + (1-L)*\left(\sum_{j=1}^{(c-1)} \left(\frac{\partial y_i}{\partial x_i}\right)*\left(\frac{dx_i}{dL}\right) + \left(\frac{\partial y_i}{\partial p}\right)*\left(\frac{dp}{dL}\right) + \left(\frac{\partial y_i}{\partial T}\right)*\left(\frac{dT}{dL}\right)\right) = 0$$

(eq. 3.10)

Stipulating the phase reaction conditions (i.e. $dx_i/dL = 0$, $dp/dL = 0$ and $dT/dL = 0$) one gets the well-known result

$$x_i = y_i \qquad i = 1 \text{ to } c. \qquad \text{(eq. 3.11)}$$

Thermodynamic textbooks usually define azeotropy as a state in which the two phase compositions are equal. Such a receipe although factual gives a poor perspective of azeotropy by missing the aspect of phase reactions.

Many thermodynamic features have two aspects; one by viewing the feature as a state produced by a phenomenon and the other by viewing it as a phenomenon induced by a state. Both are valid view points, and one is the inverse of the other. Viewed as a state, azeotropy belongs to a class of indifferent states with phase composition equalities. Such states are indifferent because the intensities are not affected by the extensity changes. Given the phase composition equalities, the converse can be proved *viz.*, that dp/dL, dT/dL, dx_i/dL and dy_i/dL are equal to zero; in other words we can establish the existence of phase reactions related to the indifferent state of equal phase compositions.

Further to the phase reaction conditions, there are pressure and temperature extreme at the azeotropic point leading to ridges (or troughs) in the ternary bubble- and dew-point surfaces. Such extremities in the binary system NH_3-CO_2 can be expressed as follows with x_n denoting the mole fraction of NH_3.

$$(dT/dx_n) = 0 \text{ at constant pressure, or} \qquad \text{(eq. 3.12)}$$

$$(dp/dx_n) = 0 \text{ at constant temperature.} \qquad \text{(eq. 3.13)}$$

3.3.8.1. *The ridge curve*:

There are many assertions in the literature [47,48,49] equating the ridges and troughs with the distillation boundaries (about to be treated shortly). There are also counterclaims to the contrary [51,52,53,54]. In order to assess these conflicting views, one needs a workable definition of ridges and troughs with no reference to the distillation boundaries. Restricting the discussion to an isobaric ternary system (illustrated in Fig. 3.11) with one binary maximum temperature azeotrope, some

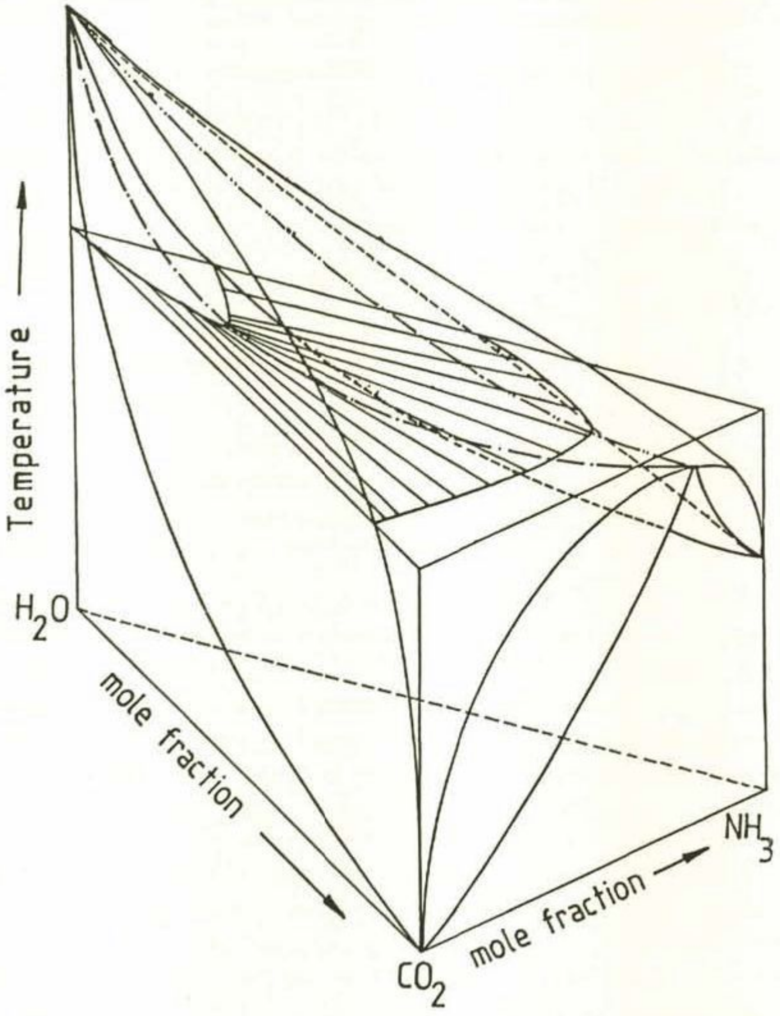

Fig. 3.11. *Bubble-point and dew-point surfaces of a ternary system with one binary maximum temperature azeotrope. The dot-dashed lines represent the liquid and gas ridge curves. Also a constant p-T cross section is shown along with tie-lines. Just for easy understanding, the bubble- and dew-point surfaces are shown as touching the pure componont boiling temperatures. In reality, with the condition being above critical, the binary envelopes on the NH_3-CO_2 side do not touch the pure component ordinate.*

of the definitions presented in the literature can be reviewed. In the figure, the components NH_3 (N) and CO_2 (C) form a binary azeotrope NH_4COONH_2 (A), and H_2O (W) influences the formation of a ridge.

These definitions as applied to the present system may be given as follows:

1. Starting from the binary maximum azeotropic composition, erect constraint planes of constant W composition. Along the intersection curves of these planes with the T-x surface, establish the maximum temperature points. The locus of such points in the T-x surface is called the ridge curve [54].

2. The ridge curve is the locus of points of maximum curvature of the isothermal isobars in the T-x surface [55].

3. The ridge curve is a curve on the T-x surface dividing the families of tie-line directions [56] .

4. The ridge curve is one in the T-x surface such that at each chosen point of the curve, if a composition constraint plane is erected normal to the ridge, the intersection of the said plane with the T-x surface shows a temperature maximum at the chosen point [57]. (This definition differs subtly from the original source.)

While all these definitions are valid, there are inefficacies and inconveniences in some of them. For example, the first one is too special for systems having one binary azeotrope. Any constaint plane will be sufficient for these systems to establish the temperature maximum, and the choice of constant W composition planes is convenient and simple. But when more binary azeotropes and in some cases a ternary azeotrope occur causing more than one ridge branch, this definition will not work. Similarly the second definition is limited to systems containing only one binary azeotrope, and algorithms based on this definition are rather difficult to implement in highly non-ideal systems. The third definition, although concise, is unworkable in the stated form, except by a very large number of phase equilibria measurements. The fourth definition is free from all these difficulties, since it uses only the intrinsic properties of the ridge curve and the T-x surfaces. One can also alternatively state the fourth definition in a still more convenient form which is easy to visualize and whose vality was established by Sobolev et al [55]. Additionally this alternative form bears a close relation to the third definition given above.

"For each point in the constant p-T bubble point curve, associate a tie line direction and a normal. Scanning all the points in the bubble point curve, find out the point having its tie-line direction coinciding with its normal. Such a point is called the ridge (trough) point. The locus of all such ridge (trough) points obtained from each p-T section and plotted at constant pressure (temperature) is called the isobaric (isothermal) ridge curve."

A general algorithm to find the ridge curves using the fourth definition is given by Doherty et al [57]. The present writer has used the first definition to establish the ridge curves of the system NH_3-CO_2-H_2O utilizing the local model of Durisch [43], and the related software is listed in Appendix B. Such a software is needed to optimize the HP condenser temperature of the stripping processes and that of the Hot Gas Recycle Process (HGRP) for urea manufacture.

Further to the application on high pressure condensers, the ridge curves are relevant in deciding which of the solutions are stripped economically by CO_2 and which are best stripped by NH_3. This aspect has been lucidly dealt with earlier by Kaasenbrood [54].

3.3.8.2. *The distillation boundaries and the residue curves*:

Leaving the ridge curves for the moment, one can move to the distillation boundaries. One of the simplest distillation process is the open evaporation process (also known as the Raleigh distillation process) [58] in which a solution of given composition is boiled isobarically and the vapour is continously withdrawn as soon as it is formed. Starting with one mole of the liquid ($L_0 = 1$), let the withdrawal rate be kept very small so as not to disturb the equilibrium inside the vessel. One may write the material balances valid at any instantaneous moment as follows.

$$L*dx_i + x_i*dL = y_i*dL \qquad i = 1 \text{ to } (c-1) \qquad \text{(eq. 3.14)}$$

Rewriting the above relation and denoting (-ln L) as , one gets

$$dx_i/d \quad = (x_i-y_i) \qquad i = 1 \text{ to } (c-1) \qquad \text{(eq. 3.15)}$$

When the still runs dry, L becomes equal to zero, and hence will tend to . Correspondingly can serve as a parameter to follow the progress of the liquid composition during the simple distillation. Since the infinitesimal amount (-dL) of the vapour withdrawn at any moment is in equilibrium with the liquid, one may again consider the y_i ($i = 1$ to c-1) to be the functions of x_i, p and T. Hence it is possible to solve the above set of autonomous differential equations, provided the pure component points are *not* included in the integral solution curves. Thermodynamically the trajectories of these differential equations, known as the simple distillation residue curves, can approach the vertices as much as one wants to, but cannot end technically at these points, and cannot intersect each other. Further, the liquid composition in a simple distillation always move in the direction of boiling point increase [45]. A qualitative illustration of residue curve trajectories in the ternary composition simplex is shown in Fig. 3.12. In addition to the residue curves, one may also follow the distillate compositions (in equilibrium with the residue compositions) and associate a distillate curve. Given these two curves, it is possible to locate the tie-lines through a simple construction, as follows.

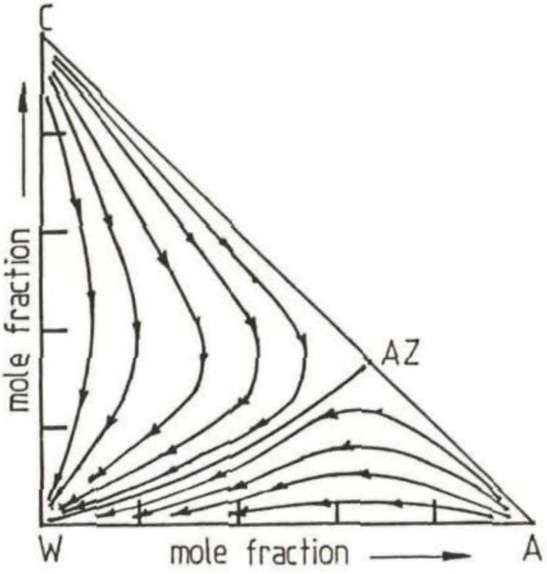

Fig. 3.12. *The qualitative behaviour of the residue curves. The distillation boundary curves separate the section into 2 regions.*

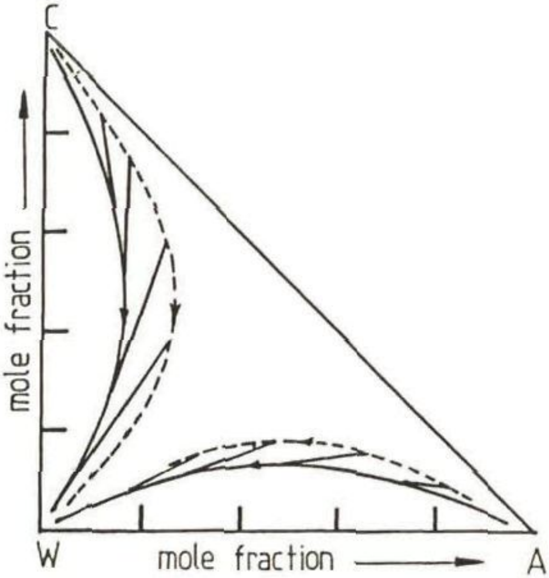

Fig. 3.13. *The tangent construction to identify the tie-lines from the residue curve (marked as full line) and distillate curve (marked as dashed line).*

First one erects tangents at various points of the residue curves. These tangents intersect the distillate curves to give the equilibrium vapour compositions of the chosen liquid compositions. An example of this construction is given in Fig. 3.13. Incidentally, the residue and the distillate curves of a binary system are just respectively the bubble- and dew-point curves themselves.

The behaviour of the simple distillation residue curve can become complicated in systems showing phase reaction at isolated composition points in addition to the pure component state. For example, introducing the phase reaction conditions ($dx_i/dL = 0$) in the simple distillation equations (eq. 3.14) suggests that the azeotropic points act as singularities in organizing the integral curves of the simple distillation. In other words, such points act as nodes, foci, saddles or centres. The residue and *distillate curves of the NH_3-CO_2-H_2O system are very similar to the one illustrated* in Fig.3.12 and Fig.3.13. More complicated systems and residue curves are beyond the scope of the present discussion, and the reader is referred to Doherty et al [45,59].

As the reader may observe in Fig. 3.12, the residue curves approaching the least volatile component split into two families, one starting from the neighbourhood of the most volatile component and the other from the neighbourhood of the component of intermediate volatility. The distillation boundary between these two families is an unusual trajectory obtained through a simple distillation of a very large amount of ternary solution having its composition equal to that of the binary azeotrope with a negligible impurity of the third component.

Having noted the features related to simple distillation one may wonder as to what use they can possibly have for processes involving continous fractionation. A simple answer is the fact that the liquid composition profiles in a continous fractionation column resembles largely the simple distillation residue curves and that these two become identical at the total reflux operation [57]. Such prior knowledge about the possible composition profiles at total reflux is very useful in tight designs of distillation coloumns.

3.3.8.3. *Are the ridge curve and the distillation boundary the same?*

Summarising, one may say that the ridge curve of the present system starts at the binary azeotrope, and the distillation boundary starts very close to the binary azeotrope. Regarding the end-points, Chermin [60] claims to prove that the ridge curve has to end in one of the non-azeotropic binary system (in the present case it appears to be NH_3-H_2O system) and not at the third vertex. It is already said that the distillation boundary approaches the third vertex, but not quite to the end. Now, the crucial question is: Are these two curves the same? It is difficult to provide a conclusive answer from a theoretical point of view, but at least in the present system in view of the available experimental VLE data, these two curves appear to be experimentally indistinguishable.

Chermin [60] also proves that each point in the liquid ridge curve is connected to another point in the the gas ridge curve through a tie-line. In other words, if a tie-line direction coincides with the normal to the bubble-point curve, it will also coincide with the normal to the dew-point curve.

Before moving on to the next ternary system, there is one final remark concerning the supposedly impassable character of the distillation boundaries.

The only restriction the distillation boundaries pose is on the set of residue compositions which are split into two regions. If a solution in region I is distilled, the residue compositions would continue to remain in the same region but the distillate composition may move to the second region. Accordingly one can always separate a given mixture by stepwise fractionation, skillfully utilizing the distillate curve and residue curve behaviour. The reader may refer to Zernike [1] and Doherty et al [45] for the underlying *rationale* of the separation. There is also the method of Schreinemakers [60] mentioned in many patents [61] to transgress the boundary using stills operating at two different pressures to obtain pure NH_3 and pure CO_2 from NH_3-CO_2-H_2O solutions.

3.4. *The ternary system ammonia-urea-water*:

Often in phase equilibria studies, investigations on one subsystem bring up similarities and differences with respect to another leading to fundamental changes in the way one looks at the global behaviour of a combined system. This is also true of the NH_3-CO_2-H_2O system (with equilibrium concentration of urea).

Adopting the reciprocal salt-pair square as a model for the p-T sections, as shown in Fig. 3.14, Lemkowitz [62] presented the bubble- and dew-point behaviour of the NH_3-CO_2-H_2O system (with equilibrium urea concentration) above and below the saddle azeotropic point.

As the reader may observe in Fig. 3.14.(a), the shape of the bubble- and dew-point curves at constant p and T in the triangular subregion of the $(2NH_3)$-CO_2-H_2O system at chemical equilibrium very much resembles the behaviour of the same system at physical equilibrium (i.e. with no urea formation). In other words, the qualitative behaviour at conditions below the saddle azeotrope is not influenced as the urea formation proceeds. Now curiosity arises as to know whether the behaviour of the system at chemical equilibrium above the saddle azeotropic conditions has an analogue in some other system at physical equilibrium. The likely canditate appears to be the $2NH_3$-H_2O-NH_2CONH_2 system whose probable behaviour is presented in this section.

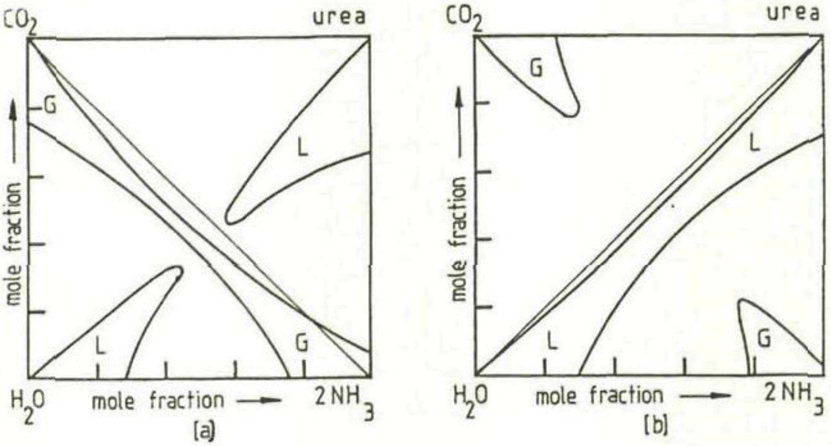

Fig. 3.14. *Reciprocal salt-pair phase model proposed by Lemkowitz [62] for the NH_3-CO_2-H_2O system at chemical equilibrium. (a) - pressure below the saddle azeotrope pressure; (b) - pressure above the saddle azeotrope pressure.*

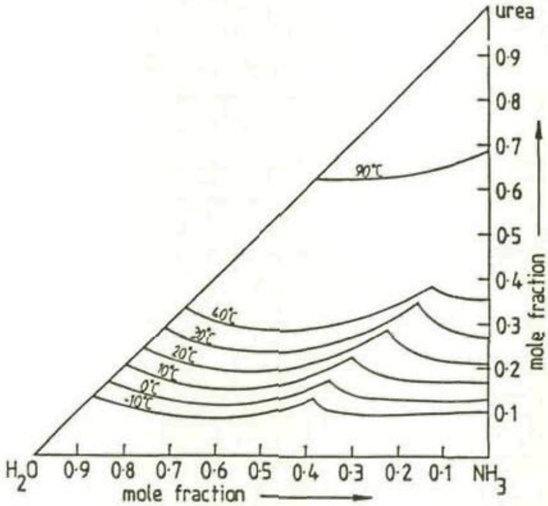

Fig. 3.15. *The solubility characteristics of the NH_3-H_2O-NH_2CONH_2.*

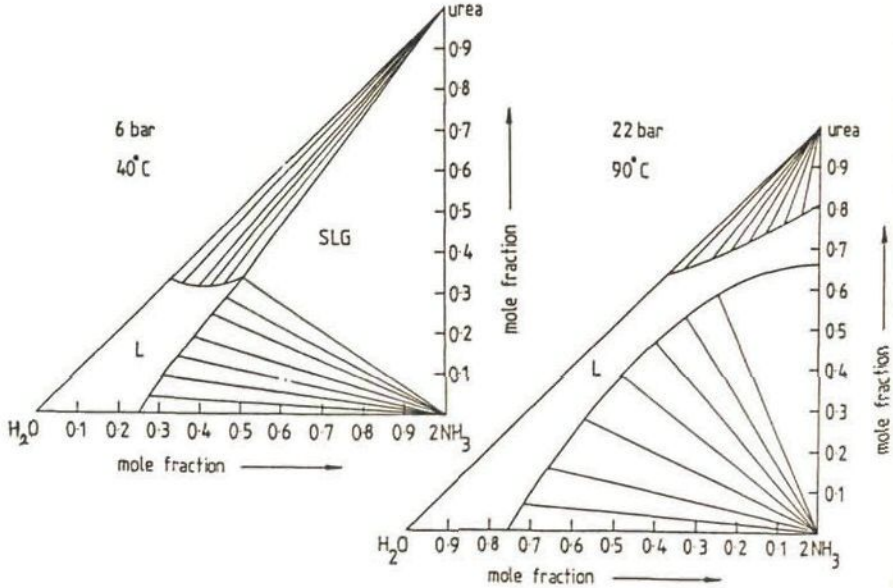

Fig.3.16. *The* NH_3-H_2O-NH_2CONH_2 *system. (a) at 6 bar-40°C and (b) at 22 bar-90°C.*

The solid-liquid equilibria of the NH_3-H_2O-NH_2CONH_2 system was investigated by Jänecke [30] and Worthington et al [63], mainly at low temperatures (i.e. up to 40°C). The binary addition compound $NH_2CONH_2.NH_3$ influences the ternary solubility behaviour up to 46°C. Since the temperature dependence of the solubility compositions at constant $(NH_3)/(H_2O)$ ratio is fairly linear, it is possible to extrapolate at least up to 90°C. The solubility characteristics of the system utilizing the (recalculated) literature and extrapolated data are represented in Fig. 3.15.

Regarding the vapour pressure data, again one has to rely on Jänecke [30] and Worthington et al [63]. While Jänecke's data were related to the saturated solutions (S-L-G equilibria), the data of worthington et al were concerned with the bubble-point behaviour of the unsaturated solutions. Combining the solubility and bubble point data of Worthington et al together with Jänecke's S-L-G data and through extrapolation, it is possible to trace the system behaviour at 6 bar-40°C and 22 bar-90°C as shown here in Fig. 3.16 (a) and (b). Now as the reader can easily observe, the bubble point behaviour of the NH_3-CO_2-H_2O system in chemical equilibrium above the saddle azeotropic conditions remarkably resembles the NH_3-H_2O-NH_2CONH_2 system at physical equilibrium.

With this brief presentation completed, the quarternary system will now be discussed in the next section.

3.5. *The quarternary system NH_3-CO_2-H_2O-NH_2CONH_2 and its transformation to the ternary system at chemical equilibrium:*

3.5.1. *The concept of a manifold:*

As suggested in the previous chapter, this system remains quarternary only in a restricted range, the limits of which are hard to establish exactly, since the range depends on the relative rates of the various chemical reactions and the speed of the phase composition measurements. Somewhat arbitrarily, one may define the quartenary system to exist up to about 100°C and about 30 bar. Beyond this range, the urea formation and hydrolysis proceed to appreciable extents at significant rates, and the system gradually turns into a ternary one at chemical equilibrium. Similarly the NH_3-CO_2-H_2O ternary system at physical equilibrium also transforms into a ternary system at chemical equilibrium. Such behaviour is associated not only with the system composed of NH_3, CO_2 and H_2O, but also with many other systems. To put it precisely, the ternary and quarternary systems at physical equilibrium are just the transitory entities in their eventual transformation to the ternary system at chemical equilibrium. Such a transitory character in turn raises the age-old basic question about the spacial representation of the reactive phase equilibria.

According to phase rule,

$$F = c + 2 - r \qquad \text{(eq. 3.16)}$$

where F is the number of intensities which can be independently varied in any equilibria, c is the number of components and r is the number of phases. Since at least one phase has to be present, one needs a space with a minimum of (c+1) dimensions to illustrate all possible phase behaviour.

This space is invariably chosen to be Cartesian orthogonal by almost every phase equilibria investigator, probably due to accepted traditions, irrespective of the presence or absence of possible simultaneous reaction equilibria. While this choice is pragmatic and in most cases sufficient, there are features like important species concentrations which cannot be represented in the Cartesian space. Afterall, the phase rule dictates only the dimensionality of the needed state space and states nothing about the representation of it. When nature prefers no special co-ordinate system imposed on it, there is a price to pay for the insistence on the Cartesian orthogonality of the working space: "The descriptions of the reactive phase equilibria will become piecemeal."

For example with the phase model of the NH_3-CO_2-H_2O system at chemical equilibrium suggested by Lemkowitz [62], one cannot deduce whether the maximum urea yield is related to the minimum bubble-point. To do that, one needs additional, more complex diagrams and/or new models. (These might be the conversion formula due to Kucheryavyi [64] or Inoue [65]). Such additions may provide acceptable numerical answers but no graphic and lucid explanations of the phenomena involved. What is needed however is a fundamentally new way of presentation through manifolds.

The use of manifolds for representing reactive phase equilibria was first suggested by Chermin [60] with a specific view of applying it to the NH_3-CO_2-H_2O ternary system at chemical equilibrium. Recently, the manifold representation of the reactive phase equilibria was hinted in a cursory manner by Perry et al [66]; but the emphasis was in developing the general formalism and not on exploring the topological features of the dew- and bubble-point surfaces.

Chermin's attempt in this direction was largely aimed at explaining the saddle azeotropy of the NH_3-CO_2-H_2O system at chemical equilibrium. While he forcefully contested the novel phase model of the Delft school [62], he barely sketched his alternative proposal at the Fertilizer Society of London [67]. Since Chermin's model is very relevant to the general problem of representing the reactive phase equilibria and not necessarily to the particular problem on urea systems, it is worthwhile to discuss the various features of the same in little more details. What is described below is largely Chermin's work together with the present author's substantial re-interpretations and explanations.

3.5.2.1. *The stoichiometric composition spaces (or the SC spaces)*:

A manifold may be intuitively understood as a hypersurface with only a local co-ordinate system defined on the neighbourhood of any chosen point. Further the manifold may be immersed in higher dimensional ambient spaces with a global co-ordinate system. An obvious example is the earth surface with the left-right and front-back co-ordinates and immersed in the 3-dimensional space.

Now moving to the phenomena of reactive phase equilibria, consider a concrete example of a two component system composed of S_1 (say NH_3) and S_2 (say CO_2) reacting further towards S_3 (say ammonium carbamate).

$$\nu_1 S_1 + \nu_2 S_2 + \nu_3 S_3 = 0 \qquad \text{(eq. 3.17)}$$

Also assume that the system composed of species S_1 and S_2 at physical equilibrium (i.e. a relatively fast transfer of species between the phases without any appreciable formation of S_3) exhibits azeotropy.

To represent this reactive system at constant pressure by a manifold, one needs a 3-dimensional ambient space. With two co-ordinates to represent the species compositions coupled with the normalisation condition of the mole fractions, the composition space may be chosen as a right triangular simplex with the hypotenuse representing the system S_1-S_2 at physical equilibrium. The temperature co-ordinate can be erected vertically above the right triangular simplex.

Now, as often stressed earlier, it is difficult to measure the physical equilibria alone by inhibiting the reaction equilibria. Nevertheless, quite a number of investigators have tried ingenious ways to circumvent this problem and have often succeeded. Plotting such data on the vertical plane erected above the hypotenuse yields the familiar bubble- and dew-point envelopes.

Now the question is how an arbitrary point in the bubble- and dew-point envelopes of the hypotenuse plane will move into the prism as the reaction proceeds. The answer is easily provided for a reaction of m species by the principle of equal proportions as follows:

$$\frac{dn_i}{\nu_i} = d\eta \qquad i=1 \text{ to } m \qquad \text{(eq. 3.18)}$$

where ν_i is the stoichiometric coefficient of the species i and n_i is the amount of i in moles and η is the reaction extent. Integrating the above expression from the start to the end of the reaction yields:

$$n_i = n_{i0} + \eta * \nu_i \qquad i=1 \text{ to } m \qquad \text{(eq. 3.19)}$$

Combining the above relation with the definitions of mole fractions one gets:

$$(x_i(\sum_{j=1}^{m} n_{j0}) - n_{i0}) = \eta(\nu_i - x_i\sum_{j=1}^{m}\nu_j) \qquad i=1 \text{ to } m-1 \qquad \text{(eq. 3.20)}$$

Eliminating η from the above independent (m-1) relations, one further gets:

$$(x_i\nu_1 - x_1\nu_i) - (x_ix_1 - x_1x_{10})\sum_{j=1}^{m}\nu_j = \nu_1x_{10} - \nu_ix_1 \qquad i=2 \text{ to } m-1 \qquad \text{(eq. 3.21)}$$

Now the above set of (m-2) relations defines a one dimensional linear subspace in the (m-1) composition space. For a particular case of a binary system at chemical equilibrium with three species, it may be stated as:

$$(x_2\nu_1 - x_1\nu_2) - (x_2x_{10} - x_1x_{20})*(\nu_1 + \nu_2 + \nu_3) = \nu_1x_{20} - \nu_2x_{10} \qquad \text{(eq. 3.22)}$$

The above linear relation between x_1 and x_2 for arbitrary values of x_{10} and x_{20} defines a subspace of the composition simplex, and also partition the simplex into disjointed subspaces, as shown in Fig. 3.17. These subspaces may be called the stoichiometric composition spaces (SC spaces). (Chermin [60] called these subspaces the reaction paths, which in the present writer's opinion may not be appropriate, since no chemical equilibrium relation is used in deriving these subspaces. Furthermore it is difficult to extend the term 'reaction path' to multireaction situations. SC spaces are entirely defined by the stoichiometric principle of equal proportions and by the number of reactions.)

Further to SC spaces, one can get SC-T hyperplanes by erecting a temperature axis over these spaces. These hyperplanes are, in a sense, analogous to the tie-lines of the L-G equilibria. These planes connect the physical equilibrium points to the chemical equilibrium points.

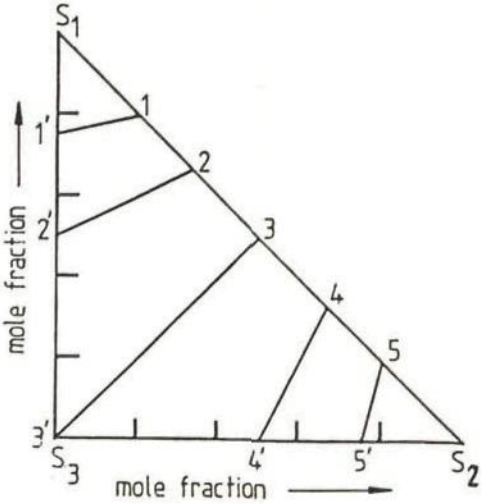

Fig. 3.17.*The stoichiometric composition spaces.*

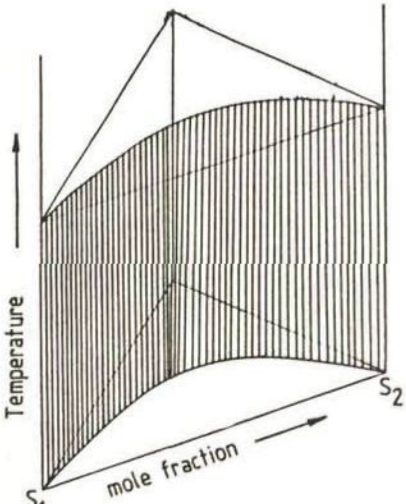

Fig. 3.18. *The reaction equilibrium surface.*

3.5.2.2. *Isobaric reaction equilibrium surface (The RE surface):*

For a simple case of one reaction in a three species system, the following relation is obtained from thermodynamics.

$$\nu_1\mu_1 + \nu_2\mu_2 + \nu_3\mu_3 = 0 \qquad \text{(eq. 3.23)}$$

Further, one may obtain from the above the following implicit relation defining an isobaric reaction equilibrium (RE) surface (Fig. 3.18) by expressing the chemical potentials to be the functions of T and x_i's.

$$g\ (x_1, x_2, T) = 0 \qquad \text{(eq. 3.24)}$$

3.5.2.3. *The intersection of the BP surface and the RE surface:*

For a non-reacting three species system with one boundary system exhibiting azeotropy and the other two behaving regularly, the isobaric bubble-point surface (BP surface at physical equilibrium) will appear as shown in Fig. 3.19.

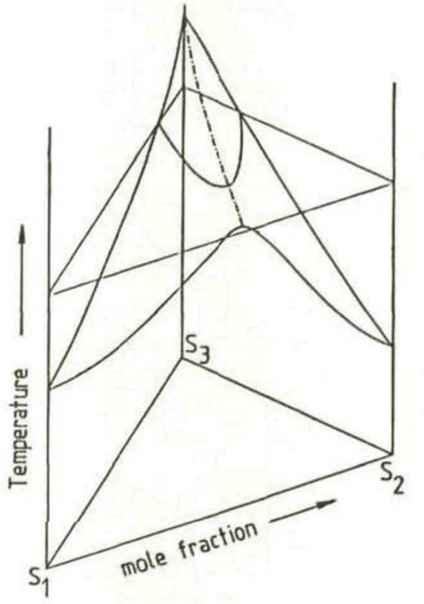

Fig. 3.19. *The bubble point surface of a three species system in which one binary system exhibits azeotropy and the other two behave regularly.*

When the BP and RE surfaces are interposed as in Fig. 3.20, one finds an intersection curve which may be called a reactive bubble-point (RBP) curve satisfying the criteria of simultaneous reaction and phase equilibria. In the same Fig. 3.20, the

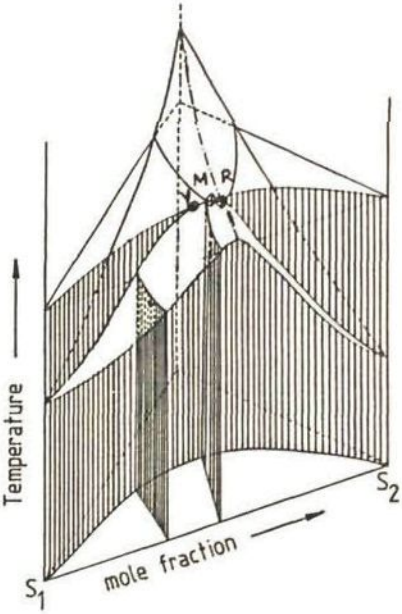

Fig. 3.20. *The intersection of BP and RE surfaces giving rise to the RBP curve. Also in the figure two SC-T planes and their intersection with the BP surface are given. The point of tangency between the RBP curve and the isobaric isothermal curve (marked M) is the maximum bubble point temperature one can achieve in a reactive phase equilibrium with high yield. Left of M the maximal yield point Y is shown. The physical ridge point R is to the right of M.*

intersection curves of the SC-T planes with the BP surface are shown as tie-line like curves connecting the physical bubble-points to the reactive bubble points. One notable feature is the tangency point M of the RBP curve with the isothermal isobaric physical bubble point curve. It is at M that one can simultaneously get a maximum conversion and the highest bubble-point temperature. The maximal yield point with no simultaneous phase equilibria is represented by the point Y and the maximal bubble point temperature with no reaction equilibria is given by R. The temperature of M is slightly less than that of R, and the conversion at M is slightly less than that Y.

The projection of RBP curve on to the composition simplex is represented in Fig. 3.21. The maximal yield point Y, the tangency point M and the ridge point R are also marked in the figure. By following the SC curve connecting the maximal yield point Y, one can identify the point Y_1 in the S_1-S_2 system which gives rise to the maximal yield. One may call such a point in the S_1-S_2 system as the maximum yielding binary point. Similarly, other points like M and R can be related to their respective binary points. Further it can be observed that the intersection point of the physical ridge

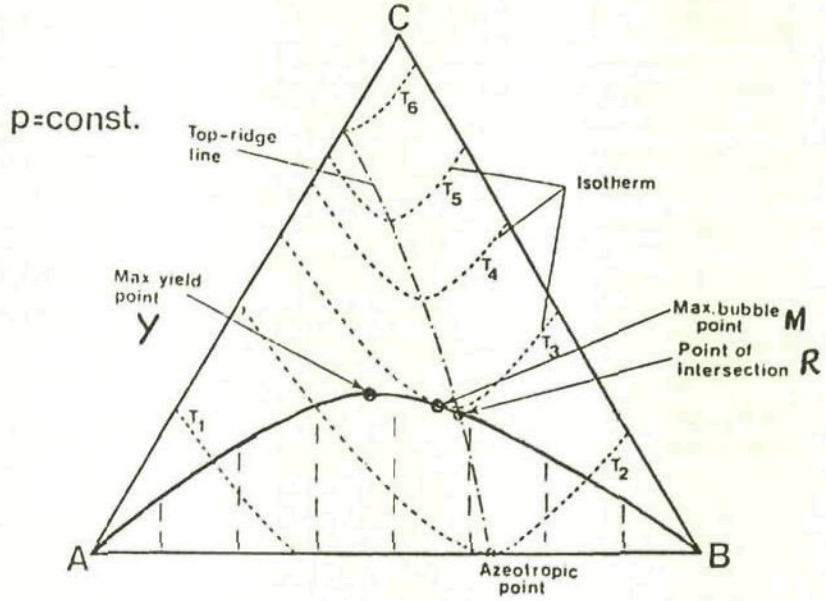

Fig. 3.21. *Projection of RBP curve onto the composition simplex.*

curve with the RBP curve has lost its earlier importance by the very presence of the reaction equilibria.

What has been achieved so far in the physical bubble point surface at one pressure can be repeated at all other pressures to generate additional RBP curves. The collection of all these curves constitutes the RBP manifold. Also one can repeat the same procedure with the dew point surface to get the reactive dew point manifold (RDP manifold). However, these manifolds do not have global co-ordinate systems. In fact, this particular aspect may be discomforting for many researchers used to smooth bubble- and dew-point surfaces in three dimensional p-x-T spaces. But then the fact that the manifold is still two dimensional and that the isobaric or isothermal representation brings up a host of new features suggests that the approach is worth persuing. Admittedly, multireaction and multispecies situation will make these features much more complicated; but a suitable algorithmic approach can be divised to handle such systems.

3.5.2.4. *Application to a four species system*:

Moving to a four species system (ABCD) with one binary azeotrope (BC), one can construct the isobaric isothermal BP and DP surfaces in a tetrahedral composition simplex as shown in Fig. 3.22. Further, if a single reaction constraint is placed on these species,

$$\text{i.e.,} \qquad B + C = A + D \qquad \text{(eq. 3.25)}$$

the resulting isobaric isothermal RE surface will have a saddle shape as shown in Fig. 3.23 due to stoichiometry and the reaction extent. In many systems, the reaction extent can be increased at a constant pressure by changing the temperature. Topologically, such increased extent is reflected by the approach of the saddle surface towards the edge connecting the product species A and D.

Now, if the isobaric isothermal BP surface and RE surface are plotted together on a composition simplex, one gets an intersection curve (i.e., the isobaric isothermal RBP curve) with two branches enclosing two liquid regions. A similar construction with the isothermal DP surface would yield the RDP curve with two branches, but enclosing a single continous gas region. The degeneration of BP and DP surfaces onto RBP and RDP curves in the case of reactive equilibria is shown in Fig. 3.24.

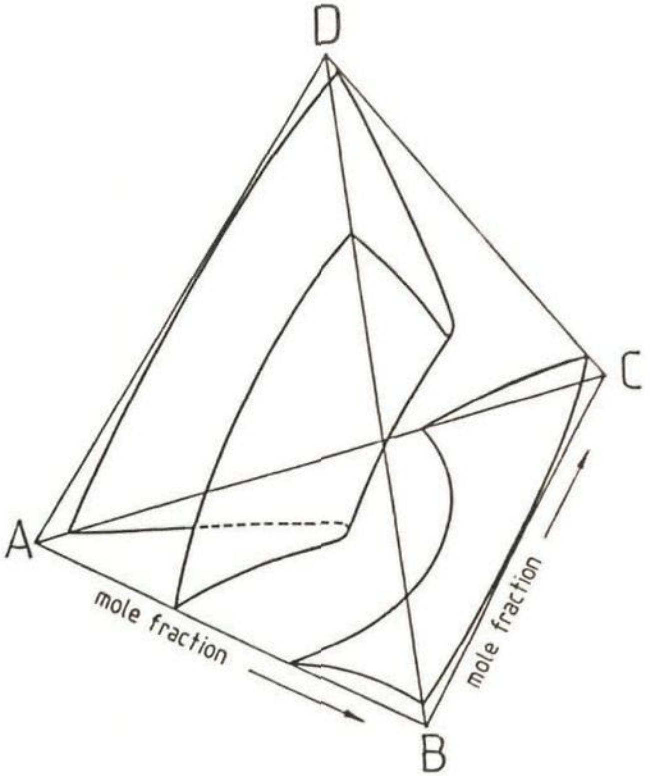

Fig. 3.22. *The isobaric isothermal bubble-point and dew-point surfaces of the quarternary system.*

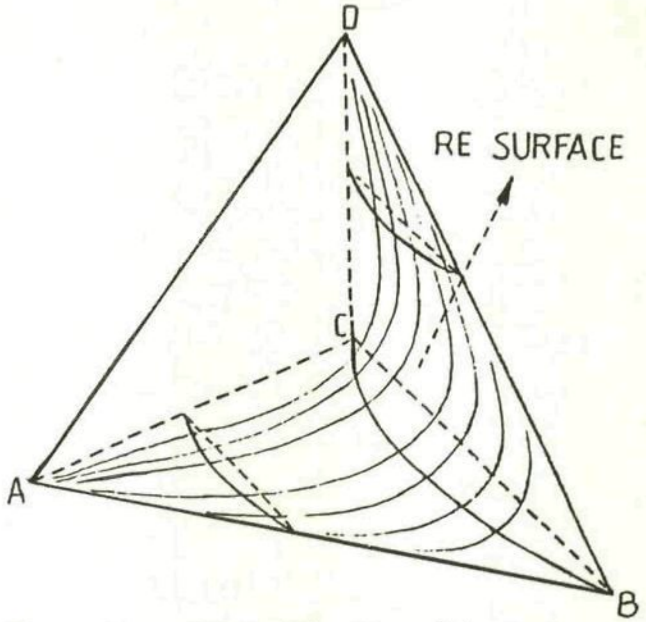

Fig. 3.23. *The reaction equilibria (RE) surface of the quarternary system.*

The existence of two branches in the isobaric isothermal RBP curve raises a question whether these branches will touch each other for some specific conditions. The answer is affirmative at one temperature for each chosen pressure. Beyond that temperature for the chosen pressure, the character of the RBP and RDP curves will reverse, i.e., the branches of the RBP curve enclose a continous liquid region while the branches of the RDP curve enclose two separated gas regions. Incidentally, Chermin [60] proved that if the two branches of the RBP curves touch each other, so do the branches of the RDP curve. Now, how does one interpret the phenomenon of the touching branches and what does one call it ? The Delft School [62] called the phenomenon reactive saddle azeotropy, and Kaasenbrood and Chermin [67] called it the indifferent point. Setting aside the semantic interludes, the significance of the *phenomenon should not be lost. The reader may refer to section 3.3.8* regarding the earlier discussion on azeotropy. If one projects the RBP and RDP curves looking from the 1:1 mole ratio of A-D composition, one will find the gas and liquid compositions to be the same *in terms of the components*, although not in terms of the *species*.

Proceeding further, the collection of the isobaric isothermal RBP and RDP curves in the four dimensional space at constant pressure would constitute the three dimensional isobaric RBP and RDP manifolds. Similarly the three dimensional isobaric RE manifold can be erected. As a result the RBP and RE manifolds would touch tangentially along a curve. The projection of the tangent curve onto the composition

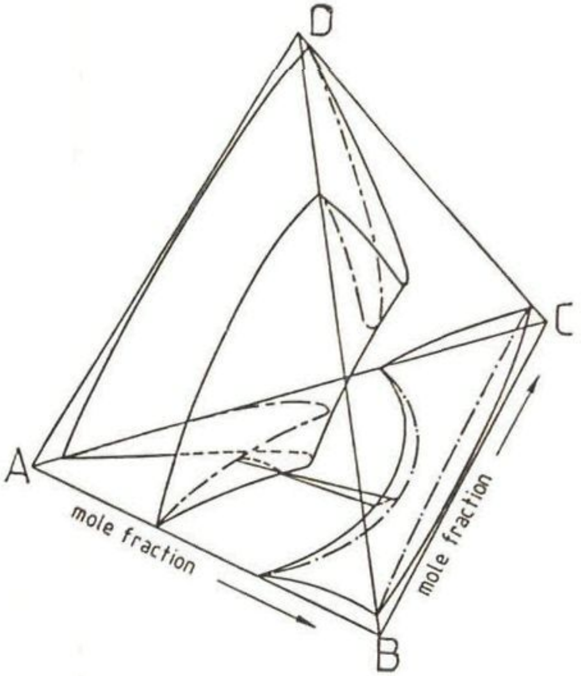

Fig. 3.24. *The degeneration of the quarternary system at physical equilibrium to the ternary system at chemical equilibrium.*

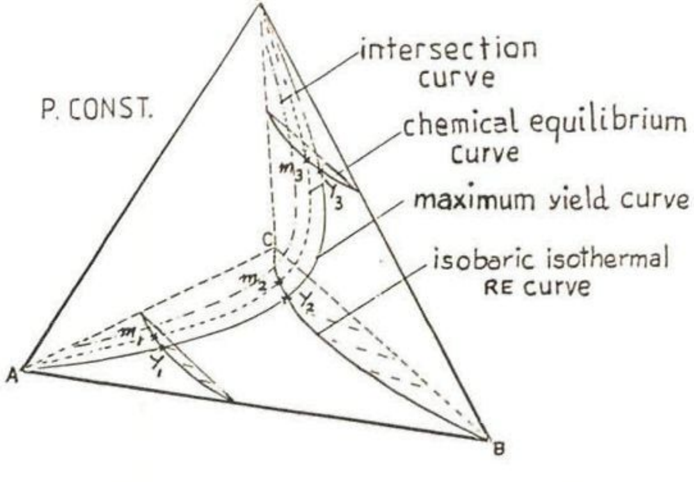

Fig. 3.25. *The CER and other curves projected onto the RE surface.*

simplex is marked on the RE surface of Fig. 3.25. This tangent curve, also known as chemical equilibrium ridge curve (CER curve) is analogous to the tangent point M discussed in the three species case. Similar projection curves like the maximum yield curve and the physical equilibrium ridge curve can all be marked on the RE surface as shown in Fig. 3.25. Further projection of the CER curve in the quarternary composition *simplex onto the reciprocal salt-pair construction (i.e.,viewing from* 1:1 *A-D* point), as mentioned earlier, will give raise to the "equilibrium ridge curve" of the Delft School model.

Following such elaborate discussion on the quarternary system and its transition to the reactive ternary system, it is now useful to move on to the experimental investigation of the ternary system at a pressure range of 5 to 30 bar and a temperature range of 80 to 130°C, in the next chapter.

References:

1. Zernike, J., "Chemical Phase Theory", Kluwer Publishing Company, Deventer, The Netherlands, 1955.
2. Malinin, S.D., "The thermodynamics of the CO_2-H_2O system", Geochemistry International, 1974, pp 1060-1085.
3. Broers, J.N., "The phase behaviour of the ternary system NH_3-CO_2-H_2O at pressures of 1 to 20 atm and temperatures of 20 to 140°C", (in Dutch), Internal report, Department of chemical technology, Delft University of Technology, The Netherlands, 1974, 110 pages.
4. van Aken, A.B. et al, I & E C Fundam., 1975, vol. 14, p 154.
5. van Krevelen, D.W. et al, "Compositions and vapour pressures of aqueous solutions of ammonia, carbon dioxide and hydrogen sulphide", Recueil.Trav. Chim.Pays-Bas, 1949, vol.68, pp 191-227.
6. Frohlich, G.J., "Vapor-liquid equilibria of aqueous systems containing ammonia and Carbon dioxide, PhD thesis, Polytechnic Institute of Brooklyn, 1957.
7. Wicar, S., "Calculation of vapour-liquid equilibrium in the system urea, ammonia, carbon dioxide and water", British Chemical Engineering, 1963, vol.8, no.12, pp 818-822.
8. Verbrugge, P., "Vapour-liquid equilibria of the ammonia - carbon dioxide - water system", PhD thesis, Delft University of Technology, The Netherlands, 1979, 133 pages.
9. Edwards, T.J. et al, "Vapour-liquid equilibria in multicomponent aqueous solutions of volatile weak electrolytes", AIChE Journal, 1978, vol.24, no.6, pp 966-975.
!0. Pawlikowski, E.M. et al, "Phase equilibrrum for aqueous solutions of ammonia and carbon dioxide", I&EC Process Design & Develop., 1982, vol.21, pp 764-770.
11. Muller, G., "Experimentelle Untersuchung des Dampf-Flussigkeits-Gleichgewichts im System Ammoniak-Kohlendioxid-wasser zwischen 100 und 200°C bei drucken bis 90 bar", (in German), PhD thesis, University of Kaiserlautern, 1983.
12. Nakamura, R. et al, "Thermodynamic properties of gas mixtures containing common polar and non-polar compounds", I & E C Process Design & Develop., 1976, vol.15, no.4, pp 557-564.
13. Belyaev, I.N. et al, "The Urea-Ammonium carbonate-water system", Russian Journal of Inorganic Chemistry, 1966, June , vol.11, no.6, pp 787-789.
14. Nitta, I. et al, "The crystal structure of potassium bicarbonate", Acta Cryst., 1952, vol.5, p 292.
15. Brooks, R. and T.C. Alcock, "Crystal structure of ammonium bicarbonate and a possible relationship with ammonium hypophosphate", Nature, 1950, vol.166, pp 435-436.
16. Nakamoto, K. et al, "Normal co-ordinate analyses of hydrogen bonded compounds.

IV. The acid carbonate ion", J.Chem.Phys., 1965, vol.43, no.4, pp 1177-1181.

17. Zernike, J., "Three phase curve of ammonium bicarbonate", Recueil.Trav. Chim. Pays-Bas, 1954, vol.73, pp 95-101.

18. Stobiecki, T et al, Chemia Stosowana, 1957, vol.1, pp 81-88.

19. Bonnier, c., Annals., 1926, vol.5, no.10, p 46.

20. Nishizawa, J.Chem.Ind.Japan, 1920, vol.23, p 630, CA 15, 1237 (1921).

21. Neumann, B. and R.Domke, Z.Elektrochemie, 1928, vol.34, p 136.

22. Hutchinson, W.K., J.Chem. Soc., 1931, p 410.

23. Bell, R.P., "Proton in Chemistry", Chapman and Hall, London, 2nd ed., 1973.

24. Scalar.N & L.C.Carrison, "Phase composition of commercial ammonium carbonate", Science, vol.140, pp 1205-1206.

25. Terres, E. and H.Behrens, Z.Phys.Chem.Abt., 1928, A 139, p 695.

26. Janecke, E., "Uber das system H_2O, CO_2 und NH_3", Z. Elektochemie, 1929, Bd 35, no. 9, pp 716-728.

27. Guyer, A and T.Piechowicz, "Losungsgleichgewichte in wasserige systemmen - das system CO_2-NH_3-H_2O bei 20^o-50^oC, Helve.Chim.Acta, 1944, vol.27, pp 858-867.

28. Takahashi, T. et al, "Equilibrium pressure for NH_3-CO_2-H_2O system", Kogyo Kagaku Zasshi, 1962, vol.65, pp 743-745.

29. Janecke, E., Z.Elektrochemie, 1929, Bd 35, pp 332.

30. Janecke, E., "Uber das system H_2O, CO_2 und NH_3. Forzetzung", Z.Electrochemie, 1930, Bd. 36, no.9, pp 645-654.

31. Otsuka, E. et al, "Equilibrium of the NH_3-CO_2-H_2O system", Kogyo Kagaku Zasshi, 1960, vol.63, no.7, pp 1214-1218.

32. Takahashi, T., "Calculation of the equilibrium for NH_3-CO_2-H_2O system by van Laar equation", Kogyo Kagaku Zasshi, 1962, vol.65, pp 837-843.

33. Jager, L. et al, "Rovnovaha kapalina-para. V. Systemu NH_3-CO_2-H_2O - I", Chemicky Prumysl, 1965, vol.15, pp 404-406.

34. Jager, L. et al, "Rovnovaha kapalina-para. V. Systemu NH_3-CO_2-H_2O - II", Chemicky Prumysl, 1965, vol.15, pp 649-651.

35. Schmidt, P.A., "Enthalpie/Zusammensetzung - diagramm fur Dreistoff systems am Beispiel des systems $NH_3/CO_2/H_2O$", Chem.Ing.Tech., 1976, vol.48, no.6, p 577.

36. Yanagisawa, Y. et al, "Vapour-liquid equilibrium for the ternary system of Ammonia-Carbon dioxide-Water", J.Chem.Soc.Japan, 1973, no.5, pp 917-923.

37. Yanagisawa, Y. et al, "Vapour-liquid equilibrium for the ternary system of Ammonia-Carbon dioxide-Water at 70-99^oC", J.Chem.Soc.Japan, 1975, no.2, pp 271-274.

38. Koren , J.G. and A.J.Andreatch, Anal.Chem., 1965, vol.37, no.2, p 256.

39. Wucherer, J., Z.ges.Kalte-Ind., 1932, vol.39, p 97.

40. A'Campo, C.P.M.G. et al, "Gas chromatographic determination of water: A source of systematic error introduced by interactions of polar compounds on porous

polymer gas chromotographic columns" J.Chromotography, 1981, vol.203, pp271-278.

41. Nakamura, R. et al, "Thermodynamic properties of gas mixtures containing common polar and non-polar compounds", I & E C Process Design & Develop., 1976, vol.15, no.4, pp 557-564.

42. Kawasumi, S., "Equilibrium of the CO_2-NH_3-Urea-H_2O system under high temperature and pressure", Bul.Chem.Soc.Japan, 1951, vol.24, no.3, pp 148-151; 1952, vol.25, no.4, pp 227-238; 1953, vol.26, no.5, pp 218-227; 1954, vol.27, no.5, pp 254-259

43. Durisch, W., "Experimentelle und thermodynamische untersuchung der siedegleichgewichte des systems $CO_2/NH_3/H_2O$ unter Harnstoffsynthese-bedingungen" PhD thesis, Eidgenossischen Technischen Hoghschule Zurich, Switzerland, 1978.

44. Altman, C.J.G., "Sublimation", Education in Chemistry, 1982, Nov., p 165.

45. Doherty, M.F. and J.D.Perkins, "On the dynamics of distillation processes- I", Chem.Eng.Sci., 1978, vol.33, pp 281-301.

46. Münster, "Thermodynamics", Springer, Berlin. 1968.

47. Schreinemakers, F.A.H., Z.Phys.Chem., 1901, vol.36, p 257.

48. Ostwald, W., "Lehrbuch der allgemeinen mischphase", Springer, Berlin, 1956.

49. Haase, R., "Thermodynamik der Mischphasen", Springer, Berlin, 1956.

50. Evell, R.H. and L.M.Welch, I & E C, 1945, vol.37, p 1224.

51. Lang, H., Z.Phys.Chem., 1950, vol.196, p 278.

52. Wilson, R.Q. et al, AIChE Journal, 1955, vol.1, p 220.

53. Bushmakin, I.N. and I.N.Kish, J. Appl. Chem. USSR. (Eng.Transl.), 1957, Vol.30, p 401.

54. Kaasenbrood, P.J.C., proceedings of the fourth European Symposium of Chemical Reaction Engineering, held at Brussels, sept 11,1968, Pergamon Press,1971, p 317

55. Sobolev, D.M. et al, J.Appl.Chem.USSR.(Eng.Transl.), 1981, vol.53, p 1917.

56. Naka, Y. et al,"Changes in distillate composition during ternary azeotropic batch distillations", Kagaku Kogaku, 1974, vol.38, pp 501-507.

57. van Dongen, D.B. and M.F.Doherty,"On the dynamics of distillation processes -V", Chem.Eng.Sci., 1984, vol.39, no.5, pp 881-892.

58. King, J.C., "Separation Processes", TMH edition, New Delhi, 1974.

59. Doherty, M.F. and J.D.Perkins, "On the dynamics of distillation processes-III", Chem.Eng.Sci., 1979, pp 1401-1414.

60. Chermin, H.A.G., DSM central laboratory internal report, Sept 22, 1976.

61. DSM patent.

62. Lemkowitz, S.M. et al, "Some fundamental aspects of urea technology", The Fertilizer Society Proceedings no.133, London, 1972, 115 pages.

63. Worthington et al, "Physical properties of ammonia solutions: ammonium nitrate-ammonia-water and urea-ammonia-water", I & E C, vol. 44, no. 4, pp 910-913.

64. Gorlovskii, D.M. and V.I Kucheryavyi, "Equation for the determination of the equilibrium degree of conversion of carbon dioxide conversion in urea

synthesis", Zh.Prikl.Khim., 1980, vol.53, no.11, pp 2548-2551.

65. Inoue,S. et al, "Equilibrium of urea synthesis I ", Bull.Chem.Soc.Japan, 1972, vol. 45, pp 1339-1345.

66. Perry, R.L. et al, "Solution thermodynamics for reactive componenets", Fluid phase equilibria, 1981, vol.5, pp 245-277.

67. Kaasenbrood, P.J.C. and H.A.G.Chermin, "The urea stripping process - stripping technology, phase equilibria and thermodynamics", The Fertilizer Society Proceedings no.167, 1977, 1 Dec, 48 pages.

CHAPTER 4

THE EXPERIMENTAL STUDY

4.1. *Introduction*:

The vapour-liquid equilibria (VLE) of the NH_3-CO_2-H_2O system have been studied during the last sixty years for many reasons. Initially these studies were performed for the coke oven industry, notably by Terres et al [1] and van Krevelen et al [2]. Later in the fifties, propelled by the sudden upsurge in urea manufacture, and because of the limited urea conversion leading to recovery and recirculation of the unreacted raw materials, the VLE study of the NH_3-CO_2-H_2O system became important.

In the fifties and sixties the process engineering companies working on urea technology carried out studies in limited regions of the p-T-x space suitable to their own processes. However, the data thus obtained were prive to these companies with a result that a unifying thermodynamic description was never developed in the open scientific literature. In fact, having concentrated very much on the individual trees, an overview of the encompassing forest was lost from sight. Formulae based on regression analysis, interpolations and safety factors became the main alleys through which the journey to scale-up was taken. Yet the results of the sixties and seventies were impressive, and it was not difficult to design plants even up to 1750 tonnes/day based on such empirical foundations. Large-scale energy economies were achieved rather easily, but only upto a point. When the process companies pushed to the extremes of the recycle techniques, the flow sheets became more complicated, and the law of diminishing returns started to cloud the future of the solution recycle processes. To improve energy economy still further by a small amount or to create a marginally simplified flowsheet, the cost of the research effort grew exponentially.

It was not long before the value of a systematic study of the NH_3-CO_2-H_2O system was appreciated in industrial and university laboratories. Although the stripping processes were an outcome of this trend, they were only the beginning. It was realized at the Delft School, based on available data, that one of the old processes, namely the Hot Gas Recycle Process (HGRP), had to be reassessed in the light of new stripping techniques, and that a new version of the HGRP could be developed by rectifying or minimizing the design deficiencies, the process constraints and the inherent operating problems.

With this objective, Lemkowitz [3] thoroughly studied the bubble-points and dew-points of the NH_3-CO_2-H_2O system with equilibrium concentrations of urea at a pressure and temperature range of 30 - 1000 bar and 130 - 260°C respectively. While he established the techno-economic feasibility of the HGRP in a general way by concentrating on the reactor, the condenser and the turbo-compressor, there was one aspect related to stripping which required a thorough study. The economy of the process, in comparision with the commercial stripping processes, was estimated to depend very much on the chosen stripping pressure [4].

Hence to establish the optimal conditions of the stripper, a systematic investigation was initiated at the Delft School to cover a pressure and temperature range of 1-30 bar and 40-130°C respectively. Under this initiative P. Verbrugge [5] carried out VLE studies at atmospheric pressure and within a temperature range of 40° - 90°C.

The present study was performed as a sequel to Verbrugge's work with the covered pressure range being $5.41<p<30$ bar and the temperature range being $88.7<T<130$°C. In the succeeding pages of the present chapter an account of the experimental rationale of the study, the experimental set-up, the procedure, the analysis methods and a discussion on the results obtained are presented.

4.2. *The rationale for choosing the present system*:

As explained in the last chapter, there are three multicomponent systems which are of interest to urea technology, namely the NH_3-CO_2-H_2O-NH_2CONH_2 system, the NH_3-CO_2-H_2O system (without the presence of urea) and the NH_3-CO_2-H_2O system (with equilibrium concentration of urea). Among these three systems, it is difficult to study the VLE of the first two unambiguously, since they are just the transitory entities of the third system.

In order to appreciate this important transitory character, it is worthwhile to consider the spatial representations of the bubble- and dew-point compositions of the three systems at a representative pressure and temperature.

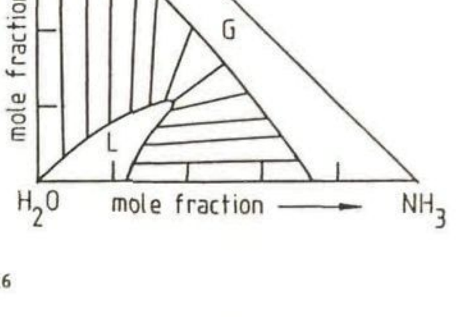

Fig. 4.1. *Typical bubble- and dew-point curves of the ternary system at physical equilibrium.*

P. Verbrugge [5] represented the bubble- and dew- point composition of the ternary system at physical equilibrium under constant pressure and temperature in a composition triangle as shown in Fig. 4.1. The bubble-point curve looks like a "tongue", while the dew-point curve is nearly straight. The most sensitive region occurs around the tip of the "tongue" at which a small change in the liquid composition causes a large change in the vapour composition. Accordingly, it becomes imperative to have reliable sampling and accurate analysis procedures for both the phases.

Regarding the quarternary system, Kaasenbrood [6] and Chermin [7] extended the spatial composition simplex to a tetrahedron. The bubble- and dew-point surfaces at each stipulated pressure and temperature had the characteristic features as shown in Fig. 4.2. The sharp curvature of the bubble- point surface at the tongue-tip once again pointed to severe composition effects.

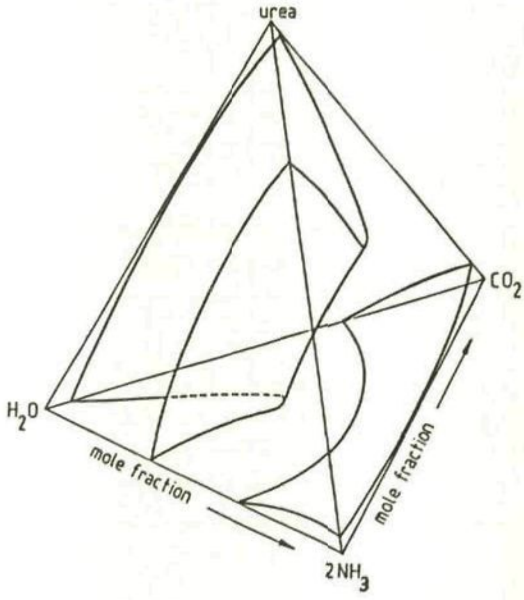

Fig. 4.2. *Typical bubble- and dew-point surfaces of the quarternary system at physical equilibrium.*

Lemkowitz et al [8] represented the ternary system at chemical equilibrium (for a given temperature and pressure) on a composition plane. Explaining the reciprocal salt-like nature of the system they outlined the bubble- and dew-point curves. The characteristic features of the bubble-point tongue-tip are also found here on both the tongues as shown in Fig. 4.3.

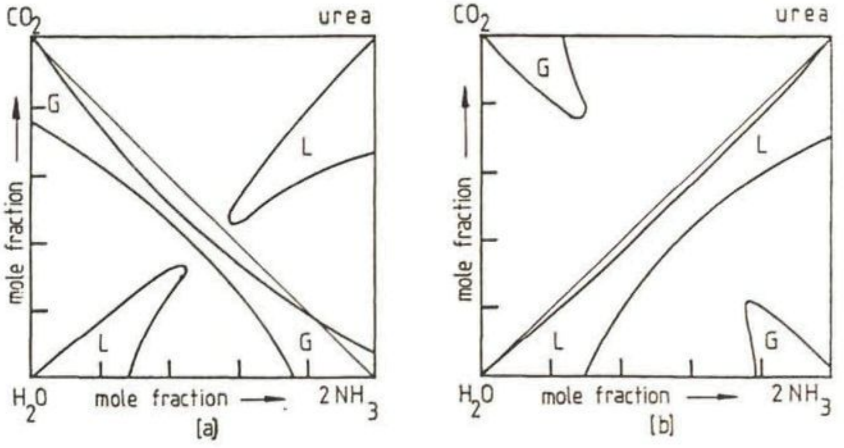

Fig. 4.3. *Typical bubble- and dew-point curves of the ternary system at chemical equilibrium. (a) Pressure above the saddle azeotrope pressure. (b) Pressure below the saddle azeotrope pressure.*

Although at the outset all these representations appear disconnected, there is an underlying transparent unity at temperatures higher than about 120°C. For example, the quarternary system is no longer stable, and it transforms into the ternary system with equilibrium concentration of urea.

In other words if we wait long enough, the two dimensional bubble- and dew-point surfaces of Fig. 4.2 will degenerate into one dimensional bubble- and dew-point curves embedded on the same surfaces but contained within the tetrahedral space, as shown in Fig. 4.4. Let us call these two curves the chemical equilibrium (CE) bubble-point and dew-point curves. If these two curves are projected down to a base looking from the equimolar point of (urea/water=1), one gets the composition plane of Lemkowitz et al [8].

Also shown in Fig. 4.4 is a curve generated by the change in the liquid composition during the transition from the quarternary physical equilibrium to the ternary chemical equilibrium. At constant temperature and pressure, such a curve can be called the reaction progress (RP) curve (shown in dashes).

An important question posed to an experimenter is whether he can measure the two end-points of the RP curve with equal ease. The answer is affirmative if the temperature is below approximately 100°C. At higher temperatures the quarternary physical equilibrium point is difficult to measure unless it is attained fast and the sampling

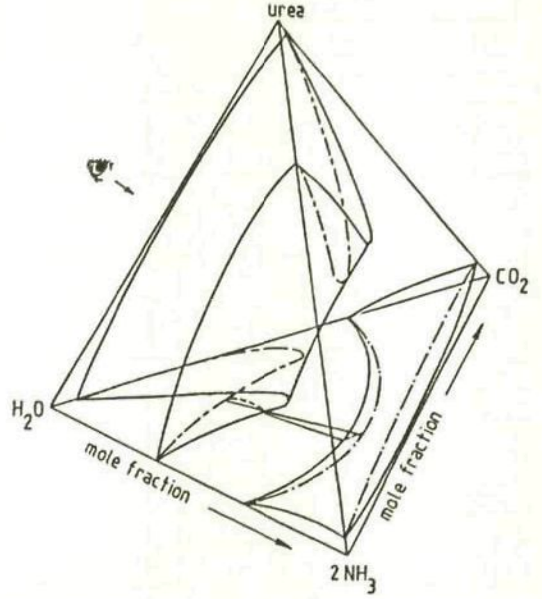

Fig. 4.4. *Degeneration of the bubble- and dew-point surfaces of the urea-CO_2-$(2NH_3)$-H_2O system into the bubble- and dew-point curves of the ternary system CO_2-$(2NH_3)$-H_2O at chemical equilibrium (shown as dot-dashed curves). Also shown is a typical physical equilibrium tie-line of the boundary system which changes into the chemical equilibrium tie-line situated inside the tetrahedron. Further the reaction progress (RP) curve is shown in dashes.*

time is insignificant relative to the rate at which the chemical reaction occurs. Otherwise one may end up finding one of the composition points in the RP curve. In essence, the experimental difficulty of VLE measurement is very severe in the case of the quarternary system and the ternary system at physical equilibrium. Such difficulty does not arise in measuring the ternary chemical equilibrium; here one only has to wait long enough.

It was this rationale which forced the present study to choose the unambiguous ternary system at complete chemical equilibrium for VLE measurements. Unfortunately the utility of such a study for the optimization of stripper conditions can be realized only through a model capable of describing both the ternary and quarternary systems. Given the intensive work carried out by various eminent researchers in the field of electrolyte solution theory in the recent decade [9,10] with regard to thermodynamic modelling, it was considered possible to derive such a specific model suitable to the present systems. Consequently, deriving the model parameters became one of the objectives of the present study.

4.3. *The experimental method*:

Among the various methods available for VLE studies, the static method was chosen by various researchers mainly due to the difficulty of recirculating vapour at small flow rates. The other methods like the distillation method, dew-point/ bubble-point method and the flow method are somewhat limited in their applications to the study of VLE at high pressure and temperature.

For example with the distillation method, one cannot take isothermal data, although the amount of time taken for measuring each individual datum is quite small. This method can, however, be quite useful in certain quick-assessment studies, provided adequate care is taken in the design of the distillation vessel with regard to the separation of phases, the carry over, the thorough mixing of the phases and the necessity of taking small samples

Alternatively, the dew-point/bubble-point method also has certain limitations when applied to ternary systems. The foremost limitation, as well as its strength, concerns the analysis aspect. While one can trace out the bubble- and dew-point surfaces elegantly and systematically, it is not possible to locate the corresponding tie-lines, for want of analyses of the individual phases.

When applied to the present ternary system, the flow method necessitates an accurate feeding of the two hot volatile gases (NH_3 and CO_2). Such accurate feeding is not hard to achieve with modern mass flow meters. Subsequently the gas streams can be heated to the required temperature. A major merit of the flow method is the flexibility in moving easily from one datum to another in a series of measurements. In spite of such an advantage, the flow method is not preferred for high pressure systems due to the non-availability of pressure control devices to maintain the pressure inside the equilibrium vessel with small flow rates. Moreover, many-a-time, there is a basic problem in attaining the equilibrium through this method. Hence the flow method is mostly preferred for low pressure and atmospheric studies.

This leaves only the static method, which is quite naturally suited to the high pressure and high temperature application. The principle involved is quite simple, although error-free practice is a bit tricky to achieve with the present system. The possibility of a three phase equilibria occurring in the experimental range desired, together with the inability to infer directly the presence of such equilibria without the aid of visual observations, is very real.

4.4. *The experimental apparatus*:

A general overview of the experimental arrangement is provided in Fig. 4.5 (autoclave side view), Fig. 4.6 (GLC side view) and Fig. 4.7 (a view of the gas storage tanks). A schematic diagram of the experimental apparatus incorporating the

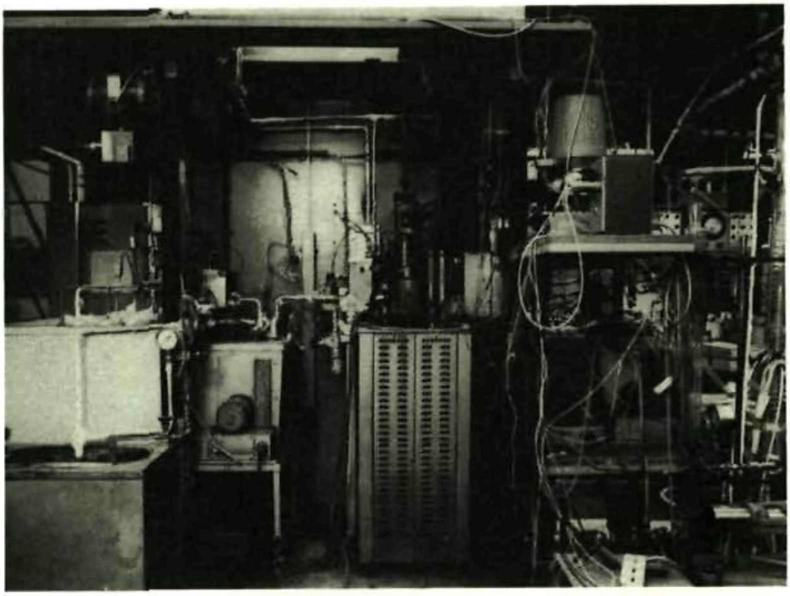

Fig. 4.5. *Autoclave-side view of the experimental arrangement.*

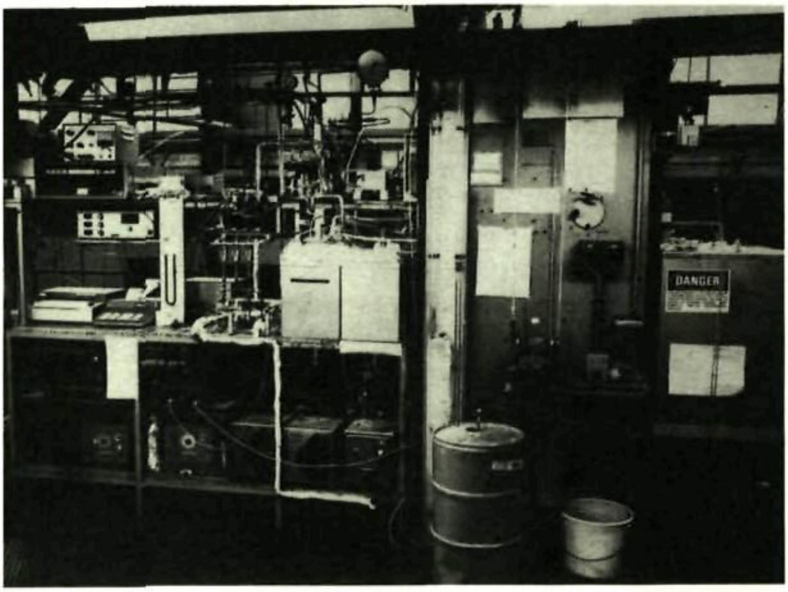

Fig. 4.6. *GLC-side view of the experimental arrangement.*

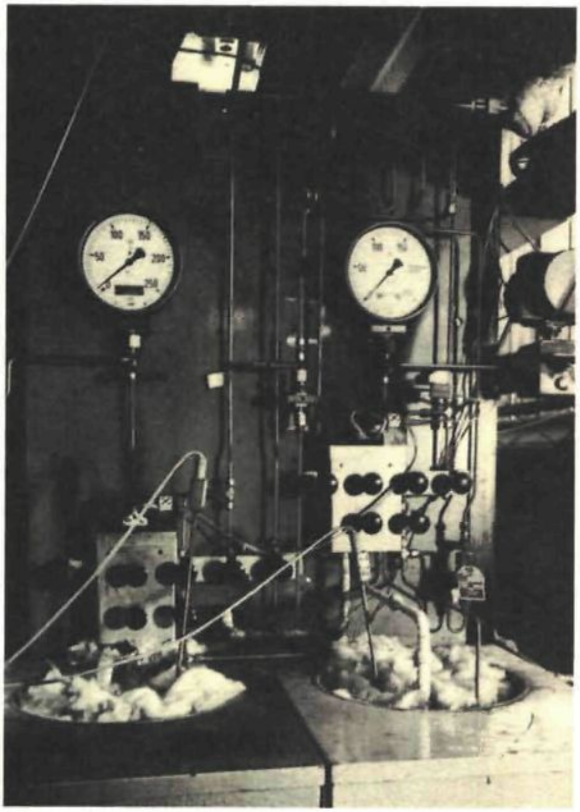

Fig. 4.7. *View of the gas storage tanks.*

autoclave, the storage tanks, the transducers and the GLC is presented in Fig. 4.8. The central part of the apparatus is the titanium autoclave fitted with a magnetically operated reciprocating agitator to effect a thorough mixing of the phases. The vessel and the agitator details are presented in Fig. 4.9 and 4.10. The volume of the vessel at 20.2^{o} C was estimated through a series of 4 capacity measurements to be 1511.7 cc with a standard deviation of 1.6 cc. The vessel is provided with a cover tightly secured to the vessel through 6 bolts. The sealing between the cover and the vessel is achieved through a tapered plug arrangement, i.e., through line closure.

4.4.1. *The agitator details*:

The top portion of the agitator shaft protruding from the cover is encased in a titanium tube. Internally, if needed, the top end of the agitator shaft containing a soft iron core, encased in titanium, can be easily dismantled from the bottom end

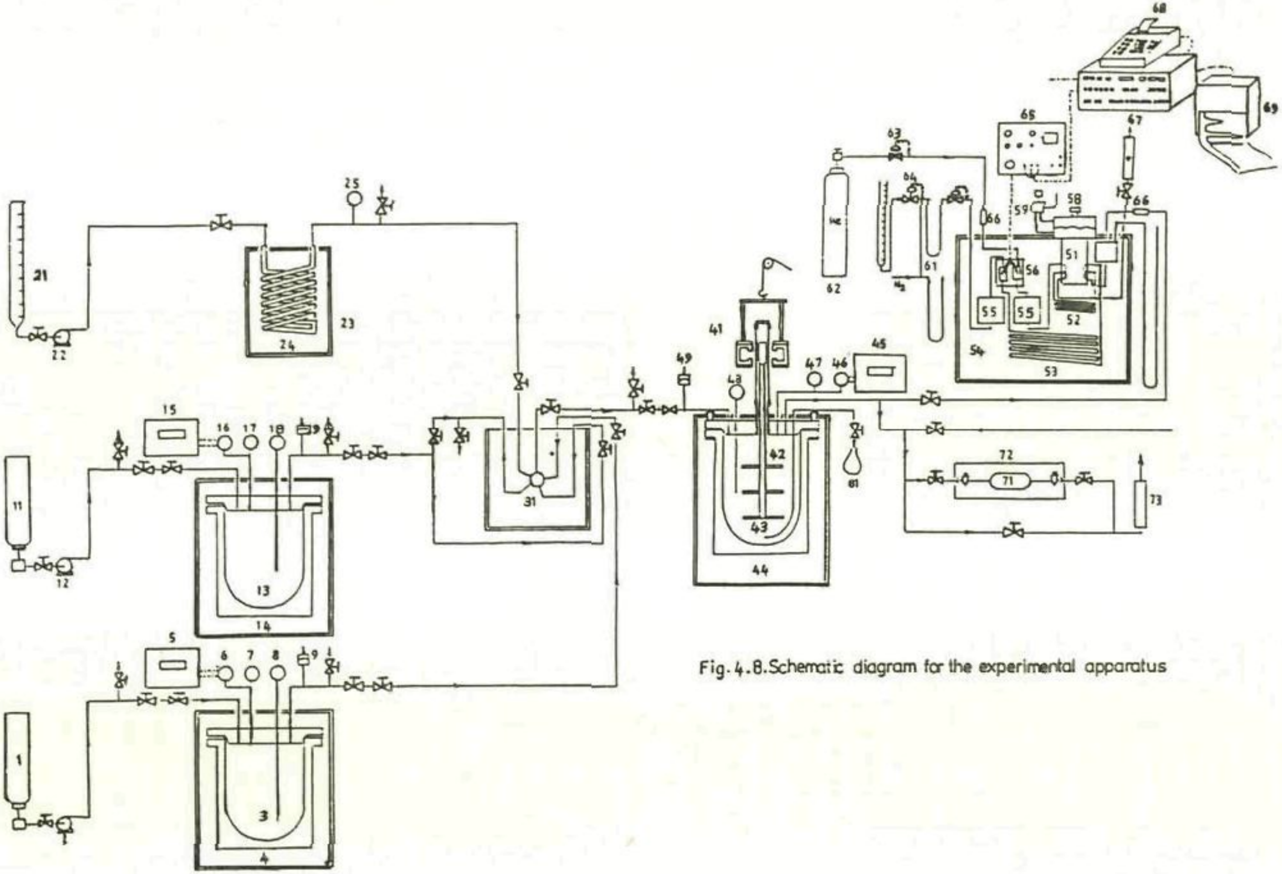

Fig. 4.8. Schematic diagram for the experimental apparatus

Index for the Fig.4.8.

1. NH_3 cylinder.
2. NH_3 feed pump.
3. NH_3 storage tank (NH_3-ST).
4. NH_3-ST air thermostat.
5. NH_3-ST pressure indicator.
6. NH_3-ST pressure transmitter.
7. NH_3-ST pressure gauge.
8. NH_3-ST temperature indicator.
9. NH_3-ST rupture disc.

11. CO_2 cylinder.
12. CO_2 feed pump.
13. CO_2 storage tank (CO_2-ST).
14. CO_2-ST air thermostat.
15. CO_2-ST pressure indicator.
16. CO_2-ST pressure transmitter.
17. CO_2-ST pressure gauge.
18. CO_2-ST temperature indicator.
19. CO_2-ST rupture disc.

21. Water feed pump suction burette.
22. Water feed pump.
23. Water heater.
24. Water heating coil.
25. Water line pressure gauge.
31. Star junction.

41. Magnetic reciprocating mechanism.
42. Stirrer.
43. Autoclave (AC).
44. AC oil thermostat.
45. AC pressure indicator.
46. AC pressure transmitter with seal.
47. AC pressure gauge with seal.
48. AC temperature indicator.
49. AC rupture disc.

51. GLC sample injection valve.
52. GLC sample loop.
53. GLC column.
54. GLC air thermostat.
55. GLC buffer capacity vessel.
56. GLC catharometer sensor cell.
57. GLC pressure tapping buffer vessel.
58. GLC manual sample injection knob.
59. Solenoid valve for air supply.
60. Sample flow rotameter.

61. GLC carrier gas outlet manometer.
62. GLC carrier gas supply cylinder.
63. GLC carrier gas inlet press. control
64. GLC carrier gas outlet flow control.
65. Catharometer.
66. Filter for GLC carrier / sample gas.
67. Integrator.
68. Printer.
69. Strip chart recorder.
70. GLC carrier gas outlet press.control
71. Alternate gas sampling bottle.
72. Heater for alter. gas sample bottle.
73. Alter.gas sample flowmeter.
81. Liquid sample ballon.

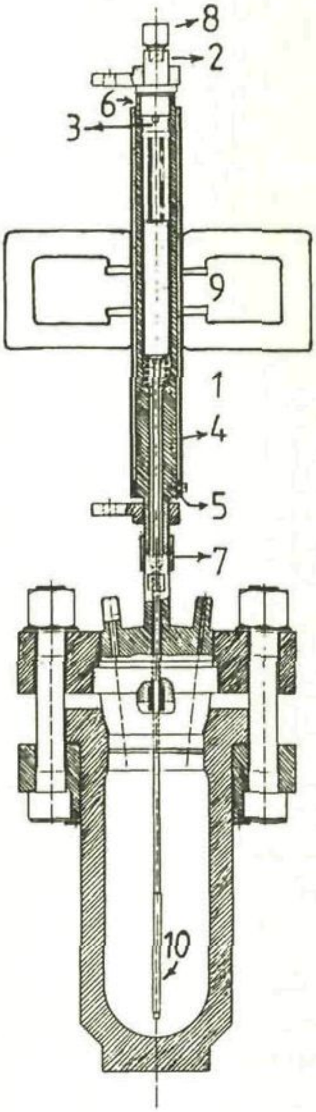

1. Agitator sheath.
2. Agitator sheath top end plug.
3. Agitator chamber thermowell.
4. Outer brass sheath.
5. Bottom spacer between the agitator sheath and the brass sheath.
6. Top spacer.
7. Shaft coupling union.
8. Top sealing nut.
9. Reciprocating permanent magnet.
10. Agitator shaft.

Fig. 4.9. Autoclave details.

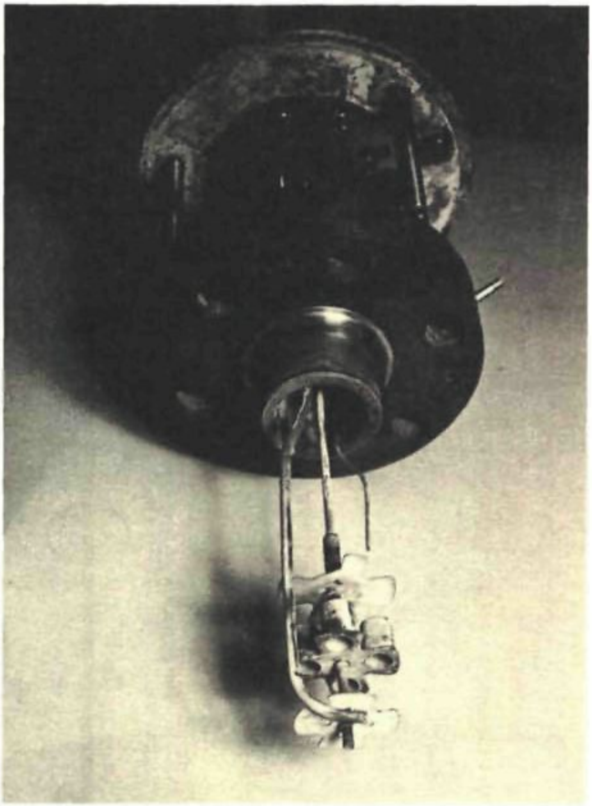

Fig.4.10.*Agitator impellers.*

containing the impellers. The impellers are shown in Fig. 4.10. On the outside of the agitator tube are two permanent magnets which are suspended through a pully arrangement and are slided up and down to cause a reciprocating movement of the agitator through magnetic action. Additionally in order to avoid carbamate condensation on the inside surface of the titanium cover tube as well as on the top end of the shaft, the titanium tube is provided with skin heating through a defroster transformer operating at 2 volts and about 500 amps. The titanium tube is surrounded by a brass tube with diatomaceous earth filling the annular section; such heat insulation prevents the titanium tube from cooling-off and the magnets from becoming too hot.

4.4.2. *The port deatails*:

The vessel is provided with 6 ports through the cover. The port A of the vessel cover is connected to a gas sampling line, and the port B is utilized for feeding the volatile gases and water. Through Port C, a platinum resistance thermometer is provided to measure the temperature. Further, in order to maintain a nearly constant level of the phase interface in all experiments, an on-off level indicator is fitted through port D. The pressure inside the vessel is sensed through port E and transmitted to the pressure transducers. Finally the liquid sampling line is extended through port F into the vessel until the entrance of the line is situated below the bottom of the agitator impeller.

4.4.3. *The level indicator*:

The on-off level indicator is a simple stainless steal 316 rod covered with a teflon sheath. Adequate sealing is provided at port D where the level indicator emerges from the cover. Just 2 cm above the inside tip of the level indicator rod, the teflon sheath is terminated and the annular gap between the sheath and the rod is sealed with *Araltite*, a thermosetting resin. A lead attached to the rod is connected through a battery and an ammeter to the cover of the vessel. The vessel and its cover are electrically isolated from the oil bath. Whenever the liquid surface touched the inside tip of the rod, the circuit closed, as shown by a sudden, discontinous increase in current. Any further increase in the level showed itself by a further, continous increase. Conversely, a decrease in the level below the desired value was indicated by a break in the circuit causing a discontinous drop in current. Such a simple level indicating device served the purpose adequately despite trivial problems, like the leakage current increasing over a period of months.

4.4.4. *The pressure transducer*:

The pressure inside the equilibrium vessel was sensed through two Foxboro diaphragm seals. One was directly connected to a liquid filled Foxboro pressure gauge to provide a rough pressure indication and the other (Mansfield and Green model by Foxboro) to a Foxboro pressure transducer (model E11GM). For a pressure range of 0 - 40 bar, the transmitter provided an output signal of 4 - 20 mA, which was measured using a multimeter. The pressure transducer and the autoclave pressure gauge were calibrated against the standard Heise pressure gauge CM37015 (p_{max} = 100 bar; accuracy and reproducibility within 0.1%). The calibration was found to be linear and reproducible. There was only a mild drift of about 0.2 % over a three year period. For a further confirmation the pressure transducer was tested and found to be in agreement with a dead weight pressure apparatus.

4.4.5. *The temperature calibration*:

Subsequent to the pressure transducer calibration, the vessel was filled with distilled water. Further, water was allowed to boil while the vapour outlet port was completely open. This procedure was followed to ensure that the outcoming water vapour was pure and air-free. With repeated additions of water nearly to the full capacity (1500 ml) of the autoclave and boiling the water at least three times, all the air inside the vessel was expelled. The quality of the water vapour that came out was checked through a GLC coloumn specially kept at 120°C. The platinum resistance thermometer (Pt-100 supplied by Klaasing Electronics BV of the Netherlands) installed through the cover into the autoclave was further connected to a digital indicator (Control and Readout Ltd, England). It was calibrated against the saturation temperature of steam. Since the pressure transducer had earlier been calibrated to a very high precision, the saturation pressure measured by the transducer became a reference, and the saturation temperature corresponding to the saturation pressure was plotted against the measured temperature shown by the digital indicator. The calibration was again linear and reproducible to within 0.1%.

4.4.6. *The thermostat*:

The autoclave securely fitted to an overhanging cover was left suspended inside a 'Tamson (The Netherlands) make' oil thermostat filled with Tamson oil 150. Although this oil had appreciable vapour pressure only above 130°C, it was susceptible to a gradual degradation above 120°C. Hence the oil had to be changed at least three times over a period of 3 years. The thermostat had, further, a stirrer, two contact thermometers with one for control and the other for safety, a booster heater to rapidly increase the temperature during start-up, and a fine tuning heater to provide an accurate temperature control of 0.1°C. Such a fine control also made the difference between the autoclave temperature and the bath temperature hardly noticeable (<0.1°C). As an additional safety precaution, if the temperature of the thermostat exceeded the preset temperature (140°C), an electric signal originating at the safety contact thermometer cut off the power supply to the thermostat, causing the heater and the thermostat stirrer to stop. The thermostat was also provided with two glass windows through which autoclave flange leaks, if any, could be observed. Except for the oil oxidation problem leading to stirrer failures once in a while, no other problem occurred with the thermostat.

4.4.7. *The autoclave safety details*:

The autoclave was provided with a safety rupture disc (John Matthey Metals Ltd, England) made of stainless steal 316 with a size of 1/2 inch orifice and a bursting pressure of 53.2 atm ± 10% at a temperature of 150°C. Since there was no practical temperature difference between the autoclave temperature and the bath, the temperature protection facility of the bath served adequately for the dual purpose. The on-off level indicator described earlier in the section 4.4.3 was mainly installed as a protection against the occurrence of high liquid level leading to a high pressure increase which would cause the safety disc to rupture. Further all inlet and outlet lines of th. autoclave were provided with heating coil or heating tape arrangements to protect those lines against cooling (which may further lead to solid carbamate plugging). Additionally hot water clearing connections were also provided to such lines in order to be able to dissolve any solid carbamate formation which might have formed in the lines.

4.5. *The feeding arrangement*:

The two volatile gases, NH_3 and CO_2, were stored in separate autoclave-like tanks which were in turn kept in air thermostats. The tanks were provided with Pt - 100 thermometers, Foxboro pressure transducers and Econosto pressure gauges (of the Netherlands). All these instruments were also calibrated in the same manner as the instruments fitted in the autoclave. The foxboro transducers fitted in the NH_3 and CO_2 tanks gave an accuracy of 0.1%, and the resistance thermometer coupled to a digital read-out performed to a precision of 0.1°C. The gases were stored at conditions close to their respective critical conditions. This was done to enable a maximal storing at one filling from the gas cylinders while maintaining the components in the gas phase.

Initially it was felt that, by utilizing accurate pressure transducers and resistance thermometers together with a known equation of state, the amount of materials drawn from each tank could be estimated and used for a material balance check across the autoclave. Unfortunately this scheme ran into problems because of the unduely large amount of line volume which came about during fabrication of the experimental set-up and which could not be estimated with sufficient accuracy. Moreover the calculation involved in finding the masses drawn out of each tank became time-consuming and almost counter-productive. As a result, the idea of a material balance check was reluctantly dropped.

Each tank was provided with a rupture disc (John Matthey metals Ltd, England) with a bursting pressure of 270 atm. Adequate shut-off and regulating valves were also provided in the inlet and outlet lines of the tanks to prevent carbamate formation by inadvertent mixing of the gases at high pressures.

The third component, water, was pumped into the autoclave through a reciprocating pump. The amount of air-free distilled water thus admitted into the autoclave was found through a burette provided at the pump suction. A variable water flow rate could be achieved by adjusting the piston stroke of the pump.

All the three feed lines joined a "five star "connection which had a drain provision and a common outlet line leading to the autoclave. Additionaly a wash-water connection was provided to the "five star" outlet line. The "five star" was kept in a separate air thermostat and kept at a fairly high temperature exceeding 160°C. Although the provision of the "five star" made the operating procedure somewhat cumbersome, it gave adequate insurance against valve failures and line blockages. Feeding was always effected through a sequential procedure consisting of interspersing the pumping of water between the additions of the volatile gases; i.e., the filling pattern resembled the order ammonia - water - carbon dioxide - water - ammonia ...etc. Such a practice very effectively avoided the carbamate blockage problem most of the times. Still there were three occasions in which the said problem did occur and had to be cleared by washing.

4.6. *The experimental procedure*:

The earlier studies on the NH_3-CO_2-H_2O system were mostly restricted to the NH_3-rich region, and the amount of data on the CO_2-rich region was very much limited in the open literature. Any CO_2-stripping process, in our case the improved HGRP, *requires that this inadequacy be rectified. Hence the present study naturally* focussed its attention mostly on the CO_2-rich region.

For each set of experiments, the first datum was always that of the binary system of carbon dioxide - water. This procedure had certain practical advantages. CO_2 being almost insoluble in water, it was very easy to build up pressure in the autoclave enabling a faster start of the experimental series. Also the establishment of equilibrium during each measurement, which was said to be attained when the pressure did not change by more than 0.1% during a period of not less than 1 hour, was fairly rapid, i.e., usually within about 3 to 4 hours.

Air-free water was added first into the autoclave almost to the full, as this was done during the temperature calibration step. With repeated boiling (not less than three full autoclave volumes) at temperatures around 120°C, the air inside the autoclave system was expelled. Subsequently the water level was reduced, and CO_2 was admitted, equilibrated and purged until air could not be detected in the gas sample through a GLC analysis. The system was then considered to be ready for starting a series of measurements.

Once again the liquid phase was built up to the predesired level and the system was brought to a desired temperature. Later more CO_2 was added or some vapour from the vessel was purged, depending on the desired pressure. Fine additions and purgings were further effected until equilibrium was achieved.

Admittedly the whole process of achieving the equilibrium at the desired pressure and temperature was very time consuming, sometimes extending as much as 8 hrs for a datum in the binary system and even 2 to 3 days for the data in the ammonia-rich region of the ternary system. In spite of this drawback, the procedure was adopted because it yielded isothermal isobaric data whose internal consistency could be checked in a straight forward manner by a simple plotting without any necessity for model interventions. Often enough in previous phase equilibria studies of the NH_3-CO_2-H_2O system, the main problem was the lack of internal consistency. On an isothermal isobaric plot, the crossing of tie-lines, which may easily happen due to analysis error or sampling problems, is very glaring, as are gas-liquid tie-lines which extend into the three phase region. Most investigators who had such probleems [11,12] do not seemed to have noticed them, probably because they never plotted their data on such a graph.

Subsequent to the achievement of equilibrium in this study, the gas sample was analysed through GLC, as described in appendix C. The liquid sample was collected in sample ballons filled with dilution water. The amount of the dilution water had an effect on the analysis, as described in the section 4.9. The liquid analyses procedures are described in appendix D.

Once the binary point of the CO_2-H_2O system was completed, some amount of ammonia and water were added. Such additions lowered the pressure due to carbamate formation and physical absorption. Again fresh CO_2 was added to raise the pressure. This process of addition of CO_2 and NH_3, interspersed with H_2O additions, was continued until the predesired pressure was achieved. During all this time, the level was maintained with the help of the on-off level indicator by draining the excess material from the autoclave through the liquid sampling line. Similarly gas purgings could be effected through the vent line provided in the autoclave. Once equilibrium was attained, samples were taken and analysed. Thus starting from the CO_2-side of the composition triangle, additional data were obtained by increasing the NH_3 and CO_2 contents as and when required.

4.7. *The preliminary results*:

In order to check the whole experimental set-up with regard to the reliability and accuracy of its functioning, initially the known system of NH_3-H_2O was investigated at 80 and 100°C, the results of which are presented in Fig. 4.11 and Fig. 4.12. Since the data obtained were quite close to the experimental curve of Clifford and Hunter [13], the experimental set-up was accepted as reliable, thus leading into the ternary measurements.

4.8. *The ternary measurements*:

In total, there are 47 ternary measurements covering a pressure range of 5.41 to 30 bar and a temperature range of 88.7°C to 130°C. For each measurement, at least four gas samples and two liquid samples were taken to check the reproducibility of the analyses. Further, the order in which the measurements were carried out at a given p and T was random so as to avoid the errors usually caused by a sequential progress of measurements.

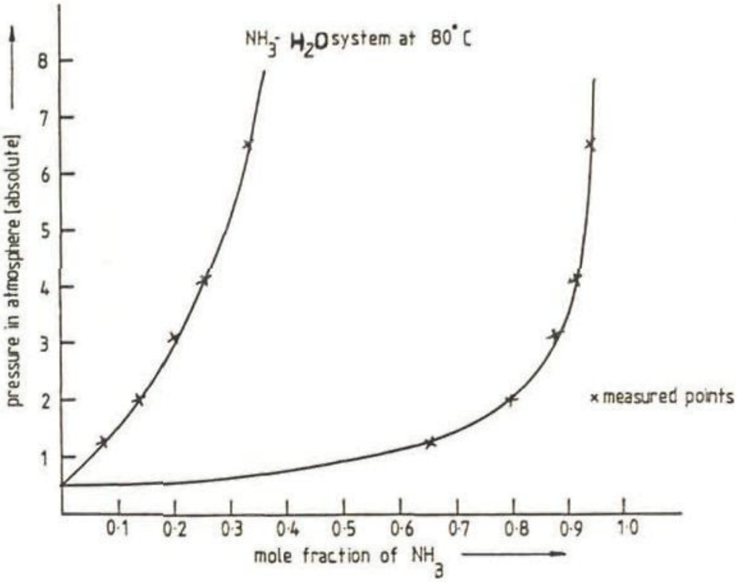

Fig. 4.11. *VLE data of the NH_3-H_2O system at 80°C. The full lines are taken from Clifford and Hunter. [13]*

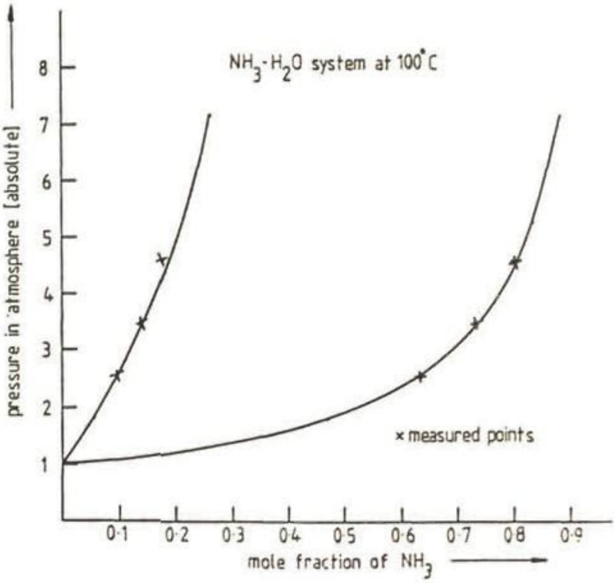

Fig. 4.12. *VLE data of the NH_3-H_2O system at 100°C. The full lines are taken from Clifford and Hunter.[13]*

Once the equilibrium was apparently attained and there was no appreciable change in pressure, the temperature of the autoclave was taken up or down by about 2°C, kept at the new temperature for about 15 min. and brought down again to the original temperature leading to a fresh equilibrium at the original conditions. This way, if the same pressure was finally obtained as earlier, one can take such agreement to be the confirmation of the attainment of equilibrium.

The results are presented in Table 4.1 and in figures 4.13 to 4.20. In taking these measurements, great care was observed in choosing regions so as to avoid measuring three phase equilibria inadvertently. With no glass windows in the autoclave, the possible presence of three phases could be checked only by indirect means (i.e. by consolidating the earlier works of Janecke [14], Guyer and Piezowitz [15], and that of DSM [16] on the onset of three phase equilibria and inferring the possible occurrence). However, the accuracy of the boundary values between S-L-G and L-G equilibria (obtained from these works) appears to be uneven and occasionaly unreliable, although the inner S-L-G region had been accurately covered.

According to the phase rule, the number of intensities one can freely set for a ternary system consisting of three phases is limited to only two, compared to three of the two phase situation. Choosing temperature and pressure, let us say one datum of our system has been measured at a pressure p_1 and temperature T_1. Unless the datum is far away from the the onset of three phase equilibria or very clearly inside the three phase region as inferred by the earlier studies, one cannot be sure whether we have inadvertently crossed into a three phase region. This is because of the uncertainty of the three phase boundary values presented by the earlier authors.

To check whether we have indeed crossed into the three phase region, one has to adopt a search procedure. In other words one can change the gross composition a little towards the well established three phase inner region and see whether the same liquid and vapour composition is obtained. If a three phase equilibrium exists, then one should get the same phase compositions irrespective of the gross composition. There were at least 7 occasions in all the series of measurements when such time consuming local explorations had to be resorted to, and two occasions proved to be real three phase situations. Additionally operating problems like the sluggishness of the pressure transducer, the erratic gas analysis and clogged feed lines were clearly dominant during such occasions; the latter problem could be rectified only by excessive water washing.

4.9. *Discussion of the results*:

At 88.7° C and 5.41 bar (Fig. 4.13), 3 gas-liquid data and 2 three phase data were measured. The three phase equilibria were observed through the search procedure

Table 4.1. *The experimental data of the NH_3-CO_2-H_2O system*

Pressure	*Temperature*	*Liquid composition*		*Gas composition*	
in bar	*in°C*	*mole% NH_3*	*mole% CO_2*	*mole% NH_3*	*mole% CO_2*
5.41	88.7	10.3	6.0	7.65	81.5
		14.4	8.0	10.0	79.5
		19.25	10.5	11.5	78.5
		42.7	22.5	58.0	41.8
		46.0	21.3	75.5	24.2
5.41	100.0	25.8	10.8	39.0	50.5
		27.8	11.2	53.6	37.0
		28.3	9.7	72.0	15.2
5.41	110.0	6.0	4.7	23.2	55.5
		11.5	5.0	24.7	55.0
		12.5	5.2	28.1	50.5
		14.5	5.55	33.5	46.0
		14.3	5.7	35.2	44.8
		15.6	5.8	40.7	39.2
		16.5	6.0	44.5	34.5
		16.2	6.0	47.5	31.8
		18.0	5.9	56.7	22.7
		18.0	4.75	67.7	12.0
10.0	110.0	9.8	5.4	6.5	80.3
		12.8	7.0	9.6	77.7
		20.0	11.5	16.2	71.8
		25.5	14.7	22.0	66.8
		27.2	16.2	25.4	64.2
10.0	120.0	14.5	6.0	17.2	65.0
		19.0	7.2	27.2	55.8
		21.1	18.5	37.0	46.0
		23.5	19.0	44.6	38.5
		24.0	8.9	50.0	34.4
		24.0	8.0	64.5	19.5
20.0	120.0	18.5	9.5	10.5	81.0
		23.2	12.0	13.8	77.8
		26.0	13.5	19.5	73.2
		28.7	14.2	32.3	70.0
		32.0	15.7	27.8	66.5

Pressure in bar	*Temperature in$^o C$*	*Liquid composition*		*Gas composition*	
		mole% NH_3	*mole% CO_2*	*mole% NH_3*	*mole% CO_2*
20.0	130.0	24.0	11.0	23.0	65.7
		26.6	12.0	27.5	61.4
		27.8	12.5	31.4	57.8
		29.0	12.7	34.3	55.0
		30.8	13.4	40.6	48.8
		32.7	14.0	46.0	43.2
		33.2	14.0	55.7	35.0
		34.5	13.2	63.4	26.5
		34.2	12.8	72.0	18.3
30.0	130.0	27.8	13.5	11.3	81.7
		32.5	16.0	20.0	79.7
		34.2	16.5	25.0	70.6
		34.3	16.6	28.0	69.0

mentioned earlier. The gas phase compositions in both cases (one in the CO_2-rich region and the other in NH_3-rich region) contained only negligible water concentrations. It was gratifying to note such observations, since these shed light on the abstract theoretical arguments raised in the previous chapter about an impossible three phase situation with solid ammonium carbamate and a binary gas phase (i.e. involving only NH_3 and CO_2) in equilbrium with a ternary liquid phase. Further, when the dew-point curve on the CO_2-rich side was extrapolated to intersect the CO_2-NH_3 diagonal to obtain the gas phase composition related to the S-G equilibria of ammonium carbamate, the value so obtained clearly matched with the predicted value (See appendix A and [17,18,19]). Similarly the gas composition of the binary CO_2-H_2O system matched with the earlier observations of Wiebe and Gaddy [20].

At 100°C and 5.41 bar (Fig. 4.14), only 3 gas-liquid data around the tongue in the liquid phase area were measured, since Müller [21] in his recent studies on the same system had already covered the non-tongue region. The interpolated data from his measurements and the present data clearly fill the entire region adequately. There are no three phase equilibria at these conditions. Once again the well-known special feature of the tongue region, where a small change in the liquid phase composition begets a much larger change in the gas phase composition, can be observed. Unlike Müller's data, Pawlikowski data [22] do not fit on the dew-point curve. Clearly there appears to be a problem in the vapour phase analysis of Pawlikowski's work. The binary data on the ammonia side (Clifford and Hunter [13]) and the carbon dioxide side (Wiebe and Gaddy [20]) are also plotted in all the figures showing the present experimental data.

At 110°C and 5.41 bar (Fig. 4.15), 10 data points were measured. Excepting one datum, all other data appear to be internally consistent. Since the tie- line concerned did not fit with the regular pattern of the other tie-lines, it was not included in the model development.

The reason for the discrepency of the said datum is suspected to be due to the sampling procedure. This particular datum was one of the earliest attempted in all of the series. During this initial period, the amount of the dilution water taken in the sample ballon was quite low, being only 100 ml., while the amount of the liquid sample was comparatively large, being around 30 ml. Accordingly all the free NH_3 might not have been captured through absorption in the ballon. Further the escaped NH_3 might have accumulated in the air space of the ballon. As a result, the final analysis of the liquid phase in the ballon would indicate a slightly NH_3-lean composition. To overcome this problem, the amount of the dilution water in the liquid sample ballon was gradually increased to 300, 500 and finally to around 800 to 900 ml. Additionally after collecting the sample, the contents were thoroughly mixed and transferred straight to a double cocked sampling bottle without exposure to the atmosphere. The diluted liquid samples were then taken from this bottle for analysis.

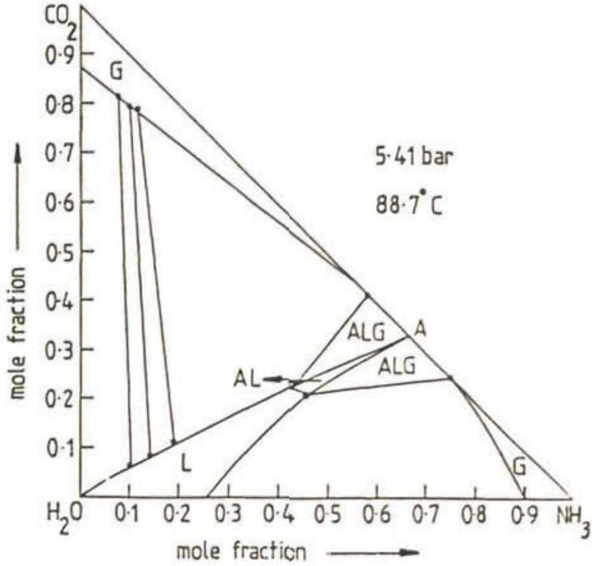

Fig. 4.13. *VLE of the ternary system NH_3-CO_2-H_2O at 5.41 bar and 88.7°C. Also the ALG equilibria compositions are marked.*

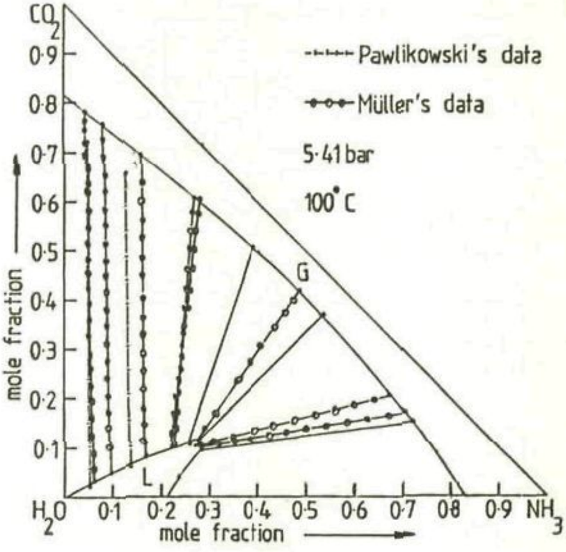

Fig. 4.14. *VLE of the ternary system NH_3-CO_2-H_2O at 5.41 bar and 100.0°C. Also the data due to Müller and Pawlikowski are plotted.*

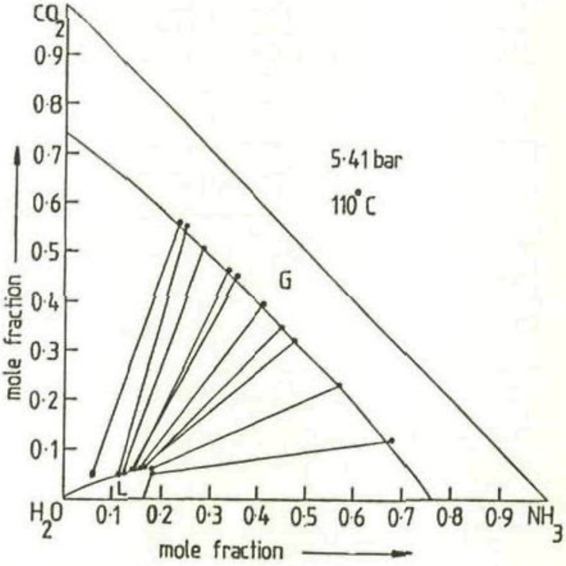

Fig. 4.15. *VLE of the ternary system NH_3-CO_2-H_2O at 5.41 bar and 110.0°C.*

During all these modifications of the liquid sampling procedures, the 110°C - 5.41 bar series was continued. The effect of the liquid sampling procedure can also be observed in the said series on the two pairs of tie-lines that cross each other. This difficulty was also due to the low volume of the dilution water, in these cases being around 400 to 500 ml. The data were accepted because the crossings were so close and the liquid composition deviation was within the analysis accuracy. Only when the dilution water was taken to a high value around 900 ml for all the remaining series could the analysis error causing the tie-line crossings be eliminated.

As the temperature is increased from 88.7°C to 110°C at a constant pressure of 5.41 bar, it can be observed that the dew-point curve moves towards the water corner and the curve increasingly becomes a straight line connecting the two binary dew-points. This behaviour is also coupled to the receding of the all-liquid region. Further temperature increase will lead to very low NH_3 and CO_2 concentrations in the liquid phase at a pressure of 5.41 bar. Such data are useful only for low pressure applications, like the sour water stripping. Since our aim at present is not related to such applications, additional data collection at still higher temperatures and at the same pressure was not attempted.

Shifting to a pressure of 10 bar, the first temperature to be tried was 110°C. At these conditions (Fig. 4.16) only 5 data could be collected starting from the CO_2-H_2O side due to operating problems like the clogging of autoclave feed line and the leakage of the liquid sample isolation valve. Instead of continuing at this temperature, the temperature was raised to 120°C and a new series was started. The same regular pattern of the tie lines was also observed in the 110°C - 10 bar series.

At 120°C - 10 bar (Fig. 4.17), only 6 data were collected, since Müller's data [21] complemented the remaining region. The present data appear to be consistent with that of Müller. Both the data put together cover a broad region nicely. Since the dew point curve had started becoming straight and the liquid region narrow, the pressure was raised once again, this time, to 20 bar at the same temperature of 120°C.

At 120°C - 20 bar (Fig. 4.18), 5 data were collected. Further measurements was not carried out due to suspicion of solid formation. This inference was given further credence by the calculation of the carbamate S-G equilibria. The dew-point curve appears to be rather straight and heading for the NH_3 - CO_2 diagonal, intersecting it very close to the solid carbamate composition point. In the same Fig. 4.18, two interpolated data points from Müller's work are also also presented. It can be easily observed that his gas compositions are too CO_2-rich. The source for the discrepancy could lie with the experimental approach he chose, as explained in the previous chapter 3.

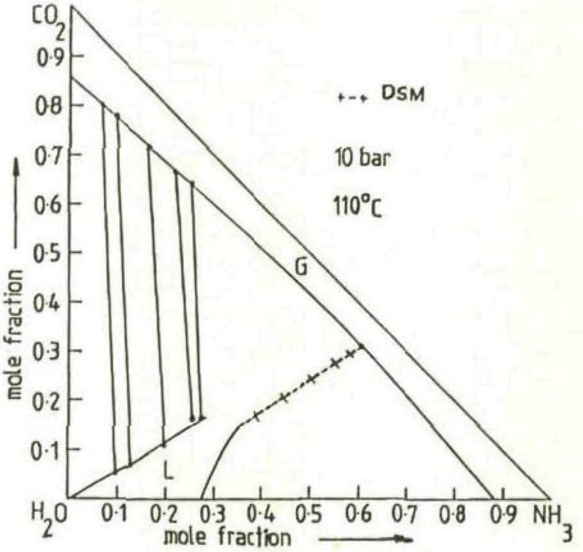

Fig. 4.16. *VLE of the ternary system NH_3-CO_2-H_2O at 10.0 bar and 110.0°C.*

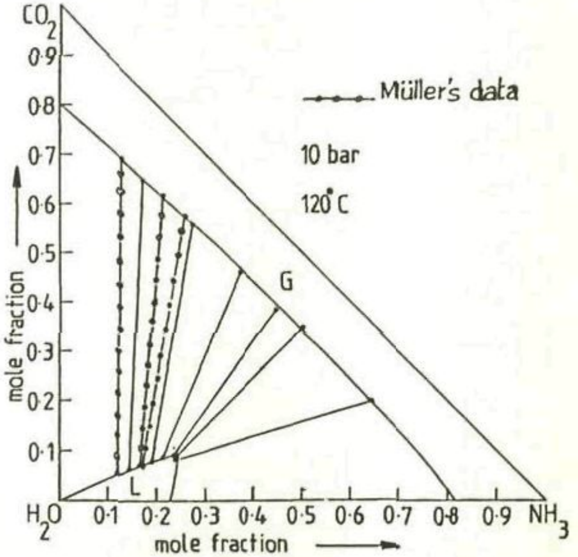

Fig. 4.17. VLE of the ternary system NH_3-CO_2-H_2O at 10.0 bar and 120.0°C.
The data of Müller are also plotted.

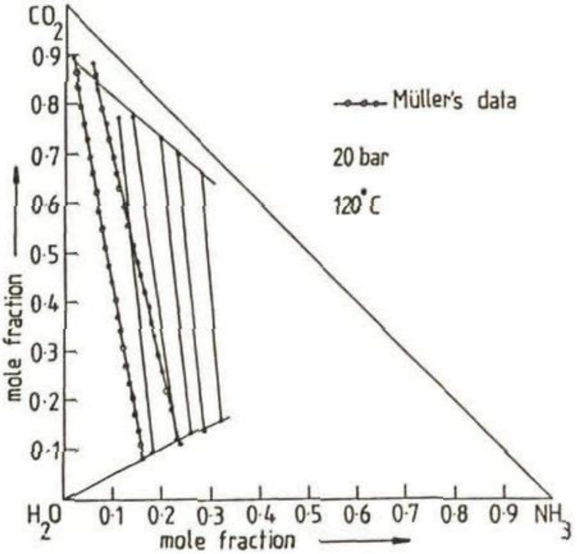

Fig. 4.18. *VLE of the ternary system NH_3-CO_2-H_2O at 20.0 bar and 120.0°C. The data of Müller are also plotted.*

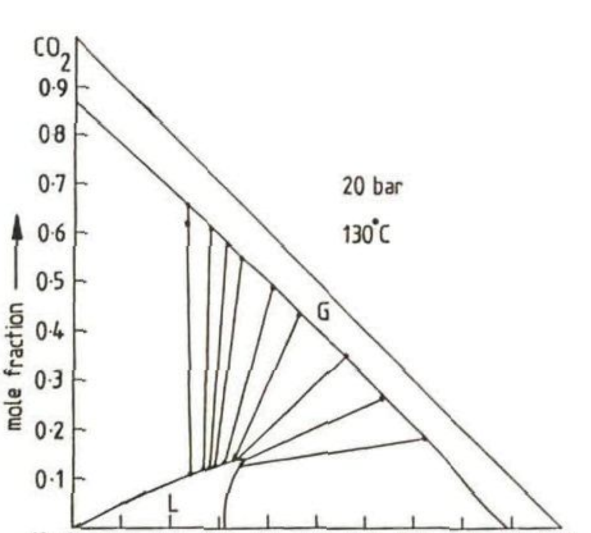

Fig. 4.19. *VLE of the ternary system NH_3-CO_2-H_2O at 20.0 bar and 130.0°C.*

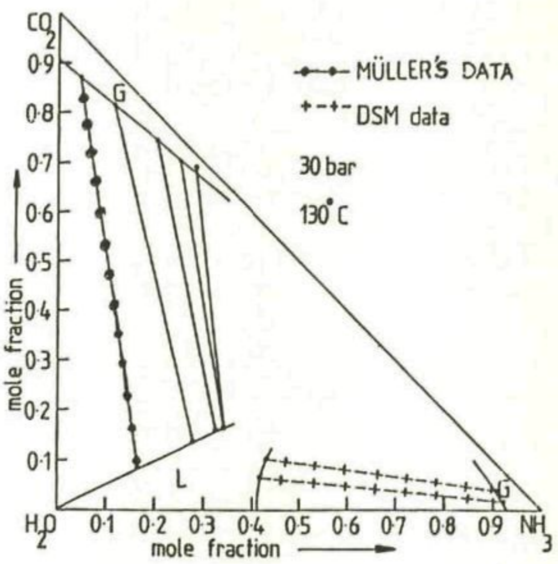

Fig. 4.20. *VLE of the ternary system NH_3-CO_2-H_2O at 30.0 bar and 130.0°C. The data of DSM are also plotted.*

Further at the same pressure of 20 bar, the temperature was increased to 130°C and a new series of measurements were started. Nine data were taken in the new series. As can be seen in Fig. 4.19, the behaviour shown is very regular and exhibits no complications. The dew-point curve at 130°C - 30 bar is less curved.

The last series of measurements were taken at a pressure of 30 bar and at a temperature of 130°C. Here only four readings could be taken. The fourth datum was plagued with solid formation. Since its reliability could not be checked thoroughly, the reading was not included in subsequent model analysis. In Fig. 4.20, one datum of Müller [21] on the CO_2-rich side and two data of DSM [16] on the NH_3-rich side are also plotted.

In all the above measurements, the pressure deviations were less than 0.5%. Similarly the temperature deviations were less than 0.2°C. The relative precision of the liquid phase analyses for each of two components was around 2 to 4 mole% and that of the gas phase analyses was around 1 to 2 mole%.

One general observation from the bubble-point behaviour at various temperatures and pressures is the narrowing of the tongue-tip with pressure increase at constant temperature and bulging of the same with temperature increase at constant pressure.

References:

1. Terres, E. et al, "Zur kenntnis der vorgange bei der ammoniakwasche von steinkohlenrohgas und der ammoniakwasser-konzentration", Das Gas und Wasserfach, 1957, vol.98, 31 May, pp 512-516.
2. Terres, E. et al, "Zur kenntnis der vorgange bei der ammoniakwasche von steinkohlenrohgas und der ammoniakwasser-konzentration", Das Gas und Wasserfach, 1957, vol.98, 7 June, pp 577-582.
3. van Krevelen, D.W. et al, "Composition and vapour pressures of aqueous solutions of ammonia, carbon dioxide and hydrogen sulphide", Recl.Trav. Chim. Pays-Bas, 1949, vol.68, p 191-227.
4. Lemkowitz, S.M., "Phase and corrosion studies of the ammonia - carbon dioxide - water system at the conditions of the hot gas recirculation process for the synthesis of urea", PhD thesis, Delft University of Technology, The Netherlands, 1975, 191 pages.
5. Verbrugge, P., "Vapour-liquid equilibria of the ammonia - carbon dioxide - water system", PhD thesis, Delft University of Technology, The Netherlands, 1979, 133 pages.
6. Kaasenbrood, P.J.C., Proceedings of the Fourth European Symposium of Chemical Reaction Engineering,held at Brussels, Sept 11, 1968, Pergamon Press, 1971,p.317
7. Chermin, H.A.G., DSM internal report.
8. Lemkowitz, S.M. et al, "Some fundamental aspects of urea technology", The fertilizer society proceedings no.131, London, 1972, 115 pages.
9. Pitzer, K.S., "Activity coefficients in electrolyte solutions", chapter7, edited by R.M.Pyckowitz, pp 157-208.
10. Pitzer, K.S., "Thermodynamics of aqueous systems with industrial applications", ACS symposium series 133, edited by J.Newman, 1980, p 106.
11. Yanagisawa, Y. et al, "Vapour-liquid equilibria for the ternary system of ammonia-carbon dioxide-water", J.Chem.Soc.Japan, 1973, no.5, pp 917-922.
12. Takahashi, T. et al, "Equilibrium pressure for NH_3-CO_2-H_2O system", Kogyo Kagaku Zasshi, 1962, vol. 65, pp 743-745.
13. Clifford, I.L. and E.Hunter, "The system NH_3-H_2O at temperatures up to 150°C and at pressures up to 20 atm.", J.Phys.Chem., 1933, vol.37, pp 101- 118.
14. Jänecke, E., "Über das system H_2O, CO_2 und NH_3", Zeitschrift fur elektrochemie, 1929, Bd. 35, Nr. 9, pp 716-728.
15. Guyer, A. and T.Piechowicz, "Losungsgleichgewichte in wasserige systemen - das system CO_2-NH_3-H_2O bei 20°-50°", Helve.Chim.Acta, 1944, vol.27, pp 858-867.
16. DSM investigations (private sources).
17. Egan, E.P. et al, "Dissociation pressure of ammonium carbamate", I & E C,1946, vol.38, no.4, pp 454-456.
19. Janjic, P.D., "Etude de l'equilibre de dissociation du carbamate d'ammonium a

l'aide d'un appareil nouveau", Helvetica Chemica Acta, 1964, vol. 47,no.206, pp 1879-1883.

20. Briggs, T.R. and V.Migrdichian, "The ammonium carbamate equilibrium",J.Phys. Chem., 1924, vol.28, pp 1121-1135.
21. Müller, G., "Experimentelle Untersuchung des Dampf-Flussigkeits-Gleichgewichts im System Ammoniak-Kohlendioxid-wasser zwischen 100 und 200°C bei drucken bis 90 bar",(in German), PhD thesis, University of Kaiserlautern, 1983.
22. Pawlikowski, E.M. et al, "Phase equilibria for aqueous solutions of ammonia and carbon dioxide", J.Am.Chem.Soc., 1982, vol.21, no.4, pp 764-770.

CHAPTER 5

THERMODYNAMIC DESCRIPTION OF THE REACTIVE VLE IN THE SYSTEM OF NH_3-CO_2-H_2O THROUGH AN ION SPECIFIC INTERACTION MODEL.

5.1. *Introduction*:

The last three decades of applied thermodynamics (both classical and statistical) have seen many developments in treating non-ideal systems of chemical engineering interest. Better equations of state based on hard sphere reference systems [1], in-depth analysis about mixing rules [2,3], and local composition models like Wilson, NRTL, UNIQUAC, UNIFAC and ASOG to describe liquid phase non-idealities are some of the developments that have taken place.

Unlike the progress in non-electrolyte systems, the progress in electrolyte systems, since the early work of Debye and Huckel [4], was slow in coming until a breakthrough was achieved by Card and Valleau [5] through molecular dynamics calculations. Subsequent theoretical developments due to Friedman [6], Rasaiah [7], Waisman and Lebowitz [8], Stillinger and Lovett [9], and Andersen, Chandler and Weeks [10] were exhaustive in describing the primitive electrolyte with equal sized cations and anions. The utility of these advances relates not only to the understanding *per se* of the electrolyte solutions but also to suggesting the type of terms to be considered in semi-empirical models.

Recourse to semi-empirical models were rather inevitable, since rigorous theoretical models could describe at the most only 2 molal solutions.

One of the earliest semi-empirical models, the ionic hydration model proposed by Stokes and Robinson (and recently improved [11]), can describe a pure electrolyte solution of molality around 20 to 30 with just two constants. Similarly, the models proposed by Bromley [12], Meissener [13], Sorensen et al [14], Pytkowicz [15], Triolo et al [16], and Cruz and Renon [17] could describe at ease the pure electrolyte solutions over wide concentration ranges. But the models available for multi-electrolyte systems are few and far between.

There are five models proposed in the literature with specific reference to multi-electrolyte systems. These are:

1. The ion specific interaction model proposed by Pitzer [18].
2. The virial coefficient model of Scatchard [19].
3. The free energy mixing model of Reilly, Wood and Robinson [20].
4. The Kirkwood-Buff model as elaborated by O'Connell and DeGance [21].
5. The local composition model as proposed by Chen et al [22].

Of these five models, the virial coefficient, and the free energy mixing models have been applied for common ion - two electrolyte mixtures. There is also a reported case [23] on the extension of Bromley's model to multi-ion mixtures. The Kirkwood-Buff model has a lot of potential for the future, provided additional semiempirical features are built into it. The attractive feature of the local composition model is its capability in also describing the non-aqueous electrolyte solutions. But unfortunately it suffers in accuracy in describing aqueous systems of molalities greater than 6 to 10, although there are exceptions. This leaves the ion specific interaction model as the one presently suitable to handle concentrated multielectrolyte systems.

Such a choice was quite natural in view of its earlier proven capabilities in describing complex electrolyte systems like artificial sea water [24] and the eight component system of $Na^+-K^+-Mg^{2+}-Ca^{2+}-H^+-Cl^--SO_4^{=}-OH^--HCO_3^--CO_3^{=}-CO_2-H_2O$ [25]. Recognising the efficacy of Pitzer's model, Edwards et al [26], Beautier et al [27], Maurer [28], Chen et al [29], and Pawlikowski et al[30] and recently Müller [31] have applied similar models to the system $NH_3-CO_2-H_2O$.

In this chapter, the ion specific interaction model is applied to the system of $NH_3-CO_2-H_2O$ with suitable modification. Important parameters, like the heats of dissolution of NH_3 and CO_2 and the reaction equilibrium constants for the formation of carbamate and urea, are also derived. Further, the optimization procedure used in arriving at the model parameters are described. Finally, the model fit is compared with the experimental data.

5.2. *Description of the problem*:

Consider the system $NH_3-CO_2-H_2O$ at chemical and physical equilibria. For this system, several reactions are possible giving rise to a number of species. Kawasumi [32], Lemkowitz [33] and Gorlovskii [34] considered the system close to urea synthesis conditions as containing five species, namely NH_3, CO_2, H_2O, NH_2COONH_4 and NH_2CONH_2. Baranski and Fulinski [35] discounted the possibility of analysing NH_4COONH_2 in solution and hence their school considered only four species. Durisch [36] followed the approach of the Delft school [33] except by inclusion of biuret and isocyanic acid. Two notable features in all the above approaches are the limitation to only molecular species and the exclusion of the two remaining ammonium salts, namely the bicarbonate and carbonate.

In contrast to the urea synthesis studies, the washing and recovery studies (pursued initially by van Krevelen [37] and followed later by Othmer and Frolich [38], Edwards et al [26], Beutier and Renon [27], Maurer [28], Pawlikowski et al [30], Müller [31], Wicar [39] and Kotula [40]) considered the system through ionic equilibria. However, none of these authors excepting Wicar and Kotula included urea formation reaction in these models. The studies of the later two authors were, however, related to the quarternary system.

One may very well ask the question as to which model, the ionic or the non-ionic, will be most suitable for describing the ternary system NH_3-CO_2-H_2O under the temperature and pressure conditions of the present study. With the concentrations of non-urea species being very high under these conditions as observed through experimental data, the choice is quite obvious in favour of ionic species and ionic reactions. Additionally the choice is supported through a recent in-situ Raman spectroscopic investigation of urea forming solutions by van Eck [41]. His study establishes the existence of bicarbonate, carbonate and carbamate as being present mostly in their ionic forms even at high concentrations at temperatures around 100°C and pressures around 20 to 30 bar.

In proposing an ionic model we consider 6 reactions and 10 species, namely 4 molecules (NH_3, CO_2, H_2O and NH_2CONH_2), 2 cations (NH_4^+ and H^+) and 4 anions (NH_2COO^-, $CO_3^=$, HCO_3^- and OH^-), and one electroneutrality constraint. Correspondingly, the system has to be ternary with three degrees of freedom in a two phase situation. The six reactions considered are the following:

1. Dissociation of aqueous ammonia.

$$NH_3 + H_2O \longleftrightarrow NH_4^+ + OH^- \qquad (\text{eq. } 5.1)$$

2. First dissociation of aqueous carbon dioxide.

$$CO_2 + H_2O \longleftrightarrow HCO_3^- + H^+ \qquad (\text{eq. } 5.2)$$

3. Second dissociation of aqueous carbon dioxide.

$$HCO_3^- \longleftrightarrow CO_3^= + H^+ \qquad (\text{eq. } 5.3)$$

4. Dissociation of water.

$$H_2O \longleftrightarrow H^+ + OH^- \qquad (\text{eq. } 5.4)$$

5. Formation of carbamate ion.

$$NH_3 + HCO_3^- \longleftrightarrow NH_2COO^- + H_2O \qquad (\text{eq. } 5.5)$$

6. Formation of urea.

$$NH_2COO^- + NH_4^+ \longleftrightarrow NH_2CONH_2 + H_2O \qquad (\text{eq. } 5.6)$$

The above equilibria can be described thermodynamically as follows:

$$K_1 \cdot a_w \cdot m_{m1} \cdot \gamma_{m1} - m_{c1} \cdot \gamma_{c1} \cdot m_{a4} \cdot \gamma_{a4} = 0 \qquad (\text{eq. } 5.7)$$

$$K_2 \cdot a_w \cdot m_{m2} \cdot \gamma_{m2} - m_{c2} \cdot \gamma_{c2} \cdot m_{a3} \cdot \gamma_{a3} = 0 \qquad (\text{eq. } 5.8)$$

$$K_3 \cdot m_{a3} \cdot \gamma_{a3} - m_{c2} \cdot \gamma_{c2} \cdot m_{a2} \cdot \gamma_{a2} = 0 \qquad (\text{eq. } 5.9)$$

$$K_4 \cdot a_w - m_{c2} \cdot \gamma_{c2} \cdot m_{a4} \cdot \gamma_{a4} = 0 \qquad (\text{eq. } 5.10)$$

$$K_5 \cdot m_{m1} \cdot \gamma_{m1} \cdot m_{a3} \cdot \gamma_{a3} - a_w \cdot m_{a1} \cdot \gamma_{a1} = 0 \qquad (\text{eq. } 5.11)$$

$$K_6 \cdot m_{c1} \cdot \gamma_{c1} \cdot m_{a1} \cdot \gamma_{a1} - m_{m3} \cdot \gamma_{m3} \cdot a_w = 0 \qquad (\text{eq. } 5.12)$$

In the above relations, m_{mi}, $i=1$ to 4, denote the molalities of molecular species NH_3, CO_2, H_2O and NH_2CONH_2 respectively. Similarly m_{ci}, $i=1$ and 2, denote the molalities of the cations NH_4^+ and H^+. The anion molalities m_{ai}, $i=1$ to 4, pertain to NH_2COO^-, $CO_3^=$, HCO_3^- and OH^- respectively. A similar nomenclature is followed in respect of the activity coefficients.

Due to the presence of volatile species, there are in addition phase equilibria involving NH_3, CO_2 and H_2O which can be formulated as follows:

$$\hat{f}_{mi,G}(p,T,\underline{x}) = \hat{f}_{mi,L}(p,T,\underline{y}) \qquad i = 1,2,3 \quad \text{(eq. 5.13)}$$

i.e.

$$y_i \cdot \phi_i \cdot P = m_{mi} \cdot \gamma_{mi} \cdot \hat{f}_{mi,L}^{\,ref}(p,T) \qquad i = 1,2,3 \quad \text{(eq. 5.14)}$$

The reference state fugacities $\hat{f}_{mi,L}^{\,ref}$ for the two volatile species NH_3 and CO_2 can be chosen to be the Henry's constants and that for the solvent water, the fugacity of the pure saturated water at the chosen temperature. As usual, all the reference state fugacities have to be corrected for pressure effects in terms of Poynting corrections using the molar volume of water and the partial molar volumes of NH_3 and CO_2 at infinite dilution.

$$\hat{f}_{mi,L}^{\,ref}(p,T) = f_{mi,L}^{\infty} \cdot \exp(v_{i,w}^{\infty} \cdot (p-p_w^*)/(R.T)) \qquad i=1 \text{ and } 2 \quad \text{(eq. 5.15)}$$

$$= H_i(T).\exp(v_{i,w}^{\infty} \cdot (p-p_w^*)/(R.T)) \qquad i=1 \text{ and } 2 \quad \text{(eq. 5.16)}$$

$$\hat{f}_{m3,L}^{\,ref}(p,T) = f_{mw,G}^{*}(p_w^*,T).\exp(v_w^*.(p-p_w^*)/(R.T)) \quad \text{(eq. 5.17)}$$

$$= p_w^*.\,\phi_w^*(p_w^*,T).\exp(v_w^*.(p-p_w^*)/(R.T)) \quad \text{(eq. 5.18)}$$

With the above choice of reference state fugacities, the activity coefficients can be normalized in terms of assymetric convention. This implies that the activity coefficients of all the solutes, both ionic and molecular, become unity when the concentrations of all the solute species approach zero. As for water, its activity becomes unity when it is pure. That is:

$$\lim_{\sum_i m_i \to 0} \gamma_{mi} = 1; \quad \lim_{\sum_i m_i \to 0} \gamma_{ci} = 1; \quad \lim_{\sum_i m_i \to 0} \gamma_{ai} = 1 \quad \text{(eq. 5.19)}$$

$$\text{and} \quad \lim_{x_w \to 1} a_w = 1 \quad \text{(eq. 5.20)}$$

In addition to the 9 relations (eq. 5.7 to 5.12 and eq. 5.14), there are 2 liquid phase mass balances and an electroneutrality constraint. The necessity of considering the mass balances stems from the difficulty of analysing the liquid phase species composition and the ease of analysing the component composition.

$$mNH_3 = m_{m1} + 2\,m_{m3} + m_{c1} + m_{a1} \quad \text{(eq. 5.21)}$$

$$mCO_2 = m_{m2} + m_{m3} + m_{a1} + m_{a2} + m_{a3} \quad \text{(eq. 5.22)}$$

$$m_{c1} + m_{c2} = m_{a1} + 2\,m_{a2} + m_{a3} + m_{a4} \quad \text{(eq. 5.23)}$$

Since this system has three degrees of freedom, one may specify the temperature and two liquid phase component concentrations mNH_3 and mCO_2 to determine uniquely the pressure and vapour concentrations. The set of 12 equations can be solved if there are models describing the gas and liquid phase non-idealities. Further, the problem can be made less complex with cartain simple assumptions.

The first assumption is the pressure insensitivity of the reaction equilibrium constants and the liquid phase model parameters in the pressure range of 1 to 30 bar. This single assumption, valid due to the low volume changes of ionic reactions, enables one to split the above system of 12 equations (eq. 5.7 to 5.12, eq. 5.14 and eq. 5.21 to 5.23) into two blocks. In other words, given T, mNH_3 and mCO_2, one can solve separately the set of equations involving the reaction equilibria (eq. 5.7 to 5.12), the liquid phase mass balances (eq. 5.21 and 5.22) and the electroneutrality (eq. 5.23), thereby determining the individual species molalities. With the molalities of free NH_3 and free CO_2 along with their activity coefficients and the activity of water thus being known, one can further calculate the gas phase mole fractions of NH_3, CO_2, H_2O and the total pressure, utilizing the remaining phase equilibria relations (eq. 5.14).

In order to realize this objective, one has to develop the working equations of the liquid and gas phase models. Choosing a gas phase model, namely an equation of state, is comparatively easy. The equation of state chosen in this study is due to Nakamura et al [42]. In an exploratory investigation (see chapter 6 and appendix B), this equation was found to describe very well the gas phase density data of Durisch and van den Berg [43], collected during the study related to urea synthesis conditions. Encouraged by this feature, the same equation is employed here to calculate the fugacity coefficients. This leaves only the liquid phase to be described in the next section.

5.3. *The liquid phase ion specific interaction model*:

The earliest proposal on ion specific interaction was raised by Bronsted [44] predating even the theoretical treatment of Debye and Huckel [4]. According to his proposal for the osmotic and activity coefficient expressions of pure electrolytes in terms of molality, one has to include a linear dependency term (to highlight the short range ion specific interaction) over and above the half power dependency term (representing the long range influences), as given below.

$$1 - \phi - \alpha m^{1/2} + \beta . m \qquad \text{(eq. 5.24)}$$

Further Bronsted postulated that the ion specific interaction occurs only between ions of unlike charges, and that the interaction between like charges is only through long range forces (i.e. through the parameter). Later Guggenheim [45] proposed a modified function for the long range term based on the *Debye-Huckel* contribution, while keeping the ion-specific term advocated by Bronsted unchanged. Guggenheim's equations are applicable for 1-1, 1-2 and 2-1 electrolytes up to an ionic strength molality of around 0.1. On further analysis of the Guggenheim expression with the osmotic coefficient data of simple electrolytes, Pitzer [18] established a few basic points. These points are:

1. The parameter β is dependent on the ionic strength at low concentrations.
2. A simlar parameter for the like ion interactions cannot be neglected.
3. The ternary terms may be necessary for very high concentrations.

These observations, which were further supported by the molecular dynamics and integral equation approaches, led Pitzer to suggest a comprehensive virial form of the Gibb's free energy of the multielectrolye solutions as given below.

$$G^{ex}/(n_w.R.T) = f(I) + \sum_{i,j} \lambda_{ij}(I).m_i.m_j + \sum_{i,j,k} \mu_{ijk}.m_i.m_j.m_k \qquad \text{(eq. 5.25)}$$

In the above equation, the function f(I) is specific to the solvent but common to all the solutes, accounting for the long range interactions between them. Further the term reduces to the Debye-Huckel limiting law, when the ionic strength tends to zero. The parameters λ_{ij} are the second virial coefficients, while the μ_{ijk} are the third virial coefficients describing the solvent moderated short range interactions which depend on temperature. It is assumed that the λ and μ matrices are symmetrical, Further in view of simplicity, the μ_{ijk} terms are considered to be independent of ionic strength.

A major weakness of the model posed above (just like many other electrolyte models) is the fact that the solvent affects the excess Gibbs energy only through the dielectric constant. In other words the model presumes the solvent water to be a structureless physical continuum.

In order to express the virial equation in terms of experimentally convenient parameters, one may define the following:

$$B^{\phi}_{ca}(I) = \lambda_{ca}(I) + I\lambda'_{ca} + (\nu_c/(2\nu_a))*(\lambda_{cc}+I\lambda'_{cc})+(\nu_a/(2\nu_c))*(\lambda_{aa}+I\lambda'_{aa}) \qquad \text{(eq. 5.26)}$$

$$C^{\phi}_{ca} = (3/(\nu_c\nu_a)^{1/2})*(\nu_c\mu_{cca} + \nu_a\mu_{caa}) \qquad \text{(eq. 5.27)}$$

$$\underline{\theta}_{cc'} = \lambda_{cc'}(I) - (z_{c'}/(2z_c))\lambda_{cc}(I) - (z_c/2z_{c'}))\lambda_{c'c'}(I) \qquad \text{(eq. 5.28)}$$

$$\psi_{cc'a} = 6\mu_{cc'a} - ((3z_{c'})/z_c)\mu_{cca} - ((3z_c)/z_{c'})\mu_{c'c'a} \qquad \text{(eq. 5.29)}$$

where λ'_{ij} stands for the derivative $(d\lambda_{ij}/dn_w)$.

The parameters B and $\underline{\theta}$ are meant for the binary interactions between ions, while *the C and ψ account for the ternary effects. Moreover, their definitions imply that B* and C are characteristic of a single electrolyte system, while $\underline{\theta}$ and ψ are descriptive of mixed electrolyte systems.

Now in view of the thermodynamic expressions,

$$(\phi - 1)\sum_i m_i = -\partial(G^{ex}/R.T)/\partial n_w \qquad \text{(eq. 5.30)}$$

$$\ln \gamma_i = (1/n_w).\,\partial(G^{ex}/R.T)/\partial m_i \qquad \text{(eq. 5.31)}$$

the following formulae for the osmotic and activity coefficients can be derived:

$$\begin{aligned}(\phi-1)\sum_i m_i/2 = {} & (-A_\phi I^{3/2}/(1+bI^{1/2})) + \sum_c \sum_a m_c m_a (B^{\phi}_{ca} + zC_{ca}) \\ & + (1/2) \sum_c \sum_{c'} m_c m_{c'} (\underline{\theta}^{\phi}_{cc'} + \sum_a m_a \psi_{cc'a}) \\ & + (1/2) \sum_a \sum_{a'} m_a m_{a'} (\underline{\theta}^{\phi}_{aa'} + \sum_c m_c\ {}_{aa'c})\end{aligned} \qquad \text{(eq. 5.32)}$$

$$\ln a_w = \ln x_w - ((\phi-1)\sum_i m_i)*0.018015 \qquad \text{(eq. 5.33)}$$

$$\begin{aligned}\ln \gamma_M = {} & z_M^2 F + \sum_a m_a (2B_{Ma} + zC_{Ma}) + \sum_c m_c (2\underline{\theta}_{Mc} + \sum_a m_a \psi_{Mca} \\ & + (1/2) \sum_a \sum_{a'} m_a m_{a'} \psi_{Maa'} + |z_M| \sum_c \sum_a m_c m_a C_{ca}\end{aligned} \qquad \text{(eq. 5.34)}$$

$$\begin{aligned}\ln \gamma_X = {} & z_X^2 F + \sum_c m_c (2B_{cX} + zC_{cX}) + \sum_a m_a (2\underline{\theta}_{Xa} + \sum_c m_c \psi_{cXa} \\ & + (1/2) \sum_c \sum_{c'} m_c m_{c'} \psi_{cc'X} + |z_X| \sum_c \sum_a m_c m_a C_{ca}\end{aligned} \qquad \text{(eq. 5.35)}$$

where M and X stand for a specific cation and anion, respectively.

The functional form of f(I) as the one given below was reached by Pitzer through empirical arguments.

$$f(I) = 4A_\phi (I/1.2)*\ln(1+1.2I^{1/2}) \qquad \text{(eq. 5.36)}$$

With this form of f(I), the function F works out to be as follows:

$$\begin{aligned}F = {} & -A_\phi (I^{1/2}/(1+1.2I^{1/2}) + (2/1.2)*\ln(1+1.2I^{1/2})) + \sum_c \sum_a m_c m_a B'_{ca} \\ & + (1/2) \sum_c \sum_{c'} m_c m_{c'} \underline{\theta}'_{cc'} + (1/2) \sum_a \sum_{a'} m_a m_{a'} \underline{\theta}'_{aa'}\end{aligned} \qquad \text{(eq. 5.37)}$$

Further, the Debye-Hückel parameter value used in the present study was obtained through the regression expression derived by Chen et al.

$$A_\phi(I) = -1.306568 + 0.01328238*T - 0.3550803*10^{-4}*T^2 + 0.3381968*10^{-7}*T^3 \qquad \text{(eq. 5.38)}$$

Pitzer proposed the following relation for the dependence of B^{ϕ}_{ca} on the ionic strength through semi-empirical arguments.

$$B_{ca} = \beta^0{}_{ca} + \beta^1{}_{ca}*\exp(-2I^{1/2}) \qquad \text{(eq. 5.39)}$$

Subsequently the related forms for the free energy and activity coefficient expressions can be derived as given below.

$$B_{ca} = \beta^0{}_{ca} + \beta^1{}_{ca}*\hat{g}(x) \qquad \text{(eq. 5.40)}$$

$$B'_{ca} = \beta^1{}_{ca}*g'(x)/I \qquad \text{(eq. 5.41)}$$

$$\hat{g}(x) = 2*(1-(1+x)\exp(-x))/x^2 \qquad \text{(eq. 5.42)}$$

$$g'(x) = -2*(1-(1+x+(1/2)*x^2)\exp(-x))/x^2 \qquad \text{(eq. 5.43)}$$

$$\text{with } x = 2*I \qquad \text{(eq. 5.44)}$$

It is to be noted that equations 5.40, 5.41 and 5.42 hold only for 1-1 and 1-2 electrolytes. For higher valence types like 2-2, there is a tendency towards pairing and additional terms must be added.

Definitions of a few more terms used in the above equations are as follows:

$$C_{ca} = C^{\phi}_{ca}/(2|z_c z_a|^{1/2}) \qquad \text{(eq. 5.45)}$$

$$Z = \sum_i m_i |z_i| = 2 \sum_c m_c z_c \qquad \text{(eq. 5.46)}$$

$$\theta^{\phi}_{ij} = \theta_{ij} + {}^{E}\theta_{ij}(I) + I * {}^{E}\theta'_{ij}(I) \qquad \text{(eq. 5.47)}$$

$$\underline{\theta}_{ij} = \theta_{ij} + {}^{E}\theta_{ij}(I) \qquad \text{(eq. 5.48)}$$

$$\underline{\theta}'_{ij} = {}^{E}\theta'_{ij}(I) \qquad \text{(eq. 5.49)}$$

The terms ${}^{E}\theta_{ij}$ and ${}^{E}\theta'_{ij}$ in the above expressions are zero for 1-1 electrolytes and are negligible for 1-2 electrolytes.

In order to extend (eq. 5.25) for molecular solutes, one can write:

$$G^{ex} = (G^{ex})_{ions} + (G^{ex})_{ion\text{-}molecule} + (G^{ex})_{molecule\text{-}molecule} \qquad \text{(eq. 5.50)}$$

On this basis, (eq.5.25) can be modified as:

$$\begin{aligned} G^{ex}/(n_w RT) = (G^{ex}/n_w RT)_{ions} &+ \sum_m \sum_i \lambda_{mi} m_m m_i + \sum_m \sum_{m'} \lambda_{mm'} m_m m_{m'} \\ &+ \sum_m \sum_{m'} \sum_{m''} \mu_{mm'm''} m_m m_{m'} m_{m''} \end{aligned} \qquad \text{(eq. 5.51)}$$

where m,m',m" stand for molecules and i for ions.

In the above expression, no terms describing molecule-molecule-ion interaction or ion-ion-molecule interaction are included. It is also assumed that the λ_{mi} and $\lambda_{mm'}$ are very weak functions of concentration, and hence they can be considered to be dependent only on temperature.

If (eq. 5.51) is differentiated, the following modifications are made to equations 5.32, 5.34 and 5.35:

$$\begin{aligned} (\phi-1) \sum_i m_i = ((\phi-1) \sum_i m_i)_{ions} &+ 2 \sum_m \sum_c \lambda_{mc} m_c m_m + 2 \sum_m \sum_a \lambda_{ma} m_a m_m \\ &2 \sum_m \sum_{m'} \sum_{m''} \mu_{mm'm''} m_m m_{m'} m_{m''} \end{aligned} \qquad \text{(eq. 5.52)}$$

$$\ln \gamma_M = (\ln \gamma_M)_{ions} + 2 \sum_m \lambda_{mM} m_M \qquad \text{(eq. 5.53)}$$

$$\ln \gamma_X = (\ln \gamma_X)_{ions} + 2 \sum_m \lambda_{mX} m_X \qquad \text{(eq. 5.54)}$$

Additionally a new expression for the activity coefficient of molecular solutes is introduced.

$$\begin{aligned} \ln \gamma_k &= 1/(n_w RT) * \partial (G^{ex})/\partial m_k \\ &= 2 \sum_c \lambda_{ck} m_c + 2 \sum_a \lambda_{ak} m_a + 2 \sum_m \lambda_{km} m_m + 3 \sum_{m} \sum_{m'} \mu_{kmm'} m_m m_{m'} \end{aligned} \qquad \text{(eq. 5.55)}$$

Although the above set of equations describing the liquid phase non-idealities together with expressions for temperature dependent quantities (to be described shortly) may look formidable, they are conceptually simple and can be implemented efficiently in a subroutine using iterative loops.

At the same time, however, a judicious choice of the right type and number of parameters based on sensitivity is very crucial in the implementation of such virial coefficient models. Afterall, there are both weaknesses and strengths attributed to virial coefficient models on this account. Müller [31] concludes that the modified Pitzer model along with the parameters suggested by Maurer [28] describe the system reasonably well up to 100°C. For higher temperatures, he mentions that the parameters derived by Maurer [28], Edwards et al [26] and Pawlikowski et al [30] are unsuitable. In fact, a detailed analysis reveals the inconsistency of the corresponding parameters from author to author not only in terms of absolute values but sometimes even in the sign and order of magnitude. Also such parameter values do not fit with the pattern proposed by Pitzer [18] in describing the analogous alkali electrolytes. Since this pattern relates to the structure making/ breaking capabilities of the ionic species in water, one finds the inconsistency hard to comprehend. Because of this uncertainty and since the measurements of this study are in the concentrated range involving free NH_3, NH_4^+ and NH_2COO^-, it is proposed to find out the optimum parameters anew for the liquid phase model, through an optimization procedure.

5.4. *The temperature dependent quantities*:

To solve the set of 12 equations (5.7 to 5.12, 5.14 and 5.21 to 5.23) one needs two kinds of temperature dependent quantities, namely the reference fugacities and the equilibrium constants.

The reference fugacities require the partial molar volumes of NH_3 and CO_2 at infinite dilution (estimated by the procedure of Brelvi and O'Connell [46]), the vapour pressure and specific volume of water, and the Henry constants.

Firstly, the data on specific volume of water in ml/gm available from the standard sources [47] are subjected to a regression analysis to yield the following quadratic expression.

$$v_w = 3.698585*10^{-9}*T^2 - 1.9475*10^{-6}*T + 1.2551797*10^{-3} \text{ in ml/gm} \qquad \text{(eq. 5.56)}$$

Likewise, the vapour pressure of water in the temperature range chosen (25-150°C) is expressed in Pascals through a Antoine-type equation shown below, using the data available in standard tables [47].

$$\text{Log}_{10}\ (P_w/(1.01325*10^5)) = (5.110545-1687.058/(229.695+(T-273.15)) \qquad \text{(eq. 5.57)}$$

Table 5.1.*The Henry constant for the system NH_3-H_2O*

t °C	$H_{1,exp}$ bar.mol/mol.	$H_{1,calc}$ (eq.5.66) bar.mol/mol	Deviation %	Reference
100.00	12.84	13.12	-2.22	Muller [31]
140.00	33.33	34.93	-4.81	
200.00	93.86	98.82	-5.28	
10.00	0.38	0.40	-4.80	Wilson [49]
21.11	0.69	0.70	-1.19	
32.22	1.17	1.17	-0.15	
43.33	1.90	1.89	0.51	
54.44	2.99	2.94	1.63	
60.00	3.67	3.62	1.26	
71.11	5.39	5.37	0.34	
82.22	7.68	7.73	-0.71	
93.33	10.64	10.84	-1.92	
104.44	14.24	14.83	-4.16	
110.00	16.37	17.20	-5.07	
97.00	12.30	12.06	1.97	Clifford and Hunter [50]
100.00	12.90	13.12	-1.74	
127.00	26.16	26.16	0.00	
80.00	7.05	7.21	-2.23	Mollier [51]
90.00	9.95	9.83	1.25	
100.00	13.50	13.12	2.78	
110.00	17.84	17.20	3.59	
120.00	22.74	22.14	2.64	
0.00	0.23	0.23	-0.24	Perman [52]
10.00	0.40	0.40	0.44	
19.90	0.68	0.66	3.20	
30.09	1.10	1.06	3.23	
40.00	1.76	1.64	6.57	
50.00	2.36	2.48	-4.87	Pierre [53]
60.00	3.52	3.62	-2.94	
70.00	5.10	5.17	-1.40	
80.00	7.12	7.21	-1.22	

t ^oC	$H_{1,exp}$ bar.mol/mol.	$H_{1,calc}$ (eq.5.66) bar.mol/mol	Deviation %	Reference
90.00	9.74	9.83	-0.88	Pierre [53]
100.00	13.21	13.12	0.65	
110.00	17.40	17.20	1.15	
120.00	22.61	22.14	2.08	
130.00	28.61	28.03	2.03	
140.00	35.68	34.93	2.09	
150.00	43.36	42.90	1.06	
160.00	52.40	51.96	0.84	
170.00	62.62	62.12	0.81	
180.00	73.97	73.35	0.84	
190.00	86.78	85.61	1.35	
200.00	100.85	98.82	2.02	

5.4.1. *The Henry constants*:

The Henry constant for NH_3 used in the present study was correlated by Edwards et al and that for CO_2 by Chen et al [29]. These constants are expressed below in Pa.kg of water/mole.

$$H_1 = \exp(-157.552/T+28.1001*\ln T-0.049227*T-149.006)*1.01325*10^5. \qquad \text{(eq. 5.58)}$$

$$H_2 = \exp(-8477.711/T-21.95743*\ln T+0.005780748*T+155.1699)*1.01325*10^5 \qquad \text{(eq. 5.59)}$$

Although these expressions perform well in describing the said constants, they fail rather poorly when pressed into use (!) for deriving the heat of solution of NH_3 and CO_2 in an infinite amount of solvent water. Such heats of solution are needed in calculating the reaction equilibrium constants K_5 and K_6. Hence, deriving new expressions for the Henry constants compatible with the earlier experimental heats of solution became necessary; this was achieved through a fresh analysis of the binary literature data.

5.4.2. *Derivation of the heats of solution of NH_3 and CO_2*:

Clarke and Glew [48] gave the following Taylor development of an equilibrium constant with thermodynamically meaningful regression coefficients.

$$\begin{aligned} R*\ln K_p = &- (\Delta G^o/\Theta) + \Delta H^o*T_1 + \Delta C_p{}^o*T_2 + (d\Delta C_p{}^o/dT)*T_3 + (d^2\Delta C_p{}^o/dT^2)*T_4 \\ &+ (d^3\Delta C_p{}^o/dT^3)*T_5 \end{aligned} \qquad \text{(eq. 5.60)}$$

where,

- the reference temperature, (here it is 298.15 K)

$$T_1 = ((1/\theta) - (1/T)) \qquad \text{(eq. 5.61)}$$

$$T_2 = ((\theta/T) - 1 + \ln(T/\theta)) \qquad \text{(eq. 5.62)}$$

$$T_3 = ((T/\theta) - (\theta/T) - 2*\ln(T/\theta))*(\theta/2) \qquad \text{(eq. 5.63)}$$

$$T_4 = ((T/\theta)^2 - 6*(T/\theta) + 3 + 2*(\theta/T) + 6*\ln(T/\theta))*(\theta^2/12) \qquad \text{(eq. 5.64)}$$

$$T_5 = ((T/\theta)^3 - 6*(T/\theta)^2 + 18*(T/\theta) - 10 - 3*(\theta/T) - 12*\ln(T/\theta))*(\theta^3/72) \qquad \text{(eq. 5.65)}$$

Choosing the above expression for the Henry constant of NH_3 in bar.mole/mole, thirtythree sets of data of the system NH_3-H_2O (given here in Table 5.1 and compiled by Müller [31]), are correlated as given below.

$$R*\ln H_1 = -0.344211679 + 8329.97039*T_1 - 4.424735*T_2 - 0.091914*T_3 \qquad \text{(eq. 5.66)}$$

The multiple correlation coefficient and the estimated standard error are 0.9999 and 0.0547, respectively, with Fischer's variance around 46407. Further inclusion of the T_4 and T_5 variables proved to be statistically insignificant.

Similarly the Henry constant data (43 in number expressed in bar.mole/mole) for the binary CO_2-H_2O system, compiled by Müller [31] and Weiss [54] and given in Table 5.2, are utilized to get the following regression expression.

$$R*\ln H_2 = 14.7140625 + 4741.96659*T_1 - 44.07944*T_2 + 0.127051*T_3 \qquad \text{(eq. 5.67)}$$

The multiple correlation coefficient and the estimated standard error are 0.9997 and 0.0342 respectively, with Fischer's variance around 30436. Once again, inclusion of the T_4 and T_5 proved to be statistically insignificant.

To get the heat of solution we use the following thermodynamic expression valid at the saturation conditions, as given by Redlich et al [55].

$$-(\Delta H_i^o/(R*T^2)) = (\partial \ln(H_i/\mathrm{bar})/\partial T)_\sigma - ((V_i/(R*T))*(\partial p/\partial T)_\sigma \qquad \text{(eq. 5.68)}$$

The second term on the right hand side is usually negligible and hence by differentiating the Henry's constant expression and multiplying by $-R*T^2$, one can arrive at the heat of solution of volatile gases.

Accordingly for NH_3 and CO_2, the following expressions are obtained.

$$\Delta H_{1,sol} = 8329.97039 - 4.424735*(T-\theta) - 0.045957*(T-\theta)^2 \quad \text{in cal/mole} \qquad \text{(eq. 5.69)}$$

$$\Delta H_{2,sol} = 4741.96659 - 44.07944*(T-\theta) + 0.0635255*(T-\theta)^2 \quad \text{in cal/mole} \qquad \text{(eq. 5.70)}$$

These two expressions are plotted in Fig. 5.1 and 5.2. In Fig. 5.1, the values of van der Zee [66], Worswick et al [67], Landolt-Bornstein [68] and Wagman et al(NBS) [69], and a recalculated value of van der Zee by the present author are also marked. It can be seen that there is a spread of about 200 cal. among the experimentally observed heat of solution of NH_3 at 25^oC. The high temperature values could

Table 5.2. *The Henry constant for the system CO_2-H_2O*

t °C	$H_{2,exp}$ bar.mol/mol.	$H_{2,calc}$ (eq.5.67) bar.mol/mol	Deviation %	Reference
100.0	5129	5065	1.25	Muller [31]
120.0	5744	5598	2.53	
140.0	5905	5890	0.25	
160.0	5775	5968	-3.34	
200.0	5498	5662	-2.98	
200.0	5839	5662	3.03	Takenouchi and Kennedy [56]
110.0	5364	5362	0.03	
150.0	5969	5953	0.26	
15.0	1275	1229	3.58	Haehnel [57]
50.0	2731	2852	-4.43	Zelvenskii [58]
100.0	4957	5065	-2.18	
10.0	1027	1044	-1.64	Stewart and Munjal [59]
12.43	1108	1132	-2.17	Wroblewskii [60]
10.0	1042	1044	-0.18	Morgan and Maass [61]
18.0	1329	1348	-1.43	
11.5	1110	1098	1.09	Novak et al [62]
20.0	1429	1430	-0.76	
30.0	1874	1871	0.17	
40.0	2389	2351	1.60	
60.0	3408	3355	1.55	
69.0	3712	3795	-2.23	
31.04	1889	1919	-1.60	Wiebe and Gaddy [63]
35.0	2051	2107	-2.73	
40.0	2382	2351	1.31	
50.0	2863	2352	0.38	
75.0	4091	4075	0.39	
100.0	5226	5065	3.08	

t °C	$H_{2,exp}$ bar.mol/mol.	$H_{2,calc}$ (eq.5.67) bar.mol/mol	Deviation %	Reference
101.0	4928	5097	-3.44	Prutton and Savage [64]
100.0	5042	5065	-0.45	Zawisza and Malesinska [65]
125.0	5827	5693	2.29	
150.0	5906	5953	-0.80	
175.0	5985	5912	1.22	
0.0	725	723	0.33	Weiss [54]
1.0	726	752	-3.53	
2.0	784	781	0.34	
3.0	815	812	0.39	
4.0	846	843	0.37	
5.0	878	875	0.37	
6.0	911	907	0.42	
8.0	978	974	0.39	
10.0	1048	1044	0.39	
12.0	1121	1116	0.43	
14.0	1196	1191	0.42	
16.0	1274	1268	0.44	
18.0	1354	1348	0.44	
20.0	1436	1430	0.41	
22.0	1521	1514	0.44	
24.0	1607	1601	0.40	
26.0	1696	1689	0.42	
28.0	1786	1779	0.39	
30.0	1878	1871	0.38	
32.0	1971	1964	0.34	
34.0	2066	2059	0.34	
36.0	2161	2155	0.27	
38.0	2257	2253	0.20	
40.0	2354	2351	0.13	

not be checked for want of data. Based on the spread, it appears that further work on calorimetric determination of heats of solution is necessary. Unlike the situation with NH_3, the regression line for CO_2 is an excellent fit of the experimental heat of solution values (by Harned aand Davis [70], Ellis and Golding [71] and Ellis [72]) over a wide temperature range.

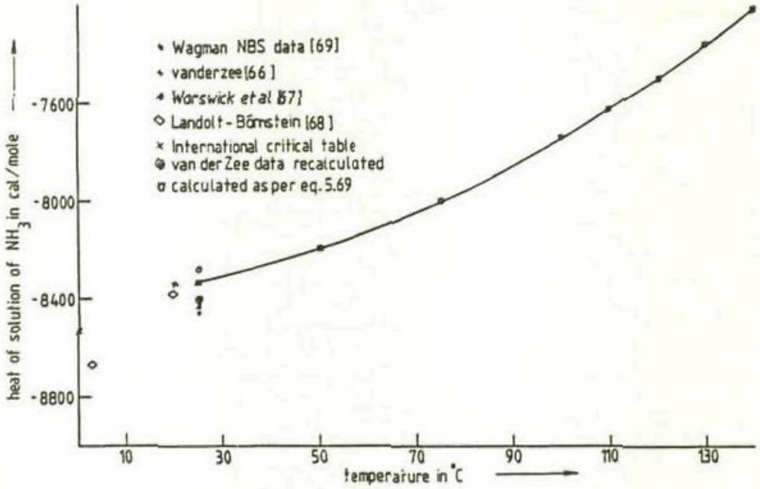

Fig. 5.1. *The heat of solution of ammonia in water.*

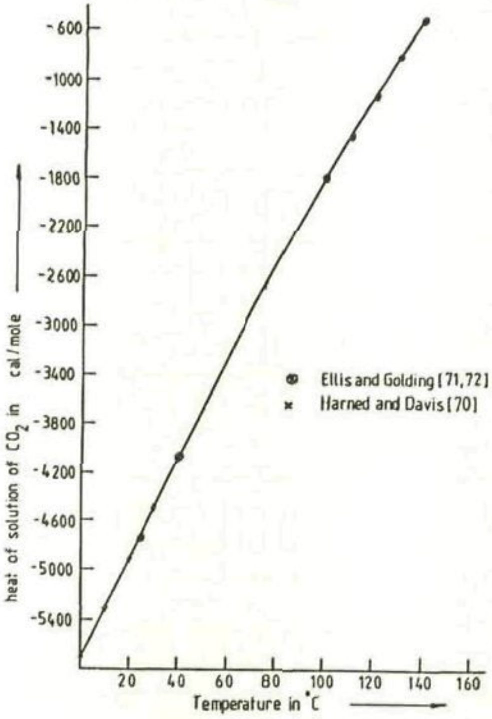

Fig. 5.2. *The heat of solution of carbon dioxide.*

5.4.3. *The reaction equilibrium constants*:

Of the six reaction equilibria, four have been studied before leading to reliable equilibrium constant expressions. The equilibrium constant expression for the dissociation of aqueous ammonia, adopted from Read [73], is given below.

$$\ln K_1 = 2814.03 - 70047.7/T - 512.21*\ln T + 1.262*T - 5.39132*10^{-4}*T^2 \qquad \text{(eq. 5.71)}$$

For the first and second dissociation of aqueous CO_2, the expressions given by Patterson et al [74] and Larson et al [75] are adopted respectively.

$$\log_{10} K_2 = -522.461 + 29688.2/T + 81.8401*\ln T - 0.0896488*T - 2.04679*10^6/T^2 \qquad \text{(eq. 5.72)}$$

$$\ln K_3 = 183.53129 - 10732.827/T - 30.0681532*\ln T \qquad \text{(eq. 5.73)}$$

For the ionization of water, the following expression given by Sweeton et al [76] is found adequate for the required purpose.

$$\log_{10} K_4 = -670.857 + 34691.6/T + 105.151*\ln T - 0.1075733*T - 2.35812*10^6*T^2 \qquad \text{(eq. 5.74)}$$

5.4.3.1. *The equilibrium constant for the formation of carbamate*:

One of the earliest determinations of the equilibrium constant at infinite dilution conditions for the formation of carbamate from bicarbonate was due to Faurholt [77]. He gave a value of 2.29 at 18°C and 3.33 at 0°C. Later Christensen et al [78] determined the same equilibrium constant at an ionic strength of 0.5 and gave four values, namely 2.13 - 25°C, 1.94 - 35°C, 1.52 - 50°C and 1.2 - 70°C. Additionally, Marion and Dutt [79] in a study on the ion association of the present system calculated a value of 2.4 for this reaction at 20°C. Further very recently, by following the progress of the carbamate formation through isotopes in the system of NH_3-CO_2-H_2O, Usdowskii [80] et al determined a value of 1.87 at 18°C. All these above values together with the value of 3.4 at 20°C given earlier by van Krevelen [37], four values given by Frohlich [38] and 6 values obtained from the work of Szarawara [81] are plotted in Fig. 5.3. It can be observed that the data due to van Krevelen [37], Frohlich [38] and Szarawara [81] are widely off the remaining points, which fall in a smooth curve. To proceed further to high temperature, one has to resort to theoretical extrapolations. This is also necessary due to the fact that the values of Christensen et al [78] at 50 and 70°C may be only qualitatively acceptable due to the ionic strength of 0.5 maintained during his measurements. This condition, however, may not have serious effects at lower temperatures.

Also Edwards et al gave two equilibrium constant expressions for the formation of carbamate, the first one [26a] with a standard heat of reaction of -3970 cal/mole and the second [26b] with -5763 cal/mole. In a follow-up study from the same school, Pawlikowski et al [30] gave the following expression.

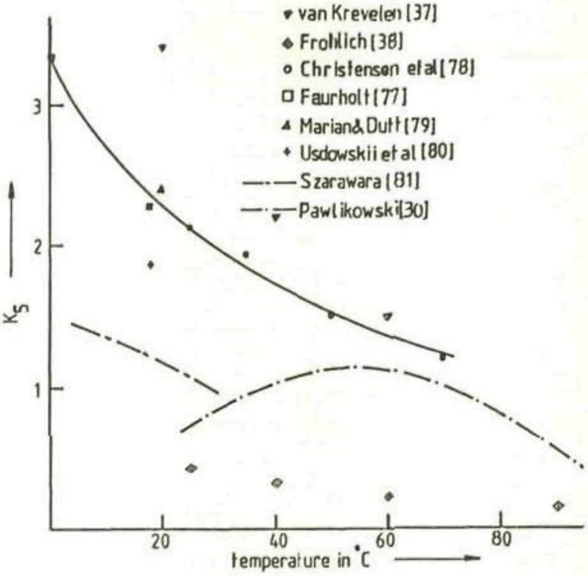

Fig. 5.3. *The values of the equilibrium constant for the formation of carbamate from bicarbonate, as presented by various researchers..*

$$\ln K_5 = 100 - 16128.57/T - 0.15152*T \qquad \text{(eq. 5.75)}$$

The above equilibrium constant expression, also plotted in Fig. 5.3, gives values very different from the experimental ones. Moreover attributing an endothermic heat of reaction at temperatures below $53^{\circ}C$ (5285 cal/mole at $25^{\circ}C$) is certainly not compatible with the observation of Christensen et al [78].

Since K_5 is a very important quantity for the present study and since no reliable expressions are available, it became essential to determine K_5 or at least the equilibrium constant K_E of the following related reaction.

$$CO_2(aq) + 2NH_3(aq) <\!\!\!-\!\!\!> NH_4^+(aq) + NH_2COO^-(aq) \qquad \text{(eq. 5.76)}$$

Fortunately the data due to Faurholt [77], Christensen et al [78], Marion and Dutt [79] and Ustowski et al [80] can be of help in arriving at the value of K_E at $25^{\circ}C$. Furthermore, to estimate K_E at various temperatures, one needs to know the heat of the above reaction (eq. 5.76) at these temperatures. This in turn necessitates a knowledge of the heat of dissolution of carbamate in an infinitely large amount of water at standard conditions and the molar heat capacity of solid ammonium carbamate at various temperatures.

Experimental determinations of the heats of formation and solution of carbamate by the earlier authors are very few. Gmelin [82] presented an approximate value of 3.8 Kcal/mole for the dissolution of ammonium carbamate in water. In an effort to find the standard heat of formation of alkali carbamates, Claude [83] and Bernard-Borrel [84] determined the heat of dissolution and hydrolysis of such carbamates. Unfortunately, it appears on detailed analysis that their values are inconclusive due to the consideration of two or three side reactions. Through a rapid thermal method, Pinsent et al [85] determined the heat of reaction (eq. 5.76) at five different temperatures as given below:

Temperature in ^{o}C	0	10	20	30	40
Observed $\Delta H_{carb,aq}$ in cal/mole	-9000	-11100	-12700	-14300	-15600

The procedure used here to arrive at the heat of solution at standard conditions is simple. Knowing the heats of solution of NH_3 and CO_2 (ΔH_1 and ΔH_2), the heat of carbamate formation through the reaction (eq. 5.76) (which is 13500 cal/mole based on the above data) and the heat of carbamate formation through the following reaction, one can arrive at the heat of solution of carbamate by Hess's law.

$$2NH_3(g) + CO_2(g) <\!\!\longrightarrow NH_4COONH_2(s); \quad \Delta H_{carb,s} \qquad \text{(eq. 5.77)}$$

The heat of formation of solid carbamate from gaseous NH_3 and CO_2 is given by the following expression (see appendix A).

$$\Delta H_{carb,s} = -13871.4781 + 199.473361*T - 0.30318*T^2 \quad \text{in cal/mole} \qquad \text{(eq. 5.78)}$$

To calculate further the heat of solution of carbamate, one can use the relation at 25^o C to obtain a value of 2000 cal/mole.

$$\Delta H_{carb,sol} = \Delta H_{carb,aq} - (\Delta H_{carb,s} - 2*\Delta H_1 - \Delta H_2) \text{ cal/mole} \qquad \text{(eq. 5.79)}$$
$$\Delta H_{carb,sol} = -13500 - (-37062 + 2*8370 + 4742) = 2000 \text{ cal/mole}$$

Now consider the following cycle:

$$\begin{tikzcd}
NH_4COONH_2(s) + \arrow[d, "\Delta H_I"'] & \text{amount of } H_2O(l) \text{ at } t^oC \arrow[r, "\Delta H_{carb,sol,t}"] \arrow[d, "\Delta H_{II}"'] & NH_4COONH_2(aq) \text{ at } t^oC \\
NH_4COONH_2(s) + & \text{amount of } H_2O(l) \text{ at } 25^oC \arrow[r, "\Delta H_{carb,sol,25^\circ C}"'] & NH_4COONH_2(aq) \text{ at } 25^oC \arrow[u, "\Delta H_{III}"']
\end{tikzcd}$$

If one makes a reasonable assumption that ΔH_{II} is equal to ΔH_{III}, then by adding ΔH_I to $\Delta H_{carb,sol,25^\circ C}$ one can arrive at $\Delta H_{carb,sol,t}$. ΔH_I is due to the contribution of the sensible heat of cooling 1 mole of carbamate from t^{o}C to 25^{o}C. The molar heat capacities of solid ammonium carbamate given in the literature are therefore processed to get the following regression expression.

$$C_{p,carb,s,exp} = 2.4333097 + 0.10539861*T - 2.8658265*10^{-5}*T^2 \qquad \text{(eq. 5.80)}$$

Accordingly the $\Delta H_{carb,sol,t}$ in cal/mole at various temperature works out to be:

t in °C	25	50	75	100	110	120	130	140
$\Delta H_{carb,sol,t}$	2000	510	-1078	-2760	-3458	-4171	-4898	-5640

Now with the help of (eq.5.79), one can calculate $\Delta H_{carb,aq}$. The values so obtained are the following:

t in °C	25	50	75	100	110	120	130	140
$\Delta H_{carb,aq}$	-13500	-16964	-19727	-21867	-22547	-23127	-23608	-23987

When the above data on the heats of reaction are coupled with the value of K_E at 18°C as given by Usdowskii et al [80], namely 2197.8, one arrives at the following expression utilizing the T_1, T_2, T_3 and T_4 variables:

$$R*\ln K_E = 14.2914 - 13475.7*T_1 - 157.13*T_2 - 1.3499*T_3 -0.0055258*T_4 \qquad \text{(eq. 5.81)}$$

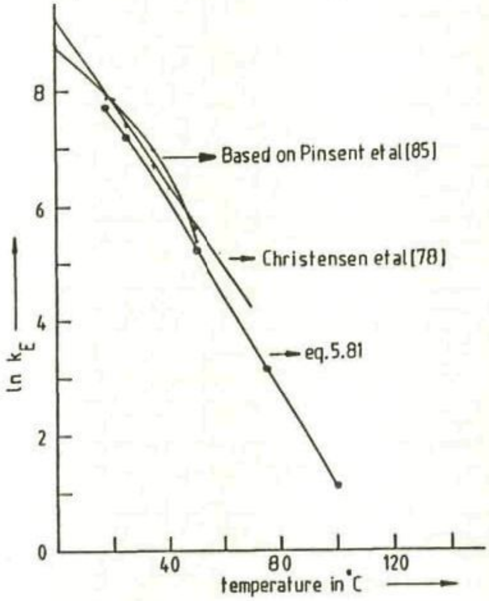

Fig. 5.4. *The equilibrium constant k_E for the formation of carbamate.*

The above expression and the experimental determinations of K_5 recalculated in terms of K_E are plotted in Fig.5.4. It can be observed that the general trend of the estimated values follows the determinations due to Christensen et al [78]. Such a behaviour is quite gratifying since only one datum on $\Delta H_{carb,aq}$ due to Pinsent et al [85], and the equilibrium constant value of Usdowski et al at 18°C [80] are employed in our estimation. As for K_5, it can be derived from K_E through the relation:

$$K_5 = K_E*K_4/K_1/K_2 \qquad \text{(eq. 5.82)}$$

5.4.3.2. *The equilibrium constant for the formation of urea*:

Unlike the equilibrium constant for carbamate formation, the equilibrium constant for urea formation at infinite dilution under standard conditions has not been experimentally determined till now. Such a lack of information is quite unexpected for a reaction which has been studied for so long in the literature. However, at concentrated conditions, there are nomograms and formulae given by Frejaques [86], Mavrovic [87], and Lemkowitz [33]. One can also arrive at a concentration dependent empirical constants through the analysis of the data due to Inoue et al [88] and Gorlovskii et al [89]. As these constants are not applicable for the infinite dilution conditions, one has to resort to free energies of formation at infinite dilution to derive the values.

Here the procedure is slightly different from the estimation of the equilibrium constant for carbamate formation. First the equilibrium constant and the heat of reaction of the following reaction at standard conditions are estimated

$$2\ NH_3(aq) + CO_2(aq) - NH_2CONH_2(aq) + H_2O(l) \qquad (eq.\ 5.83)$$

Later, the molar heat capacities of the reactants and products at temperatures around 25°C, say from 2° to 60°C, are estimated, followed by the calculation of the molar heat capacity change of the above reaction. Fitting the set of values thus obtained through a regression for Δc_p and assuming its validity over the extended range of 25° to 140°C, one can couple the same with the values of the heat of reaction and the equilibrium constant to get the final expression.

The equilibrium constant of the above reaction (eq. 5.83) K_u at standard conditions is calculated to be 2.01, utilizing the free energies of formation from elements of aqueous CO_2 (92.257 kcal/mole [69]), aqueous NH_3 (6.37 kcal /mole [90]), aqueous urea (48.72 kcal/mole [69]) and liquid water (48.72 kcal /mole [90]). Similarly, one can calculate the heat of the above reaction at 25°C to be 6732.1 cal/mole by utilizing the heats of formation of gaseous CO_2 (94.0511 kcal/mole [69]), gaseous NH_3 (10.9799 kcal/mole [90]), solid urea (79.634 kcal/mole [69]) and liquid water (68.315 kcal/mole [90]), together with the heats of solution at infinite dilution of CO_2 (4.720 kcal/mole [66]), NH_3 (8.403 kcal/mole [66a]) and urea.

The heat of solution of urea at 25°C has been determined by Egan et al (3656 cal/mole) [91] and Subramanian et al (3734 cal/mole) [92]. Additionally one can calculate the heat of solution value of 3680 cal/mole from the US NBS data collection [69] on the heat of formation of the crystal and aqueous urea from elements. This US NBS value is adopted in this study.

Now for the partial molar heat capacities of NH_3 and CO_2, one may differentiate Henry constant expressions twice to get the changes in molar heat capacities on dissolution, and add them to the ideal molar heat capacities of the gases to arrive at the partial molar heat capacities. This procedure works only when Henry constants have been measured accurately at close intervals and the derived heats of solution match at least a few experimental values in the chosen range. This is clearly the case for CO_2 (Fig. 5.2). Hence differentiating the heat of solution expression (eq. 5.70) does not pose much of a problem.

A similar procedure cannot be adopted for NH_3, since various Henry constant expressions derived in the literature including the present one do not estimate the heats of solution satifactorily in a wide range. The present expression (eq. 5.69) does it better around 25^{o}, but not beyond 60^{o}C. Hence, even though it was adopted earlier for the derivation of carbamate formation constant (which was adequate as seen in Fig. 5.4), the same procedure is not followed here in the derivation of urea formation constant. Instead, the partial molar heat capacities of ammonia reported in the literature [68a] for the temperature range of 2 to 60^{o}C are processed to get the following Clarke-Glew type expression with a correlation coefficient of 0.9999, an estimated standard error of 0.0179, and a Fischer's variance of 22988.

$$\bar{C}_{p,NH\ ,aq} = 36.3549462 + 0.088798*(T-298.15) - 3.023*10^{-3}*(T-298.15)^2 + 4.0*10^{-5}*(T-298.15)^3 \quad \text{in cal/mole/K} \qquad \text{(eq. 5.84)}$$

As for urea, the molar heat capacities reported by Gucker and Ayers [93], and Phillips and Desnoyers [94] in the range of 2^{o} to 40^{o}C are processed to yield the following expression having a correlation coefficient of 0.9999 with a standard estimated error of 0.03 and a Fischer's variance around 52600.

$$C_{p,u,} = 20.8414264 + 0.224151*(T-298.15) - 5.7*10^{-3}*(T-298.15)^2 + 2.02*10^{-4}*(T-298.15)^3 \quad \text{in cal/mole/K} \qquad \text{(eq. 5.85)}$$

Further one can couple the molar heat capacitity of liquid water, available from standard sources, to arrive at the ΔC_p of the above reaction (eq. 5.83). These ΔC_p values thus obtained can then be combined with the previously determined values of the heat of reaction and the equilibrium constant at standard condition to arrive at the following expression for K_u.

$$R\ln(K_u/2.007) = -6732.1*T_1 - 86.798*T_2 + 0.173412*T_3 + 0.000699674*T_4 \qquad \text{(eq. 5.86)}$$

Values calculated from the above expression for a few temperatures are plotted in Fig. 5.5. As for calculating K_6, one has to divide K_u by K_E.

One final remark about the expressions K_5 and K_6 concerns their reliability. These expressions have been derived on a number of assumptions. A major weak point is on the heats of solution and the partial molar heat capacitities of ammonia. Hopefully future studies will come out with reliable heats of solution values over the whole temperature range up to about 150^{o}C and these values will in turn lead to more reliable K_5 and K_6 expressions.

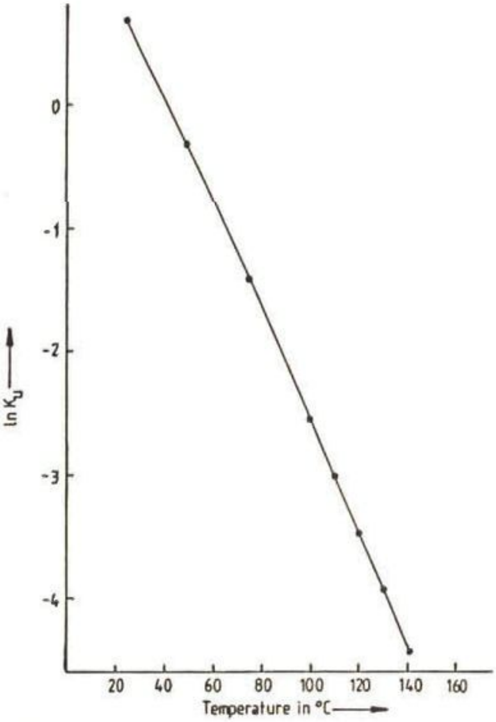

Fig. 5.5. *The equilibrium constant K_u for the formation of urea.*

5.5. *The model implementation*:

As said in the section 5.2, for a given T, mNH_3 and mCO_2, the equation block involving the reaction equilibria (eq. 5.7 to 5.12), the liquid phase mass balances (eq. 5.21 and eq. 5.22) and the electroneutrality (eq. 5.23) can be solved separately. Later, the phase equilibria proper is solved for the gas mole fractions y_1 and y_2 together with the total pressure. For this purpose, a Fortran program VANGELIS [95,96] was written using the ion specific interaction model and the Nakamura equation of state. This section describes the salient features of the program.

5.5.1. *The guidelines for selecting the model parameters*:

Since the ion specific interaction model contains a large number of parameters, parsimony in their number is to achieved through the use of previous work, theortical plausiblity, heuristic judgement and the need to make the model simple. In the present study, the Gordian knot was cut by the following guidelines [95,96] based on the typical interactions explained in Chapter 2.

1. All ternary ion-ion-ion terms, except for those involving pure electrolytes, are neglected for simplicity. Hence, only the C terms are non-zero.

2. All the molecule-cation terms are set equal to zero as per the rationale given in Chapter 2. The CO_2 molecule, with its electrophilic central carbon atom and anti-bonding orbitals on its molecular axis, may be repelled very strongly by the cations. As for NH_3 - H^+ interactions, their importance has already been recognized by including a reaction in the set of reaction equilibria. The NH_3-NH_4^+ interactions are neglected because of their similarity to the weak H_2O-NH_4^+ interactions. This is supported by the fact that the water molecules surrounding a central ammonium ion do not "feel" the change in their environment [97].

3. For the same reasons as above the C term involving NH_4^+ and OH^- is neglected.

4. The following relation between β^1 and β^0 proposed by Chen et al [29] is accepted on the grounds of minimizing the model parameters.

$$\beta^1 = 0.125 + 1.172*\beta^0 \qquad \text{(eq. 5.86)}$$

That the above relation is valid for 1-1 electrolytes has been verified through a linear regression of Pitzer's parameters so far published [18]. In fact the correlation coefficient comes out to be 0.8. Another relation by the same authors [29] for the 1-2 electrolytes is not accepted due to poor correlation.

5. The molecule-ion interaction terms involving CO_2 - $CO_3^=$ and CO_2 - OH^- are set equal to zero in view of the low concentrations of the said species.

6. The cation-cation interaction term is neglected due to the similarity of the oxonium and ammonium ions, for reasons stated in point no. 2.

7. The following rule proposed by Edwards et al [26] is accepted for the molecule-molecule interactions.

$$\lambda_{m'm''} = (\lambda_{m'm'} + \lambda_{m''m''})/2 \qquad \text{(eq. 5.87)}$$

8. The ternary interactions between CO_2 molecules are neglected due to reasons mentioned earlier in Chapter 2.

9. The binary and ternary self-interaction parameters of urea are determined from the known activity coefficient behaviour of aqueous urea solutions upto 40°C. Such activity coefficients of urea in binary aqueous solutions which have been tabulated as a function of urea molalities by Stokes [99] are first fitted to get a quadratic expression and additionally the coefficients of these quadratic expressions are fitted in terms of temperature. The expressions thus arrived at for $\lambda_{mm}(NH_2CONH_2)$ and $\mu_{mmm}(NH_2CONH_2)$ are presented in Table.5.3.

Table. 5.3. *Liquid phase model parameters which were not adjusted in the parameter optimization.*

Parameter	*Value or expression*	*Reference*
$\beta^{1}_{ca}(NH_4^{+},CO_3^{=})$	1.3	(trial and error)
$\beta^{0}_{ca}(NH_4^{+},OH^{-})$	0.10	[25,18]
$\beta^{0}_{ca}(H^{+},NH_2COO^{-})$	0.198	[28]
$\beta^{0}_{ca}(H^{+},CO_3^{=})$	0.086	[28]
$\beta^{0}_{ca}(H^{+},CO_3^{=})$	0.226	[28,29]
$\beta^{0}_{ca}(H^{+},HCO_3^{-})$	0.071	[28]
$\beta^{0}_{ca}(H^{+},OH^{-})$	0.208	[28]
$C_{ca}(NH_4^{+},CO_3^{=})$	0.003	[18]
$C_{ca}(NH_4^{+},HCO_3^{-})$	- 0.0052	[18]
$\theta_{aa'}(CO_3^{=},HCO_3^{-})$	- 0.04	[18]
$\theta_{aa'}(CO_3^{=},OH^{-})$	0.10	[18]
$\lambda_{ma}(NH_3,CO_3^{=})$	0.068	[26]
$\lambda_{ma}(NH_3,OH^{-})$	0.10	[30]
$\lambda_{ma}(CO_2,NH_2COO^{-})$	0.02	[26]
$\lambda_{ma}(CO_2,HCO_3^{-})$	0.13	[98]
$\lambda_{mm'}(NH_3,NH_3)$	$- 0.0260 + 12.29/T$	[26]
$\lambda_{mm'}(CO_2,CO_2)$	$- 0.4922 + 149.2/T$	[26]
$\lambda_{mm'}(NH_2CONH_2,NH_2CONH_2)$	$0.6677 - 122.48/T - 9.838*10^{-4}*T$	[99]
$\mu_{mm'm''}(NH_3)$	- 0.0002	(trial and error)
$\mu_{mm'm''}(NH_3,CO_2)$	- 0.0001	(trial and error)
$\mu_{mm'm''}(NH_2CONH_2)$	$- (64.25 + 11189.13/T + 0.0973*T)/1000$	[99]

All the remaining parameters except those mentioned above are retained in the model. Further, many of them, as tabulated in Table 5.3, are kept constant due to simplicity and insensitivity, irrespective of the temperature chosen. In Table 5.3, the relevant references for these values are also given.

The total number of optimized parameters is 8. Although the β^0 and the θ parameters involving $CO_3^{=}$ can be kept constant easily with no loss of accuracy, they are adjusted in view of the possible ion pair effects.

5.5.2. *The data interpolation method*:

Subsequent to the choice of the parameters to be adjusted, one needs adequate data to determine the parameter optima. Since the number of measured tie-lines (from this study, Müller [31] and DSM [100]) at each p-T cross section are limited, one has to rely on interpolation to get the pseudo-experimental points. Fortunately this can be done by a variant of the procedure suggested by Zernike [101]. According to this construction, an auxilary curve is drawn relating the liquid phase CO_2 concentration to the gas phase NH_3 concentration, as shown in Fig. 5.6, from which the data are interpolated, and used later for the optimization programme.

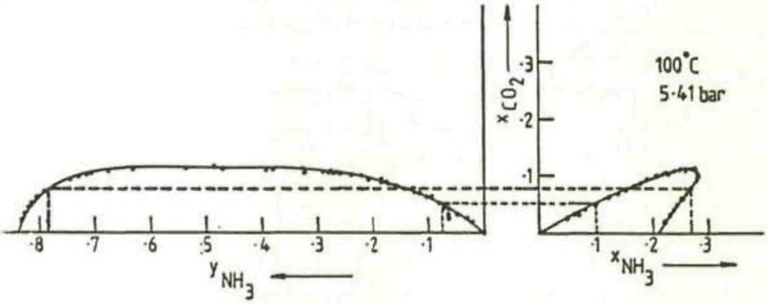

Fig. 5.6. *The data interpolation method using auxilary construction.*

5.5.3. *The software development and the optimization procedure*:

Subsequent to the data interpolation, the development of software is taken up in five stages [95,96].

Stage 1: Solve simultaneously the liquid phase reaction equilibria together with the mass balances and the electroneutrality to get an initial estimate of molalities, especially the order of magnitude, by assuming all the activity coefficients to be unity. Incidentally this trial can test the efficacy of this part of the program.

Stage 2: Assume an initial set of parameters. Include the subroutine for calculating the activity coefficients. Solve the above set of 9 equations and arrive at more realistic molalities.

Stage 3: With the molalities calculated in stage 1, test the gas phase model separately by assuming the activity coefficients of free NH_3 and free CO_2, and the activity of water to be unity. Check whether there is any snag in calculating the gas phase mole fractions and the total pressure.

Stage 4: Once all the three above stages are individually debugged, combine all the three parts into one large sub-unit and calculate the more realistic gas phase mole fractions and the total pressure.

Stage 5: Find the relative deviations of the calculated versus the experimental points in terms of the two gas phase mole fractions and total pressure. Add all the sums of squares of the relative deviations and check the optimization subroutine for its efficacy in changing the liquid phase model parameters.

At the end of stage 5, when all the individual subroutines are debugged and cleared of stability problems, they are combined into one large program called VANGELIS for the final use. A flow diagram of VANGELIS is presented in Fig. 5.7. The optimization subroutine E04JAF employed as a part of VANGELIS was originally developed by Gill and Murray [102] using a quasi-Newton algorithm and is available from the NAG subroutines library of the computer facility of the Delft University of Technology. For this library subroutine, one has to provide the boundaries of the parameters to be optimized. These boundaries are initially obtained through heuristic arguments (like the ionic radius, the ionic entropy, etc.) or from the values given by Pitzer [18] for the related alkali salts and also through a bracketing of the appropriate values of ammonium salts given by Edwards et al [26], Maurer [28] and Pawlikowski et al [30]. Once sufficient optimization trials are completed, all these boundaries are widened to a range between - 0.8 to 0.9. The optimization is further continued until it is established that the boundaries do not lead to constrained optimization. The objective function chosen for optimization is the one given below.

$$FSUM = ((y_{e,1} - y_{c,1})/y_{c,1})^2 + ((y_{e,2} - y_{c,2})/y_{c,2})^2 + ((p_e - p_c)/p_c)^2 \qquad \text{(eq. 5.88)}$$

where the subscripts e and c denote the experimental and calculated values respectively.

The optimization procedure can be described briefly as follows. First one set of liquid phase model parameters for each temperature is assumed. Normally there are 35 pseudo-experimental points for each temperature and pressure. Hence for each experimental point, knowing the component molalities of NH_3 and CO_2, the initial values of the species molalities are guessed. The activity coefficients are then calculated; the reaction equilibria, the liquid phase mass balances and the electroneutrality are simultaneously solved using another NAG subroutine called C05NBF. With the realistic molalities and activity coefficients of free NH_3 and free CO_2 thus obtained, the gas phase mole fractions of NH_3 and CO_2, and also the total pressure are calculated and compared to the experimental values. The above subcycle is repeated for all the 35 pseudo-experimental points and the sum of the deviation squares over the whole set is calculated. *At the end of the 35th subcycle this sum is passed over to the subroutine* E04JAF to arrive at a new set of improved parameters to be tried for a new cycle. This larger cycle is further repeated until successive changes in the objective function are less than the tolerence value of 1.2.

In order to reduce the computation time for solving the simultaneous equations through the subroutine C05NBF, the pseudo-experimental points are arranged in an order following the trend of the bubble point curve starting from the CO_2- rich ternary points closer to the CO_2 - H_2O binary side. It is only for the first of the 35 points that the initial guesses are given. For the second point, the calculated value of the

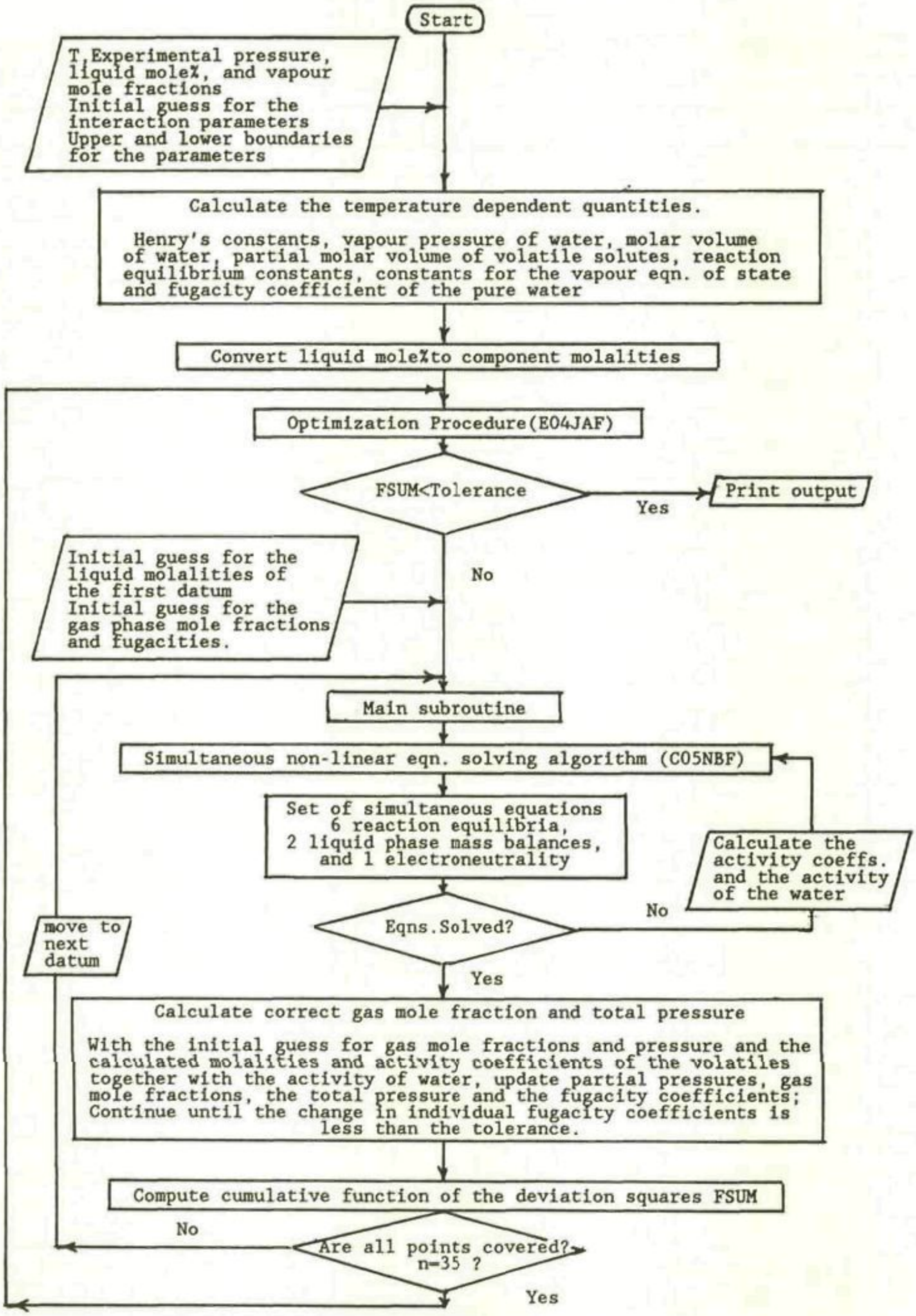

Fig.5.7.*The flow diagram of VANGELIS.*

first point is supplied as the initial guess. The same is repeated in series for the other points. However, one important aspect in solving the simultaneous equations mentioned above is that the purely binary composition points can not be given as starting guesses, in view of the stability problems in the chosen algorithm.

5.6. *The computation results and discussions*:

The computations are carried out for four sets of data having appreciable component molalities, namely 65°C - 1.027 bar, 100°C - 5.41 bar, 120°C - 10 bar and 130°C - 20 bar. The 110°C - 5.41 bar data set was not tried, since it may not have provided a severe enough test for the model in view of the low concentrations in the liquid phases. The results obtained in terms of the calculated gas phase mole fractions (y_{1c} and y_{2c}), the total pressure (p_c), the relative deviations with respect to the pesudo-experimental values ($\Delta y_1/y_{1e}$, $\Delta y_2/y_{2e}$ and $\Delta p/p_e$) are presented in Tables 5.4 to 5.7. In the tables, the pseudo-experimental liquid phase component concentrations are expressed in mole fractions and the pressure in bars. Further, the results in terms of the calculated gas phase mole fractions against the pseudo-experimental gas phase mole fractions at constant temperature are plotted in figures 5.8 to 5.11. It can be observed that the model performs satisfactorily over the temperature and liquid composition ranges with relative deviations of the gas phase mole fractions and the total pressure being less than around ± 12%, except near the binary compositions and near the bubble-point tongues. Considering the fan-like character of the tie-lines around the bubble point tongues and possible chemical analysis difficulties with compositions less than 1 mole% range, further reductions in relative deviations were not attempted due to the excessive time required for marginal improvements. Moreover the hypersurface of the function FSUM becomes very flat near the final chosen parameter values at each temperature. The obtained parameter values are plotted in Fig. 5.12 to Fig. 5.19 and presented in Table 5.8.

One possible criticism in the model implemention method concerns the separate optimization of the parameters for each temperature case. Although one can assume a functional form for the temperature dependency of the binary and ternary parameters and proceed to optimize the coefficients of the temperature dependency functions of these parameters by coupling all the experimental data, the same is not attempted because it is too premature at this stage of the investigations. This is especially so because the present attempt is the first one to describe a concentrated aqueous ammonia - carbon dioxide solutions with the inclusion of the urea formation reaction in the system. All the other earlier authors [26,27,28,29,30] who have applied the variants of the Pitzer's model [18] did not attempt so on such an exhaustive scale. Moreover the systems they described were only moderately concentrated and their approaches did not include the urea formation reaction. Müller's work [31] was the

Table.5.4.*The model estimation of the gas phase mole fractions and the total pressure.*

Experimental pressure - 1.027 bar; temperature - 65^{o}C.

x_1	x_2	y_{1e}	y_{2e}	y_{1c}	y_{2c}	P_c	$\Delta y_1/y_{1e}$ %	$\Delta y_2/y_{2e}$ %	$\Delta P/P_e$ %
0.0387	0.0242	0.0270	0.7690	0.0343	0.7310	1.0209	-27.04	4.94	0.59
0.0770	0.0430	0.0710	0.7340	0.0775	0.6859	0.9752	- 9.15	6.55	5.04
0.1150	0.0636	0.1350	0.6860	0.0940	0.7125	1.1470	30.37	- 3.86	-11.68
0.1520	0.0772	0.1950	0.6350	0.2173	0.5543	0.9269	-11.44	12.71	9.75
0.1720	0.0846	0.2420	0.5910	0.2905	0.4850	0.9148	-20.04	17.94	10.93
0.1850	0.0910	0.2870	0.5470	0.3055	0.4873	0.9695	- 6.45	10.91	5.60
0.1970	0.0938	0.3260	0.5090	0.3786	0.4159	0.9564	-16.13	18.29	6.87
0.2060	0.0982	0.3800	0.4590	0.3868	0.4207	1.0034	- 1.79	8.34	2.30
0.2230	0.1045	0.4380	0.4090	0.4365	0.3889	1.0684	0.34	4.91	- 4.03
0.2310	0.1080	0.4850	0.3630	0.4477	0.3878	1.1139	7.79	- 6.83	- 8.46
0.2377	0.1090	0.5290	0.3270	0.4840	0.3553	1.1262	8.51	- 8.65	-22.88
0.2430	0.1060	0.5790	0.2760	0.5800	0.2592	1.1161	0.17	6.09	- 8.68
0.2410	0.1030	0.6140	0.2430	0.6078	0.2276	1.0981	1.01	6.34	- 6.92
0.2390	0.1000	0.6450	0.1980	0.6333	0.1992	1.0855	1.81	- 0.61	- 0.06
0.2240	0.0900	0.7140	0.1360	0.6579	0.1562	1.0112	7.86	-14.85	1.54
0.2150	0.0790	0.7480	0.0980	0.7124	0.0969	1.0058	4.76	1.12	2.06
0.2040	0.0723	0.7720	0.0700	0.7142	0.0862	0.9674	7.49	-23.14	5.80
0.1670	0.0449	0.7990	0.0330	0.7374	0.0343	0.9049	7.71	- 3.94	11.89
0.1450	0.0260	0.8055	0.0124	0.7520	0.0132	0.9045	6.64	- 6.45	11.93
0.1890	0.0600	0.7860	0.0490	0.7337	0.0549	0.9477	6.65	-12.04	7.72
0.2110	0.0760	0.7610	0.0820	0.7174	0.0885	0.9996	5.73	- 7.93	2.67
0.2240	0.0860	0.7300	0.1165	0.6966	0.1206	1.0308	4.58	- 3.52	- 0.37
0.2360	0.0960	0.6800	0.1740	0.6617	0.1675	1.0735	3.96	3.74	- 4.53
0.2408	0.1020	0.6300	0.2280	0.6196	0.2153	1.0959	1.65	5.57	- 6.89
0.2432	0.1060	0.5900	0.2670	0.5814	0.2579	1.1170	1.46	3.41	- 8.76
0.2420	0.1080	0.5600	0.2930	0.5422	0.2982	1.1243	3.18	- 1.77	- 9.47
0.2330	0.1080	0.5000	0.3490	0.4660	0.3699	1.1123	6.80	- 5.99	- 8.53
0.2145	0.1020	0.4100	0.4310	0.4003	0.4182	1.0454	2.37	2.97	- 1.79
0.2005	0.0965	0.3600	0.4770	0.3627	0.4409	0.9941	- 0.75	7.57	3.20
0.1830	0.0900	0.2900	0.5440	0.3036	0.4864	0.9601	- 4.69	10.59	6.51
0.1620	0.0820	0.2200	0.6120	0.2326	0.5487	0.9535	- 5.73	10.34	7.16
0.1325	0.0700	0.1600	0.6650	0.1487	0.6335	0.9976	7.06	4.74	2.86
0.1090	0.0600	0.1200	0.6820	0.0962	0.6987	1.0888	19.83	- 2.45	- 6.02
0.0660	0.0380	0.0580	0.7240	0.0602	0.7117	1.0226	- 3.79	1.70	0.43
0.0250	0.0160	0.0180	0.7740	0.0309	0.6737	0.8228	-71.67	12.96	19.88

Table. 5.5. *The model estimation of the gas phase mole fractions and the total pressure.*

Experimental pressure - 5.41 bar; temperature - 100°C.

x_1	x_2	y_{1e}	y_{2e}	y_{1c}	y_{2c}	P_c	$\Delta y_1/y_{1e}$ %	$\Delta y_2/y_{2e}$ %	$\Delta P/P_e$ %
0.0500	0.0250	0.0290	0.7850	0.0629	0.7023	4.1445	-116.90	10.54	23.39
0.0620	0.0335	0.0430	0.7800	0.0460	0.7840	5.7090	- 6.98	- 0.51	- 5.53
0.0700	0.0330	0.0480	0.7780	0.0629	0.7466	5.0446	-31.04	4.04	6.75
0.0820	0.0420	0.0620	0.7670	0.0692	0.7476	5.1983	-11.61	2.74	3.91
0.0970	0.0500	0.0800	0.7550	0.0729	0.7564	5.5262	8.88	- 0.19	- 2.15
0.1220	0.0620	0.1040	0.7340	0.0936	0.7361	5.4323	1.00	- 0.29	- 0.41
0.1400	0.0700	0.1260	0.7160	0.1177	0.7070	5.1955	6.59	1.26	3.96
0.1520	0.0760	0.1430	0.7030	0.1270	0.7023	5.2804	11.19	0.10	2.40
0.1690	0.0820	0.1580	0.6900	0.1730	0.6448	4.8457	- 9.49	6.55	10.43
0.1800	0.0880	0.1820	0.6700	0.1750	0.6542	5.1137	3.85	2.36	5.48
0.1920	0.0940	0.2090	0.6490	0.1839	0.6549	5.3381	12.01	- 0.91	1.33
0.2080	0.1000	0.2400	0.6240	0.2229	0.6193	5.3151	7.13	0.75	1.75
0.2200	0.1040	0.2700	0.6010	0.2587	0.5873	5.3217	4.19	2.28	1.63
0.2220	0.1040	0.2800	0.5970	0.2749	0.5689	5.2238	1.82	4.71	3.44
0.2260	0.1060	0.2900	0.5860	0.2761	0.5730	5.3655	4.79	2.22	0.82
0.2300	0.1050	0.2670	0.6040	0.3241	0.5179	5.0743	-21.38	14.25	6.21
0.2400	0.1100	0.3800	0.5110	0.3247	0.5319	5.4679	14.55	- 4.09	- 1.07
0.2500	0.1120	0.4700	0.4320	0.3702	0.4912	5.5210	21.23	-13.70	- 2.05
0.2590	0.1100	0.3900	0.5040	0.4665	0.3921	5.2886	-19.62	22.22	2.24
0.2700	0.1140	0.4850	0.4180	0.4811	0.3914	5.6895	0.80	6.36	- 5.17
0.2740	0.1140	0.4850	0.4180	0.5065	0.3684	5.7359	- 4.43	11.87	- 6.02
0.2780	0.1120	0.5370	0.3720	0.5576	0.3172	5.6774	- 3.84	14.73	- 4.94
0.2810	0.1100	0.6300	0.2640	0.5986	0.2763	5.6545	4.98	- 4.66	- 4.52
0.2820	0.1060	0.6750	0.2070	0.6471	0.2255	5.5632	4.13	- 8.94	- 4.10
0.2800	0.1030	0.7050	0.1700	0.6672	0.2018	5.4506	5.36	-18.71	- 0.75
0.2830	0.1010	0.7120	0.1640	0.6964	0.1752	5.5296	2.19	- 6.83	- 2.21
0.2820	0.0970	0.7280	0.1430	0.7226	0.1473	5.4878	0.74	- 3.01	- 1.44
0.2800	0.0920	0.7440	0.1230	0.7474	0.1203	5.4442	- 0.46	2.20	- 0.59
0.2690	0.0800	0.7720	0.0880	0.7747	0.0834	5.2153	- 0.35	5.23	3.60
0.2600	0.0700	0.7900	0.0640	0.7892	0.0630	5.0920	0.10	1.56	5.88
0.2520	0.0600	0.8020	0.0480	0.8007	0.0478	5.0295	0.16	0.42	7.03
0.2440	0.0500	0.8120	0.0340	0.8089	0.0365	4.9795	0.38	- 7.35	7.96
0.2380	0.0420	0.8180	0.0250	0.8145	0.0289	4.9547	0.43	-15.60	8.42
0.2320	0.0320	0.8240	0.0170	0.8220	0.0204	4.9640	0.24	-20.00	8.24
0.2240	0.0200	0.8300	0.0080	0.8288	0.0113	4.9469	0.14	-41.25	8.56

Table. 5.6. *The model estimation of the gas phase mole fractions and the total pressure.*

Experimental pressure - 10.00 bar; temperature - 120^oC.

x_1	x_2	y_{1e}	y_{2e}	y_{1c}	y_{2c}	P_c	$\Delta y_1/y_{1e}$ %	$\Delta y_2/y_{2e}$ %	$\Delta P/P_e$ %
0.0220	0.0090	0.0200	0.7850	0.0424	0.6830	7.216	-112.00	12.99	27.84
0.0300	0.0130	0.0300	0.7750	0.0393	0.7573	9.775	-31.00	2.28	2.25
0.0430	0.0180	0.0400	0.7630	0.0488	0.7706	10.929	-22.00	- 1.00	- 9.29
0.0520	0.0220	0.0500	0.7580	0.0512	0.7853	12.042	- 2.40	- 3.60	-20.42
0.0600	0.0250	0.0600	0.7500	0.0587	0.7789	12.035	2.17	- 3.85	-20.35
0.0710	0.0290	0.0700	0.7400	0.0716	0.7635	11.710	- 2.29	- 3.18	-17.10
0.0800	0.0330	0.0800	0.7320	0.0765	0.7640	12.044	4.38	4.38	-20.44
0.0880	0.0360	0.0900	0.7230	0.0871	0.7502	11.709	3.22	- 2.72	-17.09
0.0980	0.0400	0.1000	0.7130	0.0994	0.7359	11.456	0.60	- 3.21	-14.56
0.1130	0.0470	0.1200	0.6960	0.1102	0.7295	11.647	8.17	- 4.81	-16.47
0.1280	0.0530	0.1400	0.6780	0.1350	0.6987	11.058	3.57	- 3.05	-10.58
0.1400	0.0580	0.1600	0.6600	0.1555	0.6751	10.731	2.81	- 2.29	- 7.31
0.1550	0.0630	0.1800	0.6430	0.2001	0.6201	9.922	-11.17	3.56	0.78
0.1600	0.0650	0.2000	0.6230	0.2118	0.6075	9.825	- 5.90	2.49	1.75
0.1700	0.0680	0.2200	0.6060	0.2493	0.5646	9.411	-13.32	6.83	5.89
0.1800	0.0730	0.2400	0.5880	0.2622	0.5565	9.577	- 9.25	3.66	4.23
0.1900	0.0770	0.2600	0.5690	0.2890	0.5312	9.544	-11.15	6.64	4.56
0.1940	0.0790	0.2800	0.5510	0.2947	0.5278	9.630	- 5.25	4.21	3.70
0.1960	0.0800	0.3000	0.5330	0.2975	0.5261	9.675	0.83	1.30	3.25
0.2080	0.0830	0.3200	0.5130	0.3542	0.4690	9.462	-10.69	8.58	5.38
0.2110	0.0840	0.3400	0.4950	0.3650	0.4593	9.480	- 7.35	7.21	5.20
0.2130	0.0850	0.3600	0.4750	0.3680	0.4579	9.954	- 2.22	3.60	0.46
0.2140	0.0860	0.3800	0.4570	0.3631	0.4647	9.648	4.45	- 1.68	3.52
0.2250	0.0880	0.4000	0.4380	0.4225	0.4082	9.609	- 5.63	6.80	3.91
0.2300	0.0890	0.4200	0.4170	0.4470	0.3863	9.669	- 6.43	7.36	3.31
0.2350	0.0910	0.4400	0.3980	0.4597	0.3780	9.847	- 4.48	5.03	1.53
0.2370	0.0910	0.4600	0.3770	0.4734	0.3652	9.859	- 2.91	3.13	1.41
0.2380	0.0920	0.4800	0.3580	0.4694	0.3708	9.947	2.21	- 3.58	0.53
0.2390	0.0930	0.5000	0.3390	0.4653	0.3765	10.039	6.94	-11.06	- 0.39
0.2400	0.0930	0.5200	0.3170	0.4721	0.3701	10.046	9.21	-16.75	- 0.46
0.2410	0.0920	0.5400	0.2980	0.4895	0.3523	9.979	9.35	-18.22	0.21
0.2430	0.0880	0.5600	0.2760	0.5405	0.3004	9.798	3.48	- 8.84	2.02
0.2470	0.0860	0.5800	0.2550	0.5779	0.2653	9.864	0.36	- 4.04	1.36
0.2460	0.0840	0.6000	0.2350	0.5876	0.2541	9.775	2.07	- 8.13	2.25
0.2480	0.0820	0.6150	0.2190	0.6105	0.2329	9.820	0.73	- 6.355	1.80

Table 5.7. *The model estimation of the gas phase mole fractions and the total pressure.*

Experimental pressure - 20.00 bar; temperature - 130^oC.

x_1	x_2	y_{1e}	y_{2e}	y_{1c}	y_{2c}	p_c	$\Delta y_1/y_{1e}$ %	$\Delta y_2/y_{2e}$ %	$\Delta p/p_e$ %
0.0200	0.0120	0.0120	0.8580	0.0149	0.8293	18.196	-24.17	3.34	9.02
0.0400	0.0200	0.0180	0.8530	0.0270	0.8385	20.905	-50.00	1.70	4.53
0.0600	0.0290	0.0360	0.8380	0.0329	0.8532	24.639	8.61	-1.81	-23.20
0.0800	0.0360	0.0480	0.8280	0.0510	0.8280	22.348	-6.25	0.00	-11.74
0.1000	0.0440	0.0640	0.8140	0.0657	0.8105	21.528	-2.66	0.43	-7.64
0.1200	0.0540	0.0860	0.7920	0.0720	0.8122	22.788	16.28	-2.55	-13.94
0.1400	0.0630	0.1060	0.7740	0.0886	0.7937	21.952	16.42	-2.55	-9.76
0.1600	0.0720	0.1280	0.7520	0.1099	0.7690	20.870	14.14	-2.26	-4.35
0.1800	0.0810	0.1490	0.7330	0.1367	0.7384	19.781	8.26	-0.74	1.10
0.2000	0.0900	0.1740	0.7080	0.1695	0.7025	18.852	2.59	0.78	5.74
0.2140	0.0960	0.1900	0.6940	0.1991	0.6708	18.200	-4.79	3.34	9.00
0.2200	0.1000	0.2030	0.6820	0.1981	0.6757	18.718	2.41	0.92	6.41
0.2300	0.1050	0.2200	0.6660	0.2140	0.6613	18.717	2.73	0.71	6.42
0.2400	0.1100	0.2300	0.6550	0.2308	0.6463	18.780	-0.35	1.33	6.10
0.2500	0.1140	0.2500	0.6380	0.2595	0.6178	18.486	-3.80	3.17	7.57
0.2550	0.1160	0.2600	0.6280	0.2742	0.6035	18.402	-5.46	3.90	7.99
0.2600	0.1180	0.2700	0.6180	0.2891	0.5894	18.361	-7.07	4.63	8.20
0.2650	0.1200	0.2800	0.6090	0.3042	0.5754	18.361	-8.64	5.52	8.20
0.2700	0.1230	0.3000	0.5900	0.3081	0.5747	18.744	-2.70	2.59	6.28
0.2750	0.1250	0.3150	0.5760	0.3232	0.5610	18.809	-2.60	2.60	5.96
0.2800	0.1280	0.3400	0.5520	0.3271	0.5606	19.249	3.71	-1.56	3.76
0.2850	0.1290	0.3520	0.5400	0.3535	0.5346	19.070	-0.43	1.00	4.65
0.2900	0.1300	0.3600	0.5320	0.3795	0.5096	18.988	-5.42	4.21	5.06
0.2950	0.1320	0.3700	0.5240	0.3941	0.4976	19.241	-6.51	5.04	3.80
0.3000	0.1340	0.3900	0.5050	0.4084	0.4861	19.538	-4.72	3.74	2.31
0.3050	0.1350	0.4000	0.4950	0.4329	0.4636	19.649	-8.23	6.34	1.76
0.3100	0.1360	0.4200	0.4740	0.4565	0.4423	19.834	-8.69	6.69	0.83
0.3150	0.1380	0.4500	0.4440	0.4693	0.4328	20.277	-4.29	2.52	1.39
0.3200	0.1390	0.4600	0.4320	0.4913	0.4137	20.578	-6.80	4.24	2.89
0.3260	0.1400	0.5000	0.3970	0.5179	0.3905	20.986	-3.58	1.64	4.93
0.3320	0.1400	0.5600	0.3420	0.5509	0.3606	21.336	1.63	-5.47	6.68
0.3380	0.1380	0.6300	0.2700	0.5950	0.3190	21.560	5.56	-18.15	7.80
0.3420	0.1360	0.6740	0.2250	0.6247	0.2910	21.736	7.31	-29.33	8.68
0.3450	0.1320	0.7020	0.2000	0.6575	0.2589	21.721	6.34	-29.45	8.61
0.3440	0.1280	0.7200	0.1820	0.6729	0.2419	21.351	6.54	-32.91	6.76

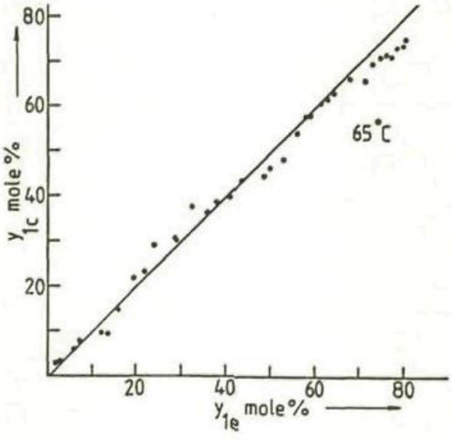

Fig. 5.8.a. *The calculated y_{1c} vs the experimental y_{1e} at 65°C.*

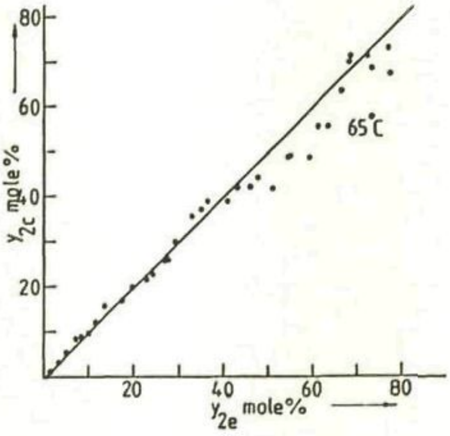

Fig. 5.8.b. *The calculated y_{2c} vs the experimental y_{2e} at 65°C.*

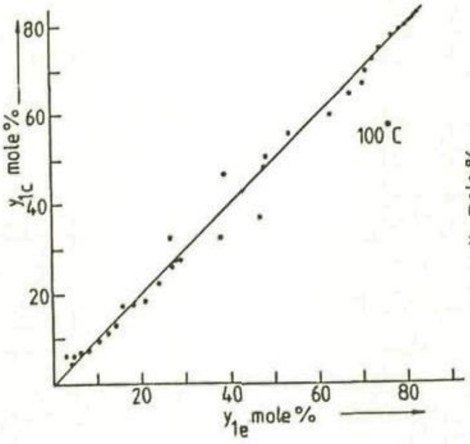

Fig. 5.9.a. *The calculated y_{1c} vs the experimental y_{1e} at 100°C.*

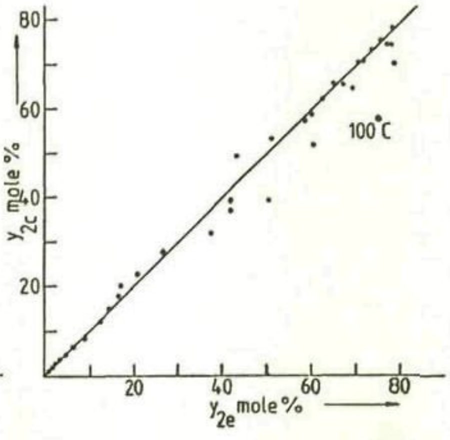

Fig. 5.9.b. *The calculated y_{2c} vs the experimental y_{2e} at 100°C.*

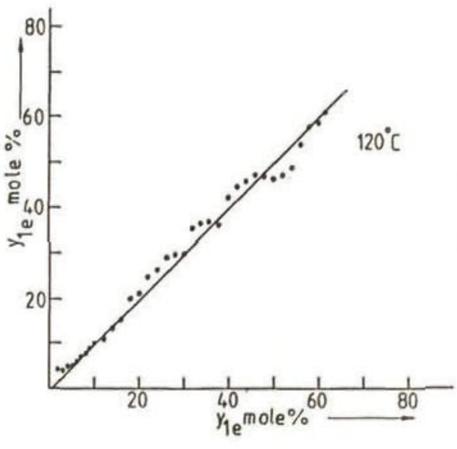

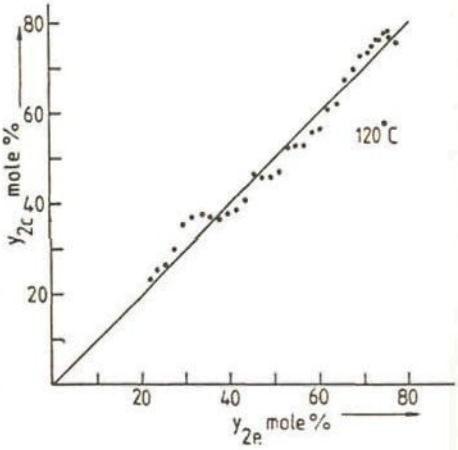

Fig. 5.10.a. *The calculated* y_{1c} *vs the experimental* y_{1e} *at 120°C.*

Fig. 5.10.b. *The calculated* y_{2c} *vs the experimental* y_{2e} *at 120°C.*

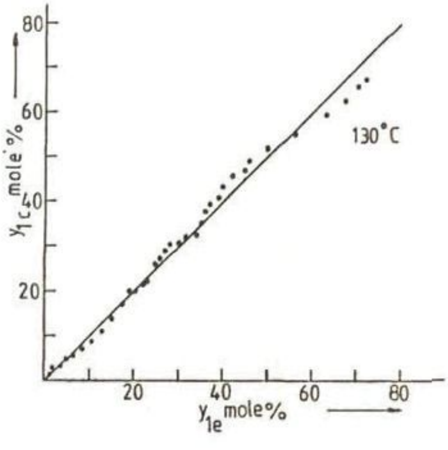

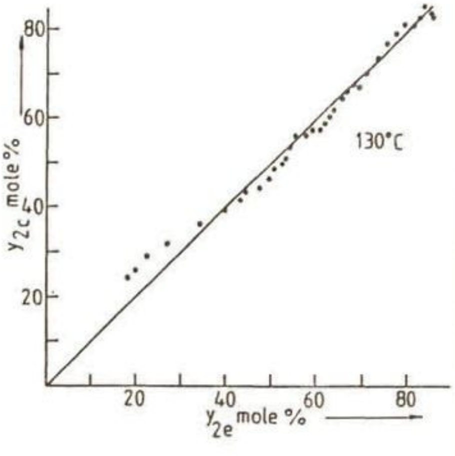

Fig. 5.11.a. *The calculated* y_{1c} *vs the experimental* y_{1e} *at 130°C.*

Fig. 5.11.b. *The calculated* y_{2c} *vs the experimental* y_{2e} *at 130°C.*

the first one which attempted to apply these models for the concentrated solutions, and his conclusions were rather pessimistic about the parameter values derived by the earlier authors [26,27,28,30] for the temperatures above 100°C. Hence it was clearly imperative for the present work to examine whether the model was adequate for the chosen experimental conditions. On this account, one can now definitely answer in the affirmative as a result of the present investigations. If one wants to achieve a still closer fit than the present one, perhaps in a future investigation, then one may have to include additional experimental data, assume the functional form of the parameters which Pitzer did for the pure NaCl case [18] and also incorporate the weight factors in the optimization function.

Leaving such a step to future investigations, it is gratifying to observe that the orders of magnitude of the optimized interaction parameters match those of Pitzer [18], wherever applicable, in his determinations for the 1-1 electrolytes. The temperature dependency trends are also similar to the one observed in his study on NaCl solutions over a wide range of temperatures. To give physical significance of these trends without additional investigations may be a bit far-fetched at present, since the parameters are obtained solely from an optimization procedure of a multi-electrolyte model. Had one been able to investigate the pure electrolytes of NH_4COONH_2, NH_4HCO_3 and $(NH_4)_2CO_3$ just like the corresponding alkali salts, one could have derived physically meaningful and explainable parameters; subsequent to such a step, one can derive the mixed ion parameters from the multielectrolyte systems. Since such a procedure is presently unavailable, the only course left, barring the regressional approaches of Kucheryavyi et al [103], is to work straight away with multicomponent systems and continue to tune the parameters fine as more and more data become available.

Table 5.8. *Optimized parameter values.*

parameter	65°C	100°C	120°C	130°C
$\beta^{\circ}_{ca}(NH_4^+, NH_2COO^-)$	-0.3965D-02	-0.5894D-01	-0.5764D-01	-0.2261D-01
$\beta^{\circ}_{ca}(NH_4^+, CO_3^{=})$	-0.1088D 00	0.1155D-02	-0.6619D-01	-0.2270D 00
$\beta^{\circ}_{ca}(NH_4^+, HCO_3^-)$	0.6788D-01	0.7628D-01	0.1385D 00	0.1799D 00
$C_{ca}(NH_4^+, NH_2COO^-)$	0.9741D-02	0.1084D-01	0.7507D-02	0.5675D-02
$\theta_{aa'}(NH_2COO^-, CO_3^{=})$	0.2686D 00	0.4009D-01	0.1355D 00	0.3062D 00
$\theta_{aa'}(NH_2COO^-, HCO_3^-)$	-0.1710D 00	-0.1714D 00	-0.2815D 00	-0.3581D 00
$\lambda_{ma}(NH_3, NH_2COO^-)$	0.4305D-01	0.3040D-01	0.3465D-01	0.4456D-01
$\lambda_{ma}(NH_3, HCO_3^-)$	-0.5156D-01	-0.1037D-01	-0.9057D-01	-0.1838D 00

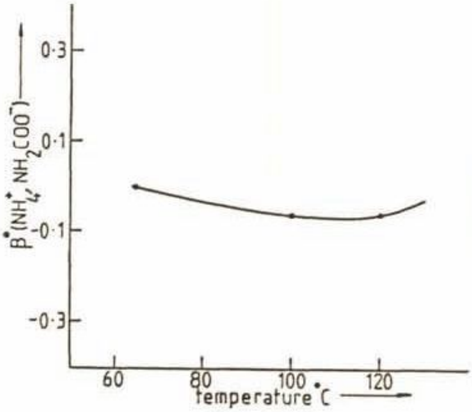

Fig. 5.12. *The temperature dependency of the parameter* $\beta^{\circ}_{ca}(NH_4^+, NH_2COO^-)$

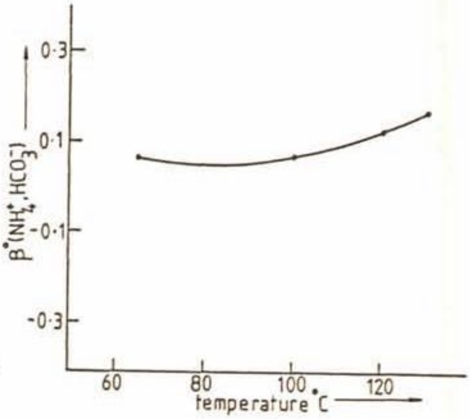

Fig. 5.13. *The deperature dependency of the parameter* $\beta^{\circ}_{ca}(NH_4^+, CO_3^{=})$

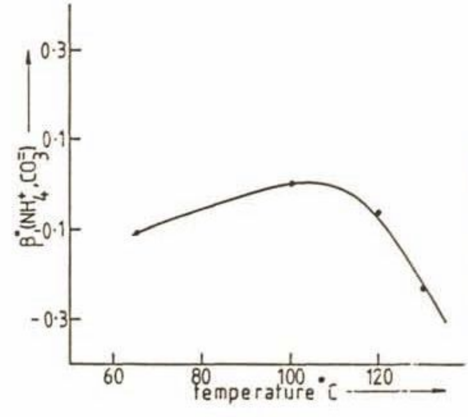

Fig. 5.14. *The temperature dependency of the parameter* $\beta^{0}_{ca}(NH_4^+, HCO_3^-)$

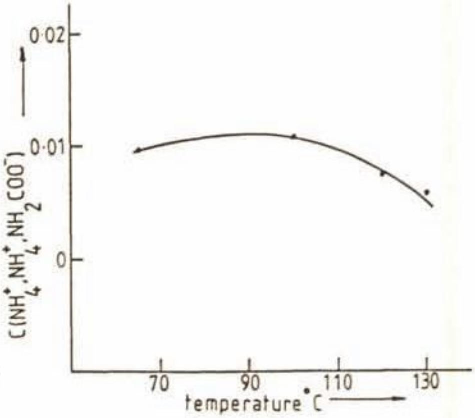

Fig. 5.15. *The deperature dependency of the parameter* $C_{ca}(NH_4^+, NH_2COO^-)$

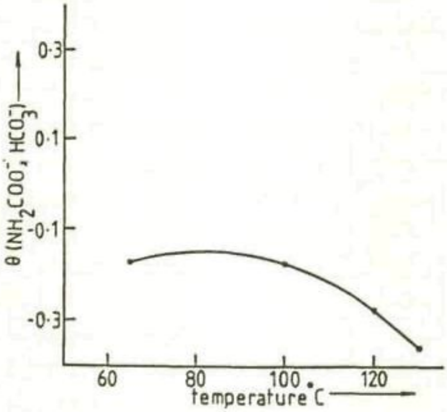

Fig. 5.16. *The temperature dependency of the parameter* $\theta_{aa'}(NH_2COO^-,CO_3^{=})$

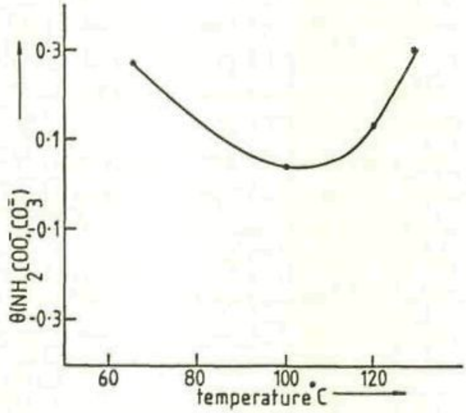

Fig. 5.17. *The deperature dependency of the parameter* $\theta_{aa'}(NH_2COO^-,HCO_3^-)$

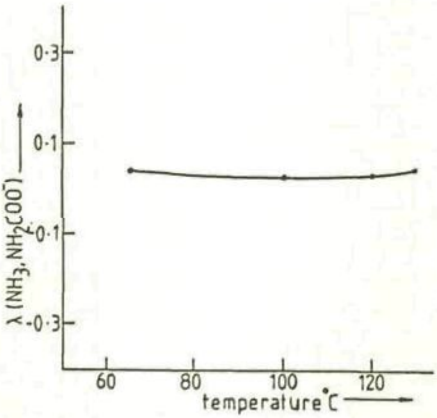

Fig. 5.18. *The temperature dependency of the parameter* $\lambda_{ma}(NH_3,NH_2COO^-)$

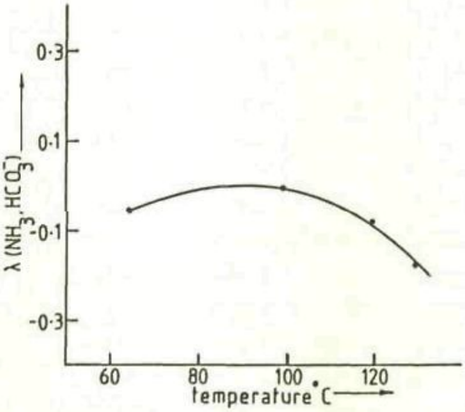

Fig. 5.19. *The deperature dependency of the parameter* $\lambda_{ma}(NH_3,HCO_3^-)$

Table 5.9.*Estimated conversion at 65°C*
m_{m3} denotes urea species molality.
x - urea % conversion based on CO_2

mNH_3	mCO_2	m_{m3}	x
2.2924	1.4335	0.0005	0.0349
4.8571	2.7124	0.0024	0.0885
7.7716	4.2980	0.0062	0.1443
10.9460	5.5600	0.0145	0.2608
12.8430	6.3170	0.0228	0.3609
14.1840	6.9770	0.0309	0.4429
15.4192	7.3418	0.0402	0.5475
16.4342	7.8342	0.0501	0.6395
18.4068	8.6256	0.0747	0.8660
19.3989	9.0696	0.0910	1.0034
20.1968	9.2615	0.1027	1.1089
20.0720	9.0384	0.1072	1.1861
20.3929	8.7156	0.0981	1.1256
20.0707	8.3978	0.0896	1.0669
18.1255	7.2826	0.0589	0.8088
16.9044	6.2114	0.0416	0.6697
15.6472	5.5456	0.0314	0.5662
11.7625	3.1625	0.0106	0.3352
9.7091	1.7409	0.0041	0.2355
13.9697	4.4348	0.0200	0.4510
16.4270	5.9168	0.0371	0.6270
18.0204	6.9186	0.0543	0.7848
19.6111	7.9774	0.0790	0.9903
20.3388	8.6153	0.0719	0.8346
20.7435	9.0412	0.1076	1.1901
20.6665	9.2231	0.1097	1.1894
19.6262	9.0971	0.0943	1.0366
17.4203	8.2838	0.0617	0.7448
15.8316	7.6197	0.0442	0.5801
13.9728	6.8719	0.0295	0.4293
11.8948	6.0208	0.0183	0.3039
9.2225	4.8723	0.0094	0.1929
7.2810	4.0079	0.0054	0.1347
4.0889	2.3542	0.0017	0.0722
1.4471	0.9261	0.0002	0.0216

Table 5.10.*Estimated conversion at 100°C*
m_{m3} denotes urea species molality.
x - urea % conversion based on CO_2

mNH_3	mCO_2	m_{m3}	x
3.0005	1.5003	0.0010	0.0660
3.8049	2.0559	0.0015	0.0730
4.3318	2.0421	0.0019	0.0930
5.3362	2.7332	0.0026	0.0951
6.5985	3.4013	0.0035	0.1029
8.2992	4.7618	0.0054	0.1141
9.8371	4.9185	0.0074	0.1505
10.9293	5.4646	0.0091	0.1665
12.5248	6.0771	0.0123	0.2024
13.6498	6.6732	0.0152	0.2278
14.9269	7.3079	0.0195	0.2668
16.6849	8.0216	0.0277	0.3453
18.0652	8.5399	0.0367	0.4297
18.2835	8.5652	0.0382	0.4460
18.7801	8.8084	0.0425	0.4825
19.1987	8.7646	0.0457	0.5214
20.4957	9.3939	0.0604	0.6430
21.7513	9.7446	0.0776	0.7963
22.7843	9.6767	0.0903	0.9332
24.3304	10.2728	0.1245	1.2119
24.8522	10.3400	0.1356	1.3114
25.2977	10.1913	0.1402	1.3757
25.6127	10.0263	0.1415	1.4113
25.5778	9.6144	0.1299	1.3511
25.1906	9.2665	0.1157	1.2486
25.5018	9.1014	0.1161	1.2756
25.2071	8.6705	0.1029	1.1868
24.7494	8.1319	0.0878	1.0797
22.9370	6.8214	0.0564	0.8268
21.5409	5.7995	0.0408	0.7035
20.3319	4.8409	0.0306	0.6321
19.1845	3.9313	0.0231	0.5876
18.3489	3.2380	0.0183	0.5652
17.4975	2.4134	0.0133	0.5511
16.4472	1.4685	0.0074	0.5039

Table 5.11.*Estimated conversion at 120°C*

m_{m3} denotes urea species molality.

x - urea % conversion based on CO_2

mNH_3	mCO_2	m_{m3}	x
1.2603	0.5156	0.0002	0.0388
1.7401	0.7540	0.0004	0.0531
2.5420	1.0641	0.0009	0.0846
3.1172	1.3188	0.0014	0.1062
3.6400	1.5166	0.0018	0.1187
4.3791	1.7886	0.0025	0.1398
5.0065	2.0652	0.0031	0.1501
5.5763	2.2812	0.0037	0.1622
6.3108	2.5758	0.0045	0.1747
7.4673	3.1059	0.0058	0.1867
8.6754	3.5922	0.0074	0.2060
9.6899	4.0144	0.0088	0.2192
11.0025	4.4720	0.0109	0.2437
11.4600	4.6556	0.0117	0.2513
12.3840	4.9536	0.0135	0.2725
13.3757	5.4246	0.0157	0.2894
14.3885	5.8311	0.0183	0.3138
14.8127	6.0320	0.0195	0.3233
15.0274	6.1336	0.0201	0.3277
16.2848	6.4983	0.0246	0.3786
16.6134	6.6139	0.0259	0.3916
16.8426	6.7212	0.0268	0.3987
16.9700	6.8197	0.0273	0.4003
18.1799	7.1104	0.0333	0.4683
18.7476	7.2545	0.0365	0.5031
19.3541	7.4946	0.0403	0.5377
19.5769	7.5169	0.0418	0.5561
19.7182	7.6222	0.0429	0.5628
19.8604	7.7281	0.0439	0.5759
19.9734	7.7397	0.0447	0.5775
20.0566	7.6565	0.0453	0.5917
20.1626	7.3017	0.0457	0.6259
20.5559	7.1571	0.0484	0.6763
20.3810	6.9594	0.0469	0.6739
20.5467	6.7937	0.0478	0.7036

Table 5.12.*Estimated conversion at 130°C*

m_{m3} denotes urea species molality.

x - urea % conversion based on CO_2

mNH_3	mCO_2	m_{m3}	x
1.1469	0.6881	0.0001	0.0145
2.3621	1.1810	0.0006	0.0508
3.6559	1.7670	0.0015	0.0849
5.0235	2.2606	0.0027	0.1194
6.4847	2.8533	0.0042	0.1472
8.0643	3.6289	0.0060	0.1653
9.7507	4.3878	0.0082	0.1869
11.5644	5.2044	0.0109	0.2094
13.5205	6.0842	0.0143	0.2350
15.6364	7.0364	0.0188	0.2672
17.2159	7.7230	0.0229	0.2965
17.9589	8.1631	0.0248	0.3038
19.1987	8.7646	0.0288	0.3286
20.4957	9.3939	0.0337	0.3587
21.8197	9.9498	0.0398	0.4000
22.5038	10.2370	0.0435	0.4249
23.2032	10.5307	0.0475	0.4511
23.9186	10.8311	0.0521	0.4810
24.6911	11.2482	0.0572	0.5085
25.4418	11.5644	0.0630	0.5448
26.2544	12.0020	0.0696	0.5799
26.9968	12.2196	0.0772	0.6318
27.7546	12.4417	0.0857	0.6888
28.5781	12.7875	0.0955	0.7468
29.4219	13.1418	0.1067	0.8119
30.2327	13.3817	0.1192	0.8908
31.0612	13.6268	0.1333	0.9782
31.9660	14.0042	0.1501	1.0718
32.8336	14.2621	0.1685	1.1895
33.8877	14.5530	0.1936	1.3303
34.9036	14.7184	0.2209	1.5008
35.8056	14.6189	0.2471	1.6903
36.3682	14.4622	0.2638	1.8241
36.6170	14.0100	0.2694	1.9229
36.1651	13.4568	0.2535	1.8838

Similarly, trying to find the pure electrolyte parameter values at present from those of alkali salts by correlating them against the ionic radii, the absolute ionic entropies, the hydrated ion radii etc., (similar to the attempt by Beutier et al [27]) can only be an ad-hoc arrangement with uncertain results, since no salts related to our present system, excepting the carbonate and bicarbonate salts of sodium and potassium, have been so far investigated. The worth of such correlations can be assessed only when other alkali carbonates, bicarbonates and carbamates are investigated in the future in a systematic way.

One important observation in the above model calculation is that the incorporation of the urea formation reaction proved to be a positive step. Despite the fact that the equilibrium constant is estimated in a circumferential way and not directly from the experimental values of the free energy and enthalpy of the reaction, it is quite revealing to know that urea as a species is present in appreciable concentrations even at 65° C, concentrations comparable to those of free CO_2 and $CO_3^{=}$. Further, the highest urea conversion at 65, 100 and 130°C is achieved in the model calculation for an $(NH_3)/(CO_2)$ ratio value slightly greater than a similar value existing at the bubble point tongue (i.e. the so called liquid ridge point mentioned in the Chapter 3). Incidentally, such a conclusion is in agreement with the predictions of Chermin [104]. As for 120°C, the available data stops even before the bubble-point tongue is reached, and hence one cannot compute the maximum urea conversion. The calculated urea molalities and the conversion to urea as a percentage of the liquid phase CO_2 component molality along with the liquid phase pseudo-experimental component molalities are represented in Tables 5.9, 5.10, 5.11 and 5.12.

There is one further observation related to the temperature dependency of the model parameters. It appears that one can afford to keep λ_{ma} (NH_3, NH_2COO^-) constant with respect to temperature and still obtain a satisfactory fit. A similar remark can be made to a limited extent on the parameter β^o (NH_4^+, NH_2COO^-). Such a step will limit the parameters to only six for further optimization.

With these discussions, we move to the next chapter to discuss a few related features of the Hot Gas Recycle Process mainly with respect to the phase equilibria implications on the process design.

References:

1. Henderson, D., "Practical calculations of the equation of state of fluids and fluid mixtures using perturbation theory and related theories", Advances in Chemistry series No.182, "Equations of state in engineering and research." ed. by. K.C.Chao and R.L.Robinson, 1979, pp.1 - 29.
2. Whiting, W.B. and J.M.Prausnitz, "Equations of state for strongly nonideal fluid mixtures: application of local compositions toward density-dependent mixing rules", Fluid phase equilibria, 1982, vol.19, no.9, pp.119-147.
3. Mansoori, G.A., "Statistical mechanical theory of local compositions", Fluid phase equilibria, 1985, vol.22, no.3, pp.253-275.
4. Debye,P. and E.Huckel, Phys.Z., 1923, vol.24, p.185 and p.334;1924, vol.25, p.97
5. Card, D.N. and J.P.Valleau, "Monte Carlo study of the thermodynamics of electrolyte solutions", J.Chem.Phys., 1970, vol.52, no.12, pp.6232-6240
6. Friedman, H.L., "Computed thermodynamic properties and distribution functions for simple models of ionic solutions", Modern aspects of electrochemistry, ed. by J.M.Bockris and B.O.Conway, 1971, no.6.
7. Rasaiah, J.C.," A View of electrolyte solutions", J.Solution Chem., 1973, vol.2, no.2/3, pp.301-338.
8. Waisman, E. and J.L.Lebowitz, " Mean spherical model integral equations for the charged hard spheres", J.Chem.Phys., I in 1972, vol.56, p.3086, II in 1972, vol.56, p.3094.
9. Stillinger, F.H. and R.Lovett, "Ion-pair theory of concentrated electrolytes. I. basic concepts", J.Chem.Phys., 1963, vol.48, no.9, pp.3858-3868
10. Andersen, H.C. and D.Chandler, "Mode expansions in equilibrium statistical mechanics", J.Chem.Phys., 1970, vol.53, p.547; 1971, vol.54, p.26; 1971, vol.55, p.1497; 1972, vol.57, p.1918; 1972, vol.57, p.1930.

    Andersen, H.C., D.Chandler and J.D.Weeks, J.Chem.Phys., 1972, vol.56, p.3812; 1972, vol.57, p.2626.
11. Stokes, R.H. and R.A.Robinson, "Solvation equilibria in very concentrated electrolyte solutions", J.Solution Chem., 1973, vol.2, no.2/3, pp.173-191.
12. Bromley, L.A., "Approximate individual ion values of β (or B) in extended Debye-Huckel theory for uni-univalent aqueous solutions at 298.15K", J.Chem. Thermodynamics, 1972, vol.4, pp.669-673.

    Bromley, L.A., "Thermodynamic properties of strong electrolytes in aqueous solutions" AIChE J., 1973, vol.19, no.2, pp.313-320.
13. Meissner,H.P. and J.W.Tester," Activity coefficients of strong electrolytes in aqueous solutions", I&EC process des.develop., 1972, vol.11, no.1, pp.128-133.
14. Sorensen, T.S., "The adjusted screened potential/excluded volume (ASPEV) theory of strong electrolytes in solution", Acta Chem. Scand., 1978, vol.A32,pp.571-594

Sorensen, T.S. et al, " Ionic radii from experimental activities and simple statistical-mechanical theories for strong electrolytes with small Bjerrum parameters", Acta Chem.Scand., 1984, vol.A 38, pp.735-756.

15. Pytkowicz, R.M., Chapter 1 of "Activity coefficients in electrolyte solutions", vol.I, CRC press, Cleveland, 1979, p.1

16. Triolo, R. et al,"Simple electrolytes in the mean spherical approximation", *J.Phys.Chem., 1976, vol.80, no.17, pp.1858-1861.*

17. Cruz, Jose-Luis and H.Renon, "A new thermodynamic representation of binary electrolyte solutions nonideality in the whole range of concentrations",AIChE J., 1978, vol.24, no.5, pp.817-830.

18. Pitzer, K.S., "Theory: ion interaction approach" in "Activiiy coefficients of electrolyte solutions" as Chapter 7. ed. by R.M.Pytkowicz, CRC press, Cleveland, 1979, pp.157-208.

    Pitzer, K.S., "Thermodynamics of aqueous electrolytes at various temperatures, pressures, and compositions", ACS symposium series 133, "Thermodynamics of aqueous systems with industrial applications", ed. by S.A.Newman, 1980, pp.451-466.

    Pitzer, K.S., "Thermodynamics of electrolytes.I.Theoretical basis and general equations", J.Phys.Chem., 1973, vol.77, no.2, pp.268-277.

    Pitzer, K.S. and G.Mayorga,"Thermodynamics of electrolytes.II.Activity and osmotic coefficients for strong electrolytes with one or both ions univalent", J.Phys.Chem., 1973, vol.77, no.19, pp.2300-2308.

    Pitzer, K.S. and G.Mayorga,"Thermodynamics of electrolytes.III. Activity and osmotic coefficients for 2-2 electrolytes", J.Solution Chem., 1974, vol.3, no.7, pp.539-546.

    Pitzer, K.S. and J.J.Kim,"Thermodynamics of electrolytes. IV. Activity and Osmotic coefficients for mixed electtolytes", J.Am.Chem.Soc., 1974, vol.96, no.18, pp.5701-5707.

    Pitzer, K.S., "Thermodynamics of electrolytes. V. Effects of higher - order electrostatic terms", J.solution Chem., 1973, vol.4, no.3, pp.249-265.

    Pitzer, K.S. and L.F.Silvester, "Thermodynamics of electrolytes. VI. Weak *electrolytes including H_3PO_4", J.Solution Chem., 1976, vol.5, no.4, pp.269-278.*

    Pitzer, K.S.et al, J.Am.Chem.Soc., 1977, vol.99, p.4930

    Silvester, L.F. and K.S.Pitzer, "Thermodynamics of electrolytes. VIII. High temperature properties, including enthalpy and heat capacity, with application to sodium chloride", J.Phys.Chem., 1977, vol.81, p.1822.

    Pitzer, K.S. et al, J.Solution chemistry, 1978, vol.7, p.45.

    Downes, C.J. and K.S.Pitzer, "Thermodynamics of electrolytes. Binary mixtures formed from aqueous NaCl, Na_2SO_4, $CuCl_2$, and $CuSO_4$ at 25^oC", J.Solution Chem., 1976, vol.5, no.6, pp.389-398.

Peiper, J.C.and K.S.Pitzer, "Thermodynamics of aqueous carbonate solutions including mixtures of sodium carbonate, bicarbonate, and chloride", J.Chem. Thermodynamics, 1982, vol.14, pp.613-638

19. Scatchard, G., J.Am.Chem.Soc., 1961, vol.83, p.2636.
Scatchard, G. et al, J.Phys.Chem., 1970, vol.74, p.3786.

20. Reilly, P.J. and R.H.Wood, "The prediction of the properties of mixed electrolytes from measurements on common ion mixtures", J.Phys.Chem., vol.73, no.12, pp.4292-4297.
Reilly, P.J., R.H.Wood and R.A. Robinson, " The prediction of osmotic and activity coefficients in mixed electrolytes", J.Phys.Chem., 1971, no.9, pp.1305-1314

21. O'connell, J.P. and A.E.DeGance, "Thermodynamic properties of strong electolyte solutions from correlation functions", J.Solution chem., 1975, vol.4, no.9, pp.763-778.

22. Chen, C.C, "Two new activity coefficients models for the vapor-liquid equilibrium of electrolyte systems", ACS symposium series 133, "Thermodynamics of aqueous systems with industrial systems, ed. by S.A.Newman, 1980, pp.61-89.
Chen, C.C. et al, "Local composition model for excess Gibbs energy of electrolytes systems", AIChE J., 1982, vol.23, no.4, pp.588-596.

23. Zemaitis, J.F., "Predicting vapor-liquid-solid equilibria in multicomponent aqueous solution of electrolytes", in ACS symposium series 133, "Thermodynamics of aqueous systems with industrial applications",ed.by S.A.Newman, 1980, pp.227-246

24. Whitefield, M., Geochim. Cosmochim. Acta, 1975, vol.39, p.1545.

25. Harvie, C.E. and N.Moller and J.H.Weare, "The prediction of mineral solubilities in natural waters: The Na-K-Mg-Ca-H-Cl-SO_4-OH-HCO_3-CO_3-CO_2-H_2O system to high ionic strengths at 25^oC", Geochim. Cosmochim. Acta, 1984, vol.48, pp.723-751.

26. Edwards, T.J. et al, a. "Thermodynamics of aqueous solutions containing volatile weak electrolytes", ATChE J., vol.21, no.2, pp.248-259.
b."Vapor-liquid equilibria in multicomponent aqueous solutions of volatile weak electrolytes", AIChE J., 1978, vol.24, no.6, pp.966-976.

27. Beautier, D. and H.Renon, "Representation of NH_3-H_2S-H_2O, NH_3-CO_2-H_2O, and NH_3-SO_2-H_2O vapor-liquid equilibria", I&EC process des.dev., 1978, vol.17, no.3, pp.220-230.

28. Maurer, G.,"On the solubility of volatile weak electrolytes in aqueous solutions", ACS Symposium series, "Thermodynamics of aqueous systems with industrial applications", ed.by S.A.Newman, 1980, pp.140-171.

29. Chen, C.C. et al, "Extension and application of the Pitzer equation for vapor-liquid equilibrium of aqueous electrolyte systems with molecular solutes", AIChE J., 1979, vol.25, no.5, pp.820-831.

30. Pawlikowski, E.M. et al, "Phase equilibria for aqueous solutions of ammonia and

carbon dioxide", I&EC process des.dev., 1982, vol.21, no.4, pp.764-770.

31. Müller, G.,"Experimentelle Untersuchung Des Dampf-flussigkeits-Gleichgewichts im system ammoniak-kohlendioxid-wasser zwischen 100 und 200°C bei drucken bis 90 bar",(in German), PhD thesis, University of Kaiserlautern, 1983.

32. Kawasumi,S.,"Equilibrium of the CO_2-NH_3-Urea-H_2O system under high temperature and pressure", Bulletin of The Chemical Society of Japan, I in 1951, vol.24, no.3, pp.148-151; II in 1952, vol.25, no.4, pp.227-238; III in 1953, vol.26, no.5, pp.218-222; IV in 1953, vol.26, no.5, pp.222-227; V in 1954, vol.27, no.5, pp.254-259.

33. Lemkowitz, S.M.,"Phase and corrosion studies of the ammonia-carbon dioxide - water system at the conditions of the hot gas recirculation process for the synthesis of urea", PhD thesis, Delft University of Technology, The Netherlands, 1975, 191 pages.

34. Gorlovskii, D.M.,"Study of reaction equilibrium in the synthesis of urea from ammonia and carbon dioxide", Author's summary of the thesis, Moscow, 1969, 19 pages.

35. Baranski, A. and A.Fulinski, "Comments on the thermodynamics of urea synthesis", J.Appl.Chem.Biotechnol., 1975, vol.25, pp.113-114.

36. Durisch, W.,"Experimentelle und thermodynamische untetsuchung des Seidegleichgewichts des systems $CO_2/NH_3/H_2O$ unter harnstoffsynthese-bedingungen" (in German) PhD thesis, Eidgenossischen Technische Hochschule, Zurich, 1978, 210 pages.

37. van Krevelen, D.W. et al, "Composition and vapour pressures of aqueous solutions of ammonia, carbon dioxide and hydrogen sulphide", Recueil des travaux chimques des Pays-Bas. 1949, Tome 68, no.3, pp.191-216.

38. Othmer, D.F. and G.J. Frohlich,"Carbon dioxide and ammonia in aqueous ammonium nitrate solutions", I&EC process des.dev.,1964, vol.3, no.3, pp.270-279.

39. Wicar, S.,"Calculation of vapour-liquid equilibrium in the system urea, ammonia, carbon dioxide, and water", Brit.Chem.Eng., 1963, vol.8, no.12, pp.818-822.

40. Kotula, E.," A vapour liquid equilibrium model of the NH_3-CO_2-H_2-Urea system at elevated pressure", J.Chem.Tech.Biotechnol., 1981, vol.31, pp.103-110.

41. van Eck, M., "Quantitative analysis of the urea synthesis by means of laser Raman spectrometry" PhD thesis, Technical University of Delft, The Netherlands, 101 pages.

42. Nakamura, R. et al,"Thermodynamic properties of gas mixtures containing common polar and nonpolar components", I&EC process des.dev., 1976, vol.15, no.4, pp.557-564.

43. Durisch, W. and P.J.van den Berg, "Die dichte gasformiger kohlendioxid-ammoniak-wasser gemische unter harnstoff-synthese bedingungen", Chemia, 1979, vol.33, no.6, pp.200-204.

44. Bronstead, J.N., J.Am.Chem.Soc., 1922, vol.44, p.938; also p.877.

45. Guggenheim, E.A., Philos.Mag., (Series 7), 1935, vol.19, p.588.
Guggenheim, E.A. and J.C.Turgeon, Trans. Faraday Soc., 1955, vol.51, p.747.

46. Brelvi, S.W. and J.P.O'Connell, "Corresponding states correlations for liquid compressibility and partial molar volumes of gases at infinite dilution in liquids", AIChE J., 1972, vol.18, no.6, pp.1239-1243.

47. Handbook of Chemistry and Physics, CRC press, Cleveland, 59th ed.,1978.

48. Clarke, E.C.W. and D.N.Glew, "Evaluation of thermodynamic functions from equilibrium constants", Trans.Faraday Soc., 1966, vol.62, pp.539-547.

49. Wilson, T.A., Refrig.Eng., 1924, vol.10, pp. 248-252.

50. Clifford, I.L. and E.Hunter, "The system ammonia-water at temperatures up to 150°C and at pressures up to 20 atmospheres", J.Phys.Chem., 1933, vol.37, pp.101-118.

51. Mollier, H., VDI-Zeitschrift, 1908, vol.52, no.33, pp.1315-1320.

52. Perman, E.P., J.Chem.Soc., 1901, vol.79, pp.718-725; 1903, vol.83, pp.1168-1184.

53. Pierre, B. Kylteknisk Tidsckrift, 1959, vol.14, pp.89-90

54. Weiss, R.F.,"Carbon dioxide in water and seawater: The solubility of a non-ideal gas", Marine Chem., 1974, vol.2, pp.203-215.

55. Redlich, T.R. et al, "Solubility of gases in liquids. 13. High-precision Determination of Henry's constants for methane and ethane in liquid water at 275 to 328", J.Phys.Chem., 1981, vol.85, pp.3230-3237.

56. Takenouchi, S. and G.Kennedy, Am.J.Sci.,1964, vol.262, pp.1055-1074.

57. Haehnel, O., Zbl. Mineralog. Geol. Palaontol., 1920, pp.25-30.

58. Zelvenskii, Y.D., Zhurn. Khim. Prom., 1937, vol.14, pp.17-18, pp.1250-1257.

59. Stewart, P.B. and P.Munjal, J.Chem.Eng.data, 1970, vol.15, no.1, pp.67-71.

60. Wroblewskii, S., Ann.Phys.chem., 1883, vol.18, p.290; Compt.Rendus, 1882, vol.94, p.1335.

61. Morgan, O.M. and O.Maass, can.J.research, 1931, vol.5, pp.162-199.

62. Novak, J.et al, Coll.Czech.Chem.Commun., 1961, vol.26, pp.2266-2270.

63. Wiebe, R. and V.L.Gaddy, Chem rev., 1941, vol.63, pp.475-477; J.Am.Chem. Soc., 1939, vol.61, pp.315-338; also 1940, vol.62, pp.815-817.

64. Prutten, C.F. and R.L.Savage, J.Am.chem. soc., 1945, vol.67, pp.1550-1554.

65. Zawisza, A. and B.Malesinska, J.Chem. Eng.Data, 1981, vol.26, no.4, pp.388-391.

66. van der Zee, C.E., "Thermodynamics of carbon dioxide and carbonic acid", J.Chem.Thermodynamics, 1978, vol.10, pp.1113-1136.
a. "The enthalpies of solution and formation of ammonia", J.Chem.Thermodynamics, 1973, vol.4, pp.675-683.

67. Worswick, R.D. et al, "The enthalpy of solution of ammonia in water and in aqueous solutions of ammonium chloride and ammonium bromide", J. Chem. Thermodynamics, 1974, vol.6, pp.565-570.

68. Landolt-Bornstein Handbook, Neue Serie, 2.1. Anorganic substances-water, pp.79-80, Item no.439. a. also 2.2. Spezifische Warme und Warmeinhalt binarer losungen, pp.274-275.

69. Wagman, D.D. et al, "Selected values of chemical thermodynamic properties. Tables for the first thirty-four elements in the standard order of arrangement", NBS Tech.note no.270-3, Jan.1968.

70. Harned, H.S. and R.Davis," The ionization constant of carbonic acid in water and the solubility of carbon dioxide in water and aqueous salt solution from 0 to 50^o", J.Am.Chem.Soc., 1943, vol.65, pp.2030-2037.

71. Ellis, A.J. and R.M.Golding, Am.J.Sci., 1963, vol.216, pp.47-60

72. Ellis, A.J., "The solubility of carbon dioxide in water at high temperatures", Am.J.Sci., 1959, vol.257, pp.217-234.

73. Read, A.J., "Ionization constants of aqueous ammonia from 25 to 250°C and to 2000 bar", J.Solution chem., 1982, vol.11, no.9, pp.649-664.

74. Patterson, C.S. et al," Carbonate equilibria in hydrothermal systems: first ionization of carbonic acid in NaCl media to 300°C", Geochim. Cosmochim. Acta, 1982, vol.46, pp.1653-1663.

75. Larson, J.W. et al,"Heat capacities and volumes of dissociation of phosphoric acid (1st, 2nd, and 3rd), bicarbonate ion, and bisulfate ion in aqueous solution", Can.J.Chem., 1982, vol.60, pp.2141-2150.

76. Sweeton, F.H. et al, "Acidity measurements at elevated temperatures. VIII. Dissociation of water", J.Solution Chem., 1974, vol.3, no.3, pp.191-214.

77. Faurholt, C., "Über die prozesse '$NH_2COONH_4 + H_2O - (NH_4)_2CO_3$' und '$CO_2 + H_2O - H_2CO_3$", Z.Anorg.Allg.Chem., 1921, vol.120, pp.85-102.
Faurholt, C., "Etudes sur les solutions aqueuses de carbamates et de carbonates", J.Chim.Phys. Phys-Chim. Biol., 1925, vol.22, pp.1-44.

78. Christensen, F. et al, "Equilibrium constants in the ammonium carbonate-carbaminate system. The acid dissociation constant of carbamic acid", Acta Chemica Scand., 1978, vol. A 32, pp.15-17.

79. Marion, G.M. and G.R.Dutt, "Ion association in the ammonia-carbon dioxide-water system", Soil Sci.Soc.Amer.Proc., 1974, vol.38, pp.889-891.

80. Usdowski, H.E. et al, "Kinetically controlled partitioning and isotopic equilibrium of ^{13}C and ^{12}C in the system CO_2-NH_3-H_2O", Z.Phys.Chemie Neue Folge, 182, Bd.130, pp.13-21.

81. Szarawara, J et al, "Badania hydrolizy karbaminianu amonowego", Przemysl Chemiczny, 1973, vol.52/12, pp.817-821.

82. Gmelin handbook on inorganic chemistry, "NH_4", p.346.

83. Claude, B., "Hydrolyse et thermochimie de quelques carbamates", Revue de Chemie minerale, 1965, tome 2, pp 327-338.

84. Bernard, M.A. and M.M.Borel, "Etude thermochimique de quelques carbamates",

Bulletin de la societe chemique de France, 1968, no.6, pp.2362-2366.

85. Pinsent et al, B.R.W. et al, "The kinetics of combination of carbon dioxide with ammonia", Trans. Faraday Soc., 1956, vol.52, pp.1594-1598.

86. Frejaques, M., "Les bases theories de la synthese industrielle de l'uree", Chimie et industrie, 1948, vol.60, no.1, pp.22-35.

87. Mavrovic, I.,"Final equilibrium urea yield", Hydrocarbon Processing, 1971, vol.50, no.4, p.161.

88. Inoue, S. et al, "Equilibrium of urea synthesis", Bull. Chem. Soc. Japan, I in 1972, vol.45, pp.1339-1345; II in 1972, vol.45, pp. 1616-1619.

89. Gorlovskii, D.M. et al, "Experimental values of the equilibrium degree of conversion of carbon dioxide into urea by the Bazarov reaction", Zh.Prikl. Khim., 1972, vol.45, no.7, pp.1533-1537.

Gorlovskii et al, "Equation for the determination of the equilibrium degree of carbon dioxide conversion in urea synthesis", Zh.Prikl.Khim., 1980, vol.53, no.11, pp.2548-2551.

90. CODATA bulletin, J.Chem.Thermodynamics, 1978, vol.10, pp.903-906.

91. Egan, E.P and B.B.Luff, "Heat of solution, heat capacity, and density of aqueous urea solutions at 25°C", J.Chem.Eng.Data, 1966, vol.11, pp.192-194.

92. Subramanian, S. et al,"Nuclear magnetic resonance and thermochemical studies on the influence of urea on water structure", J.Phys.Chem.,1969, vol.73,no.1, pp 266-269.

93. Gucker, F.T. and H.B.Pickard, "The heats of dilution, heat capacities, and activities of urea in aqueous solutions from the freezing point to 40°C", J.Am.Chem.Soc., 1940, vol.62, pp.1464- 1471.

94. Phillips, P.R. et al, "Apparent molal volumes and heat capacities of urea and methyl-substituted ureas in H_2O and D_2O at 25°C", Can.J.Chem., 1974, vol.52, pp.1709-1713.

95. Gogolides, Evangelos, "Thermodynamics of the phase and reaction equilibria in the system NH_3-CO_2-H_2O --- model development and parameter evaluation through optimization methods", IASTE internal report, Laboratorium voor Chem. tech., Technische Hogeschool Delft, The Netherlands, 29th Aug.,1984, 48 pages.

96. de Rijke, Jan, " Het gebruik van modelbeschrijvingen voor de niet-idealiteit in het system NH_3-CO_2-H_2O", Internal report, Laboratorium voor anorganische en fysische Chemie, Technische Hogeschool Delft, The Netherlands, 1984, 69 pages.

97. Böhm, H-J. and I.R. Macdonald, "An ab initio potential energy function for $NH_4^+.H_2O$ and its use in the study of ionic co-ordination in solution", Trans.Faraday Soc., part II, Chem.Phys., 1980, vol.80, pp.887-998.

98. Mason, D.M. and R.Kao, "correlation of vapor-liquid equilibria of aqueous condensates from coal processing", ACS Symposium series 133, "Thermodynamics of aqueous systems with industrial applications", 1980, pp.106-138.

99. Stokes, R.H., "Thermodynamics of aqueous urea solutions", Austrl. J. Chem., 1967, vol.20, pp.2087-2100.

100. DSM private communication

101. Zernike, J., "Chemical phase theory", Kluwer publishing company, 1955.

102. Gill, P.E. and W.Murray, "Algorithms for the solutions of the nonlinear least-squares problem", SIAM J.Numer.Anal., vol.15, no.5, pp.977-992.

103. Kucheryavyi, V.I. et al, "vapor-liquid equilibrium in the system ammonia-carbon dioxide-urea-water at pressures up to 50 atm and temperatures in the range of 100-160°,

104. Chermin, H.A.G., DSM internal report, private communication.

CHAPTER 6

APPLICATION OF THE PHASE EQUILIBRIA PRINCIPLES TOWARDS THE DESIGN OF UREA PROCESSES AND ESPECIALLY WITH REFERENCE TO THE HOT GAS RECYCLE PROCESS.

6.1. *Introduction*:

Urea is synthesized from ammonia and carbon dioxide through the formation of ammonium carbamate followed by dehydration at high temperatures and pressures ranging from 180 to 200° C and 140 to 250 bar, respectively.

$$2NH_3(aq) + CO_2(aq) <\!\!\longrightarrow NH_4COONH_2(aq)$$

$$\Delta H_1 = -\ 25.19 \text{ Kcal/mole at 1 bar and } 193^{o}\text{ C. [1]} \qquad \text{(eq. 6.1)}$$

$$NH_4COONH_2(aq) <\!\!\longrightarrow NH_2CONH_2(aq) + H_2O(liq)$$

$$\Delta H_2 = \ 6.88 \text{ Kcal/mole at 1 bar and } 193^{o}\text{ C. [1]} \qquad \text{(eq. 6.2)}$$

While the first reaction goes to near completion, the second reaction is the limiting one during synthesis. Even with excess NH_3, the industrially reported conversions span a range of only 55 to 75%, necessitating recovery and recycle of the unreacted materials in order to minimize the specific consumption of raw materials and energy. Consequently the available commercial processes differ mostly in their methods of recovery and recirculation.

There are basically two categories of urea processes. The first is the classical pressure reduction processes. Traditionally these processes have been called "the solution recycle processes," which in the author's opinion can be equally applied to the second category, namely, the stripping processes. The major criterion for classification is whether the decomposition is effected by the reduction in total pressure or by the alteration of partial pressure.

In the pressure reduction processes (PRP), the reactor exit stream is let down in at least 3 low pressures stages with adequate heating to decompose the unreacted ammonium carbamate and to expel the excess ammonia. The volatiles are then absorbed countercurrently by the aqueous carbonate/carbamate solutions obtained from the previous low pressure stages. The enriched solution is finally recirculated to the reactor. Major processes in this category are due to Mitsui-Toatsu (15), Montedison (16), and also Urea Technology Inc (19). The first two processes are not presently offered in the market, and the two companies concerned have switched over to their own stripping processes (15,16).

In the stripping processes (STRP), the volatiles in the reactor exit stream are stripped off by altering their partial pressures through the addition of at least one of the fresh reactants. The lean solution is then led to successive low pressure units to decompose the remaining carbamate (10 to 15%) and to expel ammonia. Volatile gases from the stripper are condensed at the same synthesis pressure and recycled back to the reactor. Major processes are the Stamicarbon CO_2 stripping process (14), SNAM progetti NH_3 stripping process (20), Toyo Engineering ACES process (15) and Technimont IDR process (21).

In addition to these processes, Ammonia Casale of Switzerland are offering a process called Split Reaction Recycle process (SRRP) coupling the high conversion advantage of the PRP with the efficient recovery of the STRP (22).

In the same spirit of coupling the two different approaches, Technological University of Delft (TUD) developed a Hot Gas Recycle Process (HGRP). The original HGRP, pioneered in the 1930's by I.G.Farben Industrie of Germany [2], fell out of favour due to a number of major operating problems. The TUD version of the HGRP [3] attempts to rectify such problems through consistent application of phase equilibria principles. The technical feasibility of the TUD process has been well demonstrated at a pilot plant level, and its economics appears to compare favourably with the CO_2 stripping process. However, on further scrutiny, there appears to be some more scope for improving the TUD process.

In this chapter, a synthesis of the improved HGRP, developed at the TUD, is presented in a simplified manner highlighting the relevance of the phase equilibria studies. Also certain guidelines on the process design are established.

6.2. *The basic premise of the HGRP*:

Consider a simple flowsheet of the urea synthesis consisting of just three modules, namely a reactor, a decomposer, and a condenser, as given in Fig. 6.1.

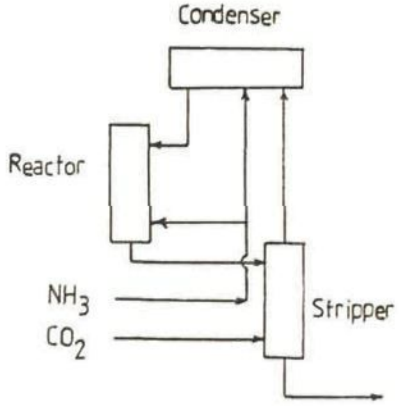

Fig.6.1. *Synthesis loop of urea process*

In a STRP, all the three units operate isobarically, while in the classical PRP the decomposer and the condenser operate at the same pressure and the reactor operates at a higher pressure. The main advantage of STRP is in the high pressure operation of the condenser leading to generation of low pressure steam instead of heat rejection to cooling water. However, such high pressure operation also leads to enhanced urea hydrolysis and biuret formation in the stripper. To achieve economy against these odds, the emphasis in STRP is usually on high stripping efficiencies [4] obtained over a thin film in the stripper tubes. Increasing the synthesis pressure further is counter-productive to stripping processes, mainly because of the increased solubility of ammonia in water and incresed energy requirement for decomposing carbamate at higher temperatures. Hence high stripping efficiencies commensurate with high stripper pressures are very difficult to achieve in these processes.

In contrast, the decomposer in the PR process operates at relatively mild conditions, and the urea hydrolysis and biuret formation are not serious. Furthermore the reactor pressure can be increased to high values to effect high conversion; but the problem of heat rejection to cooling water persists as a major detriment.

The approach of the HGRP is very different from the previous two. Here, the condenser and the reactor are kept at the same pressure while the decomposer operates at a lower pressure and a hot gas recycle compressor is interposed between the stripper and the condenser. Unlike the I.G.Farben process, in which the recycle compressor was afflicted with serious corrosion problems mainly because of inadequate knowledge, the TUD process was realized after a thorough study of the bubble- and dew-points at high pressures and temperatures and detailed metallurgical studies of the turbo-impellar. Also a model turbocompressor was run without any condensation by maintaining the gases inside the compressor above the dew-point. The downstream equipments of the TUD HGRP were very similar to those of the CO_2 stripping process.

6.3. *The improved TUD HGRP*:

The earlier version of the TUD HGRP adopted the same reactor conditions as those of the CO_2 STRP. Such a choice, although feasible to start with, need not be optimal. One of the design guide-lines of the CO_2 STRP [4] was towards the minimum pressure needed to effect the synthesis, and it was not critical in its design to aim for a maximum possible conversion. This practice was different from that of the PR processes, for example the MTC process, where it was the maximal conversion that was aimed at [5], no matter what pressure was required. There appears to be no reason why these two objectives cannot be met simultaneously.

As a result of such a pursuit, one can increase the reactor pressure and the conversion beyond those of the STRP and still adopt stripping techniques. Consequently the stripper heat duty is lower than that of the STRP. Secondly, the pressure of the condenser-generated steam can be as high as 7 bar. Thirdly, the urea hydrolysis and biuret formation are less severe in the HGRP.

In addition to the change in reactor operation (i.e. by simultaneously achieving a maximum conversion and a minimum bubble-point pressure), the earlier version of the HGRP offers further scope for modifications. The improved version, shown here in Fig. 6.2, has three major changes in the equipment layout:

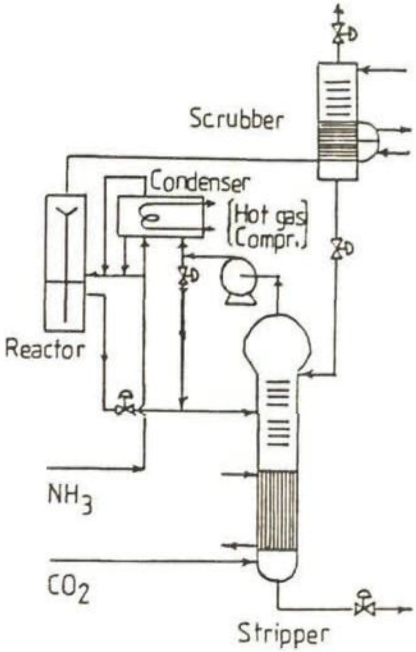

Fig. 6.2. *The improved TUD Hot Gas Recycle Process.*

1. The stipper has been made into a stripper-cum-rectifier.

2. The scrubber botttoms is used as a reflux to the stripper-rectifier.

3. The hot gas recycle comprsssor is made into a single stage compressor with no aftercooler

and,

the stripper pressure is increased to enable single stage compression of the recycle gas [6].

Various operating parameters of the process will be described in the subsequent sections in detail. As a result of these changes, the water to carbon dioxide ratio in the reactor feed can be brought down to values around 0.2.

6.4. *Basis for the pre-design calculations of the improved TUD HGRP:*

In order to explain the design philosophy of the improved TUD HGRP, a base case with the following details/assumptions is taken here as an example.

The plant capacity = 1800 tonnes/day (= 75 tonnes/hr = 1248.81 Kmoles/hr).

The purity of CO_2 entering the plant = 98.0 mole %.

The composition of the inerts entering the plant along with CO_2:

H_2 = 1.7280 %

N_2 = 0.2496 %

Ar = 0.0185 %

CH_4 = 0.0039 %

The purity of NH_3 entering the plant = 99.87 mole%.

The composition of the inerts entering the plant along with NH_3:

H_2 = 0.0530 %

N_2 = 0.0163 %

Ar = 0.0062 %

CH_4 = 0.0545 %

Projected specific consumption of CO_2 = 0.75

The required CO_2 feed (100% pure) = 1278.12 Kmoles/hr
The required CO_2 feed (98 % pure) = 1304.20 kmoles/hr.
Projected specific consumption of NH_3 = 0.57
The required NH_3 feed (100% pure) = 2510.13 Kmoles/hr
The required NH_3 feed (99.87% pure) = 2513.40 Kmoles/hr

The amount of anticorrosion air added to protect the stripper, the condenser and the reactor is assumed to be 4.16 % of the molar feed rate of CO_2.

The amount of anticorrosion air = 54.24 Kmoles/hr
Total inerts entering the stripper = 80.32 Kmoles/hr
The purity of CO_2 feed entering the stripper = 94.09%

Based on an inert balance and assuming the inerts to be insoluble in all the liquid streams of the reactor, the stripper, the condenser and the scrubber, one can fix the following.

The amount of inerts leaving the scrubber = 83.59 Kmoles/hr
The composition of the inerts leaving the reactor = 10 mole % (assumed).
The approach to equilibrium in the reactor = 0.96 (assumed).
The liquid to feed mole ratio inside the reactor = 0.9 (assumed)

6.5. *Fixing the reactor conditions*:

Now consider the system of NH_3-CO_2-H_2O at the reactive bubble point (RBP) equilibrium with urea being present as a species. The system being ternary, both the bubble-point pressure (p^*) and the conversion to urea (x) at the bubble-point can be expressed in terms of L (= the molar ratio of NH_3 to CO_2 in the liquid phase), W (= the molar ratio of H_2O to CO_2 in the liquid phase) and temperature (θ in Celcius or T in Kelvin). Thus:

$$x = \hat{X}\,(\theta, L, W) \tag{eq. 6.3}$$

$$p^* = \hat{P}\,(\theta, L, W) \tag{eq. 6.4}$$

Through a systematic experimental programme on urea conversions, Inoue et al [7] established the function X to be unimodal with respect to temperature (i.e. with one extremum) and not monotonic as suggested by the earlier authors [8]. In other words for a given L and W, the conversion is maximum at one temperature. This condition may be called the (θ-x) max condition.

$$\partial x/\partial\theta = \partial\hat{X}\,(\theta, L, W)/\partial\theta = 0 \tag{eq. 6.5}$$

Likewise, Lemkowitz [3] established the unimodal character of the bubble- point pressure with respect to L for a given θ and W. This condition may be called the (p^*-L) min condition.

$$\partial p^{*}/\partial L = \partial \hat{P}\,(\theta, L, W)/\partial L = 0 \qquad \text{(eq. 6.6)}$$

Rearranging (eq. 6.5 and eq. 6.6) we get,

$$\theta_{max} = \hat{\theta}\,(L, W) \qquad \text{(eq. 6.7)}$$

$$L_{opt} = \hat{L}\,(\theta, W) \qquad \text{(eq. 6.8)}$$

The novelty of the present approach is in simultaneously satisfying the above two equations. In other words, for a given W, the intersection of (eq. 6.7 and eq. 6.8) will exhibit the maximal conversion at the minimal bubble-point pressure; and the intersection values are the corresponding optimal L and θ .

To get these intersections, one has to resort to the data collected by the earlier researchers [3,7,11,13], the interpretation of which is problematic due to the different bases of the data collections.

6.5.1. *The Gibbs and Duhem problems*:

There are two types of situations in thermodynamic modelling of phase equilibria (with or without the interaction of reaction equilibria). They are:

1. Given a minimum of information about the unit sized extensive *phase* properties (for example per unit mass or per unit mole) or the intensities (like p and T), finding the remaining information about all the *phases and the total system. This problem is called an equilibrium* problem. One may also call it a Gibbs problem.
2. Given a minimum of information about the unit sized extensive properties or the intensities of the *total* system at equilibrium, finding the distribution of the components among all the phases and all the specific extensive phase properties. Since as yet no formal name is given to this problem in the literature, the author proposes to call it an equilibrium distribution problem or a Duhem problem. In the distillation parlance, analogous problems are called flash problems.

Both problems have relevance to the experimentation or prediction of phase equilibria. In fact, the Duhem problem is just an extension of the Gibbs problem with the inclusion of material balances. The Gibbs problem is governed by the phase rule and the Duhem problem by Duhem's theorem.

In the Gibbs problem of the ternary vapour-liquid equilibria, three sets of independent variables have been chosen traditionally. They are:

1. (p,T, concentration of one species in any one phase)
2. (ρ_{phase},T, concentration of one species in any one phase)
3. (T, concentrations of two species in any one phase)

For the Duhem problem, it is necessary to specify the gross compositions and two other variables (i.e. the intensities or the unit sized extensities of the total system). Usually either (p,T) or (ρ_{gross}, T) are specified. ρ_{gross} is called the loading density or the charge density in urea literature.

The reactive VLE of urea synthesis has been treated as a Gibbs problem by Inoue-Otsuka [7] and Lemkowitz [3], while Frejacques [8], Baranski-Fulinski [9], Effremova-Leontiva [10] and Gorlovskii-Kucheryavyi [11] treated it as a Duhem problem. Durisch [12] treated the system as a Duhem problem for experimentation and a Gibbs problem during modelling.

So much ground-laying on characterising the problems is necessary here due to the often observed apparently conflicting arguments in the urea literture. These conflicts were especially persistent because, the system being a reactive ternary one, the maximum number of variables to be set both for the Gibbs and the Duhem problems was equally four (i.e. valid for a single phase). Such conflicts could have been avoided if only the basic premises and the variables selected were clearly set forth by the various researchers in their articles.

6.5.2. *The (θ-x) max condition*:

There are mainly three sources of data regarding the urea conversions. The first is due to Kawasumi [13] and the second is due to Inoue et al [7]. Both of them analysed the liquid phase directly with respect to the NH_3, CO_2, urea and H_2O. The third set of data collected by Gorlovskii et al [11] is on a different basis, namely the overall compositions, and hence cannot be coupled with the above due to reasons mentioned in the earlier paragraphs.

In their earlier publication pertaining to a Duhem problem, Gorlovski et al [11a] presented the conversion (x) to urea in the liquid phase as a function of the gross $\{NH_3\}/\{CO_2\}$ ratio (one may call it L_o), the gross $\{H_2O\}/\{CO_2\}$ ratio (W_o), the pressure (p in atm) and the temperature (θ in °C). The reported regression expression (eq. 6.9) was claimed to represent their data well.

$$x = 34.28*L_0 - 1.77*L_0^2 - 29.3*W_0 + 3.699*L_0*W_0 + 0.9129*\theta - 0.07482*\theta*L_0$$
$$- 5.395*10^{-6}*\theta^3 + 0.002293*p - 112.1 \text{ in } \% \qquad \text{(eq. 6.9)}$$

Almost simultaneously Inoue et al [7] treated the urea conversion problem as a Gibbsian one and obtained a regression expression for the urea conversion with three variables, namely θ, L and W of the liquid phase (see eq. 6.10). Their expression was claimed to fit their data well. They also made a passing remark that the Gorlovski's expression predicted less conversions in comparison with their data and that the inclusion of *p* as a variable is unnecessary. This apparent confusion of comparing the data with different bases (i.e., the one based on (θ, L, W) and the other based on (θ, L_o, W_o, p)) was quite unfortunate.

$$x = (0.2616*L - 0.01945*L^2 + 0.0382*L*W - 0.116*W - 0.02732*L*(\theta/100) - 0.103*W*(\theta/100) + 1.64*(\theta/100) - 0.1394(\theta/100)^3 - 1.869)*100\ \% \quad \text{(eq. 6.10)}$$

In a further article [11b], not clarifying the confusion made earlier by Inoue et al, Gorlovski et al apparently combined their data with those of Inoue et al [7] and also those of Kawasumi [13] and presented a new expression (eq. 6.11) claiming to better the earlier two expressions. In the new expression there was no term involving pressure. Does this treatment mean that their raw data have been recalculated and brought to the same basis as those of the Japanese data ? It is not at all clear from their article as to whether the confusion has been eliminated or compounded.

$$x = 94.31*L - 139.9*L^{0.5} - 4.284*L^2 - 26.09*W + 2.664*L*W + 1.54*\theta - 0.09346*\theta*L - 1.059*10^{-5}*\theta^3 - 97.82 \text{ in } \% \quad \text{(eq. 6.11)}$$

Given these circumstances and unless clarified by the authors, the data and the regression expressions due to Gorlovski et al have to be separated from the other investigations. This leaves the Inoue expression which does not cover the low L values. Also a fresh regression of the Inoue data together with those of Kawasumi, by considering only those terms suggested by Inoue et al, brought out the statistical insignificance of two coefficients in the Inoue et al expression, namely the W and $L\theta$ terms. On the contrary, the inclusion of these two terms appears essential to meet the experimental trend. The correlation coefficient of the reworked Inoue expression is 0.9765 with a standard error of 1.7436 and a Fisher's variance ratio of 99.92.

In addition to their regression expression, Inoue et al presented six major trends of urea conversion behaviour which have also been corraborated by Kucheryavyi et al. Any regression expression or a model which is developed to describe the urea conversion data has to meet the following observed trends.

1. $\partial x/\partial\theta$ at constant L and W is zero at one temperature.
2. θ_{max} decreases with increase in L at constant W.
3. θ_{max} decreases with increase in W at constant L.
4. $\partial^2 x/\partial L^2$ is negative in the range considered.
5. $\partial^2 x/\partial W^2$ is positive in the range considered.
6. $\partial^2 x/\partial W \partial\theta$ is negative in the range considered.

Satisfying these trends, the following regression expression (eq. 6.12) was developed by the present author to fit the data due to Inoue et al and the data due to Kawasumi. The correlation coefficient is 0.9938 and the standard error of the estimate is 1.628%. The Fisher's variance ratio is 460.48. Except for the W^2 and $L*\theta$

terms, the coefficients are more than 99.5% significant. The W^2 term is significant up to 95% and the $L*\theta$ term is significant up to 85%.

$$
\begin{aligned}
x = {} & 332.597855 - (613.260744 + 1.56785865\ L + 9.08425388\ W)*(\theta/100) \\
& + 395.261578\ (\theta/100)^2 - 81.0783052\ (\theta/100)^3 + (27.9503989 + 140.179398W)*L \\
& - (163.692296\ W + 29.8978319\ L - 4.48784208\ W)*W
\end{aligned}
\qquad \text{(eq. 6.12)}
$$

Now the maximum conversion temperature is obtained from the following equation:

$$\theta^2_{max} - 3.2500398*\theta_{max} + 2.5212693 + 6.44586*10^{-3}*L + 0.0373476*W = 0 \qquad \text{(eq. 6.13)}$$

The calculated θ_{max} for various L and W are presented in Table 6.1 and also marked in Fig. 6.3.

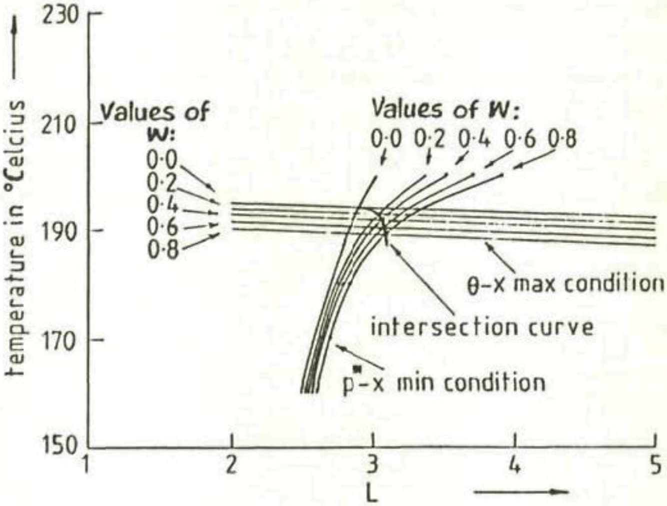

Fig. 6.3. *The θ-L optima obtained from (θ-x) max and (p^*-L) min conditions.*

Table 6.1. *The calculated maximum conversion temperatures in ° C for various L and W.*

W L	0.0	0.2	0.4	0.6	0.8	1.0
2	195.1	194.0	192.8	191.5	190.2	188.8
3	194.1	192.9	191.7	190.4	189.0	187.6
4	193.1	191.9	190.6	189.2	187.8	186.2
5	192.0	190.7	189.4	188.0	186.4	184.8
6	190.9	189.6	188.2	186.7	185.1	183.3
7	189.8	188.4	186.9	185.3	183.6	181.7

6.5.3. *The (p^*-L) min condition*:

The bubble-point pressure of the NH_3-CO_2-H_2O system at chemical equilibrium has been studied by Kawasumi [13], Lemkowitz [7] and Gorlovskii [11]. The minimum found in the bubble-point pressure with respect to L both in the physical and the chemical equilibria is attributed by these authors to the formation of the compounds like the ammonium carbamate, ammonium bicarbonate and ammonium carbonate, which are relatively non-volatile compared to NH_3 and CO_2. For our purpose, the p^*-L data given by Lemkowitz are interpolated at various W-values and are presented in Figures 6.4 to 6.7. For comparison, the bubble-point curve at 180° C calculated with the aid of the Durisch model [12] is also represented in the figure for W=0.2. Further in the figures 6.4 to 6.7, the minimal bubble-points at various temperatures but at a single W are connected by dotted curves. It should be mentioned that the x - co-ordinate of the figures 6.4 to 6.7 is in terms of the mole fraction of $2NH_3$. Lemkowitz accounted the ammonia moles in terms of $2NH_3$ for symmetry reasons in his model. However, such $2NH_3$ mole fractions can be refered back to the L values mentioned in this chapter.

Now if the θ-L optima obtained from the (θ-x) max condition and from the (p^*-L) min condition are plotted together (See Fig. 6.3), the intersection points meeting both the conditions can be obtained. Such intersection points given in Table 6.2 are the ones suitable for choosing the reactor conditions.

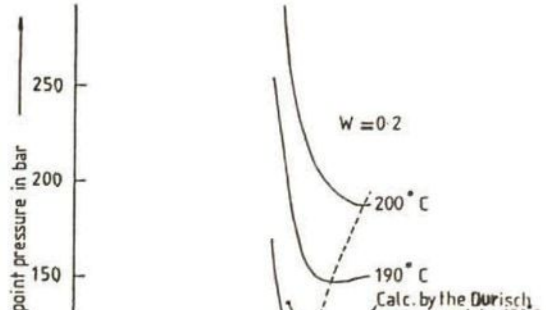

Fig. 6.4. p^* *vs. L for various temperatures at W = 0.2.*

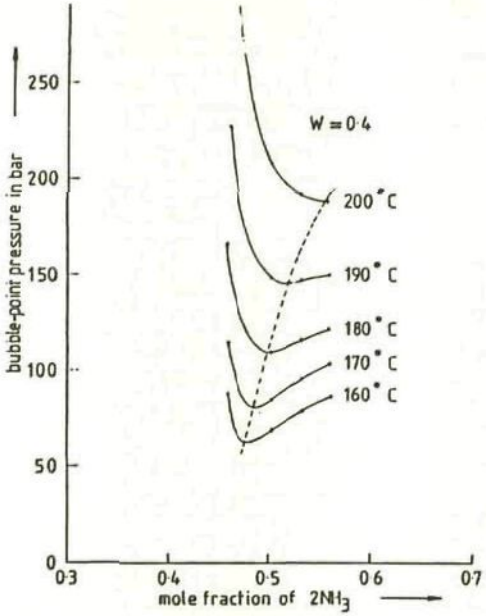

Fig. 6.5. p^* *vs. L for various temperatures at W = 0.4.*

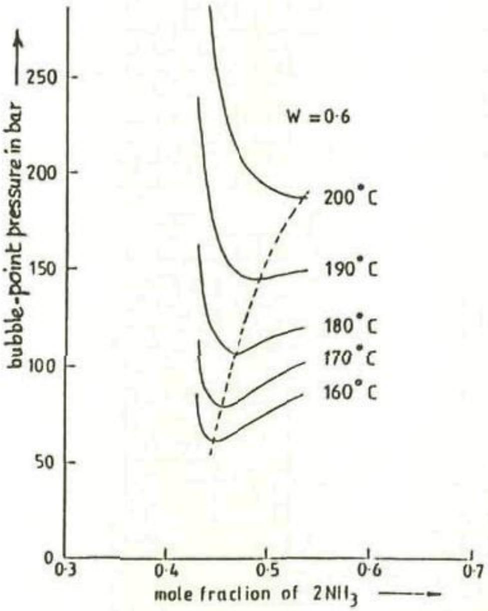

Fig. 6.6. p^* *vs. L for various temperatures at W = 0.6.*

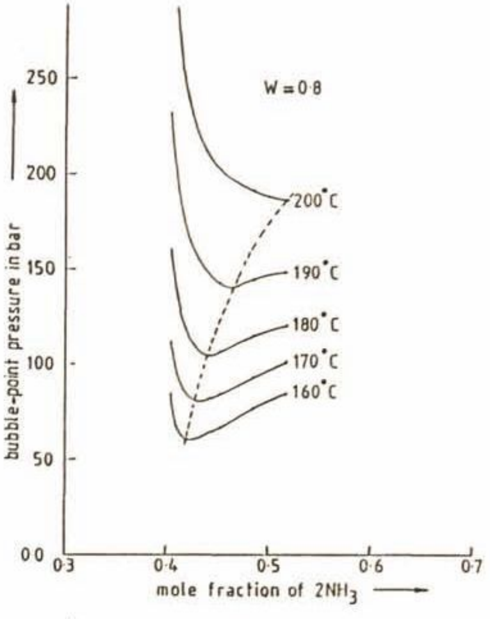

Fig. 6.7. *p^* vs. L for various temperatures at W = 0.8.*

The optimal L and θ_{opt} for each W are also plotted in Fig. 6.8. and the conversions x and the bubble-point pressures p^* are plotted against the optimal values of θ_{opt} in Fig. 6.9 and Fig. 6.10.

Table 6.2.*Optimal reactor conditions for each W*

W	L_{opt}	θ_{opt} in °C	p^*_{opt} in bar	x_{equil}
0.0	2.91	194.2	160.0	77.32
0.2	3.04	192.9	154.5	72.61
0.4	3.06	191.6	148.2	67.80
0.6	3.08	190.5	142.8	63.46
0.8	3.10	188.9	135.9	59.58

For a W of 0.4, which is normally prevailing in the stripping processes, the optimal L and θ works out to be 3.06 and 191.8° C. In comparison with these values, three stripping processes have their reactor conditions as follows:

	L_{opt}	θ_{opt} in °C	x_{equil}
Stamicarbon CO_2 stripping process [14]	2.95 to 3.1	183	66.54
Mitsui-Toatsu ACES process [15]	4.00	185	74.29
Technimont IDR process [16]	4.00	190	74.49

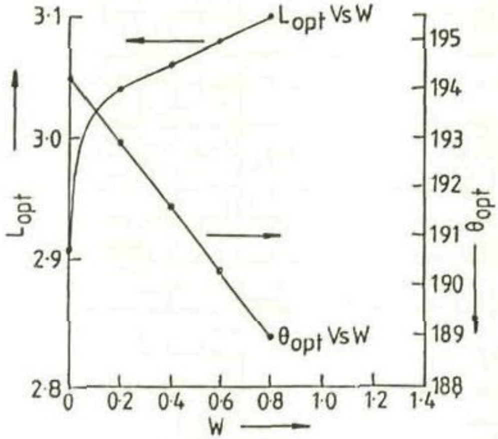

Fig. 6.8. *The* L_{opt} *and* $_{opt}$ *vs W.*

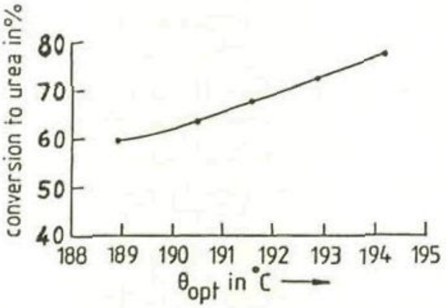

Fig. 6.9. *The conversion vs. the optimum temperatures.*

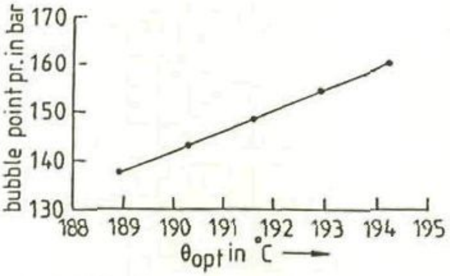

Fig. 6.10. *The bubble-point pressures vs the optimum temperatures.*

6.5.4. *Calculation of the reactor composition*:

The pressure determined by the above graphical procedure is only the bubble point pressure of the NH_3-CO_2-H_2O system with the equilibrium concentration of urea. However, in actual practice, there are inerts like nitrogen and methane, and also hydrogen coming along with the raw materials ammonia and carbon dioxide. Further it is usual to introduce air in small ammounts to the stripper, (which will further serve in the condenser and reactor) as a corrosion protection measure. Consequently, the partial pressure of the inerts in the reactor can be substantial. Also the complete thermodynamic equilibrium may not be reached inside the reactor in actual practice. Hence there will be a vapour-liquid separation inside the reactor. In order to estimate the actual vapour-liquid composition prevailing in the presence of inerts, the model due Lemkowitz [7] is employed here with suitable modifications.

The modified model can be described by the following definitions/equations.

moles of urea in the liquid = x
moles of H_2O in the liquid = $x + W$
moles of free CO_2 in the liquid = c
moles of free NH_3 in the liquid = $L - 2 + 2c$
moles of carbamate in the liquid = $1 - x - c$
total liquid moles = $L + x + W + 2c - 1$
mole fraction of CO_2 in the liquid = $x_1 = c / (L + x + W + 2c - 1)$
mole fraction of NH_3 in the liquid = $x_2 = (L - 2 + 2c) / (L + x + W + 2c - 1)$
mole fraction of H_2O in the liquid = $x_3 = (x + W) / (L + x + W + 2c - 1)$
mole fraction of urea in the liquid = $x_4 = x / (L + x + W + 2c - 1)$
mole fraction of carb in the liquid = $x_5 = (1 - x - c) / (L + x + W + 2c - 1)$
Henry's constant for CO_2 = $H_c = (0.92/0.9869) * (60 * T - 23389)$ bar
Vapour pressure of NH_3 = $p_n = (1.0287/0.9869) * 10^\wedge(5.361 - 1345/T)$ bar
Vapour pressure of H_2O = $p_w = (1/0.9869) * 10^\wedge(6.075 - 2256/T)$ bar
Urea formation constant = $K_2 = 1.37 * 10^\wedge(2367/T - 3.392)$

Phase equilibria:

mole fraction of CO_2 in the vapour = $y_1 = (H_c/P) * x_1$ (eq. 6.14)
mole fraction of NH_3 in the vapour = $y_2 = (p_n^*/P) * x_2$ (eq. 6.15)
mole fraction of H_2O in the vapour = $y_3 = (p_w^*/P) * x_3$ (eq. 6.16)

Vapour phase normalization conditions:

mole fraction of inerts in the vapour = $y_6 = 1 - (y_1 + y_2 + y_3)$ (eq. 6.17)

Reaction equilibria:

$x * (x + W) * (L + x + W + 2c - 1) = K_2 * (L - 2 + 2c)^2 * c$ (eq. 6.18)

$$\begin{aligned} x = {} & 332.597855 - (613.260744 + 1.56785865\ L + 9.08425388\ W)*(\theta/100) \\ & + 395.261578\ (\theta/100)^2 - 81.0783052\ (\theta/100)^3 + (27.9503989 + 140.179398W)*L \\ & - (163.692296\ W + 29.8978319\ L - 4.48784208\ W)*W \end{aligned} \qquad \text{(eq. 6.12)}$$

Solving the above set of equations along with the mass balances would yield the vapour-liquid composition for a given feed composition at a set pressure and temperature. (The software used for this purpose is given in Appendix B.)

Initially to tune the model, two parameters, K_2 and p_n^*, were adjusted so that the predicted bubble-points (with no inerts being present) closely matched the graphically read data due to Lemkowitz. Once the tuning was achieved, the inerts content in the feed and the reactor pressure were varied until the liquid to molar component feed ratio was 0.9 and the mole fraction of the inerts in the vapour phase 0.1. Also the approach to equilibrium was considered to be 0.96. These three values (mentioned earlier in section 6.4 as assumed) appear to be reasonable in view of the similar reactor conditions prevailing in stripping processes. The calculated optimal reactor conditions are as follows:

Reactor pressure = 169.3 bar
Reactor temperature = 192.9°C
NH_3/CO_2 ratio in the reactor feed = 3.04
H_2O/CO_2 ratio in the reactor feed = 0.2
Inerts/CO_2 ratio in the reactor feed = 0.042
Approach to equilibrium = 0.96
Equilibrium conversion in the liquid phase = 0.7237
Liquid to feed ratio in terms of components = 0.9009
Liquid component composition:
  $X_{\text{carbon dioxide}}$ = 0.2366
  X_{ammonia} = 0.7150
  X_{water} = 0.0484
Liquid species composition:
  $x_{\text{carbon dioxide}}$ = 0.0082
  x_{ammonia} = 0.3606
  x_{water} = 0.3028
  x_{urea} = 0.2339
  $x_{\text{carbamate}}$ = 0.1028
Vapour composition:
  $y_{\text{carbon dioxide}}$ = 0.2059
  y_{ammonia} = 0.6630
  y_{water} = 0.0311
  y_{inerts} = 0.1000

One other parameter to be fixed is the split of fresh ammonia to be fed to the reactor and to the condenser. Choosing the fresh ammonia split is related to the autothermic operation of the reactor. In other words, a minimal fraction of feed ammonia has to be sent to the reactor in such a way that the heat released by carbamate formation approximately matches the heat required for urea formation inside the reactor. (Here the heat of solution of ammonia is neglected due to the lack of precise enthalpy models). Autothermic operation also means that a certain amount of CO_2 fed through the recycle stream from the condenser has to be in the free form. This requirement further implies that the liquid to feed ratio of the condenser largely detemines the design fresh ammonia split.

6.6. *Fixing the condenser conditions*:

Having fixed the reactor conditions except the fresh ammonia split, one may move to the condenser operating at a pressure slightly higher than that of the reactor. This increase in operating pressure is mainly to take care of the pressure drop due to flow. In the present analysis, for all cases considered, the pressure drop between the condenser and the reactor is taken to be 0.5 bar. Further denoting the condenser pressure as p_C and considering the condenser to have attained a fast equilibrium (i.e. only carbamate formation with no urea formation), one may proceed with a distribution problem relevant to the high pressure condenser. The model employed here was developed by Durisch [12].

Taking a reference pressure of 100 bar and 170°C, Durisch considered the change in the liquid non-idealities around the vicinity of the reference point to be minimal, leading to the neglect of activity coefficients. The models similar to that of Durisch have been recently termed as local models and are very much preferred in flowsheeting programs in view of the repeated need for iteration calculations [23]. Durisch expressed the reactive VLE through equilibrium constants based solely on pressure and temperature. Also he approximated the gas phase behaviour through a truncated virial coefficient equation. The model as applied to the present case will be as follows:(See also Appendix B.)

$$y_1 = Q_1 * x_1 \qquad \text{(eq. 6.19)}$$

$$y_2 = Q_2 * x_2 \qquad \text{(eq. 6.20)}$$

$$y_3 = Q_3 * x_3 \qquad \text{(eq. 6.21)}$$

$$x_5 = K_1 * x_1 * x_2^2 \qquad \text{(eq. 6.22)}$$

$$x_1 + x_2 + x_3 + x_5 = 1 \qquad \text{(eq. 6.23)}$$

$$y_1 + y_2 + y_3 = 1 \qquad \text{(eq. 6.24)}$$

Also there are mass balances in terms of the component mole fractions:

$$N_L * (X_1 - Y_1) = N_F * (Z_1 - Y_1) \qquad \text{(eq. 6.25)}$$

$$N_L * (X_2 - Y_2) = N_F * (Z_2 - Y_2) \qquad \text{(eq. 6.26)}$$

Now in the simplified flowsheet shown in Fig. 6.2, both the liquid and gas streams of the condenser are sent to the reactor instead of just a liquid stream. Hence the ratio W has to be the same as the ratio Z_3/Z_1, where Z_3 and Z_1 are the CO_2 and H_2O feed compositions to the condenser. Accordingly with p_c set as above and for a given W, the above set of equations can be solved for various L_c (i.e the ratio existing at the condenser feed) at temperatures between the bubble- and dew-points, and in each case the component mole ratio of N_I/N_F can be calculated. The results thus obtained for $W = 0.2$ are plotted in Fig. 6.11.

It can be observed from the figure that there is a specific L_C against which one can get a maximum N_I/N_F value at each temperature. If such maximum N_I/N_F points are connected, then one gets the maximum N_I/N_F curve shown in Fig. 6.11. Such maximum N_I/N_F imply the greatest amount of heat one can obtain due to condensation at a particular temperature and still end up with a vapour-liquid mixture (which can be sent to the reactor to enable autothermic operation). There is a further interpretation of the so-called maximum N_I/N_F curve. As seen from the figure, the maximum L_C one can ever have in the condenser feed and still hope to get the maximum heat transfer is 3.21 and the corresponding temperature is 177°C. Now what does this assertion imply ? Supposing one chooses any temperature other than 177°C, then the

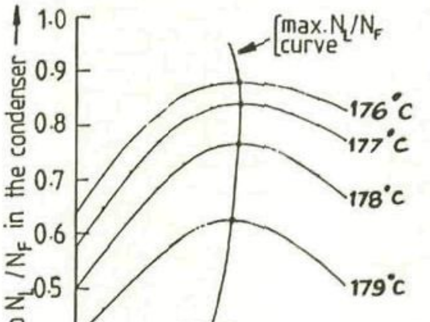

Fig. 6.11. *Molar ratio N_I/N_F vs L_C at $W = 0.2$ and at various temperatures.*

maximum possible L_C values and maximum N_L/N_F values are limited. Hence the best choice for the condenser temperature has to be 177°C. (One can compare this choice against the binary azeotropic temperature 168° C at the equilibrium pressure of 155 bar. In the earlier TUD HGRP, the condenser temperature was chosen to be 167° C.)

Now coming to the choice of L_C, a value of 3.21 can never be chosen in the present design since the reactor feed has an L value of only 3.04. Even a value of 3.04 cannot be fixed, since it would otherwise mean that fresh ammonia is not added to the reactor - a situation not so desirable for operability and control reasons. Hence further low L_C values are to be tried and in each case both the the condenser and reactor models are to be solved simultaneously until one achieves an autothermic operation of the reactor. In the present case, a value of 2.76 for L_C appears adequate. (Compare this value against the binary azeotropic L_C of 2.45 at an equilibrium pressure of 155 bar.) The value of 2.76 also means that 0.22 of the fresh ammonia (i.e. 552.95 kmoles/hr at 99.87% purity) is to be sent to the reactor and the rest (i.e. 1960.45 kmoles/hr at 99.87% purity) to the condenser. Since this calculation has neglected the heat of solution of ammonia, the final result has to be considered only as approximate. A rigorous calculation of the enthalpy balance can be carried out to determine the precise value of the ammonia split, if and when enthalpy models are available.

Proceeding with the above calculation, the total flow rate of the recycle stream (comprising both liquid and gas) is estimated to be 7882.03 kmoles/hr.

The calculated condenser inlet component compositions are:

CO_2 concentration in the condenser feed = 0.2500
NH_3/CO_2 ratio (L_c) in the condenser feed = 2.76
H_2O/CO_2 ratio (W) in the condenser feed = 0.2
Inerts/CO_2 ratio in the condenser feed = 0.0421
Liquid phase component composition: CO_2 = 0.2376
NH_3 = 0.7035
H_2O = 0.0589
Liquid phase species composition: Free CO_2 = 0.0157
Free NH_3 = 0.4529
H_2O = 0.1089
Carbamate = 0.4228
Vapour phase composition: CO_2 = 0.2999
NH_3 = 0.6331
H_2O = 0.0138
Inerts = 0.0532
Liquid to feed ratio in terms of component moles = 0.8022

As a result, the vapour feed rate from the compressor is calculated to be 5921.58 Kmoles/hr. If the inerts component flowing (at a rate of 80.32 kmoles/hr) along with the vapour is subtracted from the compressor feed rate, the inert-free-gas flow rate is 5841.26 Kmoles/hr (i.e. 1.6226 kmoles/sec).

Similarly, after subtracting the amount of fresh ammonia added to the condenser feed, one can calculate the molar composition of the inert-free gas flowing through the compressor as: CO -- 0.3372, NH_3 -- 0.5954, H_2O -- 0.0674. Now if the compressor feed gas is not to condense anywhere inside the compressor and the transfer pipe lines, its temperature should always be above the dew-point of the gas mixture at any point inside the compressor. In Fig.6.12, the dew-point curves of the compressor feed gas with inerts or without inerts (which are calculated through the earlier condenser model) are plotted. Repeating the argument just given, the gas flowing through the compressor (including at its inlet) should have pressure and temperature values above these curves (i.e in the non-condensing region marked in the figure).

6.7. *Fixing the recycle compressor conditions*:

With the allowable range of pressure and temperature at the compressor inlet fixed, one further moves to the compressor calculations. Here, in view of the tediousness of the calculations, only the power consumed for compressing the inert-free gas is calculated. Assuming Dalton's law of partial pressure to be valid for the inerts, the discharge pressure corresponding to the inerts free CO_2-NH_3-H_2O gas mixture is calculated to be 167.5 bar (i.e. with a total pressure of 169.8 bar).

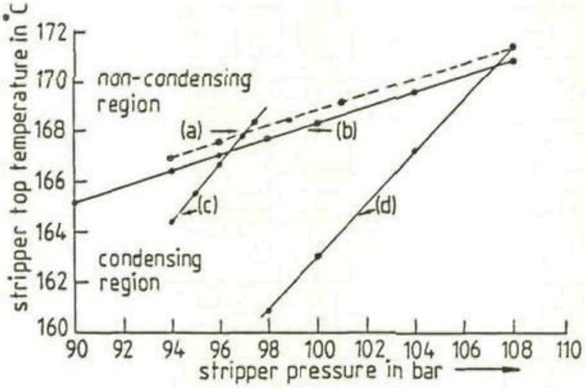

Fig. 6.12. *Fixing the suction condition of the hot gas compressor.*

a. The dew point curve of the compressor feed gas with inerts.

b. The dew point curve of the compressor feed gas without inerts.

c. Calculated suction curve for a discharge of 167.5 bar, 230°C.

d. Calculated suction curve for a discharge of 167.5 bar, 220°C.

The first aspect one has to look into, concerning the process design of a centrifugal compressor, is that relating to the limits posed on the discharge temperatures. It is reported as a design guideline [17] that the discharge temperature of centrifugal compressors is normally set to 190° C unless the process conditions demand lower discharge temperatures. Also the maximum possible discharge temperature is reported to be 230° C. If high discharge temperatures are desired, then additional care has to be taken in the mechanical design of the compressor. In the following, we consider just two different discharge temperatures, namely 230 and 220° C.

Firstly, one needs to fix at least three variables in addition to composition for a complete specification of a compressor. In the present case, the discharge pressure is set by the condenser operating condition. The discharge temperature is set by the compressor design guidelines. Hence the remaining variables to be set are only the suction pressure and the temperature. As a first case, the discharge temperature is assumed to be 230° C. Further the polytropic efficiency of the centrifugal compressor (which normally depends on the nominal inlet volume flow of the compressor and the nominal polytropic head and which usually differs from one compressor manufacturer to other) is tentatively assumed to be 0.77.

Now assuming trial values of inlet pressure and temperature, the inlet and outlet compressiblities and enthalpies of the process gas are calculated. From these values, the polytropic index is defined by the following expression [17].

$$n/(n-1) = \eta * (H_2 - H_1) / R / (Z_2 * T_2 - Z_1 * T_1) \qquad \text{(eq. 6.27)}$$

where n is the polytropic index, η is the polytropic efficiency, H is the enthalpy, Z the compressibility and T the temperature in Kelvin. The suffix "1" denotes the suction conditions and "2" denotes the discharge conditions. With this value of n, the discharge pressure is calculated by the following equation:

$$P_2 = P_1 * ((Z_2 * T_2) / (Z_1 * T_1))^{n/(n-1)} \qquad \text{(eq. 6.28)}$$

For each suction pressure and temperature assumed, the discharge pressure calculated by the above equation has to match the earlier assumed value (namely, 167.5 bar for the inert-free gas). Otherwise, a new set of suction pressure and temperature is assumed. By such trial and error calculations, a curve relating the suction pressures and temperatures for a given discharge conditions (167.5 bar and 230° C) is calculated and plotted in Fig. 6.12. Similarly another curve corresponding to the discharge conditions of 167.5 bar and 220° C is calculated and plotted in the same figure. One can now observe that any point chosen on these suction curves but within the permissible non-condensing region is an acceptable suction point. One possible suction point chosen with a minimum safety margin is the one having co-ordinates of 97.5 bar and 168.3° C, corresponding to a discharge condition of 167.5 bar and 230°C.

Similarly, for the discharge condition of 167.5 bar and 220° C, the minimum safe suction condition works out to be 108.5 bar 171.5° C. (See Fig. 6.12.)

Since the compressor suction pressure is essentially the stripper pressure, one can connect a series of such minimum safe suction points in order to constitute a curve defining feasible stripper top condition. In other words, one can use this feasibility curve to establish the stripper top temperature, once the stripper pressure is chosen. It is to be emphasized that this feasibility curve is defined for the present case only from 97.5 bar (the lowest suction pressure with a single stage hot gas compression) to 167.5 bar. The second extreme corresponds to the isobaric stripping case, as practiced in the stripping processes. Now to fix the optimal stripper pressure, one has to consider the design of stripper with the objective of minimising the energy consumed.

In the design of stripper, one has to first limit the stripper bottom temperature to avoid urea hydrolysis and biuret formation. Lacking enthalpy values/models to do a detailed enthalpy balance, the only natural course is to limit the bottom temperature to a reasonable value between 180 to 185° C (i.e. similar to the ones existing in the stripping processes). Here a value of 182.5° C is chosen.

Now the calculational procedure is simple. For each stripper pressure in the range of 97.5 to 167.5 bar, the power consumed in compressing the hot gas and the fresh CO_2 and the energy consumed in the stripper heater are calculated. The pressure which gives the lowest total energy cost (i.e. for compression and heating put together) is the optimal choice for the stripper pressure.

However the implementation of the above procedure is hampered by the lack of enthalpy values to complete the heat balance calculation across the stripper. Hence, one has to be satisfied for the present with only the calculation of power required for compressing the inerts-free hot gas and inerts-free wet CO_2. (See Appendix B for the software.) The following results are valid for the case of stripper pressure (i.e. the compressor suction pressure) at 97.5 bar.

The hot gas compressor :

Assumptions / Input variables:

The gas handled: inerts-free hot recycle gas
The polytropic efficiency : 0.77
The no. of stages: 1
The composition of the gas (in mole fraction):

CO_2 - 0.3372
NH_3 - 0.5954
H_2O - 0.0764

Suction condition: 97.50 bar and 168.3° C

Discharge condition: 167.5 bar and 230.0° C

Flow rate through the compressor: 1.6226 kmoles/sec

The results:

The calculated power: 3618.0 kw.

The CO_2 compressor:

Assumptions / Input variables:

The gas handled: inerts-free wet CO_2:

The polytropic efficiency: 0.77

The no. of stages: 4

The results:

	stage I	stage II	stage III	stage IV
CO_2 mole frac.	0.9277	0.9744	0.9911	0.9972
Suction temp. in ° C	40.0	40.0	40.0	40.0
Suction pr. in bar	1.02	2.8	8.3	26.0
Discharge temp. in ° C	178.0	178.0	178.0	182.50
Discharge pr. in bar	2.9	8.4	26.1	97.7
Flow rate in kmoles/sec	0.3827	0.3645	0.3582	0.3560
Power consumed in kw	1639.08	1600.49	1619.79	1710.33

How then does one assess the economic viability of the HGRP vis-a-vis the amply proven STRP ? The answer largely hinges on the energy spent on the stripper heater. Ultimately, it was towards providing this answer that the entire program on urea research was directed at the Technological University of Delft. In the continuing series of reaearch work [3,18], what was accomplished in the present work is only one part, namely phase equilibria studies up to 30 bar and 130° C. Only when the work is continued up to about 100 bar and 180° C and also only when new studies are initiated to estimate enthalpies, can the question of the economic viability of the improved TUD HGR process be answered in an unambiguous manner. Until then, one can only speculate on the relative merits of the HGR process over the stripping processes.

In the meantime, the present author wishes to emphasize that all this knowledge of and insight into urea technology in general and the HGRP in particular would not have been reached but for the consistent application of phase theory and phase equilibria measurements together with an inevitable mix of adequate empiricism.

Reference:

1. These values were derived from the equations (5.81 and 5.86) given in chapter 5.

2. Dewling, W.L.E and S.Robell, "Urea manufacture at the I.G. Farben-Industrie plant at Oppau", FIAT final report 889, 3 Sept 1946, 29 pages.

3. Lemkowitz, S.M, "Phase and Corrosion studies of the ammonia-carbon dioxide-water system at the conditions of the hot gas recirculation process for the synthesis of urea", PhD thesis, Delft University of Technology, The Netherlands, 1975, 191 pages.

4. Kaasenbrood, P.J.C and H.A.G. Chermin, "The urea stripping process - stripping technology, phase equilibria and thermodynamics", The Fertilizer Society Proceedings no. 167, 1977, 1 Dec., 48 pages.

5. Jojima, T., "Recent technological developments in urea production",-paper presented at the FAI-IFDC fertilizer seminar 1977, New Delhi, India, Dec. 1-3, 1977.

6. Yahya, N, "The economic evaluation of the DSM - CO_2 strip process and the TH-Delft hot gas recycle process for the production of urea - part 1", Internal report, 1976, 94 pages.

7a. Inoue, S., K.Kanai, and E.Otsuka, "Equilibrium of urea synthesis I", Bull.chem.soc.Japan, 1972, vol.45, pp 1339-1345.

7b. Inoue, S., K.Kanai, and E.Otsuka, "Equilibrium of urea synthesis II", Bull.chem.soc.Japan, 1972, vol.45, pp 1616-1619.

8. Frejacques, M., "Les bases theoriques de la synthese industrielle de l'uree", Chimie et Industrie, 1948, vol. 60, no. 1, p 22.

9. Baranski. A and A. Fulinski, " Consideration sur la description thermodynamique de la synthese de l'uree a partir de l'ammoniac et de l'anhydride carbonique", Chemie et Industrie, 1968, vol. 99, p 1605.

10. Effremova, G.D and G.G.Leontieva, "The compressibility of mixtures of ammonia and carbon dioxide and the equilibrium of urea synthesis reaction", (in Russian), Khim. Prom., 1962, vol. 10, 742

11a. Kucheryavyi, V.I, Khim.Prom. 1969, vol.3, p 200

11b. Gorlovskii, D.M. and V.I.Kucheryavyi, "Equation for the determination of the equilibrium degree of conversion of carbon dioxide in urea synthesis", Zh.Prikl.Khim., 1980, vol.53, no.11, pp 2548-2551.

12. Durisch, W., "Experimentelle und thermodynamische untersuchung der seidegleichgewichte des systems $CO_2/NH_3/H_2$ unter Harnstoffsynthese-bedingungen", PhD thesis, Eidgenossischen Technischen Hochschule, Zurich, Switzerland, 1978.

13. Kawasumi, S. "Equilibrium of the CO_2-NH_3-Urea-H_2O system under high temperature and pressure", Bul.Chem.Soc.Japan, 1951, vol.24, no.3, pp148-151;1952, vol.25, no.4, pp227-238; 1953, vol.26, no.5, pp218-227; 1954, vol.27, no.5, pp254-259.

14. Dooyeweerd, E. and J.Meessen, "Comparisons of the energy consumptions of low energy urea technologies", Nitrogen, 1983, May-June, No.143, pp 32-38.
15. Jojima, T. et al, "Commercially proven new urea technologies", CEP, April, 1984 pp 31-35.
16. Zardi, U., "Urea plants for tomorrow's world", Nitrogen, 1982, No.135, pp26-37.
17. Lapina, R.P., "Estimating centrifugal compressor performance - process compressor technology - vol I, chapter 5", Gulf Publishing Company, Houston, 1982.
18. Verbrugge, P.,"Vapour-liquid equilibria of the ammonia-carbon dioxide-water system", PhD thesis, Delft University of Technology, The Netherlands, 1979, 133 pages.
19. Kirkland, R.W.,"Energy-efficient route to granular urea", CEP, 1984, April,pp49-53.
20. Guadalupi, M. and Zardi, U.,"Here's SNAM's new urea process", Hydrocarbon Processing, 1965, Vol.44, No.7, pp 131-133.
21. Pagani, G., "IDR technology cuts to a minimum the energy consumption in urea plants", Nitrogen, 1983, sept-oct, No.145, pp 35-37.
22. Zardi, U., "Revamping Urea plants economically", CEP, 1984, April, pp 36-39
23. Macchietto, S. et al, "Simple models for non-ideal vapour-liquid equilibrium calculations", AIChEJ, 1984, Vol.30, No.4, pp 669-672.

APPENDIX A

THE SOLID-GAS EQUILIBRIA OF THE NH_3-CO_2 SYSTEM

The solid-gas equilibria of a binary system with a dissociating compound exhibit unusual features, like the occurrence of two gas compositions in equilibrium with the solid at constant p and T and the occurrence of an extremum sublimation pressure (or temperature) with respect to composition at a given temperature (or pressure). The p-T diagram of the dissociating compound also exhibits a continuous three phase region leading to the occurrence of a maximum sublimation point and a minimum melting point instead of a triple point [1].

The solid-gas equilibria of the system NH_3-CO_2 also belongs to this class of behaviour due to the formation of NH_4COONH_2, the qualitative aspects of which were dealt with earlier in Chapters 2 and 3. In this appendix, attention is restricted to the quantitative determination of the isothermal p-x curves.

In the literature, the decomposition pressure has been studied by a number of authors [2,3,4,5,6]. Also the S-G equilibria have been studied by Briggs and Migridichian [5] at low pressures and temperatures with excess NH_3 and CO_2. Thermodynamically the solid-gas equilibria can be described as follows [7]:

$$(Y_n{}^2*y_c)*(\phi_n{}^2*\phi_c)*p^3 = K_p * \exp((v_s/(R*T))*(p-p_{sat})) \qquad \text{(eq. A.1)}$$

where y_n and y_c are the mole fractions of NH_3 and CO_2, ϕ_n and ϕ_c are the fugacity coefficients of NH_3 and CO_2, p is the total pressure, T is the temperature, K_p is the equilibrium constant, V_s is the molar volume of the solid ammonium carbamate, R is the gas constant and p_{sat} is the saturation (i.e. decomposition) pressure at T.

There are two novel aspects which distinguish the present study from the previous ones [5,6,9]. The first is the inclusion of the poynting correction in the right side of the (eq. A.1) with the molar volume of the solid NH_4COONH_2 (56.57 ml/mol) given by Adams [8]. The second is the inclusion of fugacity coefficients calculated by the Nakamura equation of state [10]. The temperature variations of the solid molar volume was neglected in this study. As for the Nakamura equation, initially it was found to predict the experimental molar volumes of the NH_3-CO_2-H_2O gas mixtures [11] well within 1-2 % at urea synthesis conditions and hence was adopted here to predict the fugacity coefficients.

Regarding the saturation pressure, the data due to Briggs and Migridichian [5], Egan et al [6] and a few others [3,4] were critically examined and utilized to yield the following relation with a multiple correlation coefficient of 0.9999, an estimated error of 0.0115 and a Fisher variance of 836833:

$$P_{sat} = \exp\ (\ -\ 2.30060464 + 3.148766 * \log T - 5303.19527\ /\ T\ ) \qquad \text{(eq. A.2)}$$

The heat of decomposition of NH_2COONH_4 can be derived from this expression almost up to the maximum sublimation point by the usual means.

As for K_p, its value at each T can be calculated through eq. A.1, with y_n value equalled to (2/3).

An interactive program to predict the gas phase NH_3 mole fractions for a given p and T was written for an APPLE II microcomputer. The flow diagram (Fig. A.2) and the program listing are given at the end of this appendix. The results of the calculation for the temperatures 88.7°C, 90.36°C, 103.36°C, 119.08°C and 128.83°C are given in Fig. A.1. The decomposition pressures for these temperatures are: 4.99 bar, 5.41 bar, 10 bar, 20 bar and 30 bar, respectively.

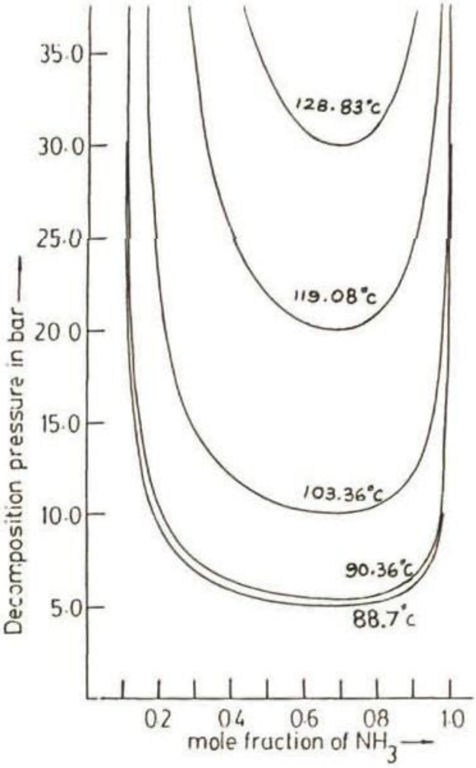

Fig. A.1. *The calculated S-G equilibria of the NH_3-CO_2 system.*

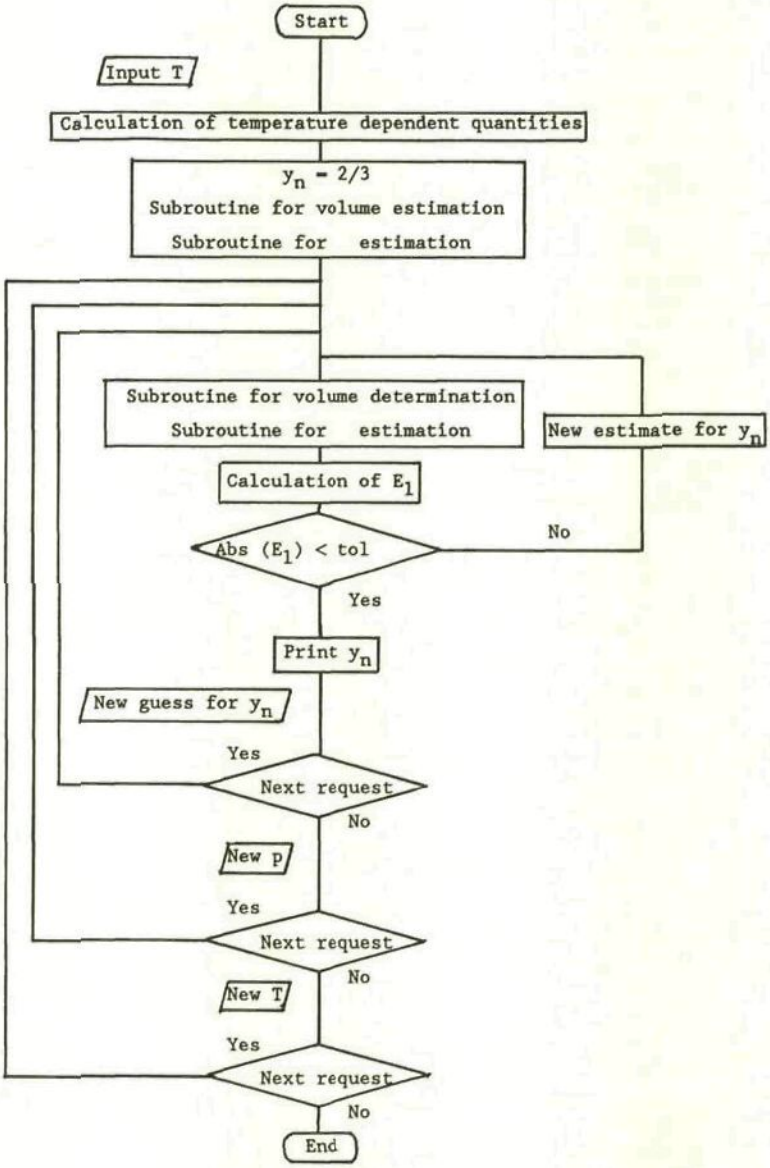

Fig. A.2. *The flow diagram of the calculation of the S-G equilibria of the NH_3-CO_2 system.*

The program listing:

```
100 Y$ = "Y"
110  PRINT "DO YOU WISH TO COMPUT
     E S - G EQUILIBRIUM OF THE N
     H3-CO2 SYSTEM?"
120  PRINT
130  INPUT "TYPE (Y/N) AND PRESS
     RETURN.  ";WISH$
140  IF WISH$ = Y$ GOTO 500
150  PRINT "VERY WELL. SEE YOU NE
     XT TIME."
160  END
500  PRINT
510  INPUT "TEMPERATURE IN KELVIN
     ?";T
515 KK = 3.1693 + (253.17 / T)
520 NN = 2.6435 + (561.63 / T)
530 KN = 3.1 + (133.235 / T)
540 BK = 10 ^ ( - 1.234 - 4.67E -
     05 * T)
550 BN = 10 ^ ( - 1.3884 - 1.47E -
     04 * T)
560 CK = 0.0
570 CN = 0.01
580 PS =  EXP ( - 2.30060464 + 3.
     148766 *  LOG (T) - 5303.195
     27 / T)
585 PR = PS / 0.9869
590  PRINT
600  PRINT "PS=";PR;" BAR"
610 R = 0.08205
620 V = R * T / PS
630 YN = 2 / 3
635 P = PS
640  PRINT
650  PRINT "COMPUTING KP"
660  GOSUB 2000
670  PRINT
680  INPUT "PRESSURE IN BAR?";PB
690 P = 0.9869 * PB
695 V = R * T / P
700  PRINT
710  INPUT "YOUR GUESS FOR YN ?";
     YN
720  FOR J = 1 TO 30
730  GOSUB 2000
740 E1 = (YK * FCO2) * (YN * FUNH
     3) ^ 2 * P ^ 3 - KP *  EXP (
     56.573913 * (PS - P) / (1000
      * R) / T)
750 YN = 0.99999 * YN
760  GOSUB 2000
770 EX = (YK * FCO2) * (YN * FUNH
     3) ^ 2 * P ^ 3 - KP *  EXP (
     56.573913 * (PS - P) / (1000
      * R) / T)
780 DER = (E1 - EX) / (0.00001 *
     YN)
790 YN = YN - EX / DER
800  IF  ABS (E1) < 1.0E - 04 GOTO
     1000
810  NEXT J
820  REM  NO CONVERGENCE
830  PRINT
840  PRINT "NO SOLUTION FOR YN AF
     TER 30 ITERATIONS"
850  END
1000  PRINT
1010  PRINT "YN=";YN
1050  PRINT
1060  INPUT "TRY FOR A NEW GUESS
     OF YN ?";WISH$
1070  IF WISH$ = Y$ THEN  GOTO 70
     0
1080  PRINT
1090  INPUT "TRY FOR A NEW P AT T
     HE SAME T ?";WISH$
1100  IF WISH$ = Y$ THEN  GOTO 67
     0
1110  PRINT
1120  INPUT "TRY FOR A NEW T ?";W
     ISH$
1130  IF WISH$ = Y$ THEN  GOTO 50
     0
1140  PRINT
1150  PRINT "SEE YOU NEXT TIME"
1160  END
1807  GOSUB 7000
1824  END
2000 YK = 1 - YN
2010 AK = KK * YK + KN * YN
2020 AN = KN * YK + NN * YN
2030 A = AK * YK + AN * YN
2040 B = BK * YK + BN * YN
2050 C = CK * YK + CN * YN
2060  GOSUB 4000
2070 XI = B / (4 * VN)
2080 Z = (P * VN) / (R * T)
2100 FCO2 = 0.0
2110 FUNH3 = 0.0
2120  IF YK <  > 0.0 THEN  GOSUB
     6000
2130  IF YN <  > 0.0 THEN  GOSUB
     6100
2300  IF YN = (2 / 3) THEN  GOSUB
     6200
2400  RETURN
4000  FOR I = 1 TO 30
4010 XI = B / (4 * V)
4020 F = (1 + XI + (XI ^ 2) - (XI
      ^ 3)) / ((1 - XI) ^ 3)
```

```
4030 DF = (2 * (XI ^ 2) + 2 * (XI
      ^ 3) - (XI ^ 4)) / ((1 - XI
     ) ^ 4)
4040 G = (R * T * F) - (A / (V +
     C)) - (P * V)
4050 DG =  - (8 * R * T * DF / B)
      + (A / ((V + C) ^ 2)) - P
4060 V = V - (G / DG)
4070  IF  ABS (G) < 1.0E ~ 06 GOTO
     4110
4080  NEXT I
4085  REM  NO CONVERGENCE
4090  PRINT
4095 PRINNT"NO SOLUTION FOR V AFT
     ER 30 ITERATIONS"
4100  END
4110 VN = V
4120  RETURN
5000 FGI = ((4 * XI - 2 * (XI ^ 2
     )) / (1 - XI) ^ 2) * (1 + (B
     I / B) / (1 - XI)) - ((XI ^
     2) / (1 - XI) ^ 2) + ((2 * A
     I - A(CI / C)) / (C * R * T)
     ) *  LOG (B / (B + 4 * XI *
     C)) - (A * CI / (C * R * T))
      * ((4 * XI) / (B + (4 * XI *
     C)))
5010 FI = ( EXP (FGI)) / Z
5020  RETURN
5500 FGI = ((4 * XI - 2 * (XI ^ 2
     )) / (1 - XI) ^ 2) * (1 + (B
     I / B) / (1 - XI)) - ((XI ^
     2) / (1 - XI) ^ 2) - (2 / (R
      * T)) * AI * (4 * XI / B)
5510 FI = ( EXP (FGI)) / Z
5520  RETURN
6000 AI = AK
6010 BI = BK
6020 CI = CK
6050  IF C <  > 0.0 THEN  GOSUB 5
     000
6055  IF C = 0.0 THEN  GOSUB 5500

6060 FCO2 = FI
6070  RETURN
6100 AI = AN
6110 BI = BN
6120 CI = CN
6150  GOSUB 5000
6160 FUNH3 = FI
6170  RETURN
6200 KP = (YK * FCO2) * (YN * FUN
     H3) ^ 2 * P ^ 3 *  EXP (VS *
     (PS - P) / (1000 * R) / T)
6210  PRINT
6220  PRINT "KP=";KP
6230  RETURN
```

References:

1. Zernike, J., "Chemical Phase Theory", Kluwer Publ. Co., Deventer, The Netherlands, 1955
2. Gmelins Handbuch der Anorganischen Chemie, "Ammonium", vol. 23, Verlag Chemie, Berlin, 1936, pp. 327-362.
3. Joncich, M.J., et al., J. Chem. Educ., 1967, vol. 38, no. 4, p. 598.
4. Bennet, R.N., et al, Trans. Far. Soc., 1953, vol. 49, p. 925
5. Briggs, T.R. and V. Migridichian, J. Phys. Chem., 1924, vol. 28, p. 1121.
6. Egan, E.P., J.E. Potts and C.D. Potts, I&EC, 1946, vol.38, no.4, p. 454.
7. Sandler,S.I., "Chemical and engineering thermodynamics", John Wiley & Sons, New York, 1977.
8. Adams, J.M. and R.W. Small, "The crystal structure of ammonium carbamate", Acta Cryst., 1973, B29, pp. 2317-2319.
9. Lemkowitz, S.M. "Phase and corrosion studies of the ammonia-carbon dioxide-water system at the conditions of the hot gas recirculation process for the synthesis of urea", PhD thesis, Delft University of Technology, The Netherlands, 1975, 191 pages.
10. Nakamura, R. et al, "Thermodynamic properties of gas mixtures containing common polar and nonpolar components", I&EC process des.dev., 1976, vol.15, no. 4, pp. 557-564.
11. Durisch, W. and P.J. van den Berg, "Die dichte gasformiger Kohlendioxid-ammoniak-wasser gemische unter harnstoff-synthese bedingungen", Chemia, 1979, vol. 33, no. 6, pp. 200-204.

APPENDIX B

THE PROGRAMMES USED IN THE PRE-DESIGN OF THE IMPROVED TUD HOT GAS RECYCLE PROCESS

B.1. *Introduction*:

As mentioned in chapter 6, the process design of the hot gas recycle loop involves seven major aspects. They are:

1. The optimal reactor conditions.
2. The optimal condenser conditions.
3. The hot gas recycle compressor.
4. The CO_2 compressor.
5. The scrubber conditions.
6. The stripper conditions.
7. The overall energy balance.

Of the above, only the first four could be accomplished in the present work. Regarding the remaining three, the design of the scrubber can be accomplished with the present knowledge, but it has to wait until the design of the stripper is complete. Moreover, the merit of using the scrubber bottom stream as a reflux to the stripper- rectifier is yet to be proved. Similarly, the necessity of transforming the stripper (a mere falling film heat exchanger type vessel) to a stripper-rectifier (i.e. with multistage contact devices for accelerating mass transport) is to established by trial calculation. All these aspects hinge on an adequate quantitative knowledge of the vapour-liquid equilibria of the system NH_3-CO_2-Urea-H_2O and of a liquid phase enthalpy model of the same system.

In the present appendix, the first programme is related to the determination of vapour-liquid separation in the reactor and condenser. This programme can easily handle the presence of inerts. Also the subprogramme meant for the condenser can be easily modified to find out the dew point of any given CO_2-NH_3-H_2O mixture. Similarly one can use it to find out the equilibrium ridge point of the ternary system (as was mentioned in chapter 3).

Further, the last programme included is an interactive one capable of calculating the discharge pressure and the power required for compressing the NH_3-CO_2-H_2O mixture. This programme utilizes the Nakamura equation of state to calculate the specific volume and the compressibilities. As for enthalpy values of pure NH_3, pure CO_2, pure H_2O, regression expressions were developed utilizing the values obtained in the literature.

B.2. *The programme incorporating the reactor and condenser models:*

```
]LIST

100  REM  REACTOR MODEL AS PER LE
     MKOWITZ.
110  REM  CONVERSION CALCULATED T
     HROUGH THE
120  REM  REGRESSION FORMULA
130  REM  DERIVED BY KRISH
140  DIM B(3,3)
150  DIM ZR(6),XR(6),YR(6)
160  DIM PR(6),ZC(6)
170  DIM QR(3),CR(3)
180  INPUT "TR ?";TR
190  INPUT "LR?";LR
200  INPUT "WR?";WR
210  INPUT "AR?";AR
220  INPUT "PR?";PR
230  INPUT "ER?";ER
240  INPUT "EN?";EN
250 ZR(1) = 1 / (1 + LR + WR + AR
     )
260 ZR(2) = LR * ZR(1)
270 ZR(3) = WR * ZR(1)
280 ZR(6) = AR * ZR(1)
290 T = TR + 273.15
300 K2 = 10 ^ (2367 / T - 3.392)
310 K2 = 1.37 * K2
320 PN = (10 ^ (5.361 - 1345 / T)
     ) / 0.9869
330 PN = 1.028732 * PN
340 HC = (60 * T - 23389) / 0.986
     9
350 HC = 0.92 * HC
360 PW = (10 ^ (6.075 - 2256 / T)
     ) / 0.9869
370 PW = 1.00 * PW
380 QR(1) = HC / PR
390 QR(2) = PN / PR
400 QR(3) = PW / PR
410 LL = 1.00 * LR
420 WL = 1.00 * WR
430  IF AR >  < 0 THEN CL = 0.025

440 I = 0
450 T = (T - 273.15) / 100
460 I = I + 1
470 X = (27.9503989 + 140.179398 *
     WL) * LL ^ (1 / 2)
480 X = X - (163.692296 + 29.8978
     319 * LL - 4.48784208 * WL) *
     WL
490 X = X + 395.261578 * T ^ 2 -
     81.0783052 * T ^ 3
500 X = X - (613.260744 + 1.56785
     865 * LL + 9.08425388 * WL) *
     T
510 X = X + 332.597855
520 X = X / 100
530 XL = ((27.9503989 + 140.17939
     8 * WL) * (0.5) * LL ^ ( - 0
     .5) - 29.8978319 * WL - 1.56
     785865 * T) / 100
540 XW = (140.179398 * L ^ (0.5) -
     (163.692296 + 29.8978319 * L
     L) + 2 * 4.48784208 * WL - 9
     .08425388 * T) / 100
550 X = ER * X
560  IF AR = 0 THEN  GOSUB 1450
570 MO = LL + WL + 2 * CL + X - 1

580 N = 1 + LL + WL
590 AM = LL + 2 * CL - 2
600 WT = X + WL
610  IF AR = 0 THEN  GOTO 1490
620 F = (AM ^ 2) * CL * K2 - X *
     WT * MO
630 F1 = 4 * AM * CL * K2 + (AM ^
     2) * K2 - 2 * X * WT
640 F2 = 2 * K2 * CL * AM - X * (
     WT * (1 + XL) + XL * MO) - X
     L * WT * MO
650 F3 =  - X * (WT * (1 + XW) +
     MO * (1 + XW)) - XW * WT * M
     O
660 G = MO * (LL * ZR(1) - ZR(2))
      + QR(2) * (LL + 2 * CL - 2)
      * (1 - N * ZR(1)) + QR(1) *
     CL * (N * ZR(2) - LL)
670 G1 = 2 * (LL * ZR(1) - ZR(2))
      + 2 * QR(2) * (1 - N * ZR(1
     )) + QR(1) * (N * ZR(2) - LL
     )
680 G2 = (1 + XL) * (LL * ZR(1) -
     ZR(2)) + MO * ZR(1) + QR(2) *
     (1 - N * ZR(1)) + QR(2) * AM
      * ( - ZR(1)) + QR(1) * CL *
     (ZR(2) - 1)
690 G3 = (1 + XW) * (LL * ZR(1) -
     ZR(2)) + QR(2) * AM * ( - ZR
     (1)) + QR(1) * CL * (ZR(2))
700 H = (1 - N * ZR(1)) * (MO - (
     QR(1) * CL + QR(2) * AM + QR
     (3) * WT)) - ZR(6) * (MO - Q
     R(1) * N * CL)
710 H1 = (1 - N * ZR(1)) * (2 - (
     QR(1) + 2 * QR(2))) - ZR(6) *
     (2 - QR(1) * N)
720 H2 = ( - ZR(1)) * (MO - (QR(1
     ) * CL + QR(2) * AM + QR(3) *
     WT)) + (1 - N * ZR(1)) * (1 +
     XL - (QR(2) + QR(3) * XL)) -
     ZR(6) * (1 + XL - QR(1) * CL
     )
```

```
730 H3 = ( - ZR(1)) * (MO - (QR(1
     ) * CL + QR(2) * AM + QR(3) *
     WT)) + (1 - N * ZR(1)) * (1 +
     XW - QR(3) * (XW + 1)) - ZR(
     6) * (1 + XW - QR(1) * CL)
740 B(1,1) = G2 * H3 - G3 * H2
750 B(1,2) = G3 * H1 - G1 * H3
760 B(1,3) = G1 * H2 - G2 * H1
770 B(2,1) = H2 * F3 - H3 * F2
780 B(2,2) = H3 * F1 - H1 * F3
790 B(2,3) = H1 * F2 - H2 * F1
800 B(3,1) = F2 * G3 - F3 * G2
810 B(3,2) = F3 * G1 - F1 * G3
820 B(3,3) = F1 * G2 - F2 * G1
830 D = F1 * B(1,1) + F2 * B(1,2)
      + F3 * B(1,3)
840 CL = CL - (B(1,1) * F + B(2,1
     ) * G + B(3,1) * H) / D
850 LL = LL - (B(1,2) * F + B(2,2
     ) * G + B(3,2) * H) / D
860 WL = WL - (B(1,3) * F + B(2,3
     ) * G + B(3,3) * H) / D
870  IF ( ABS (F) +  ABS (G) +  ABS
     (H)) < 1E - 06 THEN  GOTO 90
     0
880  IF I > 50 GOTO 1430
890  GOTO 460
900 XR(1) = CL / MO
910 XR(2) = AM / MO
920 XR(3) = WT / MO
930 XR(4) = X / MO
940 XR(5) = (1 - X - CR) / MO
950 YR(1) = HC * XR(1) / PR
960 YR(2) = PN * XR(2) / PR
970 YR(3) = PW * XR(3) / PR
980 YR(6) = 1 - (YR(1) + YR(2) +
     YR(3))
990 CR(1) = 1 / N
1000 CR(2) = LL * CR(1)
1010 CR(3) = WL * CR(1)
1020 RR(1) = (ZR(1) - YR(1)) / (C
     R(1) - YR(1))
1030 RR(2) = (ZR(2) - YR(2)) / (C
     R(2) - YR(2))
1040 RR(3) = (ZR(3) - YR(3)) / (C
     R(3) - YR(3))
1050  IF AR >  < 0 THEN RR(6) = (
     YR(6) - ZR(6)) / YR(6)
1060  IF AR = 0 THEN  GOTO 1220
1070 LM = RR(6) * MO * 83.588731 /
     (ZR(6) * N)
1080 U = XR(4) * LM
1090 ZT = 83.588731 / ZR(6)
1100 ZK = ZR(1) * ZT
```

```
1110 ZN = ZR(2) * ZT
1120 ZW = ZR(3) * ZT
1130 RC = ZK
1140 RN = ZN - EN * (570.0 * 1800
     ) / (17.031 * 24)
1150 RW = ZW
1160 RI = 83.588731 - 3.2674148 *
     EN
1170 RT = RC + RN + RW + RI
1180 ZC(1) = RC / RT
1190 ZC(2) = RN / RT
1200 ZC(3) = RW / RT
1210 ZC(6) = RI / RT
1220  PRINT "I     =";I
1230  PRINT "TR    =";TR; TAB( 22)
     "PR    =";PR;"BARS"
1240  PRINT "RR(1)=";RR(1); TAB(
     22)"RR(2)=";RR(2)
1250  PRINT "RR(3)=";RR(3); TAB(
     22)"RR(6)=";RR(6)
1260  PRINT "LM    =";LM; TAB( 22)
     "U     =";U
1270  PRINT "LL    =";LL; TAB( 22)
     "WL    =";WL
1280  PRINT "CL    =";CL; TAB( 22)
     "X     =";X
1290  PRINT "ZR(1)=";ZR(1); TAB(
     22)"ZR(2)=";ZR(2)
1300  PRINT "ZR(3)=";ZR(3); TAB(
     22)"ZR(6)=";ZR(6)
1310  PRINT "ZT    =";ZT; TAB( 22)
     "ZK    =",ZK
1320  PRINT "ZN    =";ZN; TAB( 22)
     "ZW    =";ZW
1330  PRINT "RT    =";RT
1340  PRINT "RI    =";RI; TAB( 22)
     "RN    =";RN
1350  PRINT "XR(1)=";XR(1); TAB(
     22)"XR(2)=";XR(2)
1360  PRINT "XR(3)=";XR(3); TAB(
     22)"XR(4)=";XR(4)
1370  PRINT "XR(5)=";XR(5)
1380  PRINT "CR(1)=";CR(1); TAB(
     22)"CR(2)=";CR(2)
1390  PRINT "CR(3)=";CR(3)
1400  PRINT "YR(1)=";YR(1); TAB(
     22)"YR(2)=";YR(2)
1410  PRINT "YR(3)=";YR(3); TAB(
     22)"YR(6)=";YR(6)
1420  GOTO 1640
1430  PRINT "ITRATIONS EXCEEDED";
     " I=";I
1440  END
```

```
1450 CL = ((1 - QR(2)) / (QR(1) +
     2 * QR(2) - 2)) * LL + ((1 -
     QR(3)) / (QR(1) + 2 * QR(2) -
     2)) * (X + WL) + ((2 * QR(2)
      - 1) / (QR(1) + 2 * QR(2) -
     2))
1460 CN = ((1 - QR(2)) / (QR(1) +
     2 * QR(2) - 2)) + ((1 - QR(3
     )) / (QR(1) + 2 * QR(2) - 2)
     ) * XL
1470 CW = ((1 - QR(3)) / (QR(1) +
     2 * QR(2) - 2)) * (XW + 1)
1480  RETURN
1490 F = (AM ^ 2) * CL * K2 - X *
     WT * MO
1500  PRINT "F=";F
1510 FL = (AM ^ 2) * CN * K2 + 2 *
     AM * (1 + 2 * CN) * CL * K2 -
     X * (XL * MO + WT * (1 + 2 *
     CN + XL)) - XL * WT * MO
1520 FW = (AM ^ 2) * CW * K2 + 4 *
     AM * CW * CL * K2 - X * ((1 +
     XW) * MO + WT * (1 + 2 * CW +
     XW)) - XW * WT * MO
1530 G = MO * (LL * ZR(1) - ZR(2)
     ) + QR(2) * (LL + 2 * CL - 2
     ) * (1 - N * ZR(1)) + QR(1) *
     CL * (N * ZR(2) - LL)
1540  PRINT "G=";G
1550 GL = MO * ZR(1) + (1 + XL +
     2 * CN) * (LL * ZR(1) - ZR(2
     )) + QR(2) * AM * ( - ZR(1))
      + QR(2) * (1 + 2 * CN) * (1
      - N * ZR(1)) + QR(1) * CL *
     (ZR(2) - 1) + QR(1) * CN * (
     N * ZR(2) - LL)
1560 GW = (1 + XW + 2 * CW) * (LL
      * ZR(1) - ZR(2)) + QR(2) *
     AM * ( - ZR(1)) + QR(2) * 2 *
     CW * (1 - N * ZR(1)) + QR(1)
      * CR * ZR(2) + QR(1) * CW *
     (N * ZR(2) - LL)
1570 DT = FL * GW - GL * FW
1580 LL = LL - (F * GW - G * FW) /
     DT
1590 WL = WL - (G * FL - F * GL) /
     DT
1600  PRINT "LL=";LL,"WL=";WL
1610  IF  ABS (F) +  ABS (G) < 1E
     - 05 THEN  GOTO 900
1620  IF I > 50 GOTO 1430
1630  GOTO 460
1640  REM  TO FIND THE TOPRIDGE C
     ONDITION
1650  REM  OF THE NH3-CO2-H2O SYS
     TEM
1660  REM  BASED ON DURISCH'S MOD
     EL
1670  REM  ONLY CARBAMATE REACTIO
     N EQUIL.
1680  REM  IS CONSIDERED;THERE IS
      NO UREA
1690  REM  FORMATION
1700  REM  MODEL APPLICABLE FOR A
      HIGH PRESSURE CONDENSOR
1710  DIM XC(6),YC(6)
1720  DIM QC(3),CC(3),RC(6)
1730  INPUT "TC?";TC
1740 PC = PR + 0.5
1750 XC(1) = 0.0174
1760 XC(2) = 0.428
1770 T = TC + 273.15
1780 I = 0
1790 QC(1) = PC ^ ( - 1) *  EXP (
     43.32522 - 3803.22 / T + 0.0
     019688 * T - 4.6144 *  LOG (
     T) + 0.345778 * PC / T + 460
     .42 * PC / (T ^ 2))
1800 QC(2) = PC ^ ( - 1) *  EXP (
     55.57294 - 5121.96 / T + 0.0
     01998 * T - 6.5033 *  LOG (T
     ) - 0.924275 * PC / T + 544.
     84 * PC / (T ^ 2))
1810 QC(3) = PC ^ ( - 1) *  EXP (
     60.17097 - 10114.7 / T + 0.0
     005818 * T - 5.7556 *  LOG (
     T) - 0.86031 * PC / T + 714.
     75 * PC / (T ^ 2))
1820 K =  EXP ( - 71.20722 + 1289
     6.3 / T + 7.7504 *  LOG (T) +
     0.22960 * PC / T)
1830  IF ZC(6) > < 0 THEN  GOTO
     2270
1840 I = I + 1
1850 F = (QC(1) - QC(3)) * XC(1) +
     (QC(2) - QC(3)) * XC(2) + (Q
     C(3) - 1) - K * QC(3) * XC(1
     ) * XC(2) ^ 2
1860 F1 = (QC(1) - QC(3)) - K * Q
     C(3) * XC(2) ^ 2
1870 F2 = (QC(2) - QC(3)) - 2 * K
      * QC(3) * XC(1) * XC(2)
1880 A = ZC(2) - QC(2) * XC(2)
1890 B = XC(1) * (1 - QC(1)) + K *
     XC(1) * XC(2) ^ 2 * (1 - 2 *
     QC(1) * XC(1))
1900 C = XC(2) * (1 - QC(2)) + 2 *
     K * XC(1) * XC(2) ^ 2 * (1 -
     QC(2) * XC(2))
1910 D = ZC(1) - QC(1) * XC(1)
```

```
1920 G = A * B - C * D
1930 G1 = A * (1 - QC(1) + K * XC
     (2) ^ 2 - 4 * QC(1) * K * XC
     (1) * XC(2) ^ 2) + QC(1) * C
      - D * (2 * K * XC(2) ^ 2 *
     (1 - QC(2) * XC(2)))
1940 G2 = A * (2 * K * XC(1) * XC
     (2) * (1 - QC(1) * XC(1))) -
     QC(2) * B - D * (1 - QC(2) +
     4 * K * XC(1) * XC(2) - 6 *
     QC(2) * K * XC(1) * XC(2) ^
     2)
1950 J = F1 * G2 - G1 * F2
1960 XC(1) = XC(1) - (F * G2 - G *
     F2) / J
1970 XC(2) = XC(2) - (G * F1 - F *
     G1) / J
1980  IF ( ABS (F) +  ABS (G)) <
     1E - 07 THEN  GOTO 2010
1990  IF I > 40 THEN  GOTO 2250
2000  GOTO 1840
2010  PRINT "CONVERGENCE SUCCESSF
     ULL"
2020 XC(5) = K * XC(1) * XC(2) ^
     2
2030 XC(3) = 1 - XC(1) - XC(2) -
     XC(5)
2040 YC(1) = QC(1) * XC(1)
2050 YC(2) = QC(2) * XC(2)
2060 YC(3) = QC(3) * XC(3)
2070  IF ZC(6) >  < 0 THEN YC(6) =
     J
2080 CC(1) = (XC(1) + XC(5)) / (1
      + 2 * XC(5))
2090 CC(2) = (XC(2) + 2 * XC(5)) /
     (1 + 2 * XC(5))
2100 RC(1) = (ZC(1) - YC(1)) / (C
     C(1) - YC(1))
2110 RC(2) = (ZC(2) - YC(2)) / (C
     C(2) - YC(2))
2120  IF ZC(6) >  < 0 THEN RC(6) =
     (YC(6) - ZC(6)) / YC(6)
2122 LK = RC(1) * CC(1) * RT * XC
     (5) / (XC(1) + XC(5))
2124 KA = LM * (XR(4) + XR(5)) -
     LK
2130  PRINT "I     =";I
2140  PRINT "PC    =";PC; TAB( 22)
     "TC    =";TC
2150  PRINT "ZC(1)=";ZC(1); TAB(
     22)"ZC(2)=";ZC(2)
2160  PRINT "ZC(3)=";ZC(3); TAB(
     22)"ZC(6)=";ZC(6)
2170  PRINT "YC(1)=";YC(1); TAB(
     22)"YC(2)=";YC(2)
2180  PRINT "YC(3)=";YC(3); TAB(
     22)"YC(6)=";YC(6)
2190  PRINT "XC(1)=";XC(1); TAB(
     22)"XC(2)=";XC(2)
2200  PRINT "XC(3)=";XC(3); TAB(
     22)"XC(5)=";XC(5)
2210  PRINT "CC(1)=";CC(1); TAB(
     22)"CC(2)=";CC(2)
2220  PRINT "RC(1)=";RC(1); TAB(
     22)"RC(2)=";RC(2)
2230  PRINT "RC(6)=";RC(6); TAB(
     22)"KA    =";KA
2240  END
2250  PRINT "ITERATIONS EXCEEDED"

2260  END
2270 I = I + 1
2280 J = (QC(3) - QC(1)) * XC(1) +
     (QC(3) - QC(2)) * XC(2) + K *
     QC(3) * XC(1) * XC(2) ^ 2 +
     (1 - QC(3))
2290 J1 = (QC(3) - QC(1)) + K * Q
     C(3) * XC(2) ^ 2
2300 J2 = (QC(3) - QC(2)) + 2 * K
      * QC(3) * XC(1) * XC(2)
2310 XC(5) = K * XC(1) * XC(2) ^
     2
2320 A = XC(1) + XC(5) - QC(1) *
     XC(1) * (1 + 2 * XC(5))
2330 A1 = 1 + K * XC(2) ^ 2 - QC(
     1) * XC(1) * 2 * K * XC(2) ^
     2 - QC(1) * (1 + 2 * XC(5))
2340 A2 = 2 * K * XC(1) * XC(2) -
     QC(1) * XC(1) * 4 * K * XC(1
     ) * XC(2)
2350 B = XC(1) + XC(5) - ZC(1) *
     (1 + 2 * XC(5))
2360 B1 = (1 + K * XC(2) ^ 2) - Z
     C(1) * 2 * K * XC(2) ^ 2
2370 B2 = 2 * K * XC(1) * XC(2) -
     ZC(1) * 4 * K * XC(1) * XC(2
     )
2380 D = XC(2) + 2 * XC(5) - QC(2
     ) * XC(2) * (1 + 2 * XC(5))
2390 D1 = 2 * K * XC(2) ^ 2 - QC(
     2) * XC(2) * 2 * K * XC(2) ^
     2
2400 D2 = 1 + 4 * K * XC(1) * XC(
     2) - QC(2) * XC(2) * 4 * K *
     XC(1) * XC(2) - QC(2) * (1 +
     2 * XC(5))
2410 E = XC(2) + 2 * XC(5) - ZC(2
     ) * (1 + 2 * XC(5))
2420 E1 = 2 * K * XC(2) ^ 2 * (1 -
     ZC(2))
```

```
2430 E2 = 1 + 4 * K * XC(1) * XC(
     2) * (1 - ZC(2))
2440 F = ZC(6) * A - J * B
2450 F1 = ZC(6) * A1 - J * B1 - J
     1 * B
2460 F2 = ZC(6) * A2 - J * B2 - J
     2 * B
2470 G = ZC(6) * D - J * E
2480 G1 = ZC(6) * D1 - J * E1 - J
     1 * E
2490 G2 = ZC(6) * D2 - J * E2 - J
     2 * E
2500 JC = F1 * G2 - G1 * F2
2510 XC(1) = XC(1) - (F * G2 - G *
     F2) / JC
2520 XC(2) = XC(2) - (G * F1 - F *
     G1) / JC
2530  IF ( ABS (F) +  ABS (G)) <
     1E - 07 THEN  GOTO 2010
2540  IF I > 40 THEN  GOTO 2250
2550  GOTO 2270
```

B.3. *The programme incorporating the compressor power calculations*:

```
]LIST

100 Y$ = "Y"
110  PRINT "DO YOU WISH TO CALCUL
     ATE THE"
120  PRINT
130  PRINT "POWER FOR COMPRESSING
      THE"
140  PRINT
150  PRINT "NH3-CO2-H2O MIXTURE ?
     "
160  PRINT
170  INPUT "TYPE (Y/N) AND PRESS
     RETURN.  ";WISH$
180  PRINT
190  IF WISH$ = Y$ GOTO 220
200  PRINT "VERY WELL. SEE YOU NE
     XT TIME."
210  END
220  PRINT "POLYTROPIC EFFICIENCY
      ?"
230  PRINT
240  INPUT "TYPE AND PRESS RETURN
      ";EF
250  PRINT
260  PRINT "SUCTION TEMPRATURE IN
      KELVIN ?"
270  PRINT
280  INPUT "TYPE AND PRESS RETURN
      ";T1
290 T = T1
300  GOSUB 1150
310  PRINT
320  PRINT "SUCTION PRESSURE IN B
     AR ?"
330  PRINT
340  INPUT "TYPE AND PRESS RETURN
      ";P1
350 P = P1
360 V = 0.083144 * T / P
370  PRINT
380  PRINT "FOR WHAT COMPOSITION?
     "
390  PRINT
400  PRINT "TYPE THE MULFRACTIONS
      IN THIS ORDER."
410  PRINT
420  PRINT "CO2,NH3,H2O. DO NOT O
     MIT THE COMMAS. "
430  PRINT
440  PRINT "FINALLY PRESS THE RET
     URN."
450  PRINT
460  INPUT YK,YN,YH
470  GOSUB 1400
480  FLASH
490  PRINT "COMPUTING MOLAR VOLUM
     E AT SUCTION CONDITIONS"
500  GOSUB 1470
510 Z1 = (P1 * VN) / (0.083144 *
     T1)
520 V1 = VN
530  NORMAL
```

```
540  HOME : REM  CLEAR TEXT AREA
550  GOSUB 1290
560 H1 = YK * HK + YN * HN + YH *
     HW
570  PRINT
580  PRINT "DISCHARGE TEMPERATURE
      IN KELVIN ?"
590  PRINT
600  INPUT "TYPE AND PRESS RETURN
      ";T2
610 T = T2
620  GOSUB 1150
630  PRINT
640  PRINT "YOUR GUESS FOR THE DI
     SCHARGE PRSSURE IN  BAR?"
650  PRINT
660  INPUT "TYPE AND PRESS RETURN
      ";P2
670 J = 0
680 P = P2
690 V = 0.083144 * T / P
700 J = J + 1
710  FLASH
720  PRINT "COMPUTING MOLAR VOLUM
     E AT THE DISCHARGE CONDITION
     S IN THE ";J;" TH ITERATION"

730  GOSUB 1470
740 Z2 = P2 * VN / (0.083144 * T2
     )
750 V2 = VN
760  NORMAL
770  HOME : REM  CLEAR TEXT AREA
780  GOSUB 1290
790 H2 = YK * HK + YN * HN + YH *
     HW
800 AL = EF * (H2 - H1) / 8.3144 /
     (Z2 * T2 - Z1 * T1)
810 P = P1 * ((Z2 * T2) / (Z1 * T
     1)) ^ AL
820  PRINT "J=";J;"       P=";P
830  IF  ABS (P - P2) < 1E - 04 GOTO
     870
840  IF J > 30 THEN  GOTO 1110
850 P2 = (P + P2) / 2
860  GOTO 680
870  PRINT
880  INPUT "FLOW RATE IN KMOLES/S
     EC ?";Q
890  PRINT "TOTAL NO. OF ITERATIO
     NS =";J
900  PRINT
910 HP = Z1 * (8.3144) * T1 * AL *
     ((P2 / P1) ^ (1 / AL) - 1)
920 EN = HP / EF * Q
930  PRINT
940  PRINT "V1=";V1;" LITRES PER
     MOLE."
950  PRINT "V2=";V2;" LITRES PER
     MOLE."
960  PRINT "Z1=";Z1
970  PRINT "Z2=";Z2
980  PRINT "H1=";H1;" JOULES PER
     MOLE."
990  PRINT "H2=";H2;" JOULES PER
     MOLE."
1000  PRINT "EF=";EF
1010  PRINT "HEAT INPUT=";H2 - H1

1020  PRINT "AL=";AL
1030  PRINT "P1=";P1
1040  PRINT "T1=";T1
1050  PRINT "T2=";T2
1060  PRINT "P2=";P2
1070  PRINT "POWER REQUIRED =";EN

1080  PRINT
1090  PRINT "IT IS A PLEASURE TO
     BE OF HELP TO YOU.  SEE YOU
     NEXT TIME."
1100  END
1110  PRINT
1120  PRINT "ITERATIONS EXCEEDED"

1130  PRINT "LAST VALUES ARE:"
1140  GOTO 930
1150 KK = 3.1693 + (253.17 / T)
1160 NN = 2.6435 + (561.63 / T)
1170 HH = 3.1307 + (1161.7 / T)
1180 KN = 3.1 + (133.235 / T)
1190 KH = 4.36 + (130.785 / T)
1200 NH = 2.6948745 + (806.05714 /
     T)
1210 BK = 10 ^ ( - 1.234 - 4.67E -
     05 * T)
1220 BN = 10 ^ ( - 1.3884 - 1.47E
      - 04 * T)
1230 BH = 10 ^ ( - 1.5589 - 0.593
     E - 04 * T)
1240 CK = 0.0
1250 CN = 0.01
1260 CH = 0.01
1270 R = 0.083144
1280  RETURN
1290 P = P / 100
1300 T = T / 100
1310 HW = 0.460201575 + 60.756880
     2 * (1 / T) - 256.582871 * (
     1 / T) ^ 2 + 337.952302 * (1
      / T) ^ 3
```

```
1320 HW = 10000 * HW
1330 HN = 4.95199701 - 38.7068896
      * (1 / T) ^ 3 + 48.2222936 *
     P / T - 412.211711 * (P / T ^
     2) + 852.784482 * (P / T ^ 3
     ) - 39.0882345 * (P ^ 2 / T)
      + 362.685951 * (P ^ 2 / T ^
     2) - 856.521985 * (P ^ 2 / T
      ^ 3) + 7.75491513 * (P ^ 3 /
     T) - 74.256656 * (P ^ 3 / T ^
     2) + 180.693009 * (P ^ 3 / T
      ^ 3)
1340 HN = 10000 * HN
1350 HK = 7.94521417 - 27.072388 *
     (1 / T) + 41.8004195 * (1 /
     T ^ 2) - 6.95129876 * P / T +
     58.8530229 * (P / T ^ 2) - 1
     40.147134 * (P / T ^ 3) + 2.
     30769031 * (P ^ 2 / T) - 19.
     2462632 * (P ^ 2 / T ^ 2) +
     38.9016342 * (P ^ 2 / T ^ 3)
      - 0.0785221525 * (P ^ 3 / T
     ) + 0.447346417 * (P ^ 3 / T
      ^ 2)
1360 HK = 10000 * HK
1370 P = 100 * P
1380 T = 100 * T
1390  RETURN
1400 AK = KK * YK + KN * YN + KH *
     YH
1410 AN = KN * YK + NN * YN + NH *
     YH
1420 AH = KH * YK + NH * YN + HH *
     YH
```

```
1430 A = AK * YK + AN * YN + AH *
     YH
1440 B = BK * YK + BN * YN + BH *
     YH
1450 C = CK * YK + CN * YN + CH *
     YH
1460  RETURN
1470  FOR I = 1 TO 30
1480 XI = B / (4 * V)
1490 F = (1 + XI + (XI ^ 2) - (XI
      ^ 3)) / ((1 - XI) ^ 3)
1500 DF = (2 * (XI ^ 2) + 2 * (XI
      ^ 3) - (XI ^ 4)) / ((1 - XI
     ) ^ 4)
1510 G = (R * T * F) - (A / (V +
     C)) - (P * V)
1520 DG =  - (B * R * T * DF / B)
      + (A / ((V + C) ^ 2)) - P
1530 V = V - (G / DG)
1540  IF  ABS (G) < 1.0E - 06 THEN
      GOTO 1620
1550  NEXT I
1560  REM  NO CONVERGENCE
1570  NORMAL
1580  HOME : REM  CLEAR TEXT AREA

1590  PRINT
1600  PRINT "NO SOLUTION AFTER 30
      ITERATIONS."
1610  END
1620 VN = V
1630  RETURN
```

APPENDIX C

THE GAS PHASE ANALYSIS OF THE NH_3-CO_2-H_2O MIXTURES: THE METHOD, THE PROBLEMS FACED AND THE SOLUTIONS.

C.1. *Introduction*:

Gas chromatography of NH_3-CO_2-H_2O mixtures exhibits many problems, like peak tailing, adsorption on the upstream tube walls, irreversible sorption of water vapour (or ammonia) on certain adsorbents, very long retention times of water vapour, etc. In spite of these problems, gas chromatography is preferred over chemical analysis methods [1,2] for analysing these gas mixtures mainly to avoid weighing and titration, the tediousness and time consumption of chemical analysis and the continual necessity of standardizing reagent solutions.

Techniques other than gas chromatography, like near infrared spectrometry [3] and mass spectrometry [4], have also been tried for analysing NH_3-CO_2-H_2O mixtures. In fact, analysis through mass spectrometry has reached on-line application in at least one urea plant [4]. However, gas chromatography still remains a simple, popular, and a reliable method - provided one takes adequate care in designing and maintaining the system.

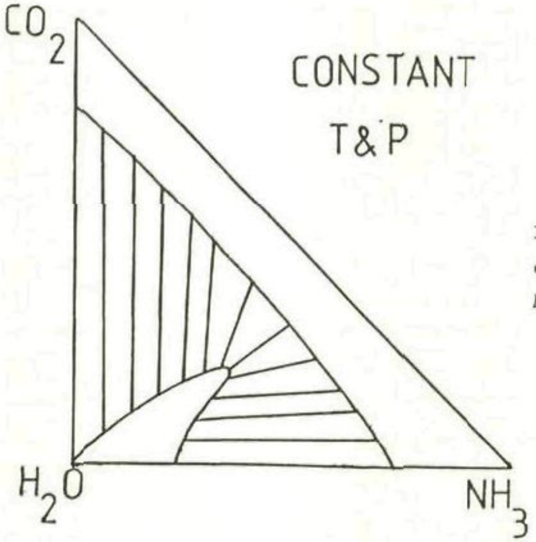

Fig. C.1. *Typical bubble- and dew-point curves of the system NH_3-CO_2-H_2O at constant T and P.*

Accurate gas sampling and analysis are very important in the VLE study of the NH_3-CO_2-H_2O system, since the tie-lines connecting the bubble- and dew-point curves at constant T and P are spread out like a fan, as shown in Fig. C.1. Around the "tongue tip" of the bubble-point curve, it can be observed that a small change in the liquid composition causes a large change in the gas composition. Such behaviour demands a reliable and accurate gas analysis. This was all the more emphasized in the present study by the prevailing ambient fluctuations of the poorly ventilated and heated pilot-plant hall where the experimental set-up was placed. It was not unusual for the hall temperature to vary as much as 20° C per day and the ambient pressure (in Delft - a low lying area) to vary not only day to day but even within a single day upto a maximum of 15 mm Hg.

All these factors were taken into account in developing the present chromatographic system. During such development, a number of simple (and in some cases, novel) procedures for the choice of the column temperature, the carrier gas flow rate, the sample volume, and the calibration of the system, were developed. It is felt that these procedures may also have applications for other systems. In what follows the broad features of the analysis system are described mainly with reference to the analysis of NH_3-CO_2-H_2O mixtures.

C.2. *The choice of the adsorbent*:

The adsorbents usually preferred for analysing NH_3-CO_2-H_2O mixtures are either the Chromosorb Century or the Poropak Series [5]. Older adsorbents, like polyethylene glycol on inert carriers, are seldom used nowadays for reliable analysis. Among the Poropak series, Poropak Q, QS, R and also R coated with 10% polyethylene-imine were employed earlier by a number of authors [6,7,8,9,10]. The qualities of separation and analytical accuracies obtained in these cases are discussed by Lemkowitz [11]. In the Chromosorb Century Series, only Chromosorb 102, 102 coated with 10% tetra-hydroxy-ethyl-ethylene-diamine, 103 and 104 have been tried for the analysis of NH_3-CO_2-H_2O gas mixtures, with varied results.

Chromosorb 103 - 60/80 mesh - was claimed by Pawlikowskii et al [12] to give optimal separation of NH_3-CO_2-H_2O mixtures (for both gas and evaporated liquid samples). The column temperature was maintained at 70°C until the NH_3 peak began to elute. Subsequently it was raised to 150°C to reduce the width of the H_2O peak. The error obtained for the gas analysis was reported to be 1.5% and that for the liquid phase 3%. However, there appears to be some error either in their analyses or in their method of sampling, since their VLE gas phase data appear to be consistently below the values reported by others [10].

Chromosorb 104 was tried at the DSM laboratories [13] and found to give large tailing of the ammonia peak at 123°C. Lemkowitz also [11] tried this adsorbent at 147°C. Being an acrylonitrile - divinylbenzene co-polymer, the nitrile group of the polymer exhibits a strong interaction with ammonia. It is suggested [13] that the nitrile groups of the polymer may react with ammonia to produce amidine groups which later react with water to release ammonia and become amide groups. The amide groups themselves can further loose water to become nitrile groups. Also the amide groups can get hydrolysed to give acid groups and ammonia. All these processes accentuate the unsymmetry, tailing and overlap of the ammonia - water peaks.

As for Chromosorb 102, it contains vinyl and phenyl groups on the surface and is classified as a low-specific adsorbent of the third type, according to Kiselev [14]. Left to itself, it performs poorly with NH_3 and H_2O leading to severe tailing and overlap, although it separates molecules like CO_2 (which interact through dispersion forces) better, as has been observed by DSM [13] and others [15]. This tailing behaviour is attributed to the unreacted vinyl groups present on the surface which must be deactivated to obtain symmetrical peaks.

The deactivation of the vinyl groups can be achieved either by chemical or physical means. Hertl and Neumann [16] describe the chemical method of saturating the unreacted vinyl groups by addition of HF to the double bond of the vinyl group. Alternatively the physical method involves the covering of hyperactive sites with low boiling, large molecular weight amines.

Earlier three amines/imines have been tried as liquid phases on a few adsorbents for the efficient separation of NH_3. They are polyethylene-imine, tetra-ethylene-pentamine (TEP), and tetrahydroxy-ethyl-ethylene-diamine (THEED). Sze et al [17] have tried TEP and THEED on Chromosorb W for the separation of lower aliphatic amines and NH_3. Moretti et al [18] and also DSM [13] have tried 10% THEED on Chromosorb 102 with efficient separation of ammonia and water.

In the present work, Chromosorb 102 with 10% THEED was chosen as the column material mainly due to its proven characteristics. The minimal temperature for the use of THEED is 50°C and the maximal temperature at which its vapour pressure becomes appreciable is around 150°C.

C.3. *The choice of the column conditions*:

Having chosen Chromosorb 102 coated with 10% THEED as the adsorbent, the next choice concerns the carrier gas. Of the three gases usually employed as carrier gases, namely hydrogen, helium and nitrogen, we rule out nitrogen because of the possible presence of air as an impurity in the gas sample. Of the remaining two, the choice is narrowed down to helium mainly for safety reasons.

C.3.1. *The operating temperature*:

It is very well known that the retention times as well as the resolution of peaks decreases with increasing temperature. While the reduction of retention times is advantageous, the reduction of resolution is detrimental to analytic accuracy. Similarly very low temperatures increase the assymmetry of the peaks and cause the resolution to become poor. Hence it is essential for the relevant adsorption isotherms at the chosen temperature to be nearly linear. Also the vapour pressure of the impregnated liquid phase has to be very low.

In order to fix the operating temperature, one may resort to the following simple and elegant method based on relative retention. By doing so, a large number of time consuming exploratory trials can be avoided.

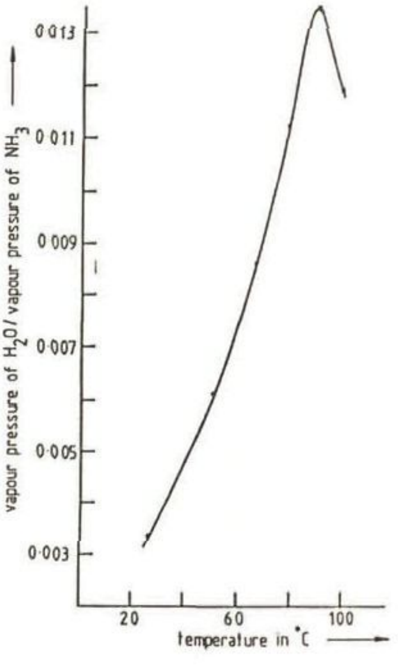

Fig. C.2. *Plot of the vapour pressure ratio of H_2O to NH_3 against temperature.*

The relative retention α of two components can be defined as the ratio of the retention volumes of the two peaks. One can also write the same as [19],

$$\alpha = \gamma_2 . P_2^o / \gamma_1 . P_1^o \qquad \text{(eq. C.1)}$$

Now limiting the situation to ammonia and water and assuming the activity coefficients γ_1 and γ_2 of ammonia and water in the polymer/liquid phase to be nearly equal, one may get the approximate relation,

$$\alpha \approx P_2^o / P_1^o \qquad \text{(eq. C.2)}$$

In other words, one can plot the ratio of the vapour pressures of H_2O and NH_3 against temperature, as shown in Fig. C.2. It can be seen from the figure that this ratio attains a maximum value around 86 to 88°C. Further there is an additional advantage of getting a symmetrical water peak because of the linear isotherm obtained in this temperature range, as shown in Fig. C.3 [15b]. Hence by narrowing down the trials to this temperature range, the optimal temperature for the resolution of ammonia and water was found out to be 87.1°C.

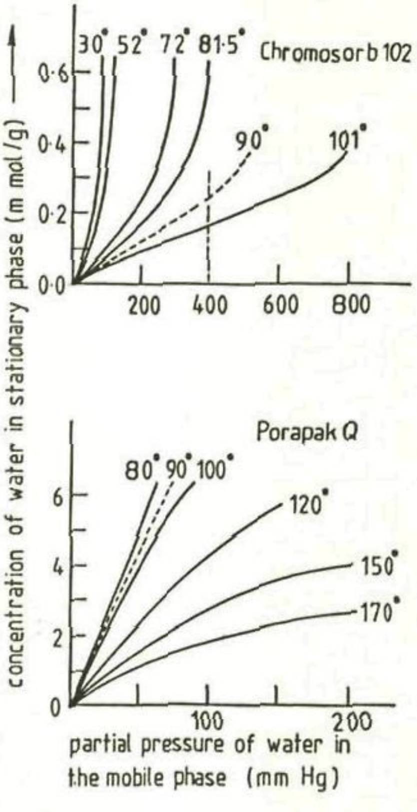

Fig. C.3. *The adsorption isotherms of water over Chromosorb 102 and Poropak Q [15b].*

C.3.2. *The choice of the column and adsorbent sizes*:

Subsequent to the choice of the temperature, the adsorbent particle size was arbitrarily chosen as 100/120 mesh mainly to have a large adsorption surface and yet offer an acceptable pressure drop for the flow. Similarly the column diameter (2.7 mm) and the length (3 m) were fixed arbitrarily without any trials.

C.3.3. The carrier gas flow rate:

The carrier gas flow rate was fixed through a simple empirical method as against the method of optimization through HETP calculation. This empirical method is based on the observation that a plot of the retention time difference between CO_2 and NH_3 peaks against the upstream pressure reveals an inflection point around the optimal pressure (3.65 bar), as shown in Fig. C.4. The corresponding optimal flow rate was found to be 62.33 Nml/min. A similar plot of the retention time difference of the NH_3 and H_2O peaks against the upstream pressure also reveals an inflection point (not shown here).

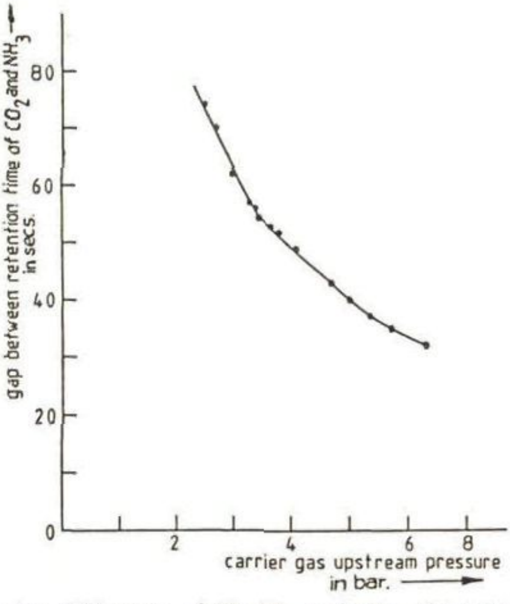

Fig. C.4. *Retention time difference of CO_2-NH_3 peaks Vs. the upstream pressure with a constant downstream pressure of 785 mm Hg.*

C.3.4. *The choice of the sample volume:*

When a sample is injected into the chromatographic column, the components are resolved into individual peaks leading to a succession of He-X mixtures with streams of helium spaced in between. Subsequently the detector senses deviations of the monitored property, (as various binary mixtures pass through it), and generates electrical signals which are subsequently transmitted to the recorder. Normally it is preferable to have a linear relation between these signals and the concentrations of X in He. In the case of a thermal conductivity detector (TCD), this means that the change in thermal conductivity of the He-X mixture with respect to the change in mole fraction of X has to be linear, at least in the range of the composition analysed. This is possible only if the sample volume is not too large. As is well known, the larger the sample volume the greater is the non-linearity of the reponse. The following method aids in estimating the sample volume for a given GC with TCD.

The thermal conductivities of the He-X mixtures are first calculated using the following relation developed by Wassilyewa [20]. These are then plotted against the mole fraction of X, as is shown in Fig. C.5.

$$\lambda_m = \sum_{i=1}^{n} ((x_i.\lambda_i)/ \sum_{j=1}^{n} (x_j.A_{ij})) \qquad \text{(eq. C.3)}$$

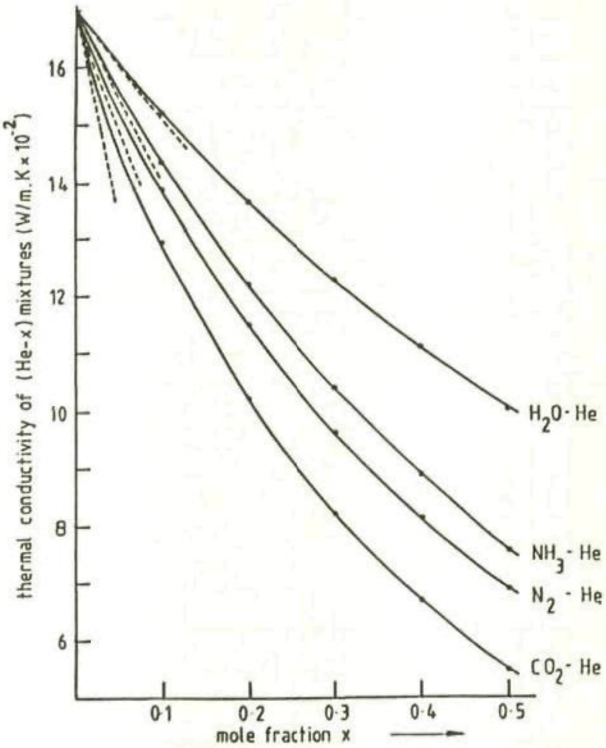

Fig. C.5. *Thermal conductivity of He-X mixtures against the mole fraction of X.*

In (eq. C.3) λ_m and λ_i are, respectively, the thermal conductivity of the gas mixture and that of the component i. The x_i and x_j are the mole fractions, and A_{ij} are the empirical interaction parameters given in Table C.1.

Table C.1. *Interaction parameters for the thermal conductivity estimation.*

i	j	A_{ij}	A_{ji}
He	N_2	2.467	0.539
He	NH_3	2.160	0.422
He	CO_2	3.220	0.424
He	H_2O	2.112	0.373

Next we calculate the maximal mole fractions of X (in He-X mixtures) which occur with the injection of pure components. These maximal concentrations are different for different components even though the amount injected is the same in each case. This difference is mainly due to the different intrinsic spread of each component caused by diffusion through the column.

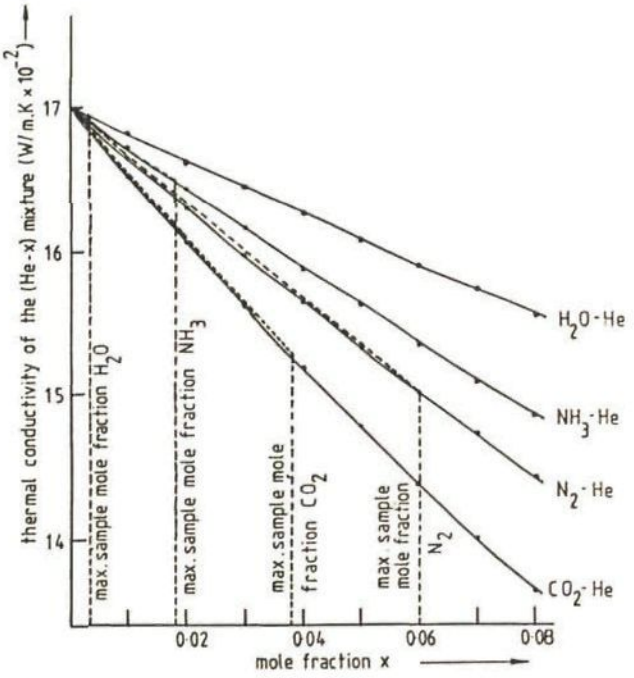

Fig. C.6. *Thermal conductivities of the gas mixtures against the mole fractions x_i - given in an expanded scale.*

Calculation of mole fractions involves two factors, namely the amount of the sample injected and the amount of helium passing through the peak duration.

The amount of the sample per injection is calculated to be 0.021 mmol for a sample volume of 0.55 ml (with an internal diameter of the sampling tube 0.8 mm and length 110 cm) at a pressure of 860 mm Hg and a temperature of 87.1°C. (The chosen pressure 860 mm Hg is the maximum allowed in the sample loop, as described in section C.5). The amount of the helium passing through the duration of each peak is calculated by multiplying the helium flow rate with the respective halfwidth. The calculated maximal mole fractions are tabulated in Table C.2 and marked in Fig. C.6.

Now the severe nonlinearity of the N_2-He and CO_2-He curves shown in Fig.B.6 becomes apparent even at low mole fractions. Hence if one prefers linear behaviour, then the maximum mole fractions have to be limited and there are two ways of doing so. The easiest is, of course, to increase the carrier gas flow rate, but this results in a straying away from the optimal flow rate and a decrease in the resolution. The other alternative is to reduce the sample volume.

Table C.2. *The maximum mole fractions of various components. (volume of the sample 0.55 ml and He flow rate 62.33 Nml/min)*

Component	Halfwidth in seconds	Amount of helium in mmole.	Amount of comp. in mmole.	Maximum mole fraction
H_2O	36.8	6.150	0.021	0.0034
NH_3	6.8	1.140	0.021	0.0180
CO_2	3.2	0.534	0.021	0.0380
N_2	2.0	0.334	0.021	0.0600

For example if the sample volume is reduced to 0.3 ml, then the amount of the sample per injection becomes 0.0115 mmol, and the maximal mole fraction of N_2 equals 0.033 and that of CO_2 0.019. With these restrictions, the thermal conductivity-mole fraction curve is easily approximated by a linear behaviour.

Based on the above analysis, the sample volume was finally set at 0.3 ml with consequent improvements in the linearity of calibration curves.

C.4. *The specification of the experimental parameters*:

Now for a given maximal error in the peak areas, the experimental parameters are to be specified to enable the design of the experimental set-up. The hardware needed for realizing the specification is described in section C.6.

It is almost customery for many workers to say that accuracies better than 2% cannot be achieved in chromatography. Yet, Goedert and Guichon [21], and also Aldorf [22] have suggested otherwise, based on a detailed error analysis of gas chromatography. They also established relevant design procedures to minimize the error. While Aldorf's work was more on the practical side, Goedert and Guichon's work was comprehensive on both the theory and practice. In what follows, their specification procedures are adopted.

For a concentration detector like the TCD, it is well known that:

$$A_i = (S_i/D) * m_i \qquad \text{(eq. C.4)}$$

where A_i is the peak area of the component i, m_i is mass of the component i in the sample, S_i is the sensitivity of the detector with reference to the component i and D is the carrier gas flow rate. As suggested by Goedert and Guichon, the carrier gas flow rate D depends on the inlet and outlet pressure of the column and the sensitivity S_i depends on the thermal conductivity of the component, the temperature and the bridge current. Hence the error in the peak area depends on the individual contributions of the parameters mentioned above.

The first two contributions towards the total error occur through the relative deviations of the inlet and outlet pressures, namely,

$$e_1 = -((2.P_i^2)/(P_i^2-P_o^2)) * (\Delta P_i)/P_i \qquad \text{(eq. C.5)}$$

$$e_2 = ((2.P_o^2)/(P_i^2-P_o^2)) * (\Delta P_o)/P_o \qquad \text{(eq. C.6)}$$

Similarly for the sample pressure, one may state:

$$e_3 = (\Delta P_s/P_s) \qquad \text{(eq. C.7)}$$

Further there is the error due to change in temperature which in the case of helium as a carrier gas can be written as:

$$e_4 = -(4.3*10^{-3}*T + 0.3) * (\Delta T/T) \qquad \text{(eq. C.8)}$$

The error due to variations in bridge current can be accounted as:

$$e_5 = 3* (\Delta I/I) \qquad \text{(eq. C.9)}$$

Table C.3. *Error contribution by the experimental variables.*

Variable	proportionality factor	absolute fluctuation	relative fluctuation %	relative contribution %	quadratic contribution $\%^2$
P_i	-2.16	10.0 mm Hg	0.365	-0.788	0.622
P_o	0.08	0.1 mm Hg	0.013	0.001	$1.08*10^{-6}$
P_s	1.00	1.0 mm Hg	0.13	0.13	0.017
T	-1.85	0.1°C	0.028	-0.052	0.0027
I	3.00	0.01 mA	0.01	0.03	0.001
e_6	1.00		0.1	0.1	0.01

There is also the integrator error e_6. All these relative contributions consist of proportionality factors and relative fluctuations, as shown in Table C.3. In this table, the inlet pressure is to be taken as 3.65 bar, the outlet pressure 1 bar , sample pressure 1 bar, the detector temperature 360.15 K and the bridge current 100 mA. (Note that all pressures are absolute.)

It can be seen from the Table C.3 that the total quadratic contribution is around 0.66, and hence the average relative error is only 0.81%. In other words, given the absolute fluctations of the variables mentioned in the table, it should be possible to limit the variations in the peak areas to less than 1%.

Now the next question is: what are the most critical variables ?

If one looks at the proportionality factors and the range of fluctuations, the detector temperature and the bridge current are ruled out from serious consideration because of the ease with which these variables can be controlled in the constant current catharometers. Among the three pressures remaining, the outlet pressure with a small proportionality factor is not so critical unless it varies by 10 to 20 mm Hg. The sample pressure may not pose much of a problem, if monitored rather than controlled, as described in the next section. This leaves only the inlet pressure requiring a close control to minimize the errors. Accordingly much attention was paid to this variable in the experimental set-up, as described in section C.6. Also the outlet pressure was controlled satisfactorily by an appropriate mechanism.

C.5. *The calibration method*:

Earlier in equation C.4, the peak area A_i was said to be proportional to the sample mass m_i. Now using the ideal gas law, eq. C.4 can be written as,

$$A_i = (S_i/D) * (p_i * V_s * M_i) / (R*T) \qquad \text{(eq. C.10)}$$

where p_i is the partial pressure of the component i in the sample loop, V_i is the sample loop volume, M_i is the molecular mass of the component i, R is the gas constant and T the detector temperature. Further by splitting p_i into total pressure P and the mole fraction x_i of the component, one can write that the peak area A_i is proportional to the mole fraction x_i, provided all the other variables are kept constant. Most importantly, this means that one has to control the total sample pressure, as Goedert and Guichon did, or correct the peak area for the varying pressure, as Aldorf did, (by multiplying the measured area with a factor (760/P)) and plot the corrected area against the mole fraction to get a stable linear calibration.

However, both these methods involve the preparation of various gas mixtures, which is not always possible, especially in the case of NH_3-CO_2-H_2O mixtures. Earlier workers [11,23] at Delft University of Technology used to employ N_2-CO_2 mixtures, N_2-NH_3 mixtures and a 2:1 mixture of NH_3-CO_2 (obtained by the volatilization of ammonium carbamate) for the calibration. As for the water calibration, nitrogen was bubbled through a water saturator to get various water compositions. However, the difficuties in preparing these mixtures have plagued the calibration procedure constantly. Hence in the present work, a novel but simple calibration procedure was developed to circumvent such difficulties and was counterchecked with the ealier system of preparing the gas mixtures.

The starting point of the method was eq. C.10 with its implication on the validity of the Dalton's law of partial pressures. In other words, if we inject a pure component i at various total sample pressures, note the peak areas and plot these variables one against the other, we should get a calibration line which is valid also for the partial pressures of mixtures. One objection to this method can be that the sample total pressure should not exceed values that invalidate the ideal gas assumption. Such an objection, however, exists also for the method of plotting peak areas against the sample mole fraction.

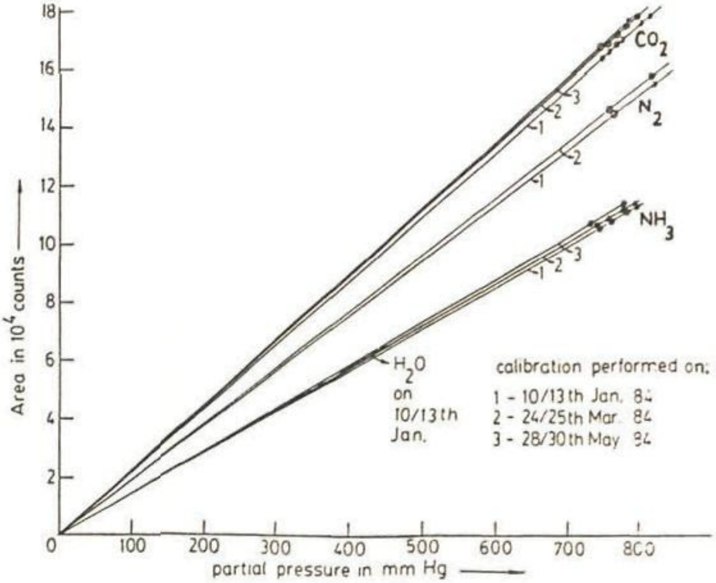

Fig. C.7. *The calibration plots of N_2, CO_2, NH_3 and H_2O*

The main advantage of the calibration plot of the peak area Vs the partial pressure is in doing away with the difficult preparation of gas mixtures, while maintaining the desired linearity. The calibration plots of the present work are shown in Fig. C.7. The maximum sample pressure employed was only 860 mm Hg. In order to check these calibrations, various compositions of N_2-CO_2 mixtures and N_2-NH_3 mixtures were prepared using thermal mass flow meters and were injected into the column; the areas obtained clearly matched with those read from the figure to within 1%, except for the case of ammonia in high concentrations, which was within 1.5%. This increased uncertainty for the high ammonia concentrations is probably due to its polar nature. Also the injection of 2:1 mixture of NH_3-CO_2 was found to confirm the calibration plot within 1.5%.

The calibration for water, which is more difficult than for the other two components, was carried out through procedures similar to those of Lemkowitz [11] and Verbrugge [23] with slight modifications. The details of the water saturator are available in the departmental internal report [24]. The maximum water concentration attempted during the calibration was only 40%. With the column temperature being only

87°C, higher water concentrations gave problems of condensation in the sample loop and in other internal parts of the GC. Fortunately there was no need to go further, since the maximum water concentration did not go above 40% for any of the vapour-liquid equilibria studied.

C.6. *The experimental set-up and the results*:

The experimental set-up is shown in Fig. C.8 and the legend and specifications in Table C.4. The carrier gas flow rate measured through a calibrated capillary flow meter was held at 62.33 Nml/mim with an abs. error of 0.1 Nml/min by maintaining the column upstream pressure at 3.65 (0.01) bar through a pressure control on the helium line and the column downstream pressure at 785 (1) mm Hg by adding nitrogen continuously into the outgoing helium stream. The flow corrections due to ambient temperature fluctuations were incorporated by charts. Both the column and the detector along with the buffer capacity vessels, the sample loop, the sample injection valve and the inside connecting lines were fixed to a deck-cover of a thermostat which was controlled to an accuracy of 0.1°C through a thyrister mechanism. The outside of the deck-cover was completely covered with fibre glass wool. The thermostat temperature was read through a Pt-resistance thermometer (precision -0.1°C). All the outside lines (3 or 6 mm dia. stainless steel) were maintained above 100°C by means of electrical tracings, wherever there was a possibility of condensation.

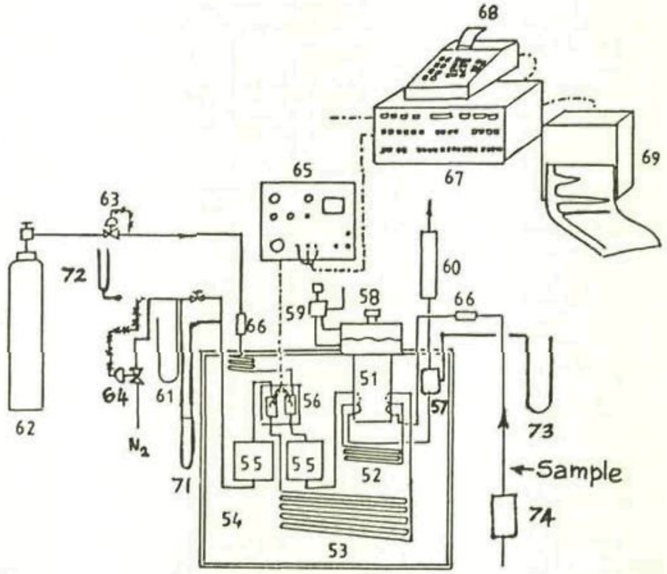

Fig. C.8 *The experimental set-up for the chromatographic analysis*

Table C.4. *The legend of the Fig. C.8 and the specifications*

51. Sample injection valve (Carle 6 port mini valve, 1 - 7 bar abs.)
52. Sample loop (0.8 mm dia, 60 cm length, 0.3 ml volume, SS 316)
53. Chromatographic column (Chromosorb 102 coated with 10% THEED, 100/120 mesh, 2.7 mm internal dia, 0.6 mm thickness, 3 m length, FEP material)
54. *Air thermostat (TH made, $0.1^{o}C$ accuracy, thyrister control)*
55. Buffer capacity vessel (5 cm dia, 5.5 cm length, 100 ml volume, SS 316)
56. Catharometer sensor (tungston-rhenium filaments, constant current, 2 cells - one for reference He and the other for the He-X mixture)
57. Buffer vessel having the sample line pressure tapping (100 ml volume)
58. GLC injection knob
59. Solenoid valve for the air supply to the injection valve (4.2 bar)
60. Sample flow rotameter (heated, Fischer-Porter 1/8-08-G-5/36, sapphire float)
61. Carrier gas outlet pressure manometer (90^{o}C and 724 - 794 mm Hg range)
62. Carrier gas cylinder
63. Carrier gas pressure control valve at the inlet (Brooks type 8601, variable downstream and constant upstream, max. temperature 140^{o}F, max. supply: 250 psi, output: 0 - 150 psi)
64. Carrier gas pressure control valve at the outlet (Brooks type 8601B, variable downstream and constant upstream, max. temperature 140^{o}F, max. supply: 250 psi, output: 0 - 10 psi)
65. Catharometer (TH Design, constant current, type A)
66. Filter for carrier gas/ sample gas (Nupro, pore size 7 micron, SS 316)
67. Integrator (Infotronics CRS - 208)
68. Printer (Monroe 1440 SN)
69. Strip chart recorder (Perkin Elmer 159, range:1 - 10 V)
71. Carrier gas capillary flow meter (0.4 mm capillary dia., 4 cm length, coloured silicon oil as the manometric fluid)
72. Bleed gas soap film flow meter
73. *Sample loop U - tube manometer ($90^{o}C$ and 120 mm Hg p)*
74. Mass flow meters (Hightech design, Inacom Instruments, max. flow: 100 ml/min at 20^{o}C, 3 bar min. and 64 bar max.)

The preparation of the calibration mixtures, namely N_2-CO_2 and N_2-NH_3, were carried out using thermal mass flow meters. The sample loop pressure was measured through a heated U - tube manometer (kept at 90^{o} to avoid the formation of ammonium carbamate). The total absolute sample pressure was taken to be the sum of the atmospheric pressure and that measured through the U-tube manometer. The sample flow rate (30 3 ml/min) was measured through a rotameter. Sample injection was done automatically every 15 minutes with the use of a timer. The total analysis time was around 12.5 min. The adopted experimental conditions are tabulated in Table C.5 and a sample chromatogram is shown in Fig. C.9.

The calibration results are shown in Fig. C.7. The reproducibility of the peak areas in any measurement was within 1% for all the components. The accuracy of the analysis as checked by the prepared mixtures containing nitrogen was 1% for CO_2 and around 1.5 % for NH_3. As for water, the accuracy was not checked by preparing mixtures of known composition. The calibration for all the components, being almost independent of the ambient fluctuations, were quite stable for at least approximately one month, after which recalibrations were found necessary. The reason for the long term drift could not be clearly ascertained.

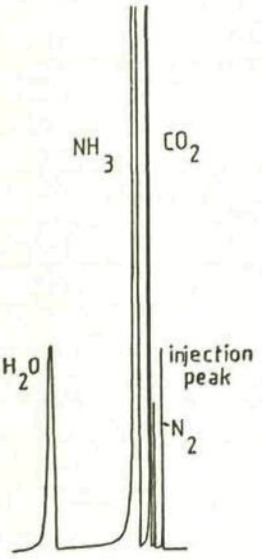

Fig. C.9. *A sample chromotogram*

Table. C.5. The experimental conditions.

Thermostat temperature	: 87.1°C
Carrier gas	: Helium
Flow rate	: 62.33 Nml/ min at 1 bar absolute and 0°C.
Sample loop volume	: 0.3 ml.
Column upstream pressure	: 3.65 (± 0.01 bar) abs.
Column downstream pressure	: 785 mm (± 1 mm) Hg. abs.
Sample flow rate	: 30 (± 3) ml/min
Range of sample pressures	: 740 - 860 mm Hg. abs.
Bridge current	: 100 mA.

References:

1 van Krevelen, D.W. et al., Recl. Trav. Chim., vol.68, 1949, p 191.

2. Kawasumi, S., Bull. Chem. Soc. Japan, vol.24, no.3, 1951, p 148.

3. Koren, J.G. and Andreatch, A.J., Anal. Chem., vol.37, no.2, 1965, p 256.

4. Lang, M.C., ISA proceedings, 1983, pp 457-465.

5. Baiulescu, G.E. and Ilie, V.A., "Stationary phases in gas chromatography", Pergamon Press, Oxford, 1975, p 169.

6. Jones, C.N., Anal. Chem., vol.39, no.14, 1967, p 1858.

7. Bathea, R.M. and Meador, M.C., J. Chromatog. Sci., vol.7, 1969, p 655.

8. Wilhite, W.F. and Hollis, O.L., J. Gas Chromatog., vol.6, 1968, p 84.

9. Mindrup, R.F. and Taylor, J.H., J. Chromatog. Sci., vol.8, 1970, p 723.

10. Müller, G., "Experimentelle untersuchung des dampf-flussigkeits-gleichgewichts im system ammoniak-kohlendioxid-wasser zwischen 100 und 200°C bei drucken bis 90 bar", PhD thesis, Universitat Kaiserslautern, 1983, 175 pages.

11. Lemkowitz, S.M., "Phase and corrosion studies of the ammonia - carbon dioxide-water system at the conditions of the hot gas recirculation process for the synthesis of urea", PhD thesis, Delft University of Technology, The Netherlands, 1975, 191 pages.

12. Pawlikowski, E.M. et al, I&EC Process Des. Dev., vol.21, 1982, pp 764-770.

13. Private communication from Dutch State Mines, The Netherlands.

14. Kiselev, A.V. and Yashin, Ya.I., "Gas adsorption chromatography", Pleanum Press, Chapter II, Ist edition, 1969.

15a. Gvosdovich, T.N. et al, Chromatographia, vol.11, no.10, 1978, pp 596-599

15b. Gvosdovich, T.N. et al, Chromatographia, vol.2, 1969, pp 234-238.

16. Hertl, W. and M.G.Neumann, J.Chromatog., vol.60, 1971, pp 319-327

17. Sze, L. et al., Anal. Chem., vol.35, 1963, p 241.

18. Moretti, E. et al., J. Chromatog. Sci., vol.12, 1974, pp 64-66.

19. Guichon, G. and Pommier, C., "Gas chromatography in inorganics and organometallics", Ann Arbor Science Publ., 2nd. ed., 1973, pp 16-17.

20. Reid, R.C., Prausnitz, J.M. and Sherwood, T.K., "The properties of gases and liquids", McGraw-Hill, Kogakusha Ltd., 3rd ed., 1974, p 508

21 Goedert, M. and Guichon, G., J. Chromatog. Sci., vol.7, 1969, pp 323-339.

22. Aldorf, H.E., "A study of the accuracy of gas chromatographic analysis, applied to the system N_2-CO_2-NH_3-H_2O", Internal report, Dept. of Chem.Eng., Delft University of Technology, 1971, 66 pages.

23. Verbrugge, P., "Vapour-liquid equilibria of the ammonia - carbon dioxide - water system", PhD thesis, Delft University of Technology, The Netherlands, 1979, 133 pages.

24. van der Steen, R., "GLC analysis in urea research", Internal report, Dept. of Chem. Eng., Delft University of Technology, 1983, 82 pages.

APPENDIX D

THE LIQUID PHASE ANALYSIS

D.1. *Introduction*:

The choice of liquid phase analysis procedures for the system NH_3-CO_2-H_2O depends on their suitability to the experimental set-up, their ease of performance, their reproducibility, precision and accuracy. All these factors strongly influence the measurement of the vapour-liquid equilibria leading to reliable and accurate data. However, before discussing these features, one should decide on the question of what to analyse: Is it the species concentration or the component concentration ?

The implication of this question is quite fundamental in describing the equilibrium situations. Although it is very desirable from a theoretical point of view to measure the species concentrations, it may not be always possible to do so due to some fast reaction-equilibria, which occur when changes of pressure and temperature takes place. Nevertheless, many attempts have been reported in the literature about the analysis of species concentrations of the system NH_3-CO_2-H_2O. The most notable in the ealy days was by Burrows and Lewis [1] who determined the extent of hydrolysis of ammonium carbamate at ambient conditions.

Barrows and Lewis analysed the concentrations of carbamate and carbonate individually by utilizing their different reaction rates with $BaCl_2$ in an alkaline media and the consequent effects on the solubility of barium salts of these anions. The same principle was adopted by Fourholt [2] and later by Christennsen et al [3] in a more refined way to determine the bicarbonate-carbamate equilibria. This method is, however, tedious and time consuming.

Lugowska [4] suggested a new method based on the different solubilities of carbamate and carbonate in 80% v/v aqueous solution of acetone. In this method, claimed to be completed in 20 min., the carbonate is easily precipitated as crystals and is quickly filtered out. The filtrate is then titrated with 0.5 M *o*-chloric acid using purple coloured o-bromocresol as indicator to determine the carbamate concentration. However, there is still one problem left unresolved, viz. the inability to distinguish between carbonate and bicarbonate.

Regarding the separate determinations of free and bound ammonia, number of methods have been mentioned in the literature. All of them exhibit problems of excessive time requirement, long term stability of reagents and also the need for many analytical steps leading to accumulated inaccuracies.

It is mainly due to these reasons that the attention in the present study was restricted to the analysis of component concentrations of NH_3 and CO_2 and not species concentrations excepting for one important species, namely urea. In what follows, the methods of analyses adopted in the present study are discussed in detail together with brief discussions about the alternative methods. Also a mention is made about the determination of potassium sulphate which was used in extremely small quantities in the liquid phase to aid the level determination through electrical contact.

D.2. *The ammonia analysis*:

D.2.1. *The possible procedures*:

There are many methods reported in the literature for the analysis of ammonia. The best known among them are, of course, the Kjeldal method [5] and the Nessler's method [6]. The other methods are the formaldehyde method [7], the ion selective electrode method [8], the steady state permeation method [9], the fluorescence method [10], the Stark magnetic cavity resonator method [11], the indophenol blue method [12] and the hypobromite reduction method [13]. There have also been some variations of these methods mainly with respect to the detection procedure adopted. All these methods are briefly described in the following sections. The method selected in the present study, the hypobromite reduction method, is discussed in detail with respect to principles, the analytical set-up and the results.

D.2.1.1. *The Kjeldal method*:

The Kjeldal method involves the addition of alkali, followed by distillation and then absorption in acid medium. It is further completed with a back-titration of the acid. Among the many variations of this method, one may describe the following one adopted by Verbrugge [5].

In this variation, no alkali is added prior to distillation. Also the distillation is completed in a very short duration of about 9 min. Weak boric acid is used as the absorbent. The pH of the acid (~4.7), measured initially, is used as a set point to drive an acid addition pump handling dilute HCl. As the pH increases, due to absorption of distilled ammonia, dilute HCl solution is continuously added to maintain the pH. The titration is recorded in a strip chart giving the volume of the titrant added as a function of time. The method is highly accurate in determining the bound ammonia, although the time taken for one determination is around 15 min.

D.2.1.2. *The Nessler's method*:

In this method [6], the Nessler's reagent (K_2HgI_4 - prepared as an alkaline solution of mercury (II) iodide and potassium iodide) reacts with ammonia to form a reddish-brown colloidal compound with the empirical formula $NH_2Hg_2I_3$. The solution is then analysed colorimetrically in the region of wavelengths around 400 to 425 nm. The accuracy of this classical method in the high concentration ranges of this study is not too high, being only of the order of 3 to 5 %. Also the interference problems are difficult to handle.

D.2.1.3. *The formaldehyde method*:

In the formaldehyde method [7], two variations are possible. In the first one, the formaldehyde reaction, written below for a typical case of ammonium chloride, is used really as a check procedure and not as an estimation method, while in the second it is directly used for estimation.

$$4\ NH_4Cl + 6\ HCHO \rightarrow (CH_2)_6N_4 + 4\ HCl + 6\ H_2O \qquad \text{(eq. D.1)}$$

In the first variation, the cold sample containing ammonium carbonate, bicarbonate and carbamate together with free ammonia is first quickly reacted with an excess of either HCl or H_2SO_4 and further boiled to release all the CO_2. The excess acid is then titrated with alkali. The titre value is subtracted from the original amount to yield the amount of the acid consumed, which is then related to the total ammonia. This estimation is cross-checked by reacting the titrated solution with formaldehyde as per (eq. D.1) to regenerate the consumed acid. The regenerated acid is further titrated with alkali to yield the acid consumed for conversion into NH_4Cl from which one can easily calculate the amount of total ammonia present in the sample.

In the second variation, the formaldehyde is quickly added in excess to the sample containing ammonium carbonate salts and free ammonia to give off CO_2, which is then slowly fixed by alkali through titration. Of couse it is essential that the evolved CO_2 is not lost from the vessel during titration. The consumed alkali quantity will then be directly related to the bound ammonia. However, free ammonia cannot be detected by this second variation.

Both the variations are time-consuming and are not easily amenable to automatic analysis, and hence have not been preferred by many users.

D.2.1.4. *The ion selective electrode method*:

The ion selective electrode is suitable only for low concentrations (around 1%) of total ammonia in aqueous solutions beyond which there is predominantly a nonlinear response. Hence the sample to be analysed has to be diluted manyfold before actual estimation. Correspondingly the error caused by dilution can be very high, even though the accuracy of the determination around 1% concentration is reported [8] to be good. Also to improve accuracy, the electrode has to be kept at constant temperature during analysis.

D.2.1.5. *The steady state permeation method*:

This method is based on appropriately altering the sample pH and allowing the transfer of NH_3 through hollow fibres (made of silicone rubber) [9] into a flowing stream of water, followed by detection using electrical conductivity. The system depends on steady state transfer rather than equilibrium transfer of the gas from the sample stream into the water stream. Hence, the typical analysis time is only around 100 s. The method is claimed to be faster, and easier to operate. Also the method can work with smaller, turbid or even coloured samples.

D.2.1.6. *The flourescence method*:

The flourescence method [10] depends on the reaction of ammonia with *o*-phthaldialdehyde (OPA) in the presence of 2 - mercaptoethanol (MCE) to produce the isoindole flourospore, whose structure is unknown. Molecular ammonia liberated by mixing the sample solution with 1 N NaOH permeates through a microporous PTFE membrane into a buffered OPA reagent stream in the inner tube. The reaction product is fed to the flow cell of a flourimeter and the flouroscence intensity is measured at 486 nm with the excitation at 370 nm. This method is very suitable for determining ammonia in environmental samples in the region from $2 * 10^{-7}$ to $2 * 10^{-4}$ M with the relative standard deviations at a pH of 13 being around 4.4 % to 1.8 %. The analysis time is around 6 min.

D.2.1.7. *The Stark magnetic cavity resonator method*:

In this method [11], the NH_3 in the sample is first liberated under alkaline conditions and is transported by permeation through a teflon membrane. It is later carried by the nitrogen carrier into a Stark magnetic cavity resonator. The steady state potential is obtained within 5 min. Using the calibration plot of the potential difference vs the concentration of ammonia, the unknown concentration can be found. The calibration is reported to be linear upto 2 mg/l. Also there appears to be very little interference problem. The reported accuracy is around 2 %. The system is eminently suitable for continous determination of environmental samples, and it can remain stable for a long time.

D.2.1.8. *The indophenol blue method*:

In the indophenol blue method [12a], a solution of ammonium salts in the presence of hypochlorite reacts with sodium phenoxide to give indophenol blue. The chemistry of this reaction is very old and the Association of Official Analytical Chemists (AOAC) has recommended this procedure [12b] as one of the most reliable ones. However, the method is reported to have an interference problem due to alkaline urea hydrolysis. The simplest way to eliminate such urea bias is by mathematical accounting, since the interference is linearly related to the amount of urea present.

Once the reaction with sodium phenoxide is completed and the colour is formed, the intensity of the sample colour is measured at 550 nm and the value is read through a calibration graph to give the ammonia concentration. The method is easily automated when the sampling rate is as much as 10 to 20 samples per hour. The standard deviation of ammonia estimation by this method has been reported [12b] to be 0.43% and that of the coefficient of variation 2.16%.

D.2.1.9. *The hypobromite reduction method*:

The last one, namely the hypobromite reduction method, involves the following reaction of ammonia with alkaline hypobromite to liberate nitrogen along with the generation of bromide ion [13].

$$2\ NH_3 + 3\ BrO^- \dashrightarrow 3\ Br^- + N_2 + 3\ H_2O \qquad \text{(eq. D.2)}$$

This method is free from interference by all substances which do not liberate nitrogen by reaction with hypobromite. Notable in these groups of substances are the amines, amides and proteins, although urea and hydrazine do interfere to some extent, especially at high temperatures.

There are three variations of the hypobromite reduction method. In the first variation [14], the nitrogen liberated by the hypobromite reduction is stripped from the solution and is transported by a carrier into a gas chromatograph where its concentration is determined using molecular sieve as the column material. This value is then related to the total ammonia present in the sample. In the second variation [15], an indirect spectrophotometric detection is used. The third variation [16] depends on the *in-situ* generation of bromine from bromide followed by its reaction with the hydroxyl ion to generate the hypobromite. Subsequently the hypobromite reacts with ammonia as per the above reaction (eq. D.2). This entire procedure is known as coulometric titration and it has a number of advantages such as:

1) The amount of the sample can be extremely small with no loss in accuracy of the determination.
2) Standard solutions need not be prepared, and calibrations need not be done, since this is an absolute method.
3) Substances which are unstable or volatile (as in the case of bromine) can be used as titrants.
4) The procedure can be easily automated and performed remotely, if needed.
5) Dilution effects do not occur and end-point detection is much simpler. It is also possible to incorporate coulometric titrations in continuous process stream analyzers.

D.2.2. *The analytical set-up and the procedure adopted in the present study for ammonia determination*:

The analytical set-up consists of a titration vessel, a titrant generation system and an indicator system, as shown in Fig. D.1. The titration vessel, placed on a base containing a magnetic strirrer, consists of a working cathode (+), an auxillary counter-anode (-) encased by a protective membrane separator, and also a pair of indicating electrodes. The working electrolyte consists of approximately 40 ml of KBr-Borax buffer (containing 5 mol/l KBr and 0.1 mol/l borax in a ratio of 2:5 with pH adjusted to 8.6 by the addition of 2 mol/l HCl). The counter-electrode is also filled with the same KBr-borax buffer (but with a different ratio, namely 1:1, without any adjustment of pH).

As part of the generation system, the working electrode and the counter-electrode are connected to an electronic constant current source (the coulostat) through a double-pole-double-throw (DPDT) switch which simultaneously activates a timer on closing. The current will remain constant as long as the reversible cell potential and cell resistence are small compared to the applied voltage and circuit resistence. With the present coulostat, one can choose a current in the range of 0.04825 to 4825 mA (or in terms of ueq/sec, $5*10^{-}$ to 5). Ideally the titration time is around 4 minutes. There is also a provision to adjust the current in a controlled fashion rather than keeping it constant. In that case, the integrator attached to the coulostat computes the amount of charge consumed for the titration. In a typical measurement, the current may be maintained constant until reaching close to end-point beyond which the current may be advantageously varied to find the titration end-point accurately.

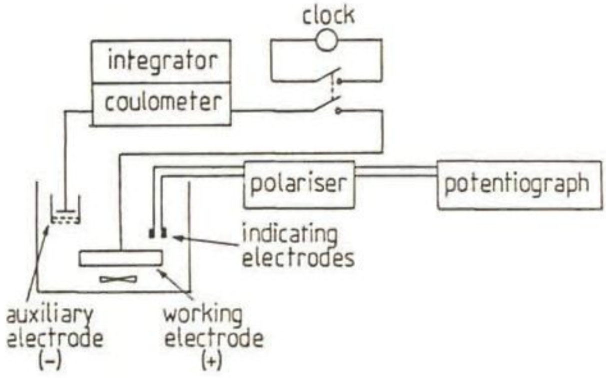

Fig. D.1. *The analytical set-up for the hypobromite method.*

The working principle of the end-point indicating system is by potentiostatic amperometry. In this system a constant voltage of 20 mV is impressed between the poles of a double platinum indicating electrode with the aid of a polarizer. The current between the poles depends on the fraction f of BrO^- in the total of Br^- and

BrO^- present in the titration vessel. When f is zero, the current-potential curve is similar to the top curve in Fig. D.2 and the indicating current is very low for the applied potential difference of 20 mV. When the f value becomes greater than 0, the running current becomes higher, as given in the bottom curve of Fig. D.2. In the polarizer, the running current between the indicating electrodes is transformed into a voltage with the help of resistors (i.e. 20 uA -- 1 V) and is fed into a potentiograph. When the indicating voltage becomes higher *than 100 mV, the potentiograph automatically* stops the titration.

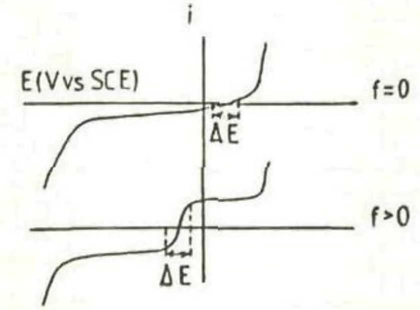

Fig. D.2. *The current-potential behaviour for (f=0) and (f>0).*

Once the sample containing ammonia is added into the titration vessel and a suitable current is chosen, the coulometric titration proceeds according to the following reactions.

At the working electrode: $2\ Br^- \rightarrow Br_2 + 2\ e$ (eq. D.3)

At the counter electrode: $2\ H_2O + 2\ e \rightarrow 2\ OH^- + H_2$ (eq. D.4)

In the solution: $Br_2 + 2\ OH^- \rightarrow Br^- + BrO^- + H_2O$ (eq. D.5)

$2\ NH_3 + 3\ BrO^- \rightarrow 3\ Br^- + N_2 + 3\ H_2O$ (eq. D.2)

Further there is a side reaction of bromine with the hydroxyl ion giving rise to bromate if the pH is not maintained around the pH of 8.6

i.e. $3\ Br_2 + 6\ OH^- \rightarrow 5\ Br^- + BrO_3^- + 3\ H_2O$ (eq. D.6)

If this side reaction takes place, then some amount of the electrogenerated bromine is lost and quantitation of ammonia through the consumption of charge is not possible. It is for this reason that there is also a provision in the analytical set-up to *add 6 mol/l HCl* to the titration vessel, if the pH drifts from the value maintained above. (Note: The pH of 0.1 mol/l of sodium tetraborate decahydrate, i.e.the borax, is around 9.2)

As long as ammonia consumes the hypobromite and is in excess, the indicating voltage will be very low (< 20 mV). It will become very high however, once all the ammonia is reacted and the ratio of BrO^-/Br^- becomes very high. *As mentioned earlier,* the titration is stopped when the indicating voltage reaches a value of 100 mV. Also to approach the endpoint more carefully, the potentiograph has the facility to contol the current of the coulostat. Once this regulating action is started, the coulometer current is no longer constant and the current is then integrated. Now, knowing the charge consumed for the titration (or knowing the ueq consumed) one can multiply the same with the equivalent mass of ammonia (i.e., the molecular mass of ammonia divided by the number of electrons involved in the reaction) to get the concentration of ammonia in gm/l. An example calculation will be as follows:

The value of the micro-equivalents read from the coulometer - 30.73
The equivalent mass of ammonia - 17.01/3 - 5.67
The concentration of ammonia - 30.73 * 5.67 - 174.24 mg of ammonia/l.

D.3. *The carbon dioxide analysis*:

Of the various methods possible for the determination of CO_2, only two are described here in detail, in view of their reliablity and accuracy. There is also the steady state permeation method similar to the one described in the determination of ammonia, except for the difference in the preferred medium (which in this case is acidic) for the liberation of CO_2. The liberated CO_2 further permeates into the receiving stream through a teflon membrane and the conductivity of the receiving stream is determined and related to the CO_2 concentration by means of a calibration.

D.3.1. *The potentiometric titration method*:

In this method [17], NaOH is first added in excess to convert all CO_2 and HCO_3^- present in the sample into $CO_3^{=}$ as per the following reactions.

$$CO_2 + OH^- \dashrightarrow HCO_3^- \qquad \text{(eq. D.7)}$$

$$HCO_3^- + OH^- \dashrightarrow CO_3^{=} + H_2O \qquad \text{(eq. D.8)}$$

Simultaneously the ammonium ion is transformed into ammonia at this high pH.

$$NH_4^+ + OH^- \dashrightarrow NH_3 + H_2O \qquad \text{(eq. D.9)}$$

As for carbamate, it is hydrolysed to carbonate and ammonium ions as per the following reaction. The freshly generated ammonium ion is further converted to free ammonia as per (eq. D.9).

$$NH_2COO^- + H_2O \dashrightarrow NH_4^+ + CO_3^{=} \qquad \text{(eq. D.10)}$$

Now the solution contains only the anions OH^- and $CO_3^{=}$, free NH_3 and the cations Na^+ and H_3O^+. The ammonia is expelled by vacuum evaporation so that it does not interfere in the titration against HCl. The titration endpoint is followed by potentiometry.

Titration against the H_3O^+ ions first brings about the neutralization of the OH^- ions followed by conversion of the $CO_3^{=}$ ions into HCO_3^-. Further the HCO_3^- ions are converted into CO_2. As a result, one must see jumps to three potential levels (or three deriative peaks) in the potential (E) vs the titrant volume (V) behaviour. In practice, there is only one jump and hence two derivative peaks (i.e. 2 numbers of dE/dV vs V peaks). This is mainly due to the fact that the last two transformations occur almost simultaneously and only the neutralization of OH^- ions get separated from the other two. The relevent titration reactions are:

$$OH^- + CO_3^{=} + 2\ H_3O^+ \dashrightarrow HCO_3^- + 3\ H_2O \qquad \text{(eq. D.11)}$$

$$HCO_3^- + H_3O^+ \dashrightarrow CO_2 + 2\ H_2O \qquad \text{(eq. D.12)}$$

The titration procedure is quite simple. First, 10 ml of the sample is pippetted into a 150 ml beaker along with the addition of 2 ml of 4 mol/l NaOH. Later, a few boiling stones are added to overcome the boiling delay which occurs under vacuum. The beaker is then kept under vacuum. Simultaneously, nitrogen at a pressure of 30 mbar and a temperature of 40°C is sent in to strip off ammonia. Whenever the the sample pH rises above 10, it is brought back to that value by the addition of 6 mol/l of HCl. Once the ammonia is stripped, the potentiometric titration using a "Metrohm potentiograph E536" is started with the addition of 0.1 mol/l of HCl. Throughout the titration, nitrogen is continously bubbled.

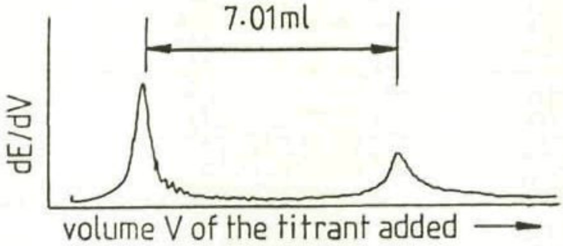

Fig. D.3. *The derivative peak diagram of the CO_2 estimation by potentiometry. dE/dV is the derivative of the potential (E) - titrant volume (V) behaviour.*

A typical derivative peak diagram is shown in Fig. D.3. Calculation of the total CO_2 concentration proceeds the same way as in any titration, once we know the volume of the titrant added between two peaks.

D.3.2. The determination of CO_2 by the permeation method using the auto-analyser and *the colorimetric detection system*:

This method is very similar to the permeation method of R.M.Carlson except in the detection procedure used. In both the methods, the sample is first acidified to convert all carbonates, bicarbonates and carbamates into free CO_2 and is made to pass through one side of a permeable membrane (made of silicon rubber). Simultaneously a water stream is passed through the other side of the membrane. As a result, a steady state transfer of CO_2, rather than an equilibrium transfer, occurs. The amount of CO_2 diffused is measured through colorimetry in the present method while Carlson has measured it by a conductimetric method. Both the methods are faster and easier to automate. They can also be used with smaller samples. The only drawback of the colorimteric detection as against the conductimetric detection is its inability to tolerate coloured or turbid solution without pretreatment. Fortunately the samples of the present study did not pose this problem. Both the detection methods give *comparable accuracies* (1 to 2%) and precisions (max. 1% standard deviation).

In the present study, the CO_2 is analysed through an auto-analyser AAII system supplied by the Technicon of USA. This system is usually offered with a number of modules suitable for different analyses [18]. Depending on the situation, particular modules are chosen and assembled. For analysing CO_2, the chosen module assembly with silicon rubber tubings is as shown in Fig. D.4.

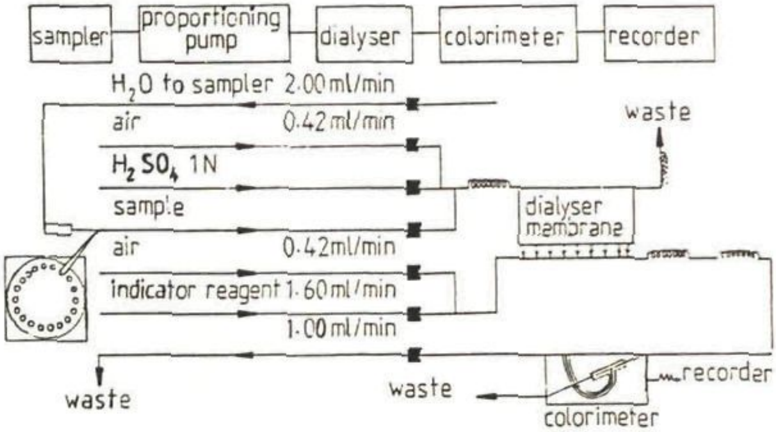

Fig. D.4. *The auto-analyzer module assembly for the colorimetric determination of carbon dioxide.*

The flow rates chosen for various streams are also indicated in Fig. D.4. The sample and the sulphuric acid flowrates *are chosen in different ratio depending on* the concentration range of CO_2 to be analysed. It can be observed from the figure that the diluted sample mixes with the air-segmented 1 N H_2SO_4 and passes through a mixing coil before entering the dialyser. Simultaneously the air-segmented indicator solution containing the colour reagent enters the other side of the membrane. The composition of the colour reagent is as follows:

0.04 g/l cresol red, sodium salt, 0.002 ml/l NH_3 solution sp.gr. 0.88
0.327 g/l tris (hydroxymethyl) methylamine, 1.0 ml/l brij 35 (a surfactant)

The above indicator reagent is to be normally kept under a nitrogen flow to avoid any contamination.

Once CO_2 diffuses through the membrane, then the indicator solution at the exit of the dialyser is taken to two long mixing coils in series and further to a colorimeter. Using a 50 mm flow cuette, the absorbance measurement is carried out at 550 nm wavelength. The stream at the exit of the colorimeter is taken to a proportioning pump from where it is sent to waste.

Since the CO_2 concentrations of the VLE samples are quite high, they are appropriately diluted so as to be in the linear region of the calibration graph. A calibration graph in the concentration range of 0 - 2000 mg/ml is shown in Fig. D.5.

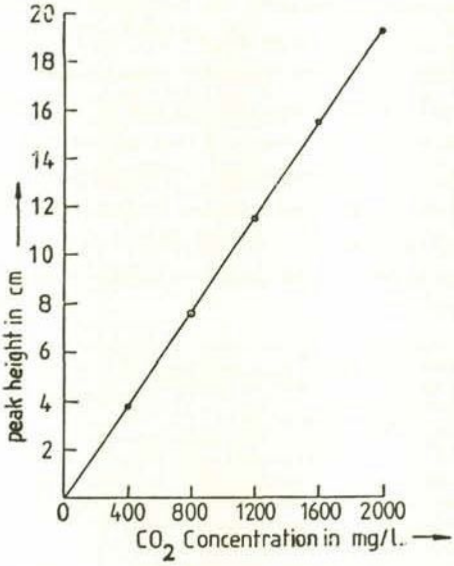

Fig. D.5. *The calibration graph for CO_2 estimation in the range of 0 - 2000 mg/l.*

D.4. *The determination of urea concentration using the auto-analyzer and the colorimetric detection system*:

Having looked at the determination methods of NH_3 and CO_2, one should now move to the determination of urea. In the present VLE study at the temperature and pressure ranges chosen, the formation of urea appears to be a significant but small quantity. The reason for analysing the urea concentration is to confirm whether the inclusion of the urea formation reaction in the proposed model is justified.

There are basically two different complexing reactions which are used for the determination of urea through colorimetry. Urea at high concentrations (0-300 g/l) is normally analyzed in urea industries [18] with para-dimethyl-amino-benzaldehyde (DMAB) as the reagent. In mildly acidic conditions urea forms a yellow coloured complex with DMAB. Subsequently the colour of the complex is measured at a wavelength of 440 nm. *The lowest range to which the DMAB method can be applied is only 0-120* mg/l. Urea at lower concentrations is measured through another method [19] based on the direct reaction of urea with diacetyl monoxime in the presence of thiosemicarbazide in mildly acidic conditions. The presence of thiosemicarbazide intensifies the colour of the reaction product. The absorbance is measured at a wavelength of 550 nm. Unlike that observed in the DMAB method, the ammonium ion does not interfere in the diacetyl monoxime method. In this section the diacetyl monoxime method is described in detail.

The analytical set-up assembled with the modules of the autoanalyzer AAII system is shown in Fig. D.6. The standard solutions and the unknown samples are placed on the sample tray. The pump transports the samples to the analytical unit where it is first mixed with the working bun colour reagent and then with the working bun acid. After this mixing, the stream is taken to a heating bath of 95°C to accelerate the formation of the colour. In the photometer, the absorbance is measured at 550 nm. Also the electrical signal from the photometer is led to a recorder. The concentration of the unknown samples are read from the calibration graph shown in Fig. D.7. The typical absorbance peaks for the chosen concentrations of the calibration are given in Fig. D.8.

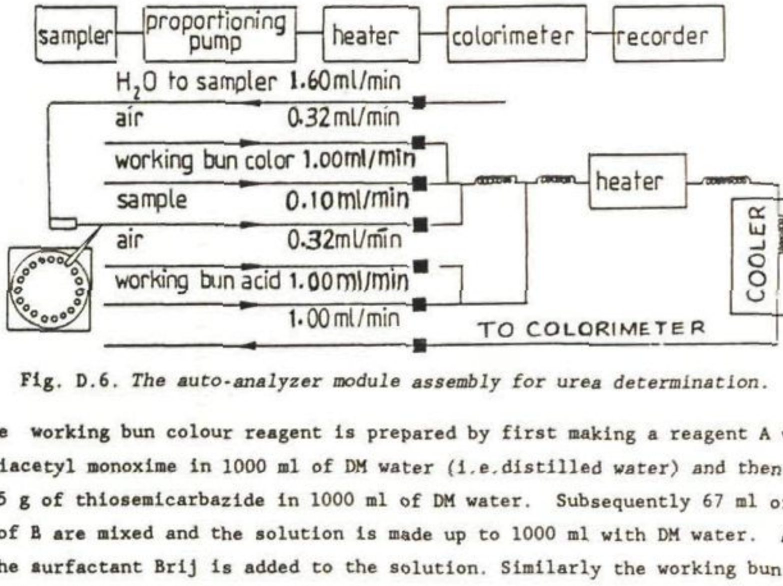

Fig. D.6. *The auto-analyzer module assembly for urea determination.*

The working bun colour reagent is prepared by first making a reagent A with 25 g of diacetyl monoxime in 1000 ml of DM water *(i.e. distilled water)* and then *reagent* B with 5 g of thiosemicarbazide in 1000 ml of DM water. Subsequently 67 ml of A and 67 ml of B are mixed and the solution is made up to 1000 ml with DM water. Also 0.5 ml of the surfactant Brij is added to the solution. Similarly the working bun acid is prepared by mixing 1 ml of reagent C and 999 ml of reagent D where reagent C is 15 g of $FeCl_3.6H_2O$ and 300 ml of 85% H_3PO_4 in 500 ml of DM water, and reagent D is 200 ml of 96% H_2SO_4 in 1000 ml of DM water.

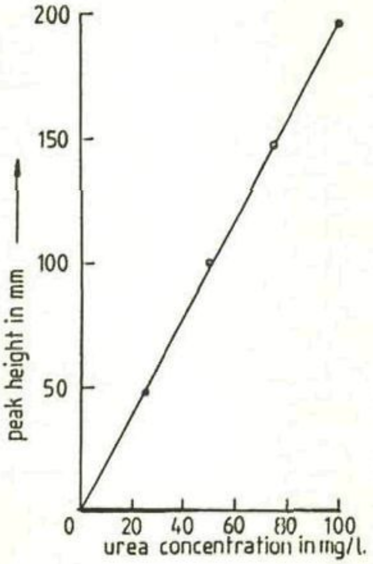

Fig. D.7. *The calibration graph for the urea determination.*

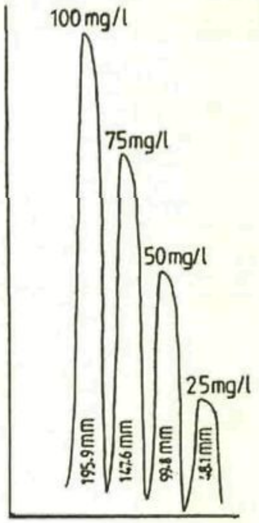

Fig. D.8. *The typical absorbance peaks for the urea determination.*

D.5. *The determination of potassium sulphate*:

In addition to the above three determinations, namely NH_3, CO_2 and urea, there is one more analysis due to addition of micro quantities of potassium sulphate at the starting of each series of VLE measurement. It may be remembered that each series of VLE at one particular pressure and temperature is always started with the binary CO_2-H_2O and proceeded further with additions of NH_3. At the binary CO_2-H_2O measurement, the conductivity of the liquid phase is quite low leading to inability of the level electrode to detect the level. This can be obviated by the addition of an ionic salt which increases conductivity. Extremely small amount of potassium sulphate (ca. 0.01 to 0.05 weight % of the total liquid phase) adequately served this purpose. Further, the extent of potassium sulphate can be determined either by analysing potassium through flame photometry or by analysing sulphate through polarography. Here only the polarographic procedure [20] is described in brief.

First 5 ml of the sample in a titration vessel is brought to alcoholic conditions (approximately 50 %) by the addition of 15 ml of 96 % ethanol. This is followed by the addition of 1 ml of 1 % gelatine solution. The pH of the solution is then brought to 2 by the addition of 65% HNO_3. Subsequently nitrogen gas is sparged through the sample solution to strip off any CO_2 being present. Now 0.1 ml of 0.33% lead nitrate solution is added to precipitate part of the sulphate as lead sulphate.

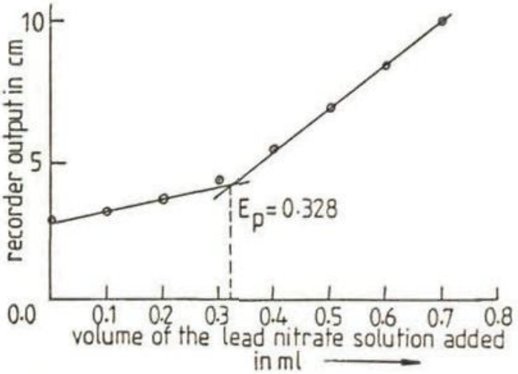

Fig. D.9. *Sulphate estimation: The graph is used to find out the volume of the lead nitrate solution needed to precipitate all the sulphate.*

$$Pb^{2+} + SO_4^{2-} \text{ --- } PbSO_4 \qquad \text{(eq. D.13)}$$

The nitrogen bubbling is continued throughout the precipitation (at least for 3 min). Now a voltage of - 0.6 V which is more negative than the half wave potential of Pb^{2+} / Pb(Hg) is applied between the working electrode and the counter-electrode. This process of measuring the diffusion limited current at a constant voltage of - 0.6 V is continued for each further addition of 0.1 ml of lead nitrate solution. Once all the sulphate in the sample is precipitated, the concentration of Pb^{2+} starts raising steadily and the measured current also does accordingly. Hence by following the limiting current against the cumulative addition of lead nitrate solution, one gets a curve given in Fig. D.9.

It can be seen from the figure that the first few points and the last few points form two separate straight lines. The intersection point obtained by extending these straight lines gives the amount of the lead nitrate solution which is just required to precipitate all the sulphate. From this volume, the concentration of sulphate present in the sample is easily calculated. In this estimation, ions like Cl^-, Br^-, I^- and $CO_3^{=}$ interfere in the analysis, while the ammonium ion does not interfere.

Reference:

1. Burrow, G.H. and G.N.Lewis, "The equilibrium between ammonium carbonate and ammonium carbamate in aqeous solution at 25°", J.Am.Chem.Soc., 1912, vol.34, pp 993-995.
2. Fourholt. C.K., Dan. Vidensk. Selsk., Mat.-Fys. Medd. 1921, vol.3, p 20.
3. Christensson. F. et al., "Equilibrium constants in the ammonium carbonate-carbaminate system. The acid dissociation constant of carbamic acid", Acta Chemica Scandinavia, 1978, vol. A32, No.1, pp. 15-17.
4. Lugowska. M., "New method of determination of ammonium carbonate and ammonium carbamate", Zeszety Nauk. politech. Slaskiej. Chemia, 1972, vol.60, pp 27-37.
5. Verbrugge,P."Vapour-liquid equilibria of the ammonia-carbondioxide-water system" PhD thesis, Delft University of Technology, The Netherlands, 1979, 133 pages.
6. Williams, S.,"AOAC official methods of analysis", 1984, 14th edition, pp623-624.
7. Medbedovskij. B. et al, "Process for the determination of bound ammonia", Russian patent no. 637669. 18 dec 1978, CA. 90:97074W
8. Viswanathan, T.S. et al., "Determination of ammoniacal nitrogen in the presence of urea", J.Assoc.Off.Anal.Chem., 1980, vol.63, No.6, pp 1248-1253
9. Carlson. R.M., "Automated separation and conductimetric determination of ammonia and dissolved carbon dioxide", Anal. Chem., 1978, vol.50, no.11, pp 1528-1531.
10. Aoki. T. et al, "Continous flow fluorimetric determination of ammonia in water", Anal. Chem., 1983, vol.55, pp 1620-1622.
11. Hirose, S. et al, "Determination of ammonia with a stark microwave cavity resonator", Anal.Chem. 1982, vol.54, pp 1690-1692.

12a. Rossum, J.R. and P.A.Villarruz, "Determination of ammonia by the indophenol method", J.Am.water works assocn., 1963, vol.55, p 657

12b. Gerke. C.W. et al., "Automated methods for total nitrogen, direct available P_2O_5 and K_2O in fertilizers", Technicon symposium, Automation in analytical chemistry, New York, N.Y., 1967, pp 241-243.

13. Schilbach. U. and E.M.Kirmse, Chem. Anal., 1978, vol. 23, no.6, pp 1025-8.(German) CA:90.202690.
14. Jenkins et al, Anal. Chem, 1966, vol.38, no.8, pp 1257-1258.
15. Halase, A. et al., "Rapid determination of bound nitrogen in the form of an ammonium ion or urea using the hypobromite ion. I. Spectrophotometric method", Acta Chim. (Budapest), 1973, vol.78, No.2, pp 129-32 (German).
16. Borecky. K. et al, Czech. patent 176532,(cl. G01N27/00), 1979, CA:90.161758
17. Vassos, B.H. and G.W.Ewing, "Electroanalytical chemistry", chapter 15, 1983, pp 208-217.
18. Wrightman, K.B., "Simultaneous automated determination of urea, ammonia, and ammonium nitrate", Advan. automat. anal., Technicon int. congr., 1969 (Publ. 1970), No.2, pp 61-67.

19. Siegert, J. "Research report on urea synthesis project", Delft University of Teccnology Internal report, 1984, 83 pages.

20. Meites, L.,"Polarographic techniques" chapter 2, 1958, 2nd. edition, Wiley-Interscience, New York.

SAMENVATTING

Deze dissertatie gaat over studies van het vloeistof-dampevenwicht van het reagerende systeem ammoniak-kooldioxide-water (met daarin de evenwichtsconcentraties van ureum) in een druk- en temperatuurgebied, resp., $5.41 < p < 30$ bar en $88.7^{o} < T < 130^{o}$ C. De noodzaak om dit onderzoek te doen ontstond uit voorgaande research betreffende een nieuw process om ureum te synthetiseren, namelijk het Heet Gas Recirculatieprocess (HGRP). In het bijzonder hebben de Delftse onderzoekers S.M.Lemkowitz en P.Verbrugge aan dit onderwerp, en de daarbij behorende fasenevenwichten, gewerkt en erover gepubliceerd.

Deze dissertatie bestaat uit 6 hoofstukken en 4 appendices. Het eerste hoofd stuk begint met een uiteenzetting van de relevantie van ureum bij het helpen oplossen van de wereldvoedselproblematiek. Daarna wordt het probleem van het optimaal gebruik van plantcapaciteit besproken, vooral met betrekking tot ontwikkelingslanden. Vervolgens worden enkele fundamentele kenmerken van de ureumsynthese uiteengezet, met name het energie-intensieve karakter van de synthese en de technologische achtergronden van de methoden die gebruikt (kunnen) worden om deze energiebehoeften te verkleinen. In dit kader wordt het onderzoek van de Technische Universiteit Delft om het HGRP nieuw leven in te blazen belicht. Het hoofdstuk eindigt met een uiteenzetting van de organisatie van het huidige researchwerk, zoals het gepresenteerd wordt in deze dissertatie.

Hoofdstuk 2 bespreekt moleculaire aspekten van de basiscomponenten, namelijk NH_3, CO_2 en H_2O, en ook de fasenevenwichten van de belangrijke binaire systemen, NH_3-H_2O, CO_2-H_2O, NH_3-CO_2, H_2O-NH_2CONH_2 (ureum), NH_2CONH_2-NH_3 en NH_2CONH_2-CO_2. Bovendien worden de moleculaire aspekten van ureumachtige stoffen, in het bijzonder carbaminezuur, behandeld. Deze discussies hebben twee doelstellingen. Ten eerste zijn ze bedoeld om de lezer enig inzicht te geven in de complexiteit van de desbetreffende systemen. Ten tweede wordt hiermee het gebruik van verschillende parameters, die worden gebruikt in het Hoofdstuk 5 ontwikkeld model, gerechtvaardigd.

Het derde hoofdstuk begint met een discussie van de multi-fasenevenwichten van het tenaire systeem NH_3-CO_2-H_2O zonder de aanwezigheid van ureum. Eerder gepubliceerde onderzoekingen worden kritisch bekeken, en het meest waarschijnlijk geachte fasengedrag van het systeem bij de tot nu toe niet onderzoekte hogedrukgebieden wordt in detail geschetst. Daarna worden enkele belangrijke details van dit fasengedrag apart besproken, met name de topologie van de kook- en dauwpuntoppervlakken, inclusief de vorm van de toprichellijnen van deze oppervlakken, en de residu- en distillatie-curven van dit systeem, in het bijzonder de grensdistillatielijnen. Daarna wordt het fasengedrag van het ternaire systeem $(2NH_3)$-NH_2CONH_2-H_2O

besproken. Om de fasenevenwichten van chemisch reactieve systemen, zols het systeem NH_3-CO_2-H_2O, te presenteren en te begrijpen, blijkt het concept van "manifolds" nuttig te zijn, en dit concept wordt daarom kort besproken. Hierna volgt een uiteenzetting van het (vijfdimensioneel) fasengedrag van het kwaternair systeem ($2NH_3$)-CO_2-H_2O-ureum en de eventuele transformatie van dit systeem tot het (vierdimensioneel) ternaire system ($2NH_3$)-CO_2-H_2O met evenwichtconcentraties van ureum.

In het vierde hoofdstuk wordt de ratio achter de keus van de meetmethode en het experimenteel systeem besproken. Hierna volgt een bespreking van het systeem en de onderdelen ervan en de experimentele procedures; ook experimentele moeilijkheden en de passende oplossingen worden genomed. De controlemeetingen van het meetsysteem, d.w.z. de fasenmetingen aan het bekend binaire systeem NH_3-H_2O worden gepresenteerd. Hierna volgt in detail een uiteenzetting en bespreking van de gemeten vloeistof-dampfasenevenwichten van het gekozen systeem binnen de al genoemde druk- en temperatuurgrenzen. Complementaire resultaten, verkregen door andere onderzoekers, worden bij deze uiteenzetting en discussie uitvoerig betrokken.

Hoofdstuk 5 begint met een review van de theorie van oplossingen van electrolyten; hierin speelt de theorie van Pitzer een bijzondere rol. Het grootste gedeelte van dit hoofdstuk gaat achter over de ontwikkeling van een eigen moleculair-thermodynamischmodel dat het gemeten fasengedrag kan beschrijven. Het ontwikkelde model blijkt de meeste experimentele data bevredigend te beschrijven. Rond de gebieden dichtbij de binaire systemen NH_3-H_2O en CO_2-H_2O is de overeenkomst tussen de metingen en de met het model berekende waarden echter minder dan bevredigend. Dit verschil zou misschien kunnen worden veroorzaakt door het gebruik van de objectieve funktie, die niet gewogen is. Een ander probleemgebied ligt rond de uiterste van de (bij constante druk en temperatuur) tongachtige vloeistofcurve; de uiterste van dit gebied is echter zeer gevoelig voor zelfs kleine fouten in de analyse. Een belangrijke conclusie betreffende de opzet van het model is, dat bij de gemeten condities het meenemen van de ureumvorming samen met de incorporatie van de ionische reacties van doorslaggevende betekenis is.

In Hoofdstuk 6 worden het eigen fasenmodel, samen met andere gepubliceerde modellen betreffende dit systeem, in combinatie met de principes van de fasenleer, zo veel mogelijk gebruikt voor procesontwerp, in het bijzonder toegepast op een verbetere versie van het Heet Gas Recirculatieproces (HGRP) voor de produktie van ureum. Een nieuwe ontwerpbenadering wordt gekozen waarin men simultaan streeft naar een minimale reactordruk, een maximale conversie, een optimale temperatuur en een optimale NH_3/CO_2-verhouding voor een gekozen H_2O/CO_2-verhouding. Gebruik makend van de genoemde modellen en principes worden de condities van de reactor, hoge-druk condenser en stripper zo volledig mogelijk berekend. Ook de compressoren voor de recirculatie van het heet-gasmensel en voor de aangevoerde CO_2 wordt berekend. Een optimalisatieprocedure voor het bepalen van een optimale stripperdruk wordt geschetst. Bij al deze berekeningen spelen samen met de gekozen modellen de numerieke waarden van veel thermodynamische gegevens, waarvan veel niet of onvoldoende nauwkeurig bekend zijn. Hierdoor is het onmogelijk een nauwkeurige economische vergelijking te maken tussen een HGRP en een stripping proces.

De dissertatie eindigt met een viertal appendices. Appendix A behandeldt de vast-dampfasenevenwichten van ammoniumcarbamaat. Deze gegevens zijn nuttig voor het bepalen van het druk-temperatuurgebied waarin alleen vloeistoff-dampevenwichten bestaan over het gehele samenstellingsgebied. Appendix B houdt zich bezig met het bepalen van de optimale condities van de reactor, hogedrukcondenser en stripper van een HGRP. Appendix C behandeld de analyse van de gasfase gebruik makend van GC, de problemen hiervan en de some unieke methoden die gebruikt zijn om optimale analyse-condities te effectueren. Appendix D bescrijft in het kort de analyse van de vloeistoffase.